RESEARCH and DEVELOPMENT PROGRAM for a COMBINED CARBON DIOXIDE REMOVAL and REDUCTION SYSTEM

Contract NAS 1-4154

Final Report - Phase I

OCTOBER 1965

Hamilton Standard DIVISION OF UNITED AIRCRAFT CORPORATION

RESEARCH and DEVELOPMENT PROGRAM for a COMBINED CARBON DIOXIDE REMOVAL and REDUCTION SYSTEM

Contract NAS 1-4154

Final Report - Phase I

OCTOBER 1965

Hamilton Standard DIVISION OF UNITED AIRCRAFT CORPORATION

FOREWORD

Hamilton Standard began company-funded research in the electrochemistry of fused salts early in 1963 with series of experiments directed toward appraising the potential of carbon dioxide decomposition through electrolysis of a molten alkali carbonate. Favorable results, together with new insights achieved, reinforced the decision to engage in a continuing program of research and advanced development in the field of non-aqueous electrodeposition. In particular, attention was addressed to the possibilities of a process in which carbon dioxide, as a constituent of a space cabin atmosphere, would be directly absorbed by an electrolyte without the need for prior separation and concentration, while elemental carbon and gaseous oxygen would be delivered as primary outputs of the electrolytic process. In September, 1964, research and engineering design studies directed toward development of a space vehicle oxygen reclamation system were consolidated in a program sponsored by the Langley Research Center of the National Aeronautics and Space Administration under contract NAS 1-4154, entitled "Research and Development Program for a Combined Carbon Dioxide Removal and Reduction System." This effort was strengthened by association with concurrent research funded by Hamilton Standard.

This is the final report for Phase I of this contract, covering the period from September 25, 1964, through October 25, 1965. Mr. P. G. Stein was Program Manager, and Mr. W. E. Arnoldi was Technical Director of the research activity. The following were principal contributors to the effort:

Dr. P. J. Birbara	Mr. D. H. Mallalieu
*Dr. C. T. Brown	Mr. D. R. McCann
*Dr. G. L. M. Christopher	*Mr. R. Roback
Mr. R. Lamparter	Mr. S. Russell
Mr. J. S. Lovell	*Dr. H. B. Urbach

*United Aircraft Research Laboratories

SUMMARY

The most significant accomplishments during the research program to date have centered about the establishment of the characteristics required in the electrolyte. This has included recognition of theoretical differences among lithium, sodium, and potassium systems and development of a working hypothesis for the electrode processes. Supporting experimental evidence for the process concept has made it possible to relate the electrolyte composition and certain contaminants to the quality of the output products of the cell. The combined theoretical and experimental development of a carbon reference electrode has been a major factor in permitting correlation of electrical observations with the chemistry and electrochemistry of the system.

In addition to the research effort directed at understanding the electrochemical process, engineering effort has been devoted to some of the problem areas involved in adapting the process to spacecraft hardware. The basic problems are positive control of the liquid electrolyte in zero gravity, recovery of carbon from the cell, and control of process gases. Engineering effort has included design and fabrication of a three phase separator model, which was delivered to NASA earlier in the program, and construction of an operating laboratory demonstration model which reflects the latest configuration utilized for process research. In addition, design effort has resulted in the preliminary selection of a porous matrix concept as a representative and potentially attractive melt containment method. This method will be studied experimentally in tests planned for the next phase.

Studies of additives indicate the strong possibility of increasing current density manyfold over the low values initially required for a coherent, graphitic deposit. Although the ultimate goal, a process in which high density carbon is continuously produced without contamination, has not been demonstrated, there is now strong evidence that this goal is achievable and that a basic conceptual framework has been established for the theoretical understanding of the process. Ability to absorb dilute CO_2 has been assured; cathode material is no longer a critical problem, and anode performance and durability have been related to electrolyte composition.

RECOMMENDATIONS

Analysis of the competing approaches indicates a clear advantage to reclamation of oxygen by the use of fused salt electrolysis due to the use of the electrolytic melt as a means for absorbing CO_2 directly from the cabin airstream as well as for the decomposition process. Recent studies have shown a significant advantage in equivalent weight for this approach over the nearest competing approach.

In order to develop this process to the point of incorporation into a practical machine, the following recommendations are made:

The understanding of the basic elemental reaction mechanisms as presently postulated should be further refined. In addition, the effects of a number of variables on system efficiency and process control should be determined. In particular, research activity should be carried out in the following areas:

- Vapor pressures of candidate electrolytes to determine the extent of melt carryover.
- Morphology of cathodic deposits under controlled environments.
- Methods to improve oxide ion transport from cathode to desorbing fluid.
- Additives that will lower the melt operating temperature.
- Additives to improve carbon homogeneity.
- Theoretical studies of thermodynamic equilibrium for mixtures of sodium, lithium, potassium and barium salts.
- Extent of dissociation of carbonates in various halide ion solvents.
- Anode surface material development such that it will be compatible with the electrochemical process of the anode.

In addition, it is recommended that the definition and solution of engineering problems be initiated. This can best be accomplished by the design, fabrication, and testing of a breadboard CO_2 removal and reduction cell module. The cell module should utilize a porous matrix to control the gas/liquid interface at the anode and should be used to evaluate this concept with regard to fabrication techniques, system performance, materials, operating procedures and applicability to zero gravity operation taking into account melt containment, carbon management, and gas control.

The effort reflected in this document is reported in two parts. Part I presents an account of the research conducted to provide an understanding of the basic atmospheric revitalization processes. Part II represents a preliminary investigation of the problem areas and the evaluation of potential solutions for a system as presently envisioned for application of the molten salt process to weightless operation. Part II also contains a comparison of integrated CO_2 management systems which include removal, transfer, and reduction subsystems and provisions for supplying makeup oxygen not available from CO_2 alone.

TABLE OF CONTENTS

TABLE OF CONTENTS (Continued)

LIST OF FIGURES

LIST OF FIGURES (Continued)

LIST OF FIGURES (Continued)

LIST OF FIGURES (Continued)

LIST OF FIGURES (Continued)

LIST OF FIGURES (Continued)

PART I

BASIC PROCESS STUDIES

1.0 INTRODUCTION TO RESEARCH STUDIES

This report presents an account of research into the process for reclamation of oxygen from carbon dioxide by electrolysis of certain molten salt mixtures, in which carbon dioxide is absorbed from a gas stream and then decomposed as a result of electrochemical and chemical processes which yield oxygen at the anode and carbon at the cathode. A similar concept had been studied by earlier investigators (References 1, 2) but was handicapped by an incomplete appreciation of the potential of the process, particularly with respect to the absorption of carbon dioxide at low partial pressure, and fundamental hypotheses for the basic processes in the cell were not firmly enough established for adequate interpretation of the experimental evidence. The work here reported, therefore, has been primarily concerned with achievement of a quantitative understanding of the characteristics of the electrolyte, the electrochemical and chemical reactions at the electrodes, and the equilibrium relationships useful as a frame of reference. Within the limitations of time and manpower and in recognition of the ultimate engineering objective of developing a reliable, working device, efforts were directed toward arriving at meaningful representations of the fundamental principles in terms of working hypotheses which could guide a continuing program of applied research and engineering development.

The accomplishments of this program should therefore be evaluated in terms of the process interpretation and its correlation with chemical theory rather than in terms of discrete measurements. The report presents this interpretation as of the end of the contract term, but also includes a review of experimental investigations and techniques which have contributed significantly to the state of knowledge achieved and to the conclusions drawn. However, it should be recognized that the process of learning is often based upon the integrated contributions of the intangible stimuli from incomplete or unsuccessful experimentation as well as the positive factual evidence gathered. If the intangibles have gone unmentioned or unrecognized in this summation, the implication is mainly that complete understanding and final perspective have not yet been attained.

The field of fused salt electrochemistry is relatively young as a scientific discipline, although there is a rapidly growing body of technical literature. Reference 3 presents an extensive survey of this subject with brief interpretive comments on several subdivisions of the field. Even without consulting the 477 references quoted, it is apparent that experimentation is difficult and often results in contentious or contradictory publications and that fundamental theory has not yet been developed to the point of providing adequate background for interpretation of much experi-

1.0 (Continued)

mental evidence. The literature is especially scanty in connection with carbonate systems, as concerned in this program. This report, therefore, is based heavily upon experimental and theoretical work performed directly under the contract and in associated research supported by the contractor, rather than upon the relatively few references quoted.

The research program was conducted by engineers and scientists in two teams, working in concert but with separate facilities, primary responsibility being vested in the Product Research Group at Hamilton Standard. The Chemical Sciences Section at United Aircraft Corporation Research Laboratories undertook a variety of assignments under the technical direction of the Product Research Group. Utilization of the two teams was based upon the professional experience and capabilities of the personnel and the facilities available, and efforts were made to achieve continuous integration in concept development.

2.3 (Continued)

gas-liquid contact, as in bubbling, is extremely rapid, being determined primarily by the excess in pressure over the equilibrium pressure of carbon dioxide in the melt contacted. Capacity of the electrolyte to absorb carbon dioxide can be maintained by the electrolytic process.

2.4 Oxygen evolution is in accord with Faraday's law, at 100% efficiency, so long as oxygen bubbles are prevented, by shielding, from reaching the cathode region, and if the anode material does not enter into the anode reactions. Nickel appears to be the most eligible anode material, but further study is necessary to insure durability and reliability.

2.5 Although the state-of-the-art in basic chemical knowledge of the properties and behavior of molten salts, particularly alkali carbonates, is at much lower level than in the chemistry of aqueous systems, fundamental chemical principles are applicable in useful and meaningful fashion to the planning and interpretation of experimental research with molten salts. Development of a carbon reference electrode, uniquely necessary to electrical measurements required in research on the electrochemical behavior of alkali carbonates, has provided an essential instrumentation technique for relating experimental observations to hypotheses, derived from basic theory.

2.6 The dissociation constant for the carbonate ion is significantly affected by the presence of chloride or fluoride in a lithium carbonate melt, despite the non-participation of these halides in the basic electrochemical or chemical processes. Equilibrium pressures are thus functions of the electrolyte as a system, rather than being determined by the individual concentrations of constituents considered independently.

2.7 Quality of carbon deposit or limiting current density for specified quality is sensitive to minor additions of certain compounds, such as borates, silicates, and phosphates. Exploration of such effects could lead to major improvements in process control.

2.8 Minor contaminant gases in the processed airstream will be significant to the basic process only insofar as they are soluble in or chemically reactive with the electrolyte, thereby providing additional reactants at the electrodes or altering the desired electrolyte composition.

2.9 Because of the solubility and reactivity of water vapor, it is highly improbable that any means can be found for incorporating decomposition of water to provide supplementary oxygen as an integral

2.0 CONCLUSIONS

2.1 Decomposition of carbon dioxide by absorption and electrolysis at low partial pressure in a molten alkali carbonate electrolyte is feasible and can be controlled so as to yield gaseous oxygen and solid carbon at the electrodes as the primary products. For a successful process, the following general conditions are necessary:

2.1.1 Temperature must be below a limit tentatively proposed to be no higher than 650°C. This represents a serious constraint on electrolyte composition.

2.1.2 Lithium cations are essential to the cathodic process, hence lithium compounds must be the predominant constituents of the electrolyte. Barium may be an alternative, but insufficient evidence is available.

2.1.3 Equilibrium partial pressures of carbon dioxide and water vapor must be maintained at levels permitting selective absorption of carbon dioxide and insuring low equilibrium partial pressures of other gases formed by chemical reaction of cathodic carbon with carbon dioxide and water vapor. The melt must thus contain carbonate, hydroxide, and oxide ions in a suitable state of dissociation, determined by carbon dioxide and water vapor pressure.

2.1.4 Anions of diluent salts necessary to obtain an acceptable melting point must not react with any constituents of the chemical system and must themselves be chemically stable. Chloride and fluoride satisfy this requirement, but oxyanions other than carbonate are severely restricted.

2.1.5 Electrode current densities are restricted by the need to limit departures from chemical equilibrium standards which govern the quality of the reaction products.

2.1.6 Contamination by chemical or physical dissolution of container, electrodes, or accessories in contact with the electrolyte must be avoided by choice of suitably inert materials.

2.2 Graphitic carbon of high purity can be deposited as an adherent coating on the cathode. In addition to control of temperature, gas partial pressures, electrolyte composition, current density, and contamination, further process understanding or control is required to insure a continuous, steady-state process in which such carbon coatings are produced in macroscopic thickness (e.g., centimeters, rather than a small fraction of a millimeter).

2.3 Absorption of carbon dioxide in dilute concentration (0.5 percent) by

2.9 (Continued)

part of the process within the electrolytic cell without prejudicing the process of carbon deposition.

3.0 RECOMMENDATIONS

3.1 Continued experimental research in the control of the cathodic gaseous environment is required in order to determine specific relationships which will insure continued deposition of carbon as a high-purity, high-density material, with minimum occluded electrolytic salts.

3.2 Studies of melt composition effects on carbonate and hydroxide dissociation should be continued, so as to provide a firm foundation for the specification of an electrolyte which will provide the necessary cathodic environment.

3.3 Anodic dissolution requires explanation of secondary chemical processes at the anode in order to establish requirements for a non-reactive or passivated anodic surface on a durable oxygen electrode.

3.4 The function of melt additives, particularly phosphates, should be studied in order to establish their role in determining equilibrium pressures and in relieving limitations on electrode current density.

3.5 Theoretical calculations of chemical equilibrium should be attempted for systems comprising combinations of lithium, sodium, potassium, and barium compounds, to determine, if possible, to what extent addition of a second cation to the electrolyte is permissible without interference with the desired process.

3.6 Improved configurations of reference electrodes should be developed to assure a reliable potential standard through greater isolation from variable environmental circumstances in the surrounding electrolyte.

4.0 DISCUSSION OF PROCESS CONCEPTS

4.1 Basic Process Concept

Decomposition of carbon dioxide into solid carbon and molecular oxygen may be accomplished by means of concurrent chemical and electrochemical processes in certain fused carbonate electrolytes. The program of experimental and theoretical research here reported has shed considerable light on the nature of these processes, providing support for working hypotheses from which system performance may be evaluated and engineering specifications laid down.

The basic configuration for this system is indicated by the diagram of Figure 4-1, showing a cell in which carbon dioxide is absorbed from a gas stream by direct contact with the electrolyte, oxygen is evolved at the anode, and carbon is accumulated in solid form at the cathode. The required operating temperature is maintained by energy losses in the process and by thermal insulation. Thermal losses to the effluent air are minimized by the use of a regenerative heat exchanger between inflow and outflow.

The fundamental concept is that lithium, electrochemically reduced at the cathode in an electrolyte containing lithium carbonate, reacts chemically with carbon dioxide in solution to deposit solid carbon adherent to the cathode surface, returning lithium ions and oxide ions to the electrolyte. At the anode, oxide ions are discharged to form gaseous oxygen. Since three oxide ions are produced at the cathode for each pair of oxide ions discharged at the anode, the extra ion is available to absorb a molecule of carbon dioxide gas, replenishing, as carbonate, the carbon dioxide reduced at the cathode. There is no substantial accretion of lithium at the cathode, since lithium atoms are promptly returned to ionic form by reaction with carbon dioxide. However, a number of secondary reactions may take place, and are indeed required for chemical equilibrium, hence a more complete exposition of the concept is necessary in order to indicate constraints in the application to an engineering process.

Notation or terminology which is peculiar to this report is explained where first used in the text. However, Figure 4-2 has been prepared to permit convenient reference to definitions of equilibrium constants and gas partial pressure symbols which are repeatedly used.

4.2 Reactions at the Electrodes

Consider first an electrolyte comprising a eutectic mixture of lithium carbonate and lithium chloride. This composition is not

4.2 (Continued)

essential, but it has a convenient melting point (509°C), is chemically stable under a small partial pressure of CO_2, and will provide a reasonably simple basis for discussing fundamental requirements in CO_2 decomposition. In the molten state - say, at 550°C - this mixture will be highly ionized. Lithium will be the only cation, but anions will include carbonate, chloride, and oxide which results from the dissociation of carbonate ions. Under equilibrium conditions, the dissociation of carbonate anions will be determined by the ionic activities and by the partial pressure of CO_2 at a free surface. Although lithium oxide and lithium chloride will both have vapor pressures, these are small and may be ignored for the purpose of this discussion.

At the cathode, lithium ions will be reduced in accordance with Equation 4-1.

$$4\,Li^{+} + 4e \longrightarrow 4\,Li \qquad 4\text{-}1$$

The atomic lithium will react with CO_2, available by dissociation of carbonate ions, to yield elementary carbon.

$$4\,Li + CO_2 \longrightarrow 4\,Li^{+} + 2\,O^{=} + C \qquad 4\text{-}2$$

It is frequently convenient to represent the net result of these cathode reactions by summation:

$$CO_2 + 4e \longrightarrow C + 2\,O^{=} \qquad 4\text{-}3$$

However, it should be noted that this is merely symbolic for the net cathodic process; the distinction between the electrochemical reaction of Equation 4-1 and the chemical reaction of Equation 4-2 should not be ignored.

At the anode, oxide ions will be oxidized in accordance with Equation 4-4.

$$2\,O^{=} \longrightarrow O_2 + 4e \qquad 4\text{-}4$$

Thus, the net electrochemical process, represented by Equations 4-1 and 4-4, is the decomposition of lithium oxide:

$$4\,Li^{+} + 2\,O^{=} \longrightarrow 4\,Li + O_2 \qquad 4\text{-}5$$

The potential difference at equilibrium between an anode and a cathode which are themselves chemically inert may be expressed by Equation 4-6, which is the summation of the Nernst equations

4.2 (Continued)

for the two electrodes.

$$E = E_o - \frac{RT}{4F} \ln \frac{(Li^+)^4 (O^=)^2}{(Li)^4 (O_2)} \qquad 4\text{-}6$$

E_o is the potential difference for unit activity of reactants and products, determined by the free energy change, ΔF_1, in Equation 4-5.

$$E_o = \frac{\Delta F_1}{4F} = 2.5 \text{ volts at } 550°C \qquad 4\text{-}7$$

The concentration terms in Equation 4-6 may be replaced by more conveniently available quantities by considering equilibrium of the chemical reaction at the cathode, Equation 4-2. The equilibrium constant may be expressed by

$$K_o = \frac{(Li^+)^4 (O^=)^2 (C)}{(Li)^4 (CO_2)} \qquad 4\text{-}8$$

whence, by substitution into Equation 4-6, we have

$$E = E_o - \frac{RT}{4F} \ln \frac{(CO_2) K_o}{(O_2) (C)} \qquad 4\text{-}9$$

Since K_o is definable in terms of the free energy change, ΔF_o, for the reaction of Equation 4-2, substitution into Equation 4-9 yields

$$E = \frac{\Delta F_1 + \Delta F_o}{4F} - \frac{RT}{4F} \ln \frac{(CO_2)}{(O_2)} \qquad 4\text{-}10$$

where (C) has been set to unity, since only solid carbon will be present. Since adding Equations 4-2 and 4-5 results in decomposition of CO_2 as a net process, the sum of the two free energy changes, $\Delta F_1 + \Delta F_o$, corresponding to these reactions, is identical with the free energy change for the decomposition of CO_2 to carbon and oxygen. This free energy change thus determines the electrode potential difference for unit activity of oxygen and carbon dioxide, and the cell voltage may be written as

4.2 (Continued)

$$E = 1.025 - \frac{RT}{4F} \ln \frac{(CO_2)}{(O_2)} \qquad 4\text{-}11$$

Since the free energy of formation of carbon dioxide is substantially constant over a wide temperature range, this equation is not restricted to the 550°C temperature proposed for this discussion. The activity of oxygen, (O_2), and of carbon dioxide, (CO_2), may be represented by the partial pressures of these gases.

4.3 Efficiency of the Electrolytic Cell

In the application of a process for oxygen reclamation to space vehicle requirements, it is appropriate to investigate the efficiency achievable. Efficiency will be defined, for this purpose, as the quotient of ideal electrolytic power input divided by actual electrolytic power input, and the ideal power input will be based upon the free energy of formation of carbon dioxide. For an electrochemical process, in which Faraday's principle applies, the current will be determined uniquely by the gram equivalent rate of decomposition, and the power input will be the product of applied potential by current. Laboratory experience has indicated that, for electrolytic decomposition of CO_2 in an alkali carbonate melt, 100% current efficiency is readily achieved, hence the power is proportional to the voltage required. Thus, 100% power efficiency may be associated with an electrode potential difference of 1.025 volts, in accordance with the definition proposed, and increases in potential due to electrode over-voltages, concentration gradients, Joule heating losses, etc., will specify operating efficiencies, generally less than 100%.

For example, consider the idealized case where the cell delivers oxygen at a partial pressure of 0.20 atmosphere, absorbing CO_2 at an input partial pressure of 0.005 atmosphere, the process taking place at 550°C. Equation 4-11, with these numerical values, becomes

$$E = 1.025 - \frac{8.31 \times 823}{4 \times 96500} \ln \frac{0.005}{0.200} = 1.090 \text{ VOLTS} \qquad 4\text{-}12$$

For these circumstances, the limiting efficiency will be 1.025/1.090 or 94%. In practice, this level is unattainable, since the electrolyte must have a CO_2 partial pressure which is substantially less than the input CO_2 pressure in order that effective chemical absorption will

4.3 (Continued)

take place. If we arbitrarily set a 90% absorption efficiency as a requirement and assume that equilibrium is attained before the gas leaves the melt, the CO_2 pressure of the melt will be 0.0005 atmosphere, resulting in a cell potential of 1.132 volts and an efficiency of 90.6%. Again, this becomes a target which cannot be closely approached in practice, since it is based upon an equilibrium which is significantly disturbed when electrode current densities are not vanishingly small.

At the anode, depletion of oxide ions by discharge of gaseous oxygen gives rise to a local gradient in oxide ion concentration, wherein electrolytic migration is balanced against diffusion processes which tend to restore equilibrium. Likewise, at the cathode, where oxide ions are generated in accordance with Equation 4-2, a balance will be attained between the rate of oxide generation and the rate of diffusion away from the cathode, resulting in a locally decreased concentration of CO_2. The consequent difference in oxide ion concentration, or CO_2 concentration, between anode and cathode will further increase the cell potential required to sustain the electrolytic process in steady state.

We shall evaluate this difference by considering two carbon cathodes, one of which is subject to the environment previously assumed while the other has an increased oxide ion concentration in its immediate vicinity. The difference in potential between these two carbon electrodes may then be added to the potential difference of Equation 4-11 in order to include the effect of the change in oxide ion concentration from the anode region to the cathode. This approach is based upon the assumption that Equations 4-1 and 4-2 represent reversible reactions at a carbon electrode, an assumption which is in accord with laboratory experience.

Using subscripts 1 and 2 to designate the two carbon electrodes and their associated environments, and representing CO_2 partial pressures by p_1 and p_2, the equation for the potential difference, $E_2 - E_1$, is written as

$$E_2 - E_1 = \frac{RT}{4F} \ln \frac{(P_2)(O^=)_1^2}{(O^=)_2^2 P_1} \qquad 4\text{-}13$$

In order to eliminate the oxide ion activities, or molal concentrations, from this equation, consider the equilibrium of oxide, CO_2, and carbonate -

4.3 (Continued)

$$CO_2 + O^{=} \rightleftharpoons CO_3^{=}, \quad K_1 = \frac{(CO_3^{=})}{(O^{=})p} \qquad 4\text{-}14$$

Since the total number of lithium ions and of chloride ions is fixed, the total number of electrochemical equivalents of oxide ions plus carbonate ions is also fixed, regardless of CO_2 pressure, each oxide ion being directly convertible to one carbonate ion, and vice versa. Their total molal concentration is thus constant and may be expressed as

$$(CO_3^{=}) + (O^{=}) = (O^{=})_e \qquad 4\text{-}15$$

where $(O^{=})_e$ may be described as an "equivalent oxide concentration."

Eliminating the carbonate concentration in Equation 4-15 by substitution from Equation 4-14 , we have

$$(O^{=})(K_1 p + 1) = (O^{=})_e \qquad 4\text{-}16$$

which, by substitution into Equation 4-13 , eliminates the oxide concentration, yielding an expression for the potential difference between two carbon electrodes in terms of their local CO_2 partial pressures:

$$E_2 - E_1 = -\frac{RT}{4F} \ln \frac{p_2(K_1 p_2 + 1)^2}{p_1(K_1 p_1 + 1)^2} \qquad 4\text{-}17$$

For all conditions of interest, K_1 is sufficiently large that $K_1 p$ is much greater than unity, hence Equation 4-17 may be simplified to the form,

$$E_2 - E_1 = -\frac{3RT}{4F} \ln \frac{p_2}{p_1} \qquad 4\text{-}18$$

Under the conditions postulated for this discussion of equilibrium relations, Equation 4-18 has been found to be in accord with experimental evidence, and an example of this relationship as experimentally determined is presented in Figure 4-3.

The anode to cathode potential difference of Equation 4-11 was written on the basis of common ionic concentrations at the two electrodes. In order to include the effect of the difference in oxide ion concentration between anode and cathode, reflected by a difference in CO_2 partial pressure between these electrodes, we

4.3 (Continued)

may add the carbon electrode potential difference given by Equation 4-18, whence

$$E = 1.025 - \frac{RT}{4F} \ln \frac{p_c^3}{(O_2)_a p_a^2} \qquad 4\text{-}19$$

in which the subscripts, a and c, denote anode and cathode quantities, respectively. The CO_2 partial pressure at the cathode, during cell operation, normally will be several orders of magnitude lower than at the anode, hence the open-circuit cell voltage, measured by establishing steady state electrolytic conditions and suddenly breaking the circuit, will be appreciably greater than previously indicated for a balanced equilibrium in the melt. For example, letting $p_a = 0.0005$, as before, but taking $p_c = 10^{-6}$, the open-circuit cell voltage will be 1.464 volts, and the limiting efficiency at zero current will be 70%. Successful operation has been achieved with applied potentials in the range, 1.6-2.0 volts, indicating efficiencies ranging from about 65% to 50% for the overall chemical/electrochemical process.

It seems worthwhile to draw attention to the fact that, while efficiency, as commonly expressed and as defined here, represents input minus losses divided by input, the losses so indicated do not all appear as thermal energy in the cell. In the example above, the 70% efficiency at zero current involves no thermal energy losses; the losses here represent "pumping power," where electrical energy is used to raise the pressure of oxygen delivered at the anode to the required output level, relative to the carbon dioxide partial pressure at the cathode. Any further losses attendant to passage of a finite current through the cell, providing the concentrations of reactants and products at the electrodes remain unchanged, will appear primarily as thermal energy and will affect the temperature of the system.

4.4 Carbon Dioxide in Effluent Gases

As mentioned earlier, effective absorption of CO_2 from a dilute atmospheric gas mixture (space cabin atmosphere) which contacts the electrolyte by bubbling, liquid spraying, or any other gas absorption technique, requires that the equilibrium CO_2 pressure of the melt be no greater than the CO_2 pressure in the effluent gas. Oxygen leaving the anode region will also be mixed with CO_2 at equilibrium pressure for a very slow process (low anode current density), or, more specifically, at the CO_2 partial pressure in the immediate vicinity of the anode, where depletion of oxide ions results in an increase in the ratio of carbonate to oxide ion

4.4 (Continued)

concentration. Thus, the anode gas output may be enriched in CO_2 above the level obtaining in the bulk of the melt. In the limit, for extremely high anode current density, where ionic diffusion is inadequate to replenish oxide ions, two moles of CO_2 will be produced for every mole of oxygen, and the gas mixture will be 1/3 oxygen and 2/3 carbon dioxide. Since this would impose an unacceptable requirement for recycling anode gas for reabsorption of CO_2, it is obvious that anode current density must be limited to a value which permits mixing processes in the melt (convection, diffusion) to hold a near-equilibrium CO_2 partial pressure in this region.

It is fortunate that the solubility and diffusion rate of oxygen in eligible electrolytes are sufficiently low that the transport of dissolved oxygen, either from the scrubber or from the anode to the cathode, may be ignored. While solubilities and diffusion rates of various gases in alkali carbonate electrolytes have not been measured directly, laboratory experience has shown that, except for carbon dioxide and water vapor, other dissolved gases such as oxygen are not transported to the cathode in appreciable quantities, relative to the rate of carbon deposition. It is nevertheless necessary to interpose a shield which prevents gas bubbles from reaching the cathode by convection, since these can directly oxidize the carbon deposit and drastically impair process efficiency. However, with simple shielding, the Faraday current efficiency of the cell, measured relative to either of the desired output materials, carbon and oxygen, is found to be substantially 100%.

4.5 Carbon Monoxide Equilibrium

Certain other gases are significant to the nature of the cathodic process and impose significant restrictions on the operating conditions required for adequate performance of the system in the application to space cabin oxygen reclamation. First, since elementary carbon is produced at the cathode in an environment which can yield carbon dioxide at a finite pressure, the reaction between carbon and CO_2 to produce carbon monoxide must be recognized. An equilibrium will tend to be established in accordance with the relations,

$$C + CO_2 \rightleftharpoons 2CO, \qquad K_3 = \frac{(CO)^2}{CO_2} = \frac{c^2}{p} \qquad 4\text{-}20$$

where, for brevity, c represents the partial pressure of carbon monoxide. If, as earlier, we take the working level of p at the cathode to be 10^{-6}, c will be about 1.5×10^{-4}, or 150 parts per

4.5 (Continued)

million in any gas mixture above the electrolyte surface at the cathode. At the least, it would be undesirable for reasons of toxicity to let this concentration of carbon monoxide appear in the cell output, hence the cathode region must be shielded from mixing with the air leaving the cell as well as from bubble communication in the melt. Figure 4-4 shows the variation of certain equilibrium constants with temperature, obtained from published free energy data, where the curve for K_3 indicates that carbon monoxide would become increasingly prominent as a cathode gas as temperature rises. However, the significance of carbon monoxide lies in another area, rather than in the toxicity and shielding aspect, as will become apparent in Section 4.8.

4.6 Water Vapor Equilibrium

Thus far, we have considered a process in which the electrolyte comprises lithium carbonate and lithium chloride, with oxide ions produced by dissociation of carbonate in equilibrium with carbon dioxide. The input gas was presumed to be an oxygen-nitrogen mixture including a small percentage of carbon dioxide, and no mention was made of the possible presence of water vapor. A space cabin atmosphere would inevitably have a significant humidity, probably with a dew point in the neighborhood of 50°F, or about 0.012 atmosphere partial pressure of water vapor. In scrubbing this gas with an oxide-containing melt, there is not only the CO_2-oxide-carbonate equilibrium to be considered but also the H_2O-oxide-hydroxide equilibrium, in accordance with the following relations:

$$H_2O + O^{=} \rightleftharpoons 2\ OH^{-},\quad K_2 = \frac{(OH^{-})^2}{(H_2O)(O^{=})} = \frac{(OH^{-})^2}{v(O^{=})} \qquad 4\text{-}21$$

The activity of water vapor, (H_2O), is represented by its partial pressure, designated by v for brevity.

The hydrolysis of LiCl might also be considered, in accordance with Equation 4-22.

$$LiCl + H_2O \rightleftharpoons LiOH + HCl \qquad 4\text{-}22$$

However, since HCl can immediately react with lithium carbonate so as to replenish lithium chloride, and since no escaping HCl has been detected, even at low ppm levels, with normal water vapor pressure, it is believed that hydrolysis of LiCl may properly be ignored in the consideration of water vapor equilibrium. Hydrolysis of LiCl, due to its extremely hygroscopic nature at room temperature,

4.6 (Continued)

is a problem in the preparation of the electrolyte if low hydroxide content is sought, and methods for eliminating moisture are relatively tedious, but in the present case we need not be concerned with hydrolysis. The direct absorption of water vapor by oxide ion, as in Equation 4-21, may be taken to represent the primary interaction between water and the electrolyte.

As in the case of the "dry" electrolyte, the total number of electrochemical equivalents of oxide, carbonate, and hydroxide ions will be fixed quantity, hence, as in Equation 4-15, we may write an expression for an "equivalent oxide concentration" in terms of the molal concentrations of the constituent ions.

$$(CO_3^=) + (O^=) + \frac{1}{2}(OH^-) = (O^=)_e \qquad 4\text{-}23$$

Replacing the carbonate and hydroxide concentrations by the use of the equilibrium relations of Equations 4-14 and 4-21, we obtain an expression relating oxide ion concentration to the partial pressures, p and v, in terms of the equilibrium constants and the equivalent oxide concentration, also a fixed quantity.

$$K_1 p\,(O^=) + (O^=) + \frac{1}{2}\sqrt{K_2 v\,(O^=)} = (O^=)_e \qquad 4\text{-}24$$

The nature of this relationship is shown in the plot of Figure 4, based upon the solution in the form,

$$K_1 p + 1 = \frac{1}{(O^=)/(O^=)_e} - \frac{1}{2}\sqrt{\frac{K_2 v/(O^=)_e}{(O^=)/(O^=)_e}} \qquad 4\text{-}25$$

Since $K_1 p$ is of interest only for values much larger than unity, this is essentially a plot of log pressure against log oxide concentration, with a dimensionless quantity indicative of water vapor pressure as a parameter.

In Figure 4-5, the oxide concentrations at the vertical asymptotes of the curves, designated by A in each case, satisfy the requirement, from Equation 4-25, that

$$\frac{(O^=)}{(O^=)_e} = \frac{4(O^=)_e}{K_2 v} \qquad 4\text{-}26$$

and the corresponding points, B, on the partial pressure scale, indicating the region of transition in slope, are defined by

4.6 (Continued)

$$K_1 p + 1 = \frac{K_2 v}{4(O^=)_e} \qquad 4\text{-}27$$

It is convenient to adopt the convention that, for operation above the transition level indicated by B, the electrolyte is termed a "dry melt," while operation below B would denote a "wet melt," these terms indicating the relative significance of the parameters, $K_1 p$ and $K_2 v/(O^=)_e$.

Note that, for a dry melt, or relatively low water vapor pressure, oxide ion concentration is inversely proportional to CO_2 pressure. A wet melt, in which water vapor effects are predominant, will have an oxide ion concentration determined by and inversely proportional to water vapor pressure, for relatively low CO_2 pressure. A dry melt will absorb CO_2 by conversion of oxide ion to carbonate, while a wet melt will need to release water vapor (increase the partial pressure) in order to provide oxide ions for CO_2 absorption. This may also be viewed as the "displacement" of water from hydroxyl ions by CO_2 to form carbonate ions. In practice, electrolysis will provide a continuous source of oxide ions, and, with the electrolytic current regulated in conformity with the CO_2 absorbed, there will be no variation in either CO_2 or H_2O partial pressure. Nevertheless, for excursions in input CO_2 pressure, the melt CO_2 pressure would be variable in the absence of water vapor but more stable under the conditions of a wet melt.

Absorption of carbon dioxide from a humid atmosphere thus involves a concurrent interaction between water vapor and the absorbent electrolyte. If the process is to provide CO_2 to the melt for electrolytic decomposition, rather than to carry on some alternative process with water vapor, it is necessary that the water input and output be identical. In terms of equilibrium relations, therefore, the water vapor partial pressure of the electrolyte must be identical with the vapor pressure in the processed atmosphere. Thus, it becomes necessary to devise and achieve an electrolyte composition which will satisfy requirements for two partial pressures, p and v, in order that CO_2 will be effectively absorbed and that the H_2O content will be unaffected by the passage of space cabin air through the cell. Alternatively stated, the hydroxide and carbonate concentrations must satisfy the relationship,

$$\frac{K_2}{K_1} = \frac{(OH^-)^2 p}{(CO_3^=)\ v} \qquad 4\text{-}28$$

4.6 (Continued)

The constants, K_1 and K_2, vary with temperature, hence, choice of a melt composition for a desired equilibrium restricts operation to a unique temperature. On the other hand, specification of operating temperature, together with the partial pressures, p and v, fixes only a concentration ratio, and some freedom is thus allowed in arriving at a composition which also has desirable qualities with regard to melting point, ionic conductivity, vapor pressure of constituent salts, and other properties which influence performance, materials compatibility, mechanical design, etc.

4.7 Oxide Ion Buffers

The effect of water vapor on oxide ion concentration is an example of a phenomenon which, by loose analogy with means for hydrogen ion control in aqueous solutions, has been considered a "buffering" action in fused carbonate mixtures. Equation 4-25, illustrated graphically in Figure 4-5, indicates that, for a sufficient concentration of H_2O, measured by the vapor pressure, formation of hydroxyl ions effectively limits the concentration of oxide ions achievable. Although this effect may be viewed as a means for limiting oxide ion concentration at the cathode so as to prevent the tendency to exceed solubility limits at high current density, the concommittant phenomenon of gas formation precludes effective use of water vapor as a "buffer." However, the same principle of oxyanion formation in the equilibrium of oxide ion and some other molecular or ionic species is an attractive subject for speculation.

The buffer need not be a volatile constituent, such as water, the primary requirement being only that a suitably stable anion be formed by combination with oxide ion. One possibility is boric oxide (B_2O_3), which is highly soluble in the electrolytes under consideration and has been observed to react with carbonate in the melt to release CO_2. We postulate an equilibrium with oxide and borate ions, as follows:

$$O^{=} + B_2O_3 \rightleftharpoons 2\,BO_2^{-}, \qquad K_6 = \frac{(BO_2^{-})^2}{(B_2O_3)(O^{=})} \qquad 4\text{-}29$$

The "total equivalent boric oxide" in the melt, representing the total of boric oxide and borate ion concentrations, may be defined as

$$(B_2O_3)_e = (B_2O_3) + \frac{1}{2}\,(BO_2^{-}) \qquad 4\text{-}30$$

Substituting this expression into the preceding expression for the equilibrium constant, we may eliminate the (B_2O_3) term and solve

4.7 (Continued)

for the borate ion concentration, which now constitutes part of the equivalent oxide. Assuming a dry melt, the equivalent oxide concentration may be written,

$$(O^{=})_e = (CO_3^{=}) + (O^{=}) + \frac{1}{2}(BO_2^{-}) \qquad 4\text{-}31$$

and by replacing the borate term, we have

$$(O^{=})_e = (CO_3^{=}) + (O^{=}) + \frac{K_6(O^{=})}{8}\left(-1 + \sqrt{1 + \frac{8(B_2O_3)_e}{K_6(O^{=})}}\right) \qquad 4\text{-}32$$

Making use of the carbonate-oxide equilibrium constant and rearranging for comparison with Equation 4-25, this becomes

$$K_1 p + 1 = \frac{1}{(O^{=})/(O)_e} - \frac{K_6}{8}\left(-1 + \sqrt{1 + \frac{8(B_2O_3)_e/(O^{=})_e}{K_6(O^{=})/(O^{=})_e}}\right) \qquad 4\text{-}33$$

For high p, or very low oxide ion concentration, the first term predominates, and the oxide ion concentration is inversely proportional to CO_2 pressure. At low p, the second term becomes significant and the limiting value for oxide ion concentration is established by the amount of equivalent boric oxide in the melt, relative to equivalent oxide, and by the equilibrium constant for the oxide-borate relationship.

Similarly, other additives may be considered as potential buffers - aluminum oxide forms an aluminate ion, silicon dioxide forms a silicate, nickel oxide forms a nickelate, etc. However, no buffer, in the sense here discussed, has yet been found which performs the desired function without undesirable side-effects. Boric oxide, in the presence of moisture, contributes to gas evolution at the cathode, apparently in the form of boranes. Aluminum oxide appears to be insufficiently soluble, except, perhaps, in a fluoride melt, where alumina appears as part of the cathodic deposit. Silicon seems to be reduced at the cathode. Nickelate ion, of low solubility, is too stable and interferes with absorption of CO_2 at low pressure. Phosphate, from meager data obtained late in the program, may have interesting possibilities, but probably due to characteristics other than a buffer function.

4.8 Gas-Forming Reactions at the Cathode

In the presence of water vapor, other gases in addition to carbon monoxide may be formed at the cathode by chemical interaction between water vapor and carbon. Hydrogen and methane have been

4.8 (Continued)

detected in measurable concentrations, hence equilibrium relations which specify these gases will be postulated. The actual mechanisms for the formation of hydrogen and methane have not been established, therefore the postulated equilibrium relations below are primarily symbolic. Nevertheless, whatever the true mechanisms may be, the postulated relations must be quantitatively satisfied in a thermodynamic sense for equilibrium and are therefore significant in the formulation of further restrictions on the process conditions.

Let us consider the reaction of water vapor with carbon to produce hydrogen and carbon dioxide:

$$C + 2H_2O \rightleftharpoons 2H_2 + CO_2, \quad K_4 = \frac{h^2 p}{v^2} \qquad 4\text{-}34$$

Here, h represents the partial pressure of hydrogen, which is uniquely determined, at any given temperature, by p and v. As discussed for carbon monoxide, hydrogen at the indicated partial pressure will appear in the gas mixture above the electrolyte at the cathode, and since, for typical operating conditions, this may be a substantial fraction of atmospheric pressure, an additional reason is provided for shielding the cathode and preventing intermixing of these gases with the atmospheric effluent from the cell. Furthermore, purging hydrogen out of this region would be highly undesirable, since more would be generated by further reaction of carbon with water vapor so long as the equilibrium pressure were not maintained, thereby depleting the carbon deposited, restoring carbon dioxide to the electrolyte, and impairing the efficiency of the cell.

Similarly, methane can also be produced, and we choose the direct reaction of carbon with hydrogen arbitrarily to represent the equilibrium requirement:

$$C + 2H_2 \rightleftharpoons CH_4, \quad K_5 = \frac{m}{h^2} \qquad 4\text{-}35$$

The partial pressure of methane is here represented by m. Methane, also, can appear in substantial concentration.

On the basis of confirmation by experimental observation, equilibrium requirements for five gases associated with the electrolyte and its cathodic carbon deposit have been discussed: carbon dioxide, water vapor, carbon monoxide, hydrogen, and methane. Since co-existence of these gases is required at an electrolyte surface, as at the cathode, a total gas pressure, g, may be expressed by

4.8 (Continued)

$$g = p + v + c + h + m \qquad 4\text{-}36$$

Suppose that the total pressure, g, were to exceed one atmosphere, and the cathode region above the electrolyte surface were vented so as to maintain one atmosphere. Then these gases would be generated continuously, would form into bubbles, and would rise to the surface and escape, to the extent that they were not restrained by adherence to the electrode surface. The growth of such bubbles could be expected to be deleterious to the orderly formation of a carbon deposit on the cathode. Formation of craters, fissures, and other types of gas passages in the carbon deposit, as has been observed in laboratory experiments, may be ascribed to such a phenomenon, therefore a rational criterion for satisfactory process control may be established on the basis that the equilibrium gas mixture total pressure must not be allowed to exceed the total pressure on the melt. Furthermore, since the working process is one of steady state non-equilibrium, some allowance must be made for local departures from equilibrium at the cathode, setting the equilibrium gas pressure limit somewhat lower than the operating pressure by a suitable margin, empirically determined.

Introducing the representations previously derived for the several gases, in terms of p and v, we have

$$y = p + v + \sqrt{K_3 p} + v\sqrt{\frac{K_4}{p}} + K_5 K_4 \frac{v^2}{p} \qquad 4\text{-}37$$

If p and v are determined by the engineering specifications for the function of the cell, setting a limit on g is equivalent to determining a limiting operating temperature, since temperature, which determines K_3, K_4 and K_5, is then implicitly a dependent variable. In view of the relation between carbonate and hydroxyl ion concentrations determined by v/p (Equation 4-28), it then remains to determine the concentration of diluent solvent, such as LiCl, necessary to achieve a melting point suitably below the limiting operating temperature.

Figure 4-6 presents calculated curves of gas partial pressures against reciprocal temperature, based upon the equilibrium constants calculated and plotted in Figure 4-4. The values of v and p were chosen arbitrarily and are based upon a normal humidity level corresponding to 50°F dew point and normal atmospheric CO_2 concentration of 0.03%. It is interesting to note that the total gas pressure reaches sea level atmospheric pressure at 650°C, and at 550°C the gas pressure is one-half atmosphere.

4.9 Carbon Electrode Potential

In Section 4.3 the potential difference between two carbon electrodes, each separately in equilibrium with the local electrolyte, was given by Equation 4-13. Concentration gradients in the electrolyte do not contribute a potential difference due to ion transference because the current is carried predominantly by the lithium ion, whose concentration is uniform throughout, being the only cation in the case under consideration. By introducing the concept of a fixed equivalent oxide concentration, Equation 4-18 was derived, relating the potential difference between two carbon electrodes to the ratio of CO_2 pressures at the two electrodes. It is evident that this suggests the use of a carbon electrode as a sensing device for local CO_2 pressure, furthermore, that by controlling the CO_2 pressure at a carbon electrode a reference potential might be established. This would be useful as a working standard against which other electrode potentials might be independently measured, as, for example, in polarography. Attempts to devise and apply other types of reference electrodes, particularly an oxygen reference, encountered problems in electrode interactions with the melt and consequent electrolyte contamination by undesired ionic species. A carbon electrode, on the other hand, is not a source of contamination, being a normal product of the cathodic process.

Carbon electrodes have been successfully used both as references and as probes, or sensors, in our work, and their behavior appears to be in good accord with theory. However, a further extension of the approach given in Section 4.3 is necessary to describe their performance.

With the presence of water vapor in a hydroxide-containing electrolyte, the oxide ion concentration required by Equation 4-13 is defined by Equation 4-25, requiring solution of a quadratic form before substitution into Equation 4-13. The algebraic format tends to obscure the meaning of the result, but since the plot of CO_2 pressure against oxide concentration for various water vapor pressures in Figure 4-4 indicates separable regimes of operation, it is more illuminating to consider two extremes, represented by predominance of the carbonate-oxide relationship at high p, low v, and by predominance of the hydroxide-oxide relationship at low p, high v. The first of these cases was essentially applied in the derivation of Equation 4-18, which is repeated below for convenient reference:

$$E_2 - E_1 = -\frac{3RT}{4F} \ln \frac{P_2}{P_1} \qquad 4\text{-}38$$

4.9 (Continued)

From Equation 4-25, when the water vapor pressure is sufficiently high so that oxide concentration is relatively independent of CO_2 pressure, the oxide concentration is found to be given by

$$\frac{(O^{=})}{(O^{=})_e} = \frac{4(O^{=})_e}{K_2 v} \qquad 4\text{-}39$$

Substituting this expression into Equation 4-13 in order to eliminate the oxide concentrations, we obtain

$$E_2 - E_1 = -\frac{RT}{4F} \ln \frac{p_2 v_2^2}{p_1 v_1^2} \qquad 4\text{-}40$$

where the equivalent oxide concentration and the equilibrium constant, K_2, do not appear, due to concellation, being the same at both electrodes.

Equation 4-38, plotted on semilog coordinates as in Figure 4-3, becomes a linear relationship between potential difference and CO_2 pressure, with a voltage coefficient, measured by the slope, of 3RT/4F, or, with logarithms to base ten at 550°C, a coefficient of 124 millivolts per decade.

Equation 4-40, if water vapor pressure is identical at the two electrodes, represents a similar relationship but with a different voltage coefficient, RT/4F, which would correspond to a slope of 41.3 millivolts per decade at 550°C. Thus, for a given water vapor pressure, the potential difference between carbon electrodes tends to be linearly proportional to the logarithm of the CO_2 pressure ratio, with the RT/4F slope at low pressures but changing to the 3RT/4F slope at higher pressures. This transition in slope has been observed experimentally, and a typical example is shown in Figure 4-7. It is interesting that the slope is changed by a ratio which is very nearly three, as pressure is varied from below to above a transition region, but it may also be significant that there is a discrepancy in the absolute values of the slopes. Whereas the theory indicates slopes of 41.3 and 124 mv/decade, these experimental data show slopes of 38 and 117 mv/decade. Although the precision of representation of the data by the straight lines may be questionable, the preponderance of evidence indicates a tendency towards lower than theoretical slopes, generally beyond the uncertainty possible through inaccuracies in temperature. Furthermore, the transition region appears to be more sharply defined than

4.9 (Continued)

would be inferred from the curves of Figure 4-5, where the stabilization of oxide ion concentration by water vapor seems to take place in a transition region extending over more than two decades of pressure. We are led to believe that the process and equilibrium relationships on which the prediction of slope is based must be inaccurate or incomplete and that there is some further variable which is not under control. It is likely that the problem lies in the interaction between water vapor and the melt, since the discrepancy in slope appears commonly to be associated with large or inadequately controlled water vapor pressure. Nevertheless, during any particular experiment, the potential/pressure relationship is found to be unique and reproducible, hence it can be useful through calibration.

The electrode configuration used in order to obtain these measurements, which is therefore also applicable to the function of a reference electrode, is shown in Figure 4-8. A graphite rod of spectrographic quality is inserted into the electrolyte through a close-fitting tube of aluminum oxide, projecting into the electrolyte about two diameters beyond the end of the tube. A controlled humidified mixture of carbon dioxide and argon is fed to the electrode tip through the clearance space inside the tube, to escape over the tip in a fine stream of bubbles. The CO_2 in the gas stream rapidly establishes carbonate-oxide equilibrium in the vicinity of the electrode tip, which is restricted by enclosure within an outer shield, also of aluminum oxide. The shield also serves to isolate the effluent gas stream from the bulk of the electrolyte, restricting the controlled environment to the small volume of electrolyte within the assembly. In order to provide ionic conductivity to the outside melt, the lower end of the shielding tube is punctured by a small hole, effectively constituting a salt bridge to the surrounding electrolyte.

This configuration may be used to provide a reference potential for voltage measurements on other electrodes in the same cell. Also, by using two such assemblies and holding CO_2 partial pressure constant at one while varying CO_2 partial pressure at the other, the characteristics of a carbonate melt of unknown composition can be obtained in the form of an E versus log p curve as in Figure 4-7, thus to determine the location of the transition region.

4.10 Materials Compatibility

While the subject of corrosion and electrolyte contamination by container and electrode materials is primarily an engineering development problem, beyond the scope of the research program discussed here, it seems nevertheless appropriate to mention

4.10 (Continued)

several aspects of experience accumulated in more than two years of laboratory experimentation with fused carbonate electrolytes. Molten mixtures of alkali carbonates and halides are potentially reactive with many common materials, especially in the presence of oxygen, and, although chemical theory may provide some guidance, the state of the art rests primarily upon laboratory observation.

For limited experimental purposes, as, for example, in polarographic studies where avoidance of electrolyte contamination by foreign ions is important, graphite crucibles have been outstandingly successful containers for the melt. However, they are useful only when oxygen may be excluded and when the generation of CO, H_2, and CH_4 is of little consequence, hence carbon is not a universally suitable material. Nickel, stainless steel (AISI 304), and gold-palladium alloy (80% Au) may be used as containers for extended periods, but a slow oxidation occurs which can ultimately result in objectionable contamination. Most satisfactory experience thus far has been with 99% purity alumina crucibles, whose solubility in various electrolyte compositions used appears to be extremely small and, moreover, not deleterious to the electrolytic process. Alumina is preferable to nickel for electrode shields, especially in the presence of oxygen above the melt surface. Magnesia has been suggested on the basis of its successful use by others in the literature, but no direct experience has been acquired in this program.

The choice of an anode material is especially difficult and appears to restrict the choice of melt composition. All of the metals mentioned suffer dissolution when used as anodes in an electrolyte containing a high mole fraction of chloride (95-99%), but the problem is significantly ameliorated in the vicinity of the eutectic mixture of Li_2CO_3 and LiCl (70% mole fraction of LiCl). Nickel has been satisfactorily used as an anode in a mixture based upon the eutectic but with LiOH added to reach equilibrium with water vapor at moderate dew points. Under these circumstances, a protective oxide coating of reasonable stability appears to form on the anode. It is expected that a combination of chemical preconditioning and the use of an optimum anode current density can be devised to achieve a passivated oxide coating, but no firm conclusions can yet be drawn.

The cathode material is more specifically a design and development problem, since the electrode surface becomes carbon shortly after electrolysis is started. Most favorable adherence is obtained on iron, stainless steel, nickel, and cobalt, but the choice of substrate for an oxygen reclamation system will undoubtedly depend more

4.10 (Continued)

upon cathode configuration, carbon removal technique, etc.

4.11 Composition of Electrolyte

The basic process concept introduced in Section 4.1, whereby lithium is electrolytically reduced to provide an oxidizable reactant for the decomposition of carbon dioxide, would superficially appear to be applicable to other alkali metal carbonates. Calculations of equilibrium compositions of a number of alternatively conceivable systems on the basis of the thermodynamic properties of their reactants and products, with the restriction that such systems must be physically possible, in accordance with the Gibbs Phase Rule, indicate that the alternatives are severely limited. A detailed discussion of the calculations is presented in Section 4.12.

Experimental attempts to deposit carbon at the cathode in melts based upon sodium and potassium carbonates, both separately and in combination, as well as in combination with lithium carbonate, have met with varying degrees of success. Calculations of thermodynamic equilibrium in closed systems with arbitrarily fixed quantities of carbon, oxygen, and alkali metal atoms have provided a tentative framework for the evaluation of these experiments, and the general result has been to indicate that the presence of lithium ions at significant concentration appears to be essential to a successful process of the type under consideration.

According to the results of the calculations, there are only two product combinations in which solid carbon can exist, M_2O-C-M_2CO_3 and M-C-M_2CO_3, representing condensed phases in the melt, with M as the alkali metal. The former combination is possible with lithium or sodium as the alkali metal, and the sodium system is restricted to temperatures below 900°K. The latter combination is possible only with sodium or potassium. Co-existence of carbon and an alkali metal in appreciable concentration at the cathode is undesirable for two reasons: first, a significantly higher potential is required for cell operation when the alkali metal is present in finite quantity at the cathode, and second, sodium and potassium metals tend to form interstitial compounds with carbon which are physically unstable, resulting, for the case of potassium, in relatively violent disintegration of the deposit. However, although the dissolution of the cathodic deposit has been observed experimentally in electrolytes where sodium and potassium compounds were predominant, an apparently stable deposit has been achieved in a lithium-potassium melt. Calculations have not been made for a two-metal system, but we infer that, since the lithium system is based upon electrolytic reduction of lithium at a lower potential than would be required for potassium, no appreciable amount of

4.11 (Continued)

potassium will be reduced in the two-metal system, and only the Li_2O-C-Li_2CO_3 relationship will be pertinent.

On the other hand, although the same type of reasoning would indicate that a sodium-potassium system, operated in a suitable temperature range, should be acceptable, experimental results appear to indicate carbon deposits of unsatisfactory quality. Similarly, a three-metal system, specifically, the ternary eutectic mixture of lithium, sodium, and potassium carbonates, despite its favorable melting point (390°C), has shown inferior performance. At the present state of knowledge, therefore, it appears that lithium salts are essential, potassium salts may be tolerable as additives, but that the inclusion of sodium salts is of questionable value and possibly detrimental.

Although lithium carbonate, lithium oxide, and lithium hydroxide are the only essential ingredients of the electrolyte insofar as requirements for chemical process and gaseous equilibrium are concerned, the relatively high melting point of lithium carbonate (726°C) makes it necessary to include suitable additives or a solvent so as to permit operation at the lower temperatures indicated by the necessity for inhibiting gaseous outputs at the cathode. As previously mentioned, the use of lithium chloride as a solvent is a conservative possibility, since the eutectic mixture melts at 509°C. A ternary mixture of lithium carbonate, chloride, and fluoride is also suitable, and potassium chloride or fluoride may be incorporated without deleterious effects. From an engineering point of view, it would be desirable to operate the cell at as low a temperature as possible. No limiting low temperature has yet been deduced on the basis of the chemical or electrochemical requirements of the system, so that the problem of reducing the temperature is primarily one of discovering a combination of the eligible ingredients which will achieve a low melting point, have acceptable conductivity and viscosity, and provide adequate solubility for the increased oxide concentration developed at the cathode during steady-state non-equilibrium operation.

4.12 Thermodynamic Equilibria in the Melt

4.12.1 Summary

The chemical constituents of melts considered for the electrolytic decomposition of carbon dioxide were determined theoretically as the melts underwent physical and chemical change while subjected to temperatures ranging from 500° to 1000°K. Various fixed ratios of the atomic constituents, carbon, oxygen, and one of the three alkali metals (Li, Na, or K), were chosen, corresponding to

4.12.1 (Continued)

variations from a pure alkali carbonate composition. This work was initiated as the result of experimental observations which indicated differences in quality and quantity of carbon deposited at the cathode, according to the initial composition of the electrolyte, particularly with variations in the choice of alkali metal. It was postulated that the difference might be due to the different thermodynamic properties of the several conceivable molecular species which might exist in the melt at various operating temperature levels. In order to evaluate this possibility, it was undertaken to determine the equilibrium compositions of pertinent chemical systems.

Since the possible constituents of the melts comprise several different condensed phases, the determination of the concentration of each individual component becomes very complex. It was found that the available machine computation procedures for calculating chemical equilibria of chemical systems containing condensed phases could not be utilized because of convergence difficulties encountered with the iterative routines. As a result, it was necessary to employ a series of hand calculations from which a qualitative determination of the individual chemical species was possible.

This work is not truly representative of the conditions existing in a fused salt electrolyte, since no account was taken of the ionic dissociation of the various molecular species. Nevertheless, the results are viewed as a meaningful first approximation to the problem, especially as some degree of correlation with experimental observations is indicated.

One significant result of the calculations is that for the entire temperature range considered the only carbon-depositing process for lithium carbonate involves equilibrium among lithium oxide, carbon, lithium carbonate, CO, and CO_2. For systems comprising sodium or potassium carbonate, carbon may be produced in equilibrium with the free alkali metal and the carbonate. For temperatures below 900°K, carbon may exist in equilibrium with sodium oxide, sodium carbonate, Na, and Na_2.

4.12.2 System Equilibrium Relations

The possible chemical species which may be present in the carbonate melts include condensed alkali metal, M, condensed carbon, condensed M_2CO_3, condensed M_2C_2, M_2O, M_2O_2, and MO_2 and the gases M, M_2, O_2, O, C, CO, CO_2, MO, and M_2O. Therefore, this reacting system could contain eight different reacting phases (seven condensed and one gaseous phase). The gaseous phases of M_2C_2,

4.12.2 (Continued)

M_2O_2 and MO_2 were not included since it is presumed that they decompose upon vaporization. Although all the chemical species above are theoretically possible, their simultaneous existence is physically impossible, as can be demonstrated by utilizing the Gibbs Phase Rule. The phase rule may be written

$$f = c - p + 2$$

where f = number of degrees of freedom for the reacting system, p = number of different phases, and c = number of components, i.e., the minimum number of products of reaction whose composition is required in order to determine the composition of all other products of reaction. The number of components for the alkali metal-carbonate system is three and, therefore, if all the possible phases were considered at one time, the number of degrees of freedom would be f = 3 - 8 + 2 = -3, a physically impossible situation. Further consideration indicates that the maximum number of phases which may exist simultaneously is five, resulting in a reacting system having no degrees of freedom; i.e., the five phases may exist only at one unique temperature and pressure. Since compositions for the reactions involved in this study are desired as a function of temperature, a reacting system having at least one degree of freedom is necessary, and therefore the maximum number of phases which can be considered is four; one gas phase and three condensed phases. The total number of combinations of reaction products which contain four or fewer phases is 64: 35 four-phase combinations, 21 three-phase combinations, seven two-phase combinations, and one one-phase combination.

Since detailed calculations of the composition of each of these possible combinations would require considerable expenditure of machine time and machine input setup time, efforts were made to reduce the total number of combinations of potential reaction products by examining the properties of the individual products and their role in the proposed reacting system. Many of the possible product combinations do not include the alkali carbonate and, since experimental results had indicated that appreciable quantities of carbonate are present, only those combinations containing carbonate as one of the condensed phases were considered in the calculations. With the restriction that carbonate be included as a reaction product, the total number of possible combinations is reduced to 23: 15 four-phase combinations, six three-phase combinations, one two-phase combination, and one single-phase combination. These combinations are shown in Figure 4-9. A brief search of the literature indicated that thermodynamic data for LiO_2, Na_2C_2, and K_2C_2 was virtually nonexistent and that LiO_2 was probably unstable in the temperature

4.12.2 (Continued)

range under consideration and that Na_2C_2 and K_2C_2 would be easily oxidized to the carbonate in the presence of oxygen. Gaseous Na_2O and K_2O are also presumed to be unstable; they were therefore not included in any product combination examined.

With the four-phase systems, manipulation of the system of equations which describe the chemical equilibrium (i.e., the expressions for equilibrium constants) gives a set of equations for the partial pressures of each gas phase constituent as a function of equilibrium constants only. Therefore, specification of temperature of the reacting system fixes the concentration of the gaseous constituents and the total pressure of the reacting system.

Evaluation of the expressions for the partial pressure of the gaseous constituents for each four-phase combination is a simple but extremely tedious hand calculation. A brief IBM program was therefore written to evaluate the expressions and this program was used to determine the partial pressures for the various four-phase combinations for a temperature range between 500 and 1000°K. The partial pressures of Li, Na, K, C, and Li_2O were compared with the vapor pressures for these compounds at these temperatures to determine if any of these compounds should be condensed. The partial pressures for only these species were examined because the other species would either decompose upon vaporization or would not condense in the temperature range under consideration because of their high vapor pressures. If any one of the compounds considered should be condensed in a product combination which does not contain its condensed phase, then there is a possibility that the particular product combination should contain four condensed phases. However, this possibility has previously been eliminated because it represents a system having no degrees of freedom. Results of this first phase of calculations indicated that the following combinations containing four phases may exist.

Systems containing Li, Na, and K

$M_2O - M_2O_2 - M_2O_3$

Systems containing Li, and Na only

$M_2O - C - M_2CO_3$

Systems containing Na and K only

$M - C - M_2CO_3$
$MO_2 - M - M_2CO_3$

4.12.2 (Continued)

$M_2O - M - M_2CO_3$
$M_2O_2 - M - M_2CO_3$
$M_2O - MO_2 - M_2CO_3$
$M_2O_2 - MO_2 - M_2CO_3$

The system containing $Na_2O - C - Na_2CO_3$ is possible only at temperatures below 900°K. The possibility of the existence of the above combinations is based only on the fact that calculations of the partial pressures of the gas phase species indicate that no other species would condense. Other factors such as the total pressures obtained and the atom ratios required to give a particular combination also affect the choice of reaction mechanism for the particular process under consideration.

The total pressure of each reaction system is completely specified for each temperature because each four-phase system has only one degree of freedom. Since the composition of all the gaseous products of reaction is completely determined for each temperature, the composition of each condensed phase and the atom concentration of carbon, metal, and oxygen required to give a particular reacting combination may be determined from a simultaneous solution of the three atom-balance relationships. The gas phase composition fixes the minimum atom concentration, and any excess of atoms would be distributed among the three condensed phases. Calculations were performed for each possible combination, and the permissible atom ratios for each combination are shown in Figure 4-10. It appears from the figure that a particular set of atom ratios could result in two or more different four-phase combinations. It should be noted, though, that each system results in a different total pressure, and therefore no two combinations could exist simultaneously. The total pressure for each permissible system is shown in Figure 4-11.

When a three-phase combination is considered (two condensed phases - one gas phase), examination of the phase rule indicates that one more degree of freedom is possible, and therefore specification of the temperature no longer fixes the total pressure of the system and the determination of the partial pressures of the gaseous species by hand calculation becomes impractical. The atom ratios for which each three-phase combination is permissible may be calculated from the atom balance relationships without actually knowing the gas phase concentrations, since the concentration of the gaseous species specifies the minimum concentration of each atom. These atom ratios for each three-phase combination are shown below.

4.12.2 (Continued)

Three-Phase System	C/M Atom Ratio	O/M Atom Ratio
$M_2O - M_2CO_3$	> 0.5	> 0.5 but < 1.5
$M_2O_2 - M_2CO_3$	< 0.5	> 1.0 but < 1.5
$MO_2 - M_2CO_3$	< 0.5	> 1.5 but < 2.0
$M - M_2CO_3$	< 0.5	> 0 but < 1.5
$C - M_2CO_3$	> 0.5	$= 1.5$

The results of calculations shown in Figure 4-9 and Figure 4-11 present a qualitative means for predicting the constituents present in carbonate melts. It can be seen that there are only two product combinations which involve the deposition of solid carbon; namely, M_2O-C-M_2CO_3 and M-C-M_2CO_3. The latter combination is possible only with sodium and potassium as the alkali metal, while the former combination is possible with lithium and sodium as the alkali metals. Since each system was assumed to have one degree of freedom, the pressures shown in Figure 4-11 are thermodynamically the only ones possible. Therefore, it appears that of the four combinations containing carbon, the combination Li_2O-C-Li_2CO_3 would produce pressures near atmospheric in the temperature range of interest.

If an inert gas such as argon were added to the gas mixture above the carbonate melts, then the systems under consideration would have two degrees of freedom and pressure could be controlled. The results of the calculations which were used in Figure 4-9 would still be valid since the inert gas would not chemically react with the other constituents, but would be used only to obtain a desired pressure. However, since pressure is now a variable, it would appear from Figure 4-9 that more than one product combination is possible for a particular set of atom ratios. From thermodynamic considerations, the co-existence of the different product combinations is not possible since chemical equilibrium would occur only for that system whose free energy was a minimum. Therefore, the chemical reaction involving the formation of the product combination which would give the most negative free energy change would be the one most likely to occur.

Examination of Figure 4-9 indicates that there is no possibility of the existence of two different product combinations containing lithium. However, there is the possibility that Na_2O-C-Na_2CO_3 and Na-C-Na_2CO_3 may exist together. The free energy changes for these two product combinations were calculated for various atom ratios. These calculations indicated that the system Na_2O-C-Na_2CO_3 would likely be present. It should be noted, though, that the gas phase is predominantly CO and CO_2 if Li is the alkali metal for the M_2O-

4.12.2 (Continued)

C-M_2CO_3 system, while Na and Na_2 are predominant when Na is the alkali metal.

4.13 Summation

The correlation and interpretation of experimental evidence obtained during this research program has necessitated not only the application of existing chemical theory but also the extension of available knowledge by means of hypothesis and speculation. Because of the emphasis on earliest possible accomplishment of the ultimate engineering objective, to enable the construction of a practical system for oxygen reclamation in space vehicles, it has appeared necessary to forego indicated opportunities for extended research which might lead to more rigorous establishment of theories and principles. Instead, the philosophy has been to make use of the hypothesis which would best fit experimental observations in the simplest manner, taking advantage of such means for planning and interpreting continued experimentation, but being always ready to criticize, modify, or reject such a hypothesis if contrary evidence were found.

Accordingly, the basic concept of electrochemical reduction of lithium, followed by chemical reaction of lithium with CO_2 to yield carbon and oxide ions, must be regarded as a strongly supported hypothesis rather than an established theory. Alternatives can be devised, but they are repugnant on the basis of undue complexity or the necessity for making broader assumptions in unexplored areas of the behavior of fused salts. The variation of carbon electrode potential with CO_2 concentration, as predicted from the Nernst equation for electrode potential, and the differences among sodium, lithium, and potassium, considered in terms of thermodynamic equilibrium of chemical systems, are so simply and conveniently compatible with the experimental results that our confidence in the basic hypothesis is strong.

The identification of ions in the melt is another area of speculation and hypothesis, resting partly on similar hypothesizing in the literature as well as on the desire for the simplest explanation of observations. We postulate the existence of carbonate, hydroxide, and oxide ions in their simplest form, setting aside the possibility that more complex associations may occur. For example, by analogy with the OH^- ion, it is possible that LiO^- may be more common than free $O^=$ ions. However, in the present state of knowledge, it is not possible to establish which is true, and it is not clear that it matters in terms of the engineering objective. In connection with studies of dissociation pressures of carbonate

4.13 (Continued)

in the presence of halides, it has been speculated that oxyhalous ionic associations may account, at least in part, for the variation in heat of dissociation between chloride and fluoride mixtures, but no sufficiently firm hypothesis has yet been established to justify representation of the electrolyte on this basis.

These cautionary comments are made, not to indicate weakness of hypotheses, but rather to emphasize that the strength of the working hypotheses lies in their adaptability to circumstances of increasing availability of experimental evidence. When an irreconcilable contradiction is discovered, a valid experiment must be accepted and the contrary hypothesis abandoned, however, our most basic hypotheses are considered relatively strong in the sense that they have endured through a period of rapidly accumulating experimental evidence which has strengthened them through evolutionary modification.

In the preceding sections a number of constraints have been described for the basic process concept of carbon dioxide decomposition by chemical reaction with an electrochemically reduced alkali metal. The fundamental process is deceptively simple; it will take place as described and satisfy the functional requirements for engineering application only if adequate control is exercised over the internal and external environmental factors which determine the course of the reactions required. In summary, the following conditions must be imposed:

> Carbonate-oxide-hydroxide concentration balance in the electrolyte must establish suitable CO_2 and H_2O concentrations such that CO_2 is absorbed at low partial pressure and H_2O is not.
>
> Electrolyte composition must permit an operating temperature such that the total pressure of gases required for equilibrium at the cathode does not exceed ambient pressure.
>
> Contamination of the electrolyte by materials which may alter the electrochemical or chemical processes at the electrodes must be avoided.

Some further comment on the third condition is appropriate. Dissolution of the melt container, thermocouples, cathode shield, anode, or any other system elements in contact with the electrolyte can introduce foreign ions into the melt which may be reduced and

4.13 (Continued)

contribute outputs at the cathode and/or at the anode if their redox potentials are lower than the normal operating potentials. Iron, and cobalt are prime offenders in this regard, resulting in significant contamination of the carbon deposit at trace contamination levels and in virtual exclusion of the carbon-forming process at higher levels. This also results in a loss in capacity for absorbing CO_2, since the oxide ions formed in the cathode process are required to maintain the ability to absorb.

The general quality of the cathodic carbon deposit is discussed in detail in Section 5.1. The objective of 100% purity and high density has been approached, but continuous accomplishment of this goal requires better control of the cathode environment and, probably, more detailed understanding of the cathode process than has yet been achieved. Nevertheless, the formation of a porous, cratered, fissured deposit showing evidence of gas evolution during deposition, commonly experienced in early experiments, is avoidable by compliance with the requirements here discussed for equilibrium of gases at the cathode. A relatively smooth-surfaced carbon deposit, without gas-containing voids, can be produced repeatedly.

However, there is a tendency for entrapment of electrolyte salts in the micro-structure of the carbon deposit, possibly because of the dendritic nature of the deposit formed, which tends to inhibit the diffusion of oxide ions away from the sites of cathodic reaction. The carbon purity thus is found to approach 100% in the initial layers but decreases due to occluded salts beyond the first several thousandths of an inch, so that the average composition in a deposit of several millimeters thickness may be significantly lower, the purity being a strong function of current density.

From an engineering point of view, less than 100% carbon in the deposit does not constitute an insurmountable problem, since the extraction of the deposit, particularly in zero gravity conditions, represents a demand for design ingenuity in any case. Since the occluded salts are soluble in the melt and presumed to be liquid in the deposit as formed, carbon removal by expressing salts through a filter and formation of a carbon cake appears to be a feasible process.

The need to devise a system configuration suitable for operation in zero gravity poses engineering design problems in a number of areas, since the electrolytic cell concept inherently involves interfaces between liquid and gaseous phases as well as between liquid and solid phases. It is evident that a rotating, axially symmetric cell could provide a centrifugal field as a substitute for gravity, but more elegant approaches are under study to avoid the

4.13 (Continued)

necessity for slip rings, rotating seals, and structural compromises. Possibilities in the use of surface tension, vortex flow, porous matrices, and other principles for liquid stabilization or containment in zero gravity, however, are beyond the scope of the research study presented here but are discussed in Part II of this report.

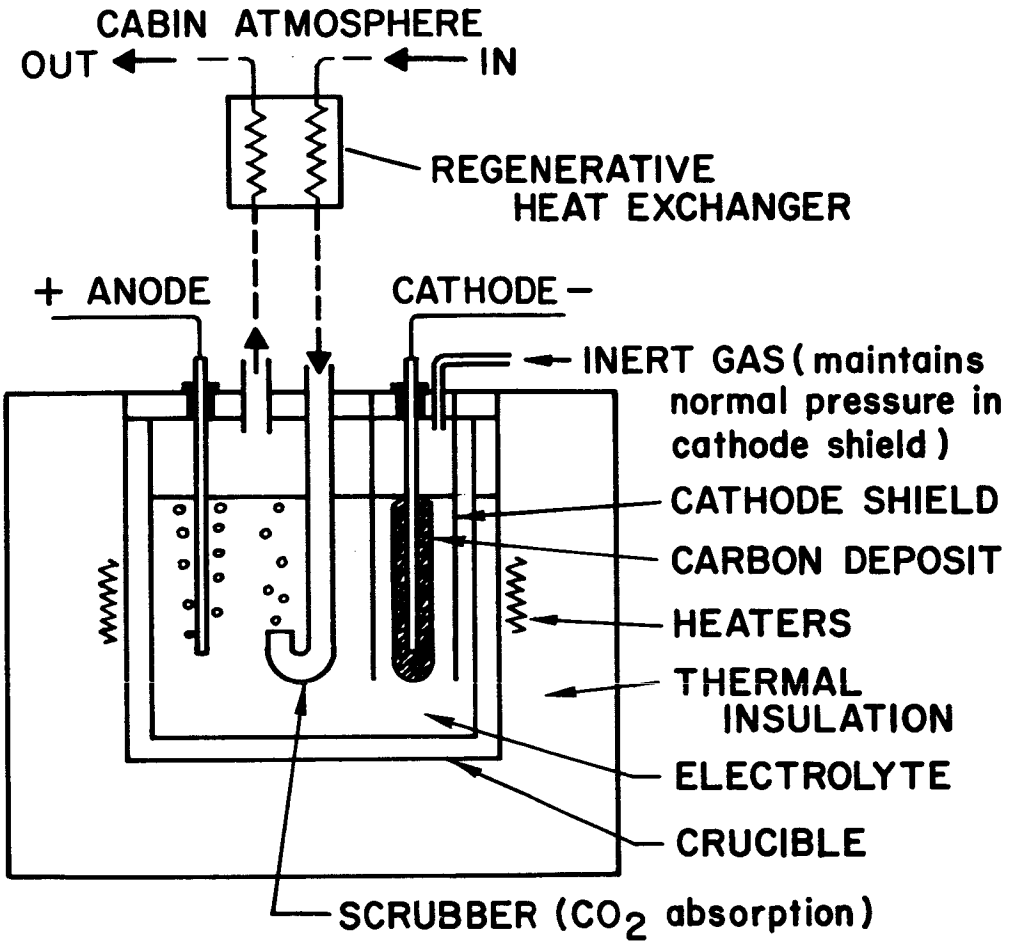

FIGURE 4-1 SCHEMATIC DIAGRAM CO_2 ELECTROLYTIC CELL

1. Equilibrium Constants

Symbol	Reaction	Equation No.
K_o	$4\ Li + CO_2 \longrightarrow 4\ Li^+ + 2O^= + C$	4-2
K_1	$CO_2 + O^= \rightleftharpoons CO_3^=$	4-14
K_2	$H_2O + O^= \rightleftharpoons 2\ OH^-$	4-21
K_3	$C + CO_2 \rightleftharpoons 2\ CO$	4-20
K_4	$C + 2\ H_2O \rightleftharpoons 2\ H_2 + CO_2$	4-34
K_5	$C + 2\ H_2 \rightleftharpoons CH_4$	4-35
K_6	$B_2O_3 + O^= \rightleftharpoons 2\ BO_2^-$	4-29

2. Gas Partial Pressures

Symbol	Gas
p	Carbon Dioxide
v	Water Vapor
c	Carbon Monoxide
h	Hydrogen
m	Methane

FIGURE 4-2 SPECIAL SYMBOLS AND NOMENCLATURE

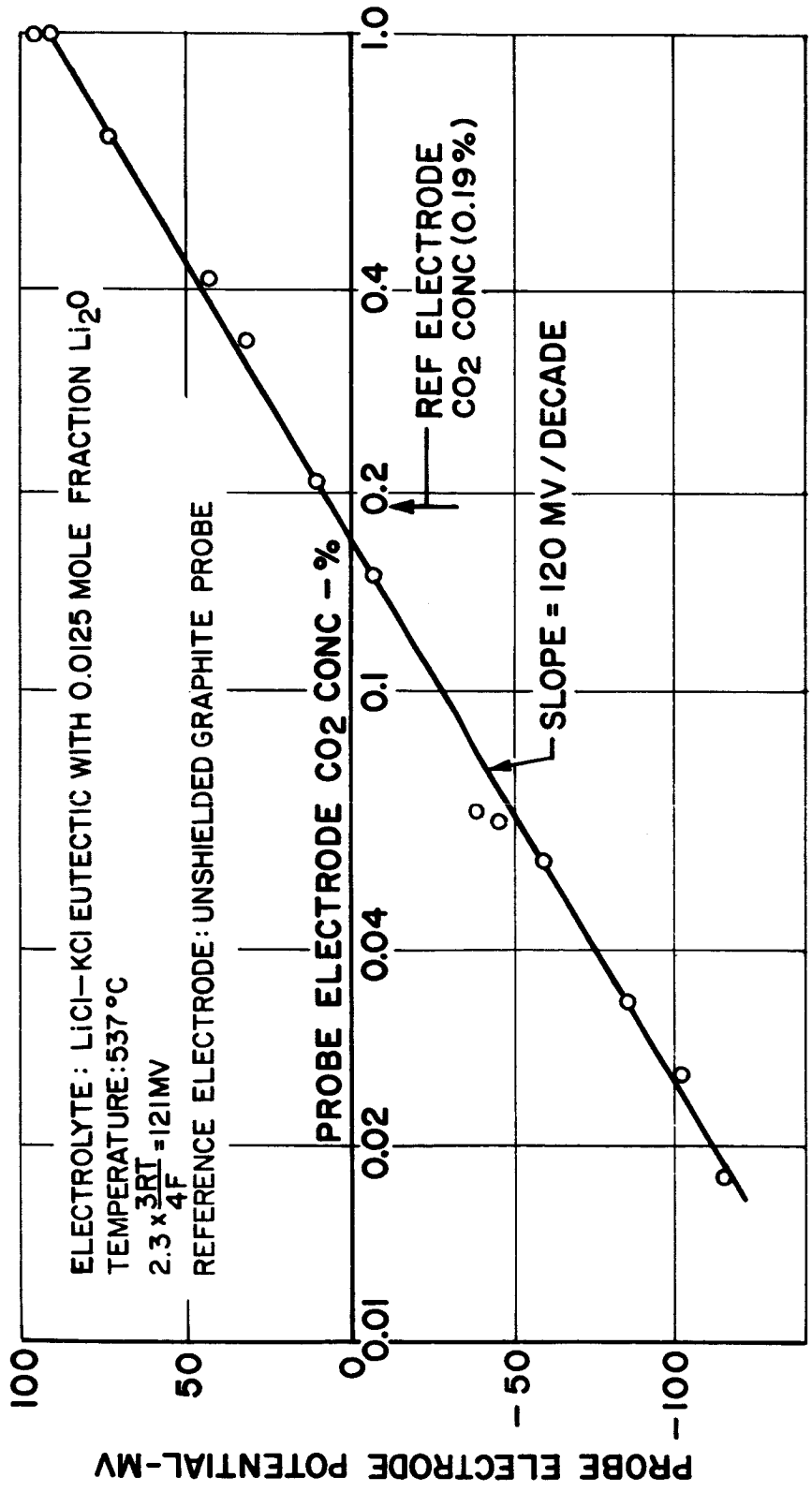

FIGURE 4-3 CARBON ELECTRODE POTENTIAL DIFFERENCE

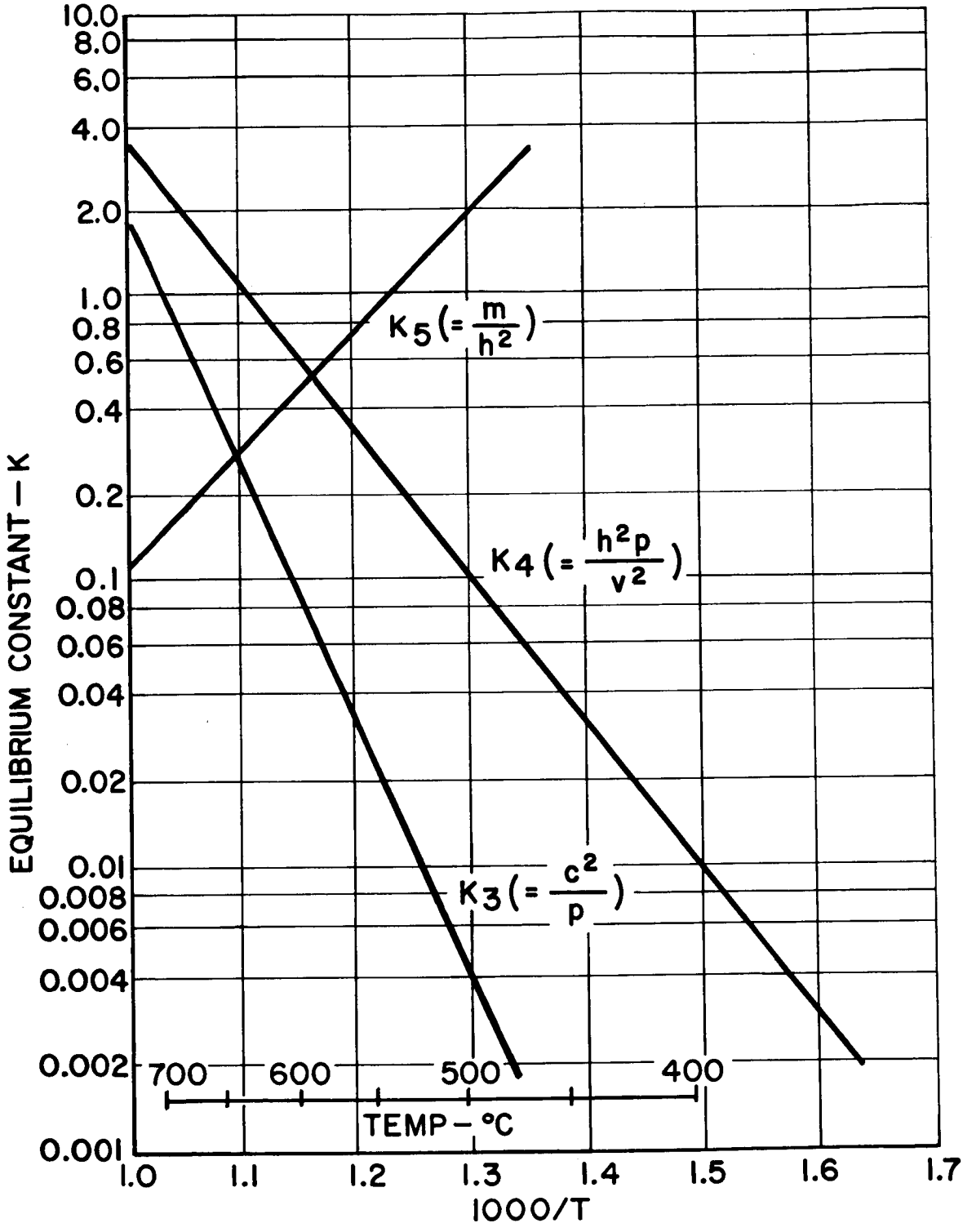

FIGURE 4-4 EQUILIBRIUM CONSTANTS

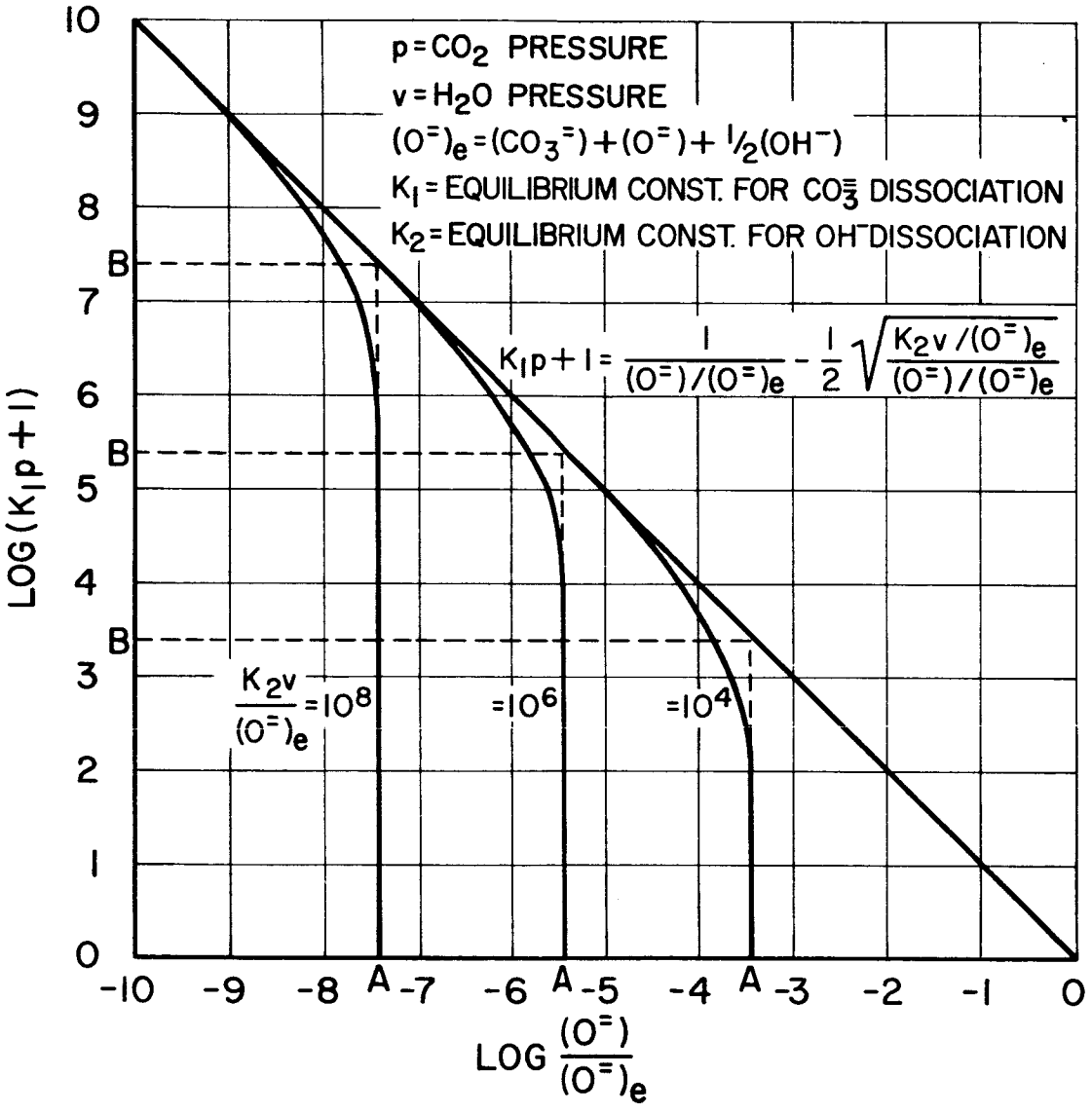

FIGURE 4-5 PARTIAL PRESSURES OF CO_2 AND H_2O IN A SOLUTION OF Li_2CO_3 AND LiOH IN LiCl

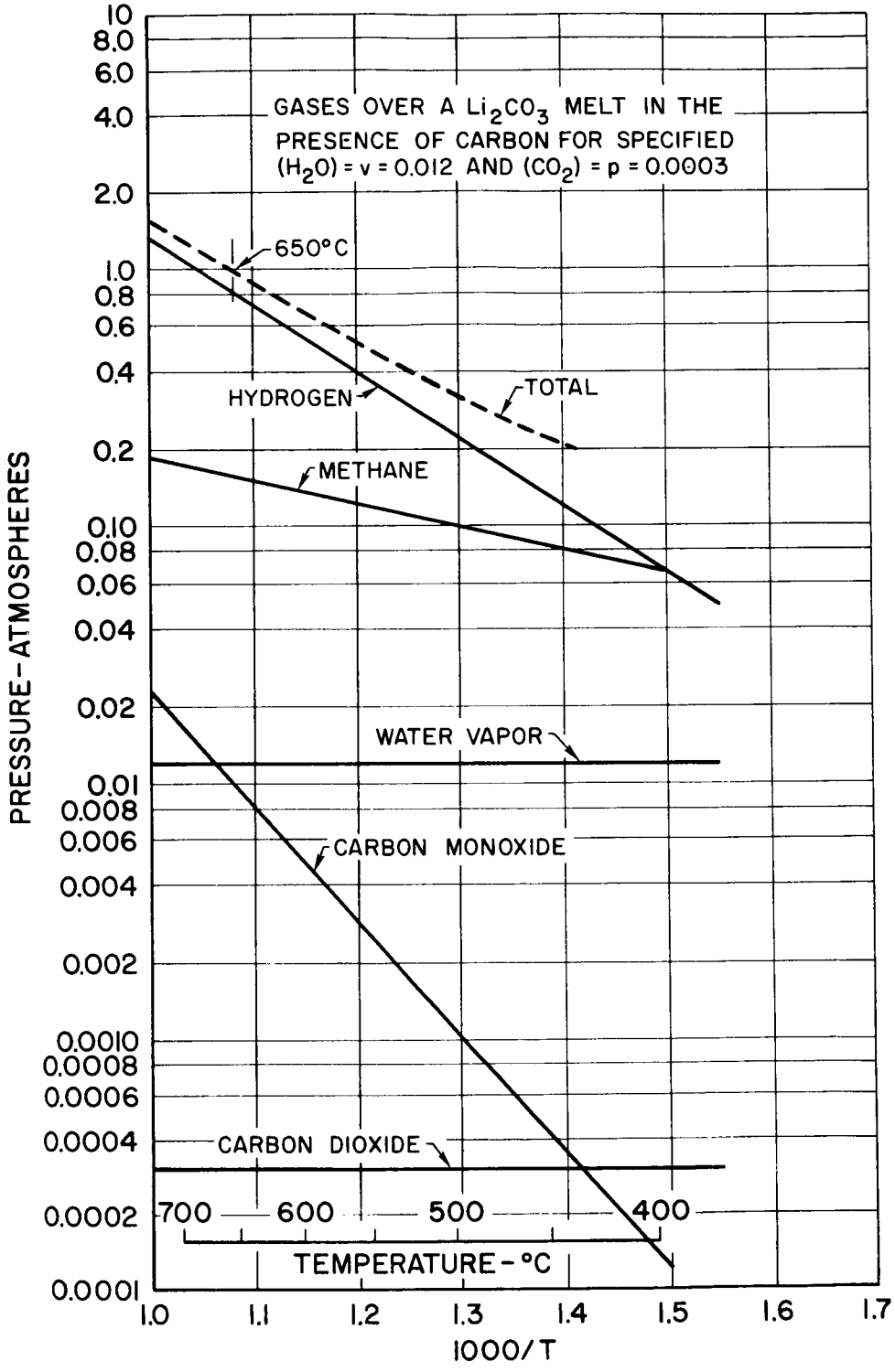

FIGURE 4-6 CALCULATED EQUILIBRIUM PRESSURES

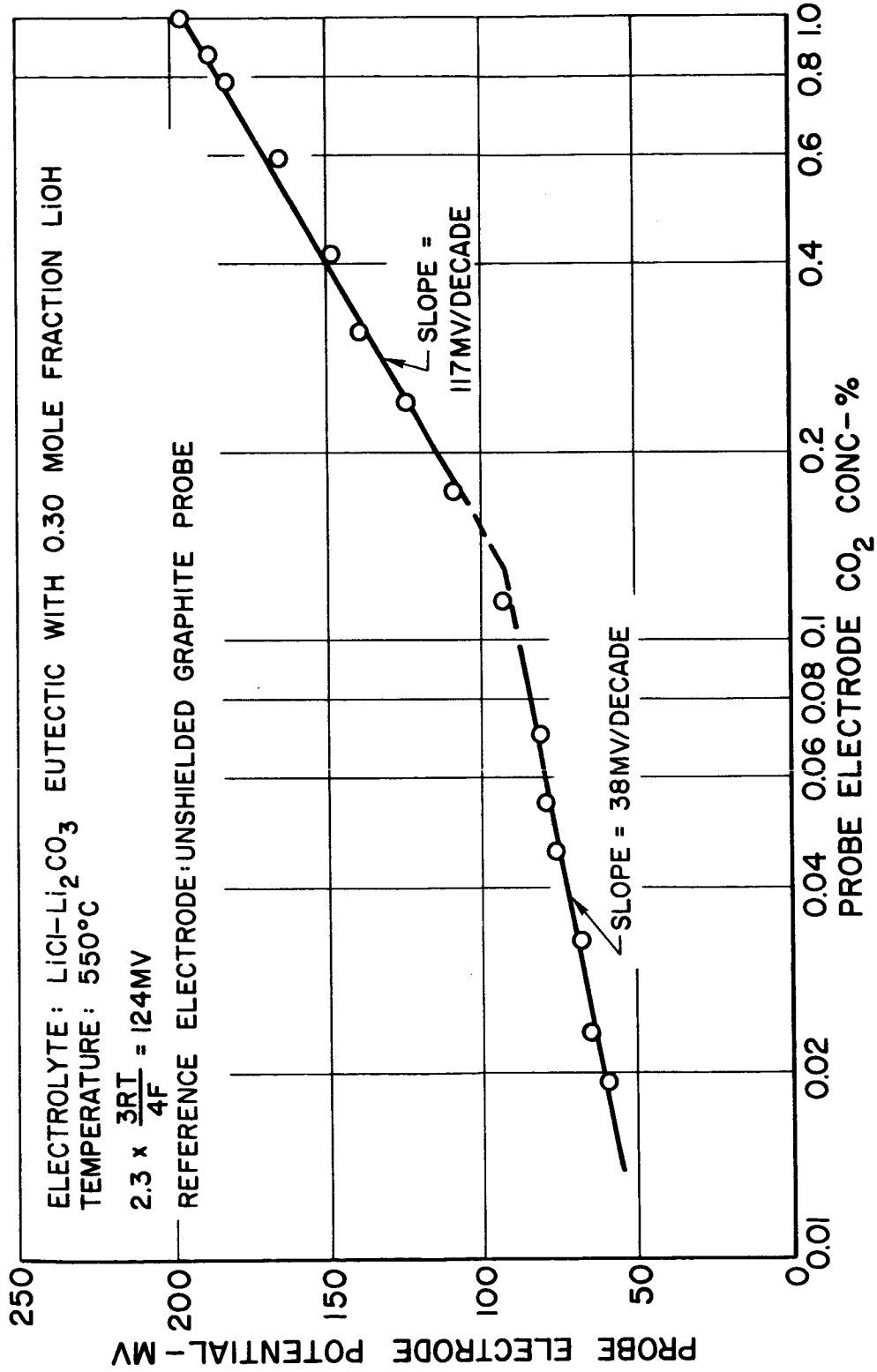

FIGURE 4-7 CARBON ELECTRODE POTENTIAL DIFFERENCE

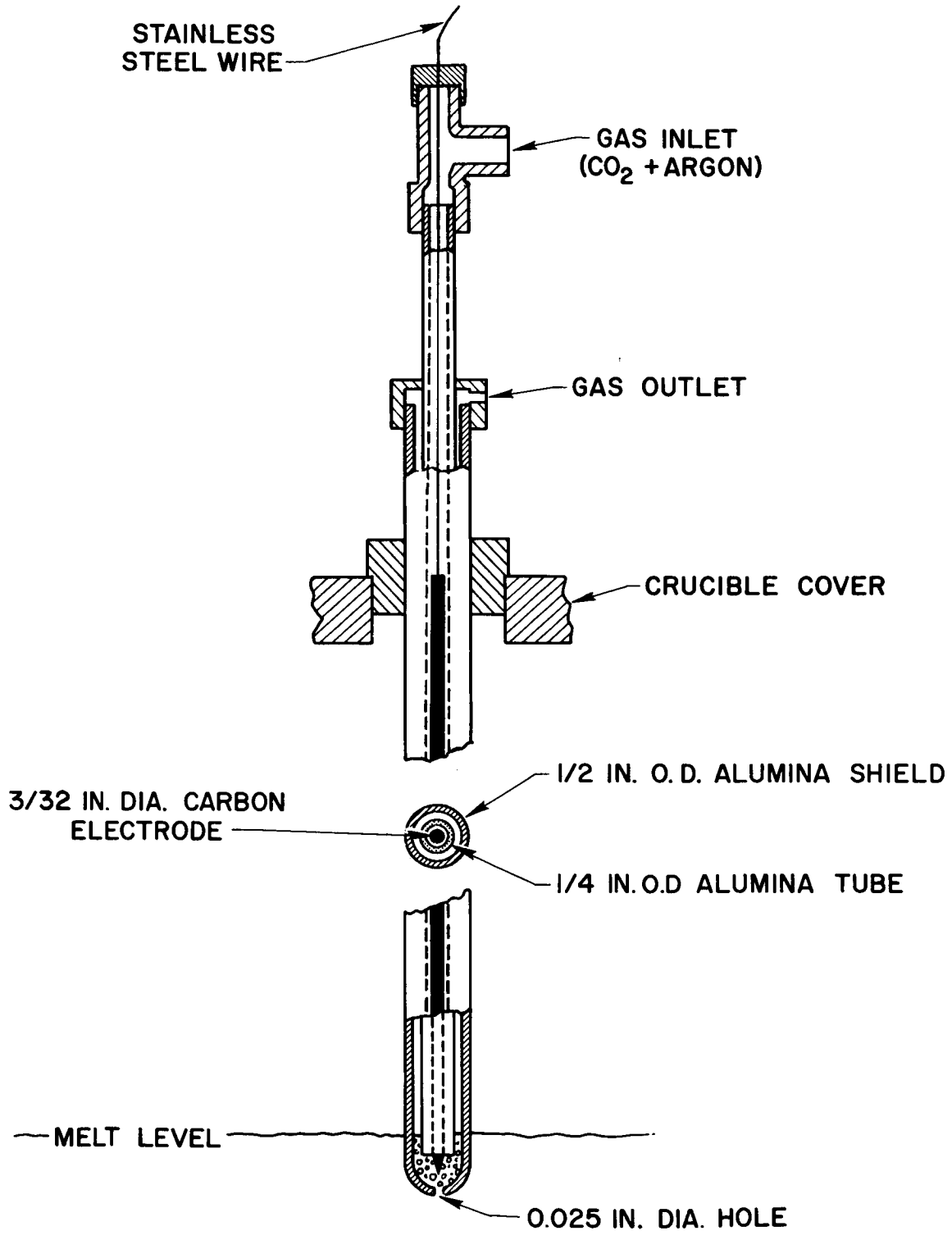

FIGURE 4-8 CARBON REFERENCE ELECTRODE

M indicates alkali metal

Four-Phase Combinations (three condensed - one gas*)

M_2C_2-M_2O-M_2CO_3
M_2C_2-M_2O_2-M_2CO_3
M_2C_2-MO_2-M_2CO_3
M_2C_2-M-M_2CO_3
M_2C_2-C-M_2CO_3
M_2O-M_2O_2-M_2CO_3
M_2O-MO_2-M_2CO_3
M_2O-M-M_2CO_3
M_2O-C-M_2CO_3
M_2O_2-MO_2-M_2CO_3
M_2O_2-M-M_2CO_3
M_2O_2-C-M_2CO_3
MO_2-M-M_2CO_3
MO_2-C-M_2CO_3
M-C-M_2CO_3

Three-Phase Combinations (two condensed - one gas*)

M_2C_2-M_2CO_3
M_2O-M_2CO_3
M_2O_2-M_2CO_3
MO_2-M_2CO_3
M-M_2CO_3
C-M_2CO_3

Two-Phase Combinations (M_2CO_3 - gas*)

One-Phase Combination (gas*)

*Gas phase consists of gaseous M, M_2, M_2O, MO, C, CO, CO_2, O, and O_2

FIGURE 4-9 POSSIBLE COMBINATIONS OF REACTION PRODUCTS CONTAINING ALKALI METAL CARBONATES

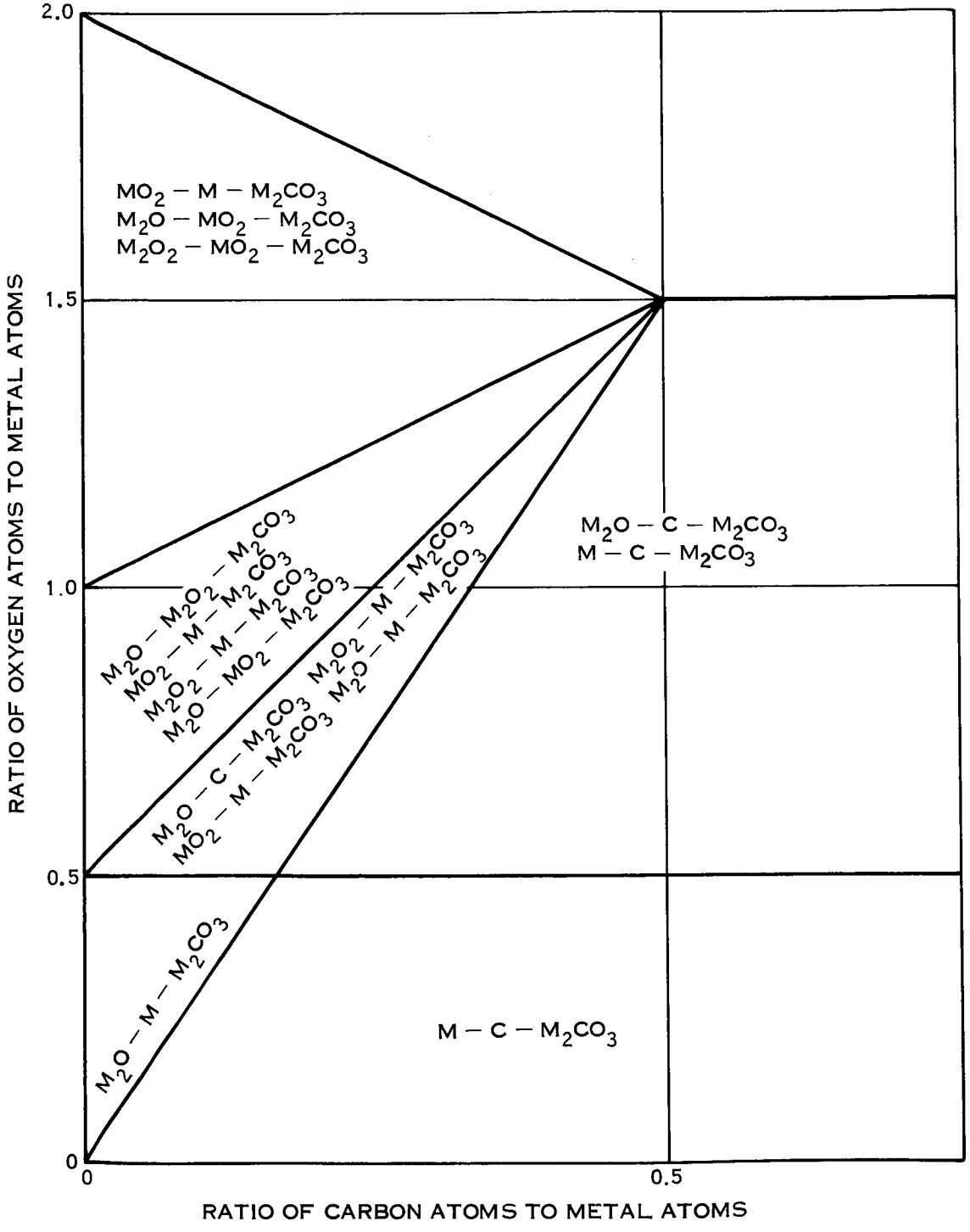

FIGURE 4-10 CATHODIC TRACES IN Na_2CO_3-NaCl

Temperature (°K)	500	600	700	800	900	1000
			Pressure in Atmospheres			
			System M_2O-M_2O_2-M_2CO_2			
M						
Li	44.833	624.7	3907	14852	40318	86796
Na	7.441×10^{-12}	1.342×10^{-8}	2.715×10^{-6}	1.355×10^{-4}	2.342×10^{-3}	2.200×10^{-2}
K	9.030×10^{-16}	2.801×10^{-12}	8.393×10^{-10}	5.955×10^{-8}	1.662×10^{-6}	2.486×10^{-5}
			System M_2O-M-M_2CO_3			
Li	*	*	*	*	*	*
Na	*	*	*	*	5.012×10^{-2}	1.950×10^{-1}
K	3.138×10^{-5}	9.207×10^{-4}	1.007×10^{-2}	5.979×10^{-2}	2.363×10^{-1}	1.0244
			System M_2O-C-M_2CO_3			
Li	2.379×10^{-11}	1.910×10^{-7}	1.014×10^{-4}	1.101×10^{-2}	4.411×10^{-1}	8.65
Na	2.657×10^{-8}	5.957×10^{-6}	2.828×10^{-4}	5.194×10^{-3}	*	*
K	*	*	*	*	*	*
			System M_2O_2-M-M_2CO_3			
Li	*	*	*	*	*	*
Na	8.582×10^{-7}	5.368×10^{-5}	1.014×10^{-3}	9.136×10^{-3}	5.012×10^{-2}	1.9505×10^{-1}
K	3.138×10^{-5}	9.207×10^{-4}	1.007×10^{-2}	5.979×10^{-2}	2.363×10^{-1}	1.0244

FIGURE 4-11 TOTAL PRESSURE FOR CARBONATE MELTS CONTAINING THREE CONDENSED PHASES

System M-C-M_2CO_3

Li	*	*	*	*	*	*
Na	8.582×10^{-7}	5.368×10^{-5}	1.014×10^{-3}	9.136×10^{-3}	5.012×10^{-2}	1.951×10^{-1}
K	3.138×10^{-5}	9.207×10^{-4}	1.007×10^{-2}	5.979×10^{-2}	2.363×10^{-1}	1.0244

System M_2O-MO_2-M_2CO_3

Li	*	*	*	*	*	*
Na	6.352×10^{-3}	8.677×10^{-2}	5.238×10^{-1}	1.911	4.991	*
K	4.399×10^{-9}	8.038×10^{-7}	3.113×10^{-5}	4.624×10^{-4}	3.651×10^{-3}	1.865×10^{-2}

System M_2O_2-MO_2-M_2CO_3

Li	*	*	*	*	*	*
Na	185.6	220.6	230.0	226.9	230.4	224.6
K	9.097×10^{-4}	1.137×10^{-2}	6.41×10^{-2}	2.242×10^{-1}	5.774×10^{-1}	1.2198

System MO_2-M-M_2CO_3

Li	*	*	*	*	*	*
Na	8.582×10^{-7}	5.368×10^{-5}	1.015×10^{-3}	9.144×10^{-3}	5.025×10^{-2}	1.963×10^{-1}
K	3.138×10^{-5}	9.207×10^{-4}	1.007×10^{-2}	5.98×10^{-2}	2.365×10^{-1}	7.072×10^{-1}

*Three-phase system does not exist at these temperatures

FIGURE 4-11 TOTAL PRESSURE FOR CARBONATE MELTS CONTAINING THREE CONDENSED PHASES (Continued)

5.0 PROCESS EXPERIMENTS

5.1 Cathode Processes

5.1.1 Cathode Deposit Morphology

Carbon deposits generally comprise one or a combination of several structures. The carbon obtained may (1) be graphitic and free of electrolyte, Figure 5-1a and b; or (2) consist of carbon with occluded salts, Figure 5-2; or (3) contain many gas pockets, Figure 5-3; or (4) be spalled off and freely circulating in the electrolyte. Cathode deposits may also at times contain heavy metal or alkali metal inclusions. Carburization of the cathode substrate metal is frequently observed.

5.1.1.1 Graphitic Carbon

With appropriate selection of electrolyte composition and electrolysis conditions, carbon deposits at the cathode in a highly oriented form which has a structure closely resembling graphite grown pyrolytically at 2100°C or higher when compared on the basis of x-ray diffraction analysis. Such analysis indicates strongly ordered crystallites with reference to the c-axis, while a- and b-axes are much less distinct. Spacing of atomic layers along the c-axis have been estimated at 3.37 Angstroms from this analysis which closely approaches that of the ideal, with 3.35 Angstroms spacing. An x-ray defraction pattern for electrodeposited graphite is reproduced in Figure 5-4 alongside similar patterns for graphite grown pyrolytically. Leaders denote lines specific to graphite.

5.1.1.2 Carbon with Occluded Salts

Under other electrolytic circumstances, particularly when deposits are obtained at high current densities, the carbon is deposited in the form of long filaments. Electron microscope examination shows that these filaments are approximately 1000 Angstroms in diameter and more than 25 times that in length. They are remarkably uniform in diameter, as is evident in Figure 5-5. They are structurally almost identical to carbon deposits described by numerous workers who have studied gas phase carbon deposition on nickel, iron, and cobalt metal substrates, Reference 4. Growth of the dendritic carbon from specific crystal faces of metal nuclei, as shown in vapor phase deposition studies, has not been ascertained in the electrolytically grown deposits, although these deposits typically show magnetic properties when ferromagnetic materials are used for cathodes. These magnetic properties are retained after acid leaching. Owing to the filamental structure, carbon of this morphology invariably retains substantial amounts of electrolyte. Thoroughly black, uniform looking deposits of this carbon structure

5.1.1.2 (Continued)

have been obtained in thicknesses dependent only on deposition time; even though carbon content may be well below 10 weight percent, cooled blocks of this material typically show electrical conductivity from one face to another. As the deposit is growing it appears "mushy" when poked, but it also gives the appearance of having a very fragile filamental carbon superstructure.

5.1.1.3 Gas Pocked Deposits

Under certain melt conditions, as anticipated from theory, gases are evolved from the cathode during the carbon electrodeposition process. These gases have been experimentally identified as comprising carbon monoxide, hydrogen, and methane. The amounts of these gases relative to each other and to the carbon varies with such factors as humidity in equilibrium with the melt and operating temperature, as will be discussed in detail in the following sections. The result of gas evolution is the production of carbon-walled bubbles, volcanic looking craters, and long hollow carbon tubes. These structures are shown in Figures 5-6a and b. The remarkable uniformity of the hollow tube structure and its silvery brilliance precipitated a brief investigation to determine whether an organized growth pattern could be inferred and whether a specific crystalline habit was associated with the carbon. X-ray diffraction analysis proved the carbon to be amorphous, and at this writing it is presumed that the structures are an artifact of gas outflow channels. Figure 5-7 shows the evolution of gas bubbles at the cathode during electrolysis under conditions which favor such.

5.1.1.4 Spalled-Off Carbon

Carbon which has spalled off the cathode is most often found floating at the surface of the electrolyte. It normally has the appearance of a frothy black foam. It is commonly associated with cathodic gas evolution - the bubble of gas rupturing as it breaks the surface of the electrolyte, leaving a film of carbon behind. Under other circumstances however, particularly in the presence of alkali cations other than lithium, carbon has been found widely dispersed in the melt and it is believed that this results not from gas formation but rather from (1) too slow a reaction of deposited alkali metal with carbon dioxide or carbonate to produce carbon, so that this reaction is only completed at a distance from the electrode, or (2) intercalation of deposited carbon with alkali metal and subsequent carbon delamination. A further characterization of this carbon has not been made.

5.1.1.5 Deposits with Heavy Metal Inclusions

Electrolysis of electrolytes with certain compositions has produced alternately metallic cobalt, iron, gold, or lead at the cathode. These metals may be co-plated with carbon; for example, co-deposited cobalt and carbon have been observed, as well as heavy stoichiometric coatings of iron carbide, Fe_3C, Figure 5-8. Nickel is not generally plated out although this has been encountered with certain melt compositions. When the metal is a small fraction of the total cathode deposit, it is commonly associated with a sooty appearing carbon layer external to any graphitic carbon layer. In cases where carbon is barely present in the cathode deposit, the metal typically has the appearance of feathers, needles, and spikes, Figure 5-9.

Accumulation of boron, silicon, and aluminum at the cathode have been noted at times, when these elements were present in certain electrolytes, but as a salt, presumably the oxide, rather than the reduced metal. Crystals, Figure 5-10, of compositions as yet not precisely defined have been obtained in these circumstances.

5.1.1.6 Alkali Metal Deposition

When electrolytes which are extremely low in carbonate content are electrolyzed at high current densities it has been possible to obtain metallic lithium (this was the only alkali cation present) and a fraction of what is believed to be lithium carbide. Hydrogen and acetylene are released as gas bubbles when this deposit is submerged in water. Potassium metal is much more readily obtained owing to its slower reactivity with the electrolyte and has been evident a number of times. The deposition of potassium on carbon cathodes results in severe delamination and disintegration of the carbon. Metallic sodium has been likewise observed.

5.1.1.7 Carburization

When ferrous cathodes are employed, their surfaces are rapidly carburized to substantial depths. This is illustrated in Figure 5-11 which also shows some observed hardness distributions. Only minor penetration of nickel by carbon has been observed. Extensive carbide formation in manganese has been indicated.

5.1.2 Cathode Process Variables

As is evident from the previous discussions of theory pertaining to the cathodic processes, and from description and comments of cathode deposit structures, there are a number of recognized process variables which require control to permit the deposition of dense carbon at the cathode. The theoretical implications of each of these variables have already been presented; such theory

5.1.2 (Continued)

will be amplified where appropriate in the following detailed description of that portion of the experimental program devoted to cathodic process investigation. The following list summarizes these variables.

Recognized Cathode Process Variables

- Electrolyte Cationic Species
- Hydroxide/Carbonate/Oxide Ion Concentrations (P_{CO_2}, P_{H_2O})
- Oxide Ion Buffers
- Diluent Anionic Species
- Dissolved Metal Ions
- Current Density
- Temperature
- Cathode Substrate Material
- Cathode Shielding
- Catholyte Agitation
- Applied Current Patterns (Time Variable)

5.1.2.1 Electrolyte Cationic Species

In the early experimental work, the importance of the presence of a predominant quantity of lithium cations in the melt for the deposition of adherent carbon at the cathode was noted. Some success was also achieved with barium salts in producing adherent deposits, but there was a notable lack of success using sodium and potassium as predominant cations. When the latter ions predominated either no carbon was obtained at the cathode, or the carbon was patchy, or dispersed in the electrolyte. In a few instances it was possible to obtain thin graphtic films in completely sodium or potassium systems when a small portion of boron oxide had been added to the electrolyte. Some of these early experiments are summarized in Figure 5-12. In the light of current understanding, when such data are reviewed, it seems evident that other variables unrecognized at the time were not being adequately controlled or widely enough varied to allow a definitive answer to the question

5.1.2.1 (Continued)

of whether some range of satisfactory process conditions might be determined for all of the cationic species studied. Recently repeated electrolysis of the potassium chloride-carbonate eutectic and the sodium chloride-carbonate eutectic, with more careful control of those variables, however, continues to reaffirm practical differences from lithium systems. Again here, neither melt yielded any visible carbon deposits. Carbon rods used as cathodes were eroded in both these melts; the carbon rod was completely destroyed in the potassium system.

All of the above observations are consistent with theory based upon thermodynamic studies, Section 4.12, which predicts that with sodium or potassium systems, the alkali metal rather than its oxide as in the case of lithium, will be in equilibrium with carbon, so that the carbon structure will probably be undermined by intercalation with alkali metal. Polarographic data indeed show substantially higher cathodic deposition potentials for sodium and potassium melts, which would be characteristic of the existence of appreciable amounts of free metal. A thermodynamic consideration of barium systems has not been carried out as of this writing.

When lithium predominates, even in the presence of the other alkali metals, its high reactivity with carbonate apparently allows it to be plated out at lower potentials (concentration polarization) than the others. Very little experimental work has been done with the lithium and sodium mixture; however, extensive work has been done with the lithium-potassium system which has shown that at sufficiently high lithium concentrations, system performance is in accord with all-lithium cation systems in the presence of chloride diluent. In fluoride diluent systems, however, even in the presence of substantial lithium, potassium metal shows a high tendency to plate out. Sodium metal shows greater tendency to plate out from an equimolar mixture of sodium, potassium, and lithium carbonates.

5.1.2.2 Hydroxide/Carbonate/Oxide Ion Concentrations (P_{CO_2}, P_{H_2O})

The immediate interdependence of carbonate, hydroxide, and oxide ion concentrations makes their simultaneous consideration almost mandatory. At all times the electrolyte is seeking to achieve an equilibrium ratio among these three ions in accord with the partial pressures of carbon dioxide and water vapor to which it is exposed. At the cathode, oxide ions are generated continually during electrolysis so that the catholyte tends generally to be richer in oxide than the bulk of the melt. The kinetics of the catholyte achieving near equilibrium with the bulk melt depends on the diffusion rates of carbon dioxide and water into the region and the oxide diffusion rate away from the cathode.

5.1.2.2 (Continued)

Theory predicts that the ratio of carbonate to hydroxide ions at the cathode (Section 4.6) determines whether carbon deposition is favored, or whether gas evolution or other interfering process prevails. Theory further predicts (Section 4.8) that the ratios of carbonate and hydroxide ions to oxide ions in the catholyte, as these reflect absolute partial pressures of carbon dioxide and moisture, determine whether cathodic gas pressures will be sufficiently high to generate bubbles. Accordingly, the great bulk of experimentation has involved the manipulation of the ratio of these anions, development of experimental techniques for doing so, and the construction of suitable measuring devices.

Before describing experiments where these factors are dealt with, it is appropriate to consider one further aspect of catholyte composition affecting concentration limits of these anions. That is, should oxide concentration become too high, or carbonate, hydroxide, or any other melt constituent accumulate or be deleted from the catholyte, partial crystallization may occur since the electrolyte systems of interest are based heavily on eutectic compositions in order to permit low operating temperature.

Cathodic gas evolution is highly visible, so that the effect of increasing catholyte oxide ion concentration (decreasing partial pressures of carbon dioxide and water) on bubble formation can be readily observed. It has been shown that the evolution of cathodic gases can be quickly halted by small additions of lithium oxide solid to the system. Also, it has been shown in many experiments that gas evolution at the cathode can be stopped by an appropriate increase in cathodic current density. In the latter case, if excess oxide accumulates at the cathode, the current density may be lowered once more without gas evolution until accumulated oxide ion is completely spent, at which time bubbling commences once again.

By using as a reference electrode a carbon rod over which a constant, low partial pressure of carbon dioxide is bubbled, it is possible by measuring potential difference from this reference to a simple carbon rod dipped into the electrolyte, to deduce the effective oxide ion content of the electrolyte. This has been treated in theory, Section 4.9 , and is treated in experimental detail in Section 6.3 . In this manner it has been possible by simple voltage readings to monitor oxide ion concentration changes as a result of carbon dioxide or moisture exposure to the system, also to re-establish substantially the same effective oxide ion concentrations when desired upon subsequent additions of solid oxide or electrolyzing to produce oxide.

5.1.2.2 (Continued)

Having chosen different oxide levels for experiment in the manner just described, differences in the cathode deposit were commonly ascertained by noting effects on cell current-voltage relationships, appearance and fraction of carbon in deposit, and open circuit potential difference between the cathode deposit and a spectroscopic carbon rod immersed in the melt. Composition differences between the cathode deposit and pure carbon are readily apparent in this last test. The rate of voltage decay to a steady state value after breaking the electrolytic circuit also gives insight into the nature of the catholyte concentration gradients. In illustration, voltage decay as a function of cathode current density (oxide accumulation along with carbon) is shown in Figure 5-13. Visual observations of cathode deposits were sometimes deceiving in that all deposits look black, and deposits of the same nominal size may have a wide range of occluded salts. When the cathode plus the deposit was removed from the cell upon completion of a given run, it was transferred to a dry atmosphere glove box and weighed. The salt was then leached from the deposit with a 1:1 HCl solution. The use of an acid leach also removed metallic impurities which might co-deposit with the carbon. In most cases a deposit containing a high percent carbon would adhere to the electrode during the leaching process whereas a low percent carbon deposit would usually break apart when treated with acid. In all cases the carbon that flakes off was filtered, washed, dried, and weighed. This weight was then added to the carbon deposit still remaining on the cathode. In cases where the metal content of the deposit was of interest a small portion of the deposit was removed for spectrographic analysis and the remainder was used for the percent carbon determinations.

By varying catholyte oxide content by the two means described above it has proved possible to readily shift from conditions of no visible carbon and all gas obtained at the cathode to high carbon, with gas pockets, Figure 5-14.

Although it was relatively easy to control oxide ion concentration at the cathode, it proved much more difficult to regulate carbonate to hydroxide ratio with any degree of certainty. First, although we can charge an electrolyte with a given ratio of carbonate to hydroxide and can ascertain this ratio to a reasonable degree by observing off-gas partial pressures of carbon dioxide and water, it is not possible to directly or even indirectly measure that ratio at the cathode. Attempts to regulate catholyte oxide by current density and at the same time to control carbonate to hydroxide ratio by impressing appropriate partial pressures of carbon dioxide and moisture on the system have been only partially successful. Effect of constant water and varied carbon dioxide partial pressure on observed open circuit potential between the cathode deposit and a carbon rod and on the rate of voltage decay are illustrated in

5.1.2.2 (Continued)

Figure 5-15. The effects are small; as would be anticipated, deposits from each run looked alike. There is some evidence that a small amount of water or hydroxide is desirable. Results of a series of runs where water vapor pressure above the electrolyte was varied are summarized in Figure 5-16. In Run 23-3 a smooth adherent deposit was obtained with quality equal to or better than that obtained in similar runs in a dry atmosphere. Since the humidifed blanket gas was passed over the melt for less than one hour prior to electrolysis in this case, it would appear that only a small amount of water could be absorbed by the melt, and suggests the possibility that in small amounts water was beneficial.

In those runs where exposure to higher humidity was longer, the deposits contained relatively low percentages of carbon and were rough and cratered in appearance. Once these cratered deposits were formed it was only necessary to partially dry out the melt by passing the blanket gas through magnesium perchlorate in order to reverse the effect. In general, high carbon dioxide partial pressure and low water pressure were required to produce beneficial effects - neither of which is attractive in the ultimate process.

An alternate approach has been to select an electrolyte composition that initially combined the appropriate ratios of carbonate, hydroxide, oxide, moisture, and carbon dioxide that theory predicted, and log pressure-voltage relationships (Section 4.6) indicated as satisfactory for carbon deposition, and then try to maintain these conditions in the catholyte during electrolysis. Experiments quickly showed that such equilibria could not be sustained in the catholyte. In systems where an equilibrium with a low water partial pressure was selected, oxide began to accumulate at the cathode at current densities lower than 10 ma/cm^2. In systems in equilibrium with high water partial pressure, cathodic gas evolution was observed, even at high current densities. Thus, it appears that in a carbonate-halide system of high hydroxide content without other additives, oxide recombination with water is so favored as to interfere with the carbon deposition process. In low hydroxide systems, oxide recombination with carbon dioxide is too slow to prevent the accumulation of excess oxide with the carbon. It has therefore been the approach of most recent experimentation to reduce moisture partial pressure and to provide electrolyte buffers that will maintain a suitable oxide ion concentration in the catholyte while fixing the excess oxide in the form of soluble compounds-phosphates, borates, etc., capable of subsequent displacement by fresh carbon dioxide. Laboratory investigation of oxide buffers and fluxes is described in the next section.

In the preceding discussion of test results, the terminology "carbon

5.1.2.2 (Continued)

dioxide diffusion rates" and "moisture diffusion rates" has been intentionally avoided. The problem appears to be one of oxide availability and not one strictly of gas diffusion rates through the bulk electrolyte. The distinction becomes important when one considers extremely rapid carbon dioxide absorption rates in the bulk melt, Section 5.3.1, and the observed prompt availability of the cathodic oxide when the electrical circuit is broken, Figure 5-17. The problem may be one of gas diffusion rate through the cathode "double layer" but should be considered as distinct from diffusion rate through the bulk electrolyte.

Reducing electrolyte carbonate concentration from 40 weight percent to as low as 0.1 weight percent does not affect the percent carbon obtained under identical electrolysis conditions, as shown below.

Effect of Electrolyte Composition

Number	Dry Atmosphere	Melt	Percent C
22-7	Ar-CO_2(380 mm)	LiCl-40 wt % Li_2CO_3	22
24-1	Ar-CO_2(380 mm)	LiCl-10 wt % Li_2CO_3	21
27-3	Ar-CO_2(380 mm)	LiCl-0.1 wt % Li_2CO_3	22

Conditions: Temperature - 600°-700°C
Current Density - 100 ma/cm^2
Cathode - Carbon
Time - 2 hours

In the latter case the electrolysis was carried out using reagent grade LiCl with a partial atmosphere of CO_2. The 0.1 weight percent is estimated on the basis of the possible hydrolysis of the melt to form hydroxide, and the subsequent reaction of the hydroxide with CO_2 to form carbonate.

5.1.2.3 Oxide Ion Buffers

Boron oxide, aluminum oxide, silicon dioxide and lithium phosphate have been added to electrolytes in separate experiments in an attempt to buffer catholyte oxide ion to a specific range. As would be anticipated the additions of boron oxide, aluminum oxide, and silicon dioxide result in the evolution of an appropriate quantity of carbon dioxide from the carbonate of the electrolyte. Addition of the boron oxide as lithium metaborate, again as would be expected,

5.1.2.3 (Continued)

does not result in any carbon dioxide displacement. An initial capacity for added boron oxide to combine with available oxide ions is immediately apparent. The effect is readily seen in Figure 5-18, which shows open circuit cathode voltage decay rate after addition of the borate. However, continued testing shows the capacity for oxide ion to be finite in that the effect wears off. In other words, the borate anion is formed but the process is not sufficiently reversible in subsequent exposure even to high carbon dioxide pressure so as to free up the boron oxide once more for oxide ion scavenging. The same is true of aluminum oxide and silicon dioxide; buffering does not occur in a satisfactory concentration range. In addition the borates, aluminates, and silicates formed are of high melting points and appear to have low solubility in electrolytes studied, as evidenced by the frequent accumulation of these materials at the cathode.

The case is somewhat different with phosphate. A lithium carbonate-hydroxide-chloride electrolyte was used as a base melt for the phosphate addition. Such a base melt before phosphate addition exhibits an appreciable affinity for water. Addition of lithium orthophosphate resulted in the evolution of an extremely large volume of water, many times that which could have come directly from the additive or have entered during the addition process. Subsequent experiments showed the electrolyte to have lost most of its capacity for water. Yet, when the system was electrolyzed it was found possible to scrub out moisture, presumably by combination with the oxide ions being formed. It therefore seemed that water was being retained in the initial electrolyte in two forms - as hydroxide and as "dissolved" water. Capacity for the latter appeared destroyed by the presence of the phosphate. The melt now exhibited a carbon dioxide partial pressure of about .04 percent and a water vapor pressure represented by a dew point of $+10^{o}$F. Under these conditions only cathodic gases were evolved (no carbon) during electrolysis at both low and high current densities. Addition of a small amount of solid lithium oxide enabled carbon deposition but only at higher current densities (100 milliamps per square centimeter). Open circuit voltage readings suggested no appreciable oxide buildup under these conditions. It would appear that sufficient oxide solubility had been achieved so that higher current densities were required to adequately decrease catholyte P_{CO_2} and P_{H_2O} so as to inhibit gas formation.

5.1.2.4 Diluent Anionic Species

Experimental study has been made of chloride and fluoride diluent anions chiefly, with some brief looks at bromide and nitrate anions. Initially, it was believed that these diluents could be considered

5.1.2.4 (Continued)

substantially "inert," serving only as non-participating solvents for the primary electrolytic species, and allowing the process to be carried out at lower temperatures. It appears now that all of these diluents have substantial effects on the cathodic process. Specific effects have not yet been completely resolved although three effects appear prominent. They are:

- Carbonate decomposition pressures appear to be markedly altered by the anionic diluent species
- Chloride systems generally retain appreciable amounts of water proportional to vapor pressure and generally produce more gas pocked deposits than fluoride systems
- Metal oxide solubilities greatly differ; aluminum oxide, for instance, is more soluble in fluoride systems than in chlorides and appears to enter into cathodic processes

5.1.2.4.1 Carbonate Decomposition Pressures

Lithium carbonate decomposition pressure is found to be altered in the presence of lithium chloride or lithium fluoride as evidenced by changes in slope of an Arrhenius plot of reciprocal temperature against carbon dioxide partial pressure. This effect is described in experimental detail in Section 8.2 . Resultant differences in electrolyte P_{CO_2}, P_{H_2O}, and in carbonate, hydroxide, and oxide ion ratios accordingly affect the deposition process.

5.1.2.4.2 System Moisture Retention

Electrolysis at relatively high current densities, 300-500 milliamps per square centimeter, has commonly produced carbon deposits which were cratered and contained gas pockets in chloride systems, and smooth carbon deposits with high oxide content in fluoride systems. This has generally been attributed to the hygroscopic nature of the chloride systems. For example, in our attempts to establish the displacement of water by carbon dioxide on a mol/mol basis from a lithium chloride, lithium carbonate, lithium hydroxide electrolyte, only 25 percent of the expected water could be accounted for. However, when an auxiliary flow of dry argon was passed over the electrolyte so as to maintain outlet water vapor pressure at the inlet level, it was possible to obtain a reasonable moisture balance. This appeared to confirm speculation that solubility of water as water molecules in the melt was appreciable and proportional to vapor pressure changes, and accounted for the inability to obtain a balance during the previous experiments.

5.1.2.4.2 (Continued)

Water retention by molten lithium chloride melts is reported by Burkhard and Corbett (Reference 5), and by Laitinen (Reference 6), but absolute amounts fall short of those being observed here. It must be concluded that the co-presence of the hydroxide and/or carbonate with the chloride results in a higher moisture capacity. Some moisture is found to be expelled when this electrolyte freezes. The behavior of fluoride electrolytes has as yet not been adequately characterized in these same respects.

5.1.2.4.3 Metal Oxide Solubility

Oxide solubilities in molten fluorides are well known. For example, cryolite, comprising a mixture of fluorides in which aluminum oxide is dissolved, is the electrolyte from which aluminum is won by electrodeposition. Similarly we have noted, in working with lithium fluoride-carbonate eutectics, the solubility of aluminum and silicon oxides. Such solubility has not been noted in other halide systems. An increase in oxide ion concentration in the fluoride system appears to retard the solution of the metal oxide.

In attempting to explain differences caused by various diluent anions, it has been useful at times to reflect on the dipolar properties of melt diluents. For example, the lithium fluoride bond has a distribution of ionic and covalent fractions so as to favor the formation of dipoles in the same sense that water forms dipoles. From this viewpoint it is readily appreciated how diluent ligands might surround an anion such as carbonate and alter its reactivity. In one test series barium fluoride was added to a lithium fluoride system in an attempt to disrupt the probability of high density packing by the speculated lithium fluoride ligands. An immediate change in electrolytic cell current-voltage relationship was observed, and carbon was deposited under identical electrolysis conditions where cathode gases were being evolved until the addition.

A second viewpoint wherein the relative affinity of various diluent anions for cationic electrolyte species on the basis of volume density of ionic charge is compared with that of carbonate, hydroxide, and oxide, has also proved interesting. On this basis, a tabulation of some of the molecular and ionic entities in the electrolyte can be arranged in order of tendency for dissociation. Lithium chloride would dissociate more readily than lithium oxide, which, in turn, is more readily dissociated than lithium fluoride. Accordingly, lithium fluoride should be a more satisfactory diluent than lithium chloride, since it would favor the dissociation of lithium oxide and thereby enhance the diffusion of excess oxide away from the cathode. It may be that the observed change in dissociation pressures of carbonate also may be related to relative ease of dissociation of

5.1.2.4.3 (Continued)

the diluent alkali halides.

Dilution with nitrate anions has been studied only so far as to demonstrate that less than five mol percent carbonate in lithium nitrate permitted the deposition of carbon below 500°C without the evolution of detectable nitrogen oxides. At higher temperatures, nitrogen dioxide was observed. Bromide diluted systems vaporized profusely and were passed over for that reason.

5.1.2.5 Dissolved Metal Ions

Results of studies where low concentrations of iron and nickel were electrolytically introduced into an equimolar lithium carbonate-chloride melt and the nature of cathodic deposits observed are summarized in Figure 5-19, listing test results from a series of 10 runs. In four of these runs (287, 290, 291-2, 294-5) there was no carbon buildup on the spectroscopic carbon cathode, but rather iron was deposited. In the remaining six runs some carbon was deposited on the spectroscopic carbon. Of these latter runs, only in Run 288 was a trace of iron found in the deposit, but this was accompanied by a much higher nickel content; iron was not found in any of these remaining cases where carbon was obtained. When spectroscopic carbon was coupled with nickel and the pair used as a single cathode, with iron present in the melt (Runs 291-2, 294-5), the nickel became coated with carbon as did the area of the carbon rod immediately adjacent to the point of contact between the two materials; the remainder of the carbon became coated with iron, Figure 5-20. Appearances suggested also that when the nickel became coated with carbon, it, too, like the carbon rod, became susceptible to iron deposition, resulting in an iron fringe to the carbon deposit. A further visual illustration of co-deposited metal effects is presented in Figure 5-21 where high nickel - higher carbon, and high iron - lower carbon are again coincident. From these test runs a beneficial effect of nickel to carbon deposition may be inferred, and an interfering effect by iron. Most uniform looking carbon deposits showed neither iron nor nickel by wet chemical analysis, although spectrographic analysis commonly showed small fractions. Experiments with cobalt metal ions added as cobalt chloride to an electrolyte base of higher halide and boron oxide content LiCl, Li_2CO_3, B_2O_3 (3, 1, 0.125 mole ratio) showed that when a cobalt anode was used, cobalt metal plated out on the cathode, but when a carbon anode was used in alternating runs, carbon was plated out. We might expect that the absence of a continuing supply of cobalt, if melt saturation was limited, would result in carbon deposition once the supply was exhausted. However, in the case of iron, iron deposition continues for extended periods after removal of the iron source. It may be that carbon and cobalt

5.1.2.5 (Continued)

deposition voltages are more similar and therefore, which material was deposited would be more sensitive to concentration changes over the range studied.

It may be generalized that certain melt compositions favor the deposition of metals, specifically, those which have a high ratio of halide to oxyanion. It has been found possible to halt the deposition of nickel and favor carbon deposition, for instance, by increasing the ratio of lithium carbonate to lithium chloride from 2 mol percent to 50 mol percent. High fluoride systems cause the solution of alumina and silica; higher fractions of aluminum and silicon are found in the cathode deposit under these circumstances.

It appears that metallic ions even in extremely low concentrations generally affect the carbon deposition process unfavorably. A measure of control over the concentration of such metal ions in the electrolyte is possible by judicious anode and cathode material selection, electrolyte composition control (oxyanion/halide ion ratio), and by electrolysis at anode passivating current densities, see Section 8.2 . Currently, particular efforts are made to restrict the use of ferrous materials in electrolytic cell construction since the presence of iron has always been associated with a lack of carbon deposit. It would seem that nickel interferes least and may actually offset the harmful effects of other metal ions such as iron; hence, nickel system components are allowed.

5.1.2.6 Current Density

Experimental data show a strong correlation between current density, referred to the cathode area, and the weight fraction of lithium oxide in the solid deposit at the cathode, as determined by chemical analysis after removal from the electrolytic cell. The relationship in an equimolar lithium carbonate-lithium fluoride electrolyte, for instance, appears to be a curve rising from zero lithium oxide at zero current density and asymptotically approaching a level of 65-70 percent as current density becomes infinite, Figure 5-22. Based upon considerations of equilibria, observed reaction products, and the predominance of electrolytic processes over processes of diffusion, a limiting level of 71.4 percent lithium oxide by weight has been deduced for that system.

Most successful carbon deposits to date have been at current densities between 10 and 30 milliamperes/square centimeter, although the addition of borate has enabled deposition of graphitic carbon for a limited period at 1 ampere/square centimeter. Most recently, the addition of phosphate has enabled carbon deposition

5.1.2.6 (Continued)

at 150 milliamperes/square centimeter for extended periods without significant oxide accumulation.

5.1.2.7 Temperature

Electrolytic deposition of carbon has been most frequently carried out between 500 and 700°C although deposits have been made at as low as 375°C and as high as 800°C. The usable temperature range appears to be bounded for practical purposes on the low end by catholyte freezing point and on the high end by carbon - gas (CO_2, CO, H_2O, H_2, CH_4, etc.) equilibria considerations. Some results of a study of temperature effects are summarized in Figure 5-23. The percent carbon in the deposits formed in the Li_2CO_3-LiF eutectic mixture and the LiCl-Li_2CO_3 eutectic mixture are considerably different at the same temperature. The melting points of the two mixtures are 610°C for the LiF-Li_2CO_3 eutectic and 510°C for the LiCl-Li_2CO_3 eutectic. Densest carbon seems to be related to the difference between the operating temperature and the melting point. If this is the case, it would appear that quasi-structural effects in the melt may be important, since it is known that molten salts have a high degree of order at temperatures considerably above their melting point (Reference 7). It is more likely however, that differences are better related to differing carbonate and hydroxide activities in the presence of fluoride or chloride.

5.1.2.8 Cathode Substrate Material

The nature of an electrode deposit often depends on the substrate. That is, a greater adherence may be achieved if the deposit forms a diffusion layer with the substrate, and a smoother deposit may be obtained if the substrate surface is conducive to the formation of many nucleating sites. If the first layer of deposit is laid down in an orderly manner, then the crystal growth should be regular for some finite thickness of deposit. The energy of nucleation must be less on the substrate surface than the nucleation energy on the surface of the deposit already formed in order to produce a regular deposit. If this is not the case carbon will deposit on a few nucleation sites on the surface and this will be followed by the deposition of carbon on deposited carbon (in this particular case) to form dendritic deposits. The net result is an open carbon structure which contains a large amount of salt.

Early experiments in lithium carbonate-fluoride systems showed that under similar electrolysis conditions, graphitic carbon coatings could be obtained on nickel, on AISI 304 stainless steel, on cast iron, on cobalt, and on manganese. Negative results were obtained in attempts to deposit on titanium, tungsten, copper, silver,

5.1.2.8 (Continued)

platinum, gold, and on pyrolytic graphite. Similarities in the crystal form of the carbides of each of the successful substrates, all of which were geometrically compatible with the graphite structure and involved low heats of formation (readily reversible reactions), suggested an associated catalytic behavior. Since that time, however, in repeat runs on tungsten and graphite substrates with greater control of electrolyte composition, P_{CO_2}, and P_{H_2O}, graphitic carbon has been obtained. It would appear that the original successful substrates more likely owed satisfactory performance to a capacity to buffer oxide, carbonate, and hydroxide ions in a proper relationship. However, as soon as these substrates became coated with carbon, such capacity was lost and interfering processes such as gas formation then prevailed, resulting in thin carbon coatings. In view of the above considerations spectroscopic carbon cathodes have been used almost exclusively in more recent experimentation to ensure that system aspects leading to sustained carbon deposition were being observed, although in a working system cathodes of nickel would be favored. Attempts to co-deposit a small fraction of "successful" substrate metal with carbon so as to sustain a suitable catholyte environment proved too difficult to accomplish, due to the opposing circumstances which tend to influence carbon versus metal deposition.

A comparison of nickel pretreatment procedures showed no major variation among acid etch only, an anodic alkali treatment followed by an acid etch, vapor blast, or a brief anodic etch period in the melt itself. All specimens showed graphite growth beginning at randomly spaced sites, the larger sites up to 1/4 inch apart, with a more black-appearing carbon deposit (dendritic looking) filling the area between sites and giving rise to a gross reticulated carbon pattern, Figure 5-24. This pattern was not affected significantly by current density. An increase in electrolyte temperature, however, produced a marked improvement in uniform initial graphite coverage. Deposits on both hard and soft nickel (electro-deposited in aqueous plating baths) whereby an altered surface nickel orientation was anticipated, displayed no noticeable change in the reticulated carbon coating pattern.

Metal-carbon couples as electrodes were briefly investigated to ascertain the current directions between the metal and carbon when the couple was made anodic or cathodic, and under different gaseous environments. It was contemplated that in this fashion we might gain insight into differences between nickel, iron, and gold, as a more inert material, each in the presence of carbon. Results in an equimolar lithium carbonate-chloride electrolyte are summarized in Figure 5-25. It will be noted that at zero cell current, carbon is anodic to both nickel and iron in the presence

5.1.2.8 (Continued)

of air. In an argon atmosphere the nickel becomes anodic to the carbon whereas the iron remains unchanged. Under both environments the gold remains anodic to the carbon. As cathodic current is increased in an air environment iron changes from a condition of carbon being anodic to it to one of it being anodic to carbon at a much lower current than that at which nickel changes in the same fashion. These slight differences allow speculation as to conditions under which carbon or the metal may more likely go into solution or be deposited out, and into possible buffering properties.

The following electromotive series was developed for a lithium carbonate-fluoride melt, no applied potential, in air.

External current direction ----------►

Au; Co; Ni; C; Ni; Cr; Fe; B; Mo; W

The dual position of the nickel with respect to the carbon reflects what has been termed a "flop-over." Initially, upon introduction of the nickel to the electrolyte it is in one location with respect to carbon; after several minutes the current shifts steadily from a condition of current from nickel to carbon to one of carbon to nickel.

5.1.2.9 Cathode Shielding

Initial experiments to determine cathode efficiency by comparing the weight of carbon collected at the cathode with that predicted by Faraday's law showed only about 25 percent efficiency when no effort was made to shield the cathode from the anodically produced oxygen. (A similar anode efficiency was indicated through measurement of cell off-gases.) It was also noted that efficiencies could be related to the degree of electrolyte agitation, more specifically to the speed of rotation of the cathode. In subsequent experiments, when a nickel shield (hollow tube with opening in bottom) was placed around the anode to shield the cathode deposit from anode gases, efficiencies approaching 100 percent were achieved. Such cathode efficiencies were obtained both at higher current densities, where dendritic carbon with entrained salts were obtained, and at lower current densities, where a substantial fraction of the cathode deposit was graphitic.

Since the carbon deposited at the cathode must seek an equilibrium with carbon dioxide, water, carbon monoxide, hydrogen, etc., it is advantageous also to maintain the cathode in as near a stagnant gaseous environment as possible so that none of the competing cathode processes - hydrogen, carbon monoxide formation, etc., are

5.1.2.9 (Continued)

favored by constant removal. In practice, however, it has been possible to sweep a low flow of inert gas (helium) over the cathode with no noticeable effect on carbon production efficiency. This is perhaps due to low diffusion rates of those gases from the cathode area. It is important to minimize the partial pressures of carbon dioxide and water, in addition to oxygen, in the gas phase above the cathode so as to minimize attack of the carbon depositing at the electrolyte interface. For, although gases such as carbon dioxide and water are immediately absorbed by the electrolyte and their partial pressures may be readily reduced below levels which may affect that portion of the carbon which is submerged, high concentrations at the interface cause severe carbon attrition. For example, when high humidity is maintained above a carbon cathode, the cathode is found to neck down and eventually drop off into the electrolyte.

Recently, it has been found possible to utilize the gaseous atmosphere above the cathode to control catholyte composition. This is accomplished by withdrawing the cathode in an oscillating fashion into the gaseous environment so as to permit the electrolyte as a thin film rapidly to achieve an equilibrium with the carefully controlled gas phase. By regulating the absolute pressures and relative ratios of carbon dioxide and water in the gas phase it has been possible to control the quality of the carbon deposit. Deposits grown in this manner are shown in Figure 5-26. It should be noted that the deposit grown on the portion of cathode always submerged shows the result of catholyte deviation from a preferred composition (gas pocked, 25 weight percent carbon); above the melt the carbon is much more smooth and dense (78 weight percent carbon). Upon appropriate change in gas phase composition, the porous deposit can be made to extend the full length of the cathode.

5.1.2.10 Catholyte Agitation

Several different cathode configurations which allow rotation and axial motion during electrolysis have been studied. Two of these are shown in Figure 5-27. In general, even with the disc type cathode shown, which was designed to allow examination of varying catholyte flow speeds across its radius, carbon coatings appeared quite uniform throughout. When the catholyte was at a temperature too close to its freezing point, however, swirl patterns could be observed in the cathode deposit. Open circuit cathode voltage decay rates were shown to be speeded up with electrolyte stirring, Figure 5-28. Some benefits attributable to agitation may be deduced from Figure 5-23, comparing Run 8-2 to Run 8-4 and perhaps Run 5-2 to Runs U-5-1 and U-5-2.

5.2.1 (Continued)

Major Anode Process Variables

- Hydroxide, Carbonate, Oxide Ion Concentrations (P_{CO_2}, P_{H_2O})
  a. Current Density
  b. Temperature
- Electrolyte Cationic Species
- Diluent Anionic Species
- Anode Substrate Material, Surface Coating
- Dissolved Metal Ions

5.2.2 Anode Process Variables

5.2.2.1 Hydroxide, Carbonate, Oxide Ion Concentrations (P_{CO_2}, P_{H_2O})

At any instant every given electrolyte has a characteristic partial pressure of carbon dioxide and water. Thus, it may be experimentally demonstrated that the electrolyte P_{CO_2} can be readily bracketed by passing into it an inert sweep gas of low CO_2 content and observing the higher CO_2 out, followed by passing in a sweep gas of high CO_2 and monitoring the low CO_2 out. The same can be done for moisture. Related to these gas partial pressures is a specific ratio of carbonate, hydroxide, and oxide ion concentrations. As we increase the oxide ion concentration, electrolyte P_{CO_2} and P_{H_2O} decrease.

Because anode off-gas must reflect the partial pressures of all other gases in the electrolyte as did our sweep gas above, it becomes evident that oxygen purity is set for the most part by the level of oxide ion concentration maintained in the electrolyte. As this concentration increases and P_{CO_2} and P_{H_2O} decrease, oxygen purity increases. Such oxide ion concentration is controlled by the rate of oxide availability from the cathode region and the rate of CO_2 feed. Absolute oxide ion concentrations for fixed P_{CO_2} and P_{H_2O} will vary with temperature, the nature of other electrolyte constituents and so on, as will be discussed in subsequent sections.

When the feed rate of carbon dioxide is balanced with the electrolysis rate according to Faraday's law, it is necessary that no oxide accumulate at the cathode (unavailable oxide) in order to

5.1.2.11 Applied Current Patterns (Time Variable)

In addition to evaluating deposits grown under constant current densities, evaluations have been made using interrupted current, constant voltage, and AC superimposed upon DC. It might be presumed that an interrupted electrolytic process might better allow time for secondary chemical and physical processes of the types theorized to take place. Although this has proved a possible diagnostic tool with respect to monitoring open circuit cathode potential (oxide buildup), Figures 5-29a and b, no definite advantage over a continuous equivalent mean current has been demonstrated.

Cell voltage has commonly been found to rise slightly with time (oxide accumulation). If voltage were controlled rather than current, it may be hypothesized that chemical and physical processes might be self-regulatory. No noticeable change in carbon deposit, however, has been found using this technique.

It was also speculated that, as in electroforming processes, it might be advantageous to superimpose an alternating current over a direct deposition current, thereby perhaps to increase agitation and decrease polarization. No improvement in the quality or quantity of carbon deposit was noted where AC frequency was varied from 500-50,000 cycles per second.

5.2 Anode Processes

5.2.1 Oxygen Production

In early experiments, electrolysis of electrolytes comprising Li_2CO_3, Na_2CO_3, and K_2CO_3 resulted in the release of a 2:1 ratio of carbon dioxide to oxygen at the anode which persisted after many hours of electrolysis. On the other hand, electrolysis of mixtures of LiF-Li_2CO_3 or LiCl-Li_2CO_3 provided essentially 100 percent oxygen. Electrolysis of the latter electrolytes at high current densities showed carbon dioxide given off with oxygen for a brief period but diminishing with time as shown in Figure 5-30. Other studies employing a shrouded anode at low current densities produced essentially pure oxygen almost immediately with no chromatographically detectable methane, hydrogen, or carbon monoxide gases. Chromatograph sensitivities were in the order of a few parts per million. Experiments to determine Faradaic efficiencies confirmed 100 percent efficiencies when the anode was shrouded and electrolysis rates were appropriately low. As is evident from the above brief synopsis a number of system variables affecting the anode processes have been recognized. In general, they comprise most of the same variables which affect the cathode processes. Effect on the anode processes is considered in the following sections.

5.2.2.1 (Continued)

sustain a low P_{CO_2} in the oxygen leaving the anode. Conversely, when high purity oxygen is being obtained for sustained periods under balanced conditions, a good quality carbon deposit at the cathode is heralded - hence the observed correlations between low current density runs (where oxide accumulation is least) and immediate high oxygen purity as noted previously.

5.2.2.2 Electrolyte Cationic Species

Effects of different cationic species are twofold. First, carbonate dissociation pressures are affected by the nature of the cation; for example, at a given temperature electrolyte P_{CO_2} is markedly different for lithium as opposed to potassium - the latter being much lower. Effect on oxygen purity is obvious in the light of the preceding discussion. Potassium systems would seem to fare better on the basis of this criteria except for a second effect. This effect relates to the property of cations, such as sodium and potassium, to be reduced and accumulate at the cathode, or to form cathode products other than carbon and oxide ion, perhaps peroxide ion, whence such cathode inefficiencies do not allow maintenance of sufficiently high oxide concentration within the electrolyte for high oxygen purity at the anode.

5.2.2.3 Diluent Anionic Species

It was shown previously in discussions of cathode process variables that when halides were added as diluents to carbonate systems the activity of the carbonate was changed as reflected in different slopes of log CO_2 pressure against reciprocal temperature. As before, such changes in P_{CO_2} are noted in variations of oxygen purity. In this same manner, oxyanion buffers such as borates and phosphates alter the effective electrolyte oxide ion concentration, additions increasing the P_{CO_2} and altering oxygen purity in the process.

5.2.2.4 Anode Substrate Material, Surface Coating

Two specific problems are associated with selection of a suitable anode material. The first of these is dissolution of the anode, and the second is the gradual formation of a non-conductive oxide film; electrolytes of high halide constitution promote dissolution, the anode metal typically being found in the cathode deposit. Gold, platinum, nickel, and cobalt anodes readily dissolve in high chloride systems containing about one mole percent carbonate. Solution does not occur at 50 mole percent carbonate. The cut-off concentration within this broad range has not been established. At the higher carbonate concentration a heavy oxide film is formed on

5.2.2.4 (Continued)

nickel anodes, and the film is still observed to conduct current. It is currently believed that the capacity to form a stable oxide film at the anode is desirable as long as the oxide is conductive, as nickel oxide appears to be. A similar film has been found on cobalt anodes, which have likewise retained conductivity. In that nickel seems to interfere least with cathode processes, at present it tends to be favored for anodic use.

5.2.2.5 Dissolved Metal Ions

When dissolved metal ions are present in an electrolyte and oxyanion content is low, so that the metal ions presumably persist as metal-halogen complexes, the metal is plated out at the cathode. However, when oxyanion content is significant, metal ions when present appear to associate within the melt as oxyanion complexes (nickelates, ferrates, etc.). Under the latter circumstance nickel oxide coatings have been observed on iron anodes when nickel was present in the electrolyte, and iron oxide coatings have been found on nickel anodes under reverse circumstances. Anodic discharge of the metal oxyanion may be presumed. A loss in oxygen production efficiency might be expected when this happens, but when electrolyte oxyanion content is high relative to halide, metal dissolution is extremely slow, so that in practice a significant decrease in anode efficiency has not been experimentally noted.

5.3 Carbon Dioxide Absorption

5.3.1 Efficiency

Experimental studies have shown carbon dioxide absorption to be exceptionally rapid. For example, pure carbon dioxide has been bubbled into electrolytes containing a small fraction of oxide at flow rates which cause violent agitation of the electrolyte, yet absorption is so rapid that no bubbles are observed to persist long enough to break through the melt surface. At lower concentrations, such as one percent by volume, flow rate through a straight 1/8 inch I. D. tube dipped one inch below the surface has been increased from 250-1800 cubic centimeters/minute without any observed change in scrubbing efficiency, which was well over 90 percent initially. An increase in CO_2 inlet concentration in one test series from 0.5 percent to 20 percent by volume resulted in an increase in scrubbing efficiency from an initial 90 percent to a final 95 percent, reflecting the increased fraction of CO_2 removed.

$$\text{Scrubbing Efficiency} = \frac{\%\ CO_2 \text{ in} - \%\ CO_2 \text{ out}}{\%\ CO_2 \text{ in}} \times 100$$

5.3.1 (Continued)

At 250 cubic centimeters/minute no decrease in scrubbing efficiency was noted when bubbler depth was varied to as little as 1/8 inch submergence. Currently it is believed that melt splash and gas-liquid separation will be controlling factors in the selection of scrubber designs rather than carbon dioxide absorption kinetics.

5.3.2 Scrubbing Process Variables

5.3.2.1 Oxide Ion Concentration

It has already been noted that gas outflow from any electrolyte reflects the partial pressures of carbon dioxide and water vapor in equilibrium with the electrolyte and that these equilibria depend upon electrolyte constitution, in particular, the oxide ion concentration. Thus, the minimum carbon dioxide content to which a gas stream can be scrubbed is set by initial melt selection which has been governed by P_{CO_2} and P_{H_2O} limits in which the desired cathode and anode processes are favored. The ability simultaneously to deposit dense carbon at the cathode and to discharge high purity oxygen at the anode, as was found in cell electrolysis efficiency studies, indicates that scrubbing to below 0.01 percent carbon dioxide by volume will be possible. This latter level, in combination with the inlet concentration to be scrubbed, will determine maximum scrubbing efficiencies possible; it is therefore desirable that the characteristic electrolyte P_{CO_2} be as low as possible.

5.3.2.2 System Moisture Balance

In a system which contains hydroxide, the absorption of one mole of carbon dioxide results in the displacement of one mole of water. Without electrolysis this water would be expected to be found in the effluent gas stream from the system. When the system is electrolyzed and oxide ions produced, this water is reabsorbed. Thus, a sustained water balance between entering and leaving gases assures that only carbon dioxide is being involved in the long term sense in the electrolytic process. Variation from such a balance indicates that water is being dissociated or that the electrolyte composition is changing. Experimental results of water balance studies are shown in Figure 5-31 and 5-32. Good correlation is indicated in Runs 3 and 4 between carbon dioxide absorbed and moisture displaced without electrolysis, where the electrolyte comprised lithium chloride, lithium hydroxide, lithium carbonate, and a small fraction of lithium phosphate. Poor correlation was shown in Run 1 in a similar electrolyte without the phosphate. It was subsequently shown in Run 2 that the moisture displaced during Run 1 was being retained by the melt in some fashion (solubility) that responded to

5.3.2.2 (Continued)

the partial pressure of moisture in the gas phase, and that if the outlet moisture was diluted by an auxiliary flow of dry inert gas through the system, a carbon dioxide-moisture balance could be shown. Run 5 illustrates the reabsorption of the moisture upon initiation of electrolysis.

5.3.2.3 Electrolyte Hydroxide "Bank"

It has been shown that carbon dioxide will displace water mole for mole from an electrolyte containing hydroxide. The presence of hydroxide in any significant concentration in the electrolyte has accordingly resulted in extremely low system carbon dioxide partial pressure, and correspondingly in high carbon dioxide scrubbing efficiencies. Because in general, free oxide in the electrolyte will be low, the presence of hydroxide also provides a buffering action in allowing oxide ions to be delivered on demand for carbon dioxide scrubbing thereby, a requirement for precise balance at all times of oxide generation rate at the cathode and carbon dioxide feed rate to the system is considerably ameliorated.

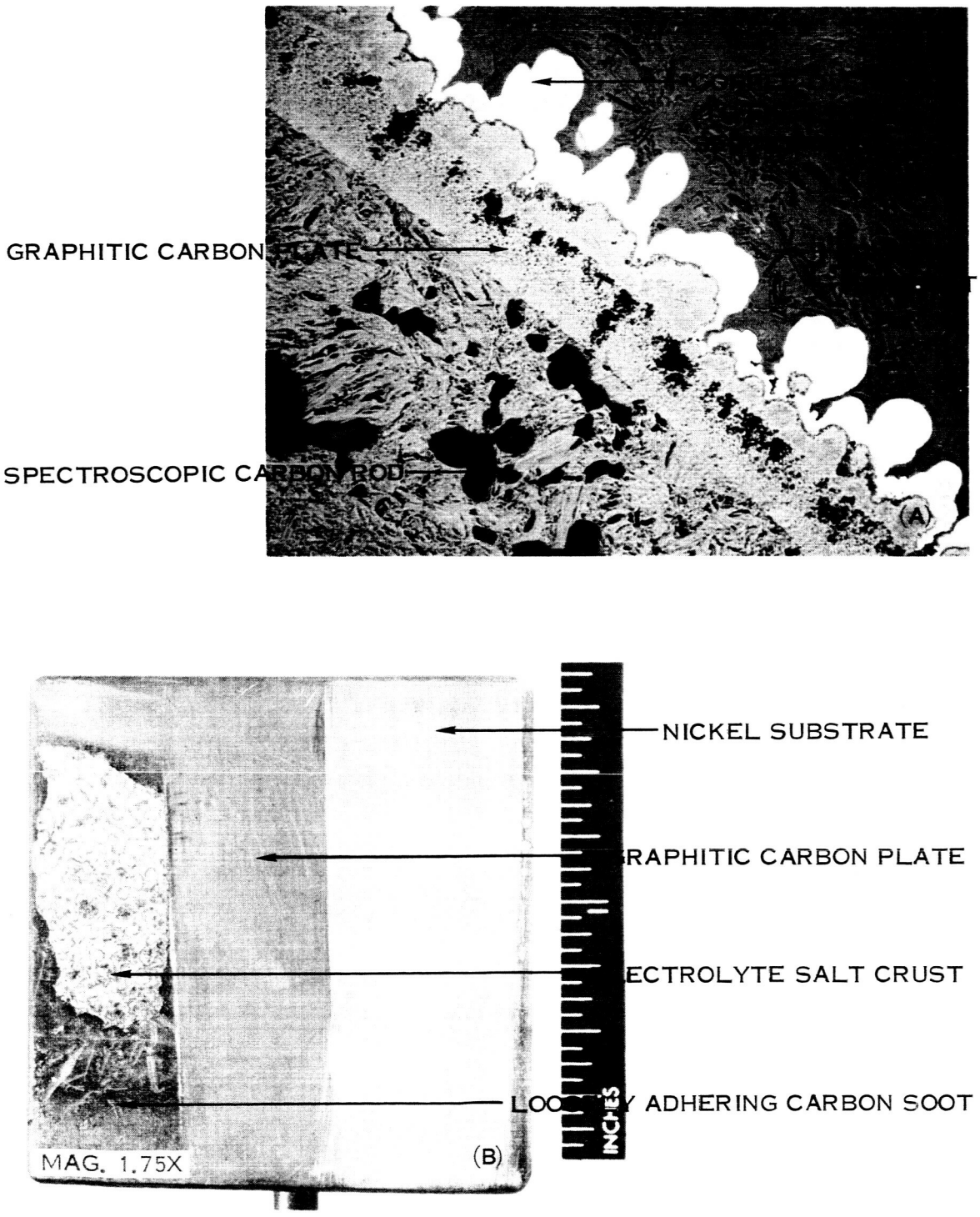

FIGURE 5-1 (a and b) GRAPHITIC CARBON DEPOSITS

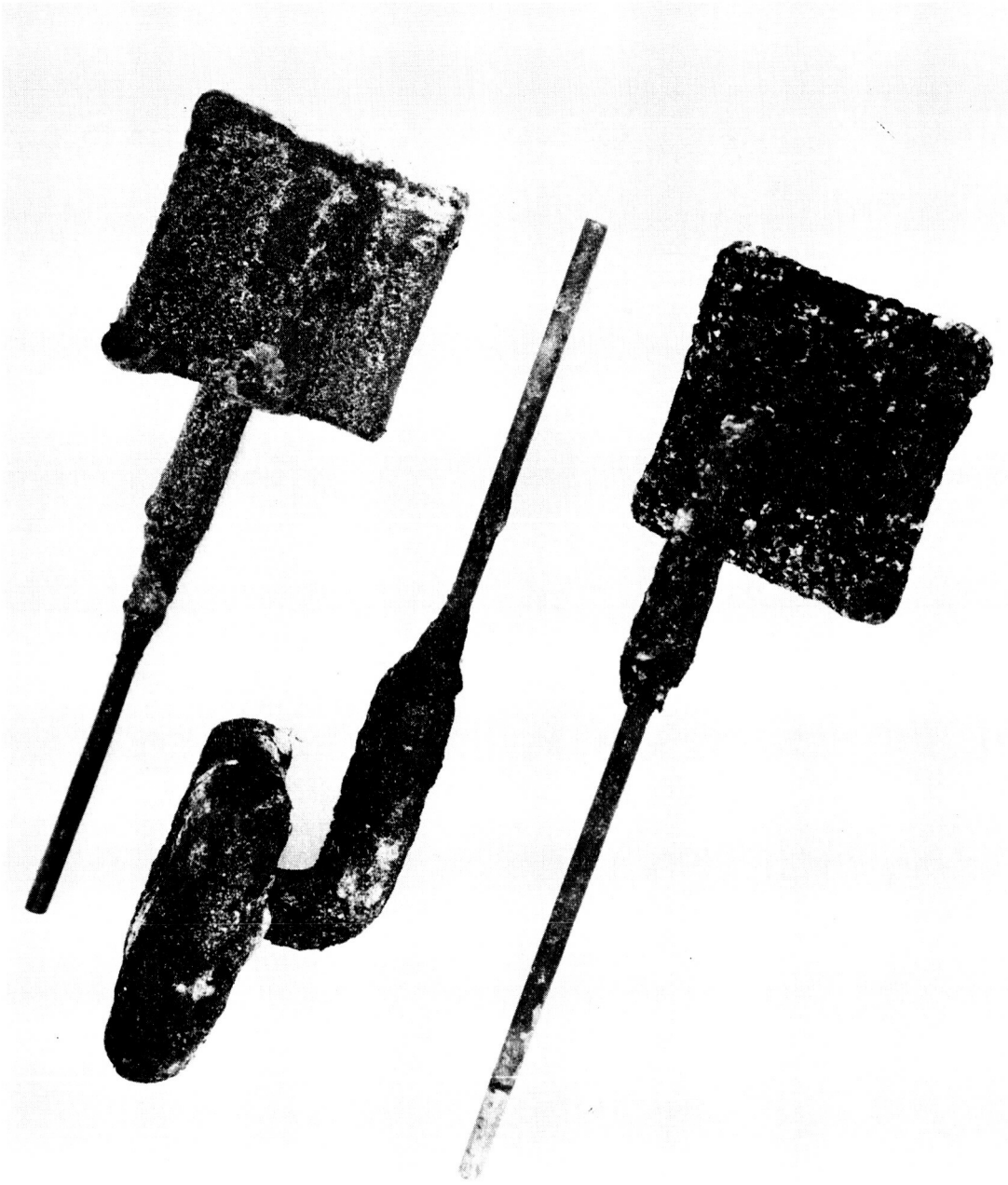

FIGURE 5-2 CARBON WITH OCCLUDED SALTS

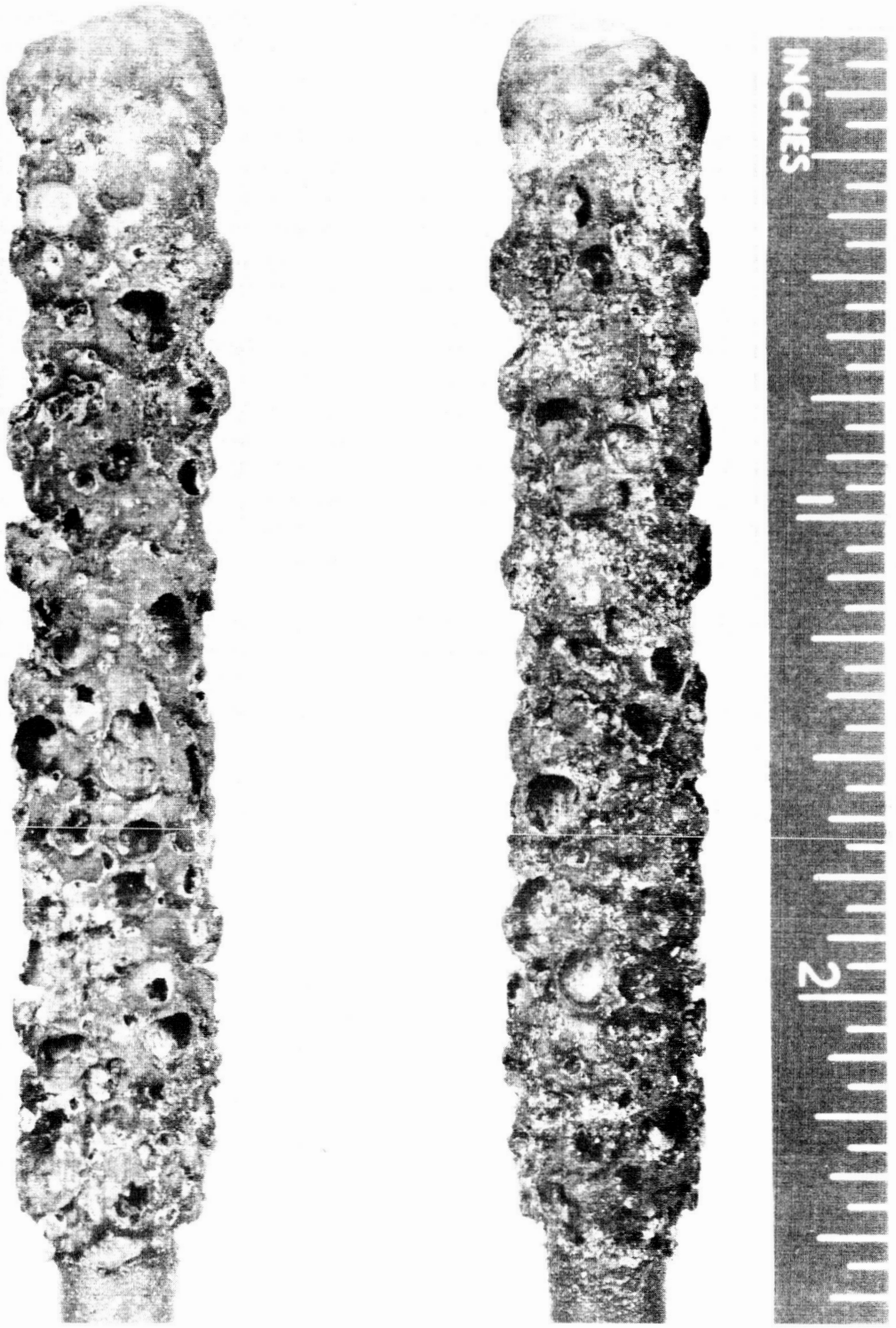

FIGURE 5-3 GAS POCKED CARBON DEPOSITS

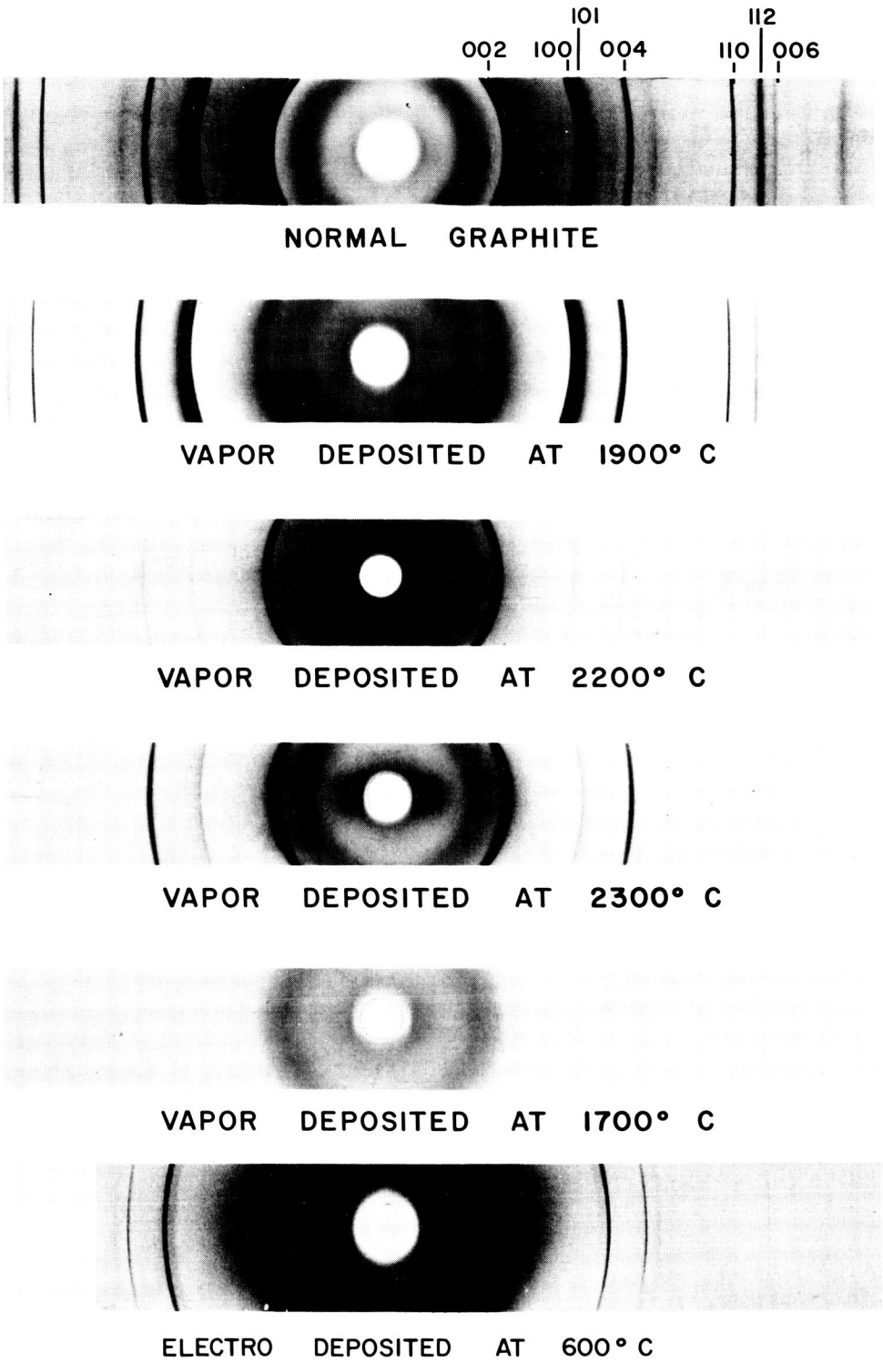

FIGURE 5-4 X-RAY DIFFRACTION PATTERNS

FIGURE 5-5 CARBON FILAMENTS

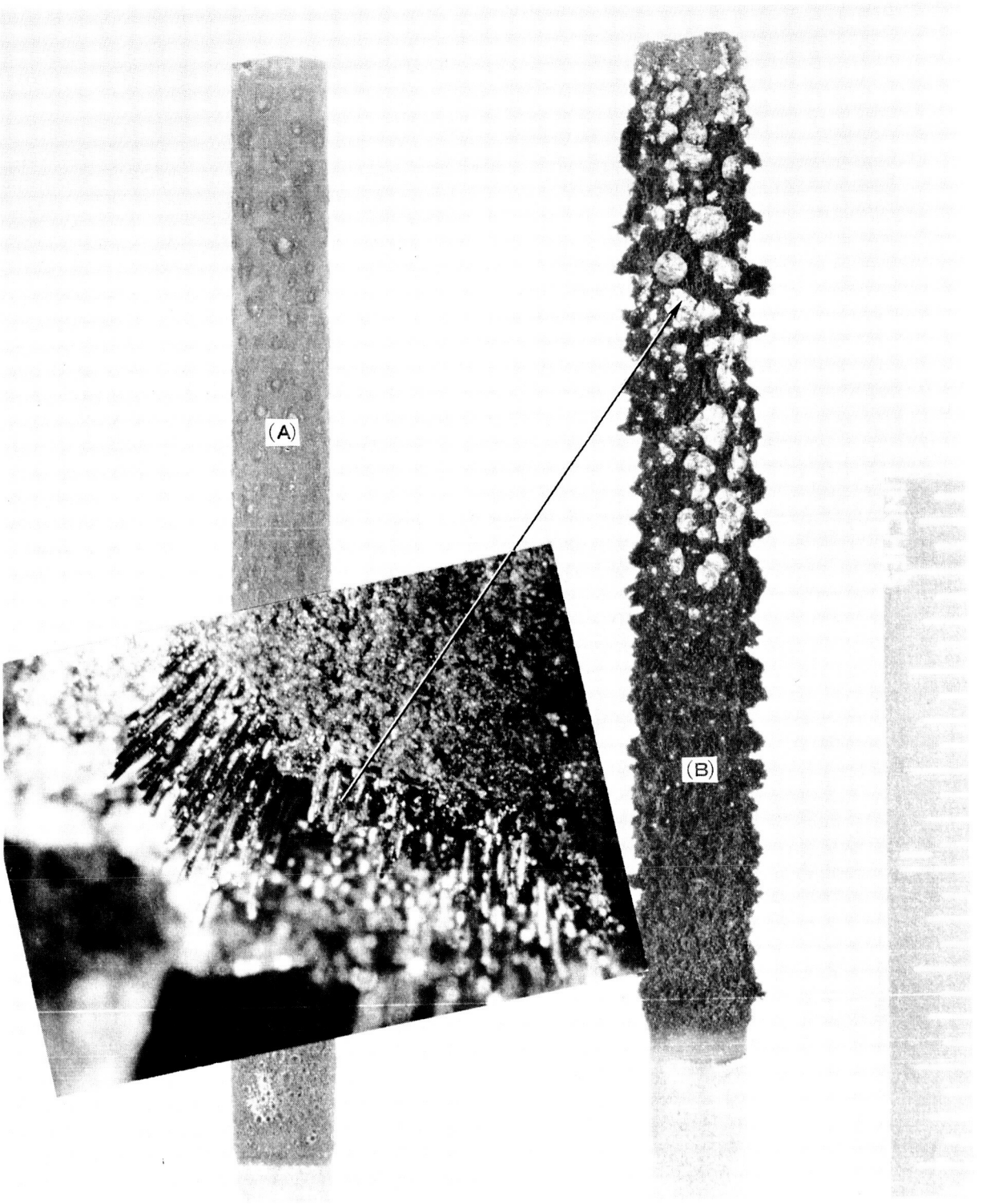

FIGURE 5-6 GAS POCKED DEPOSITS; CRATERS AND TUBES

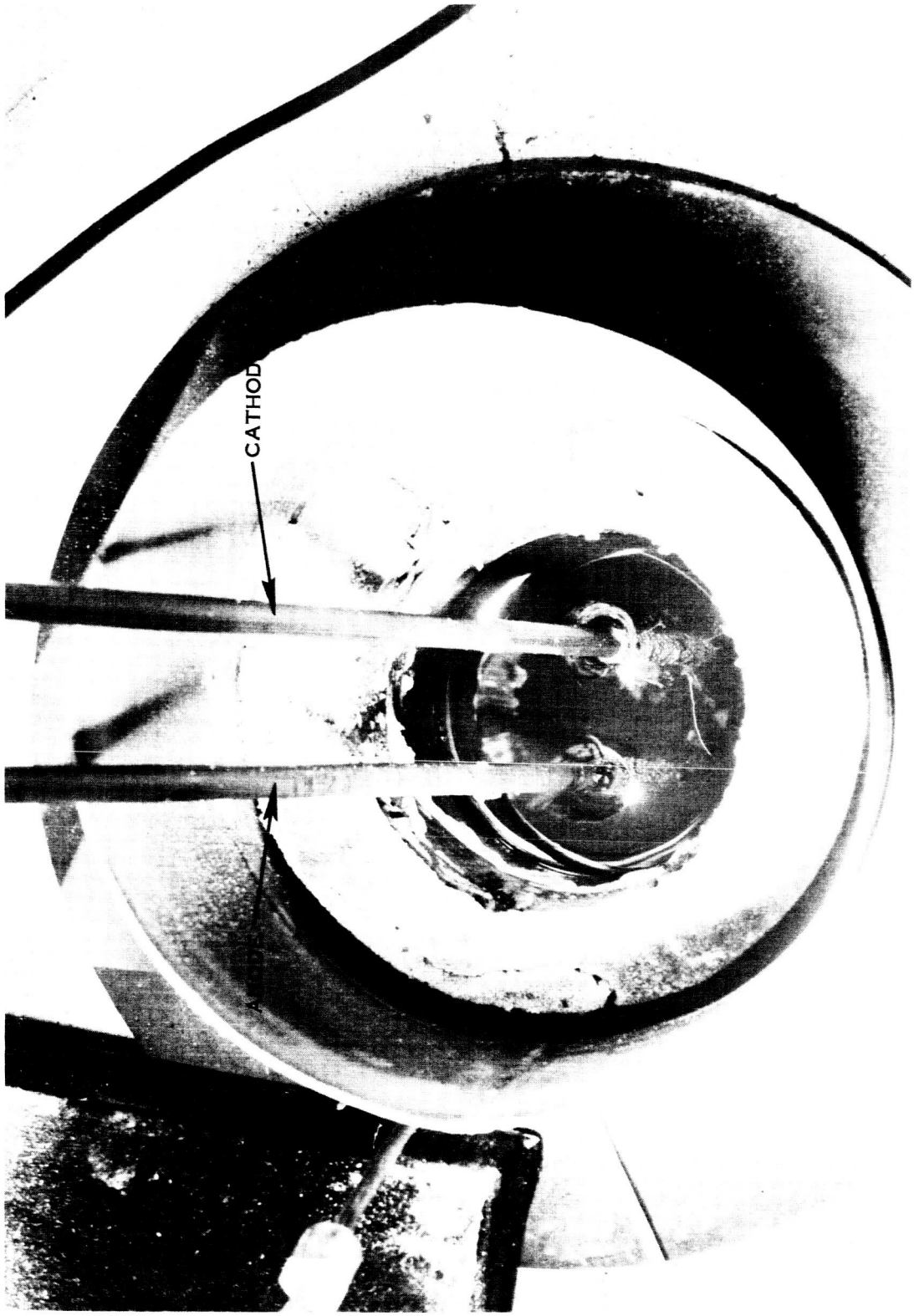

FIGURE 5-7 CATHODIC GAS EVOLUTION

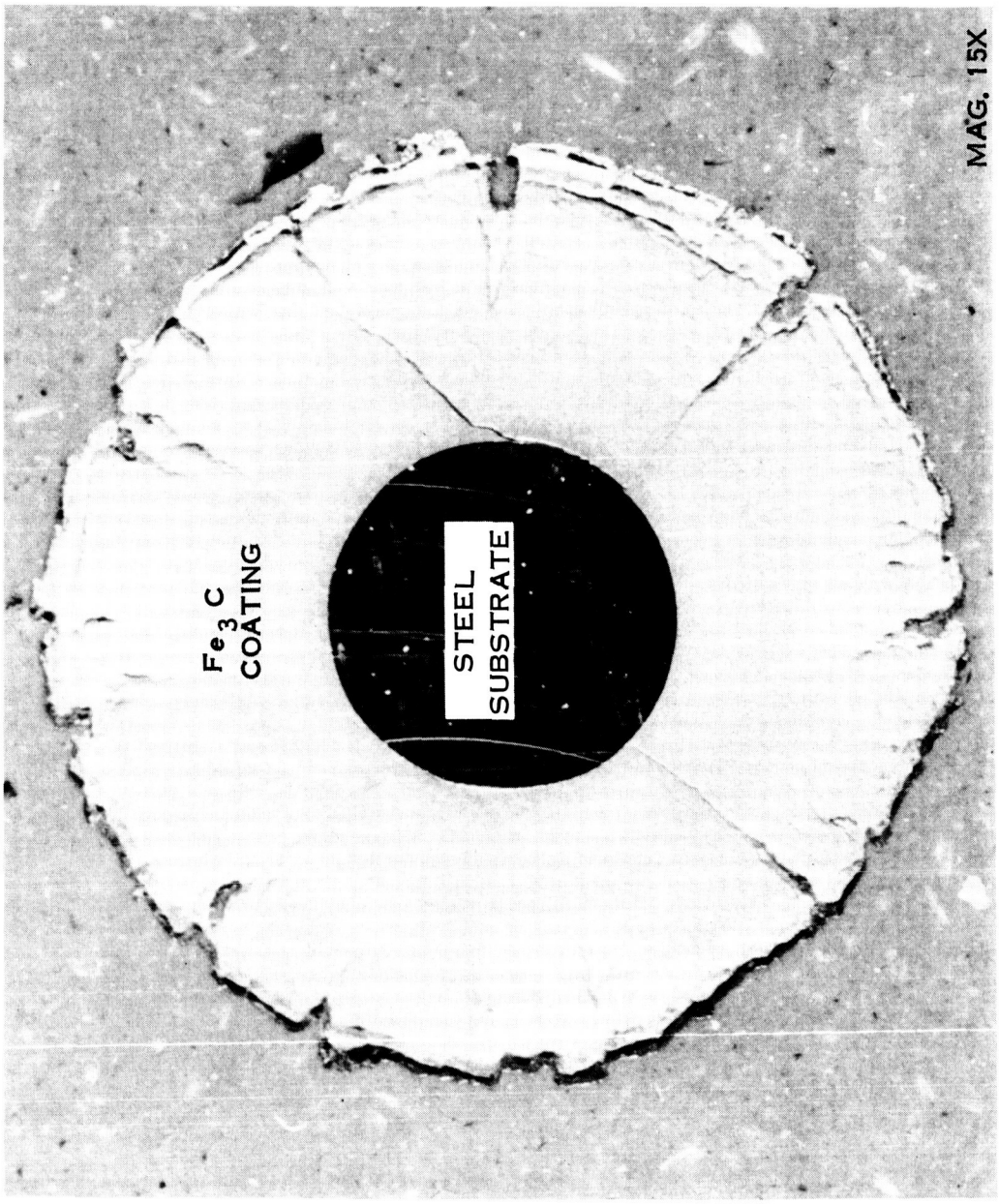

FIGURE 5-8 STOICHIOMETRIC IRON CARBIDE COATING

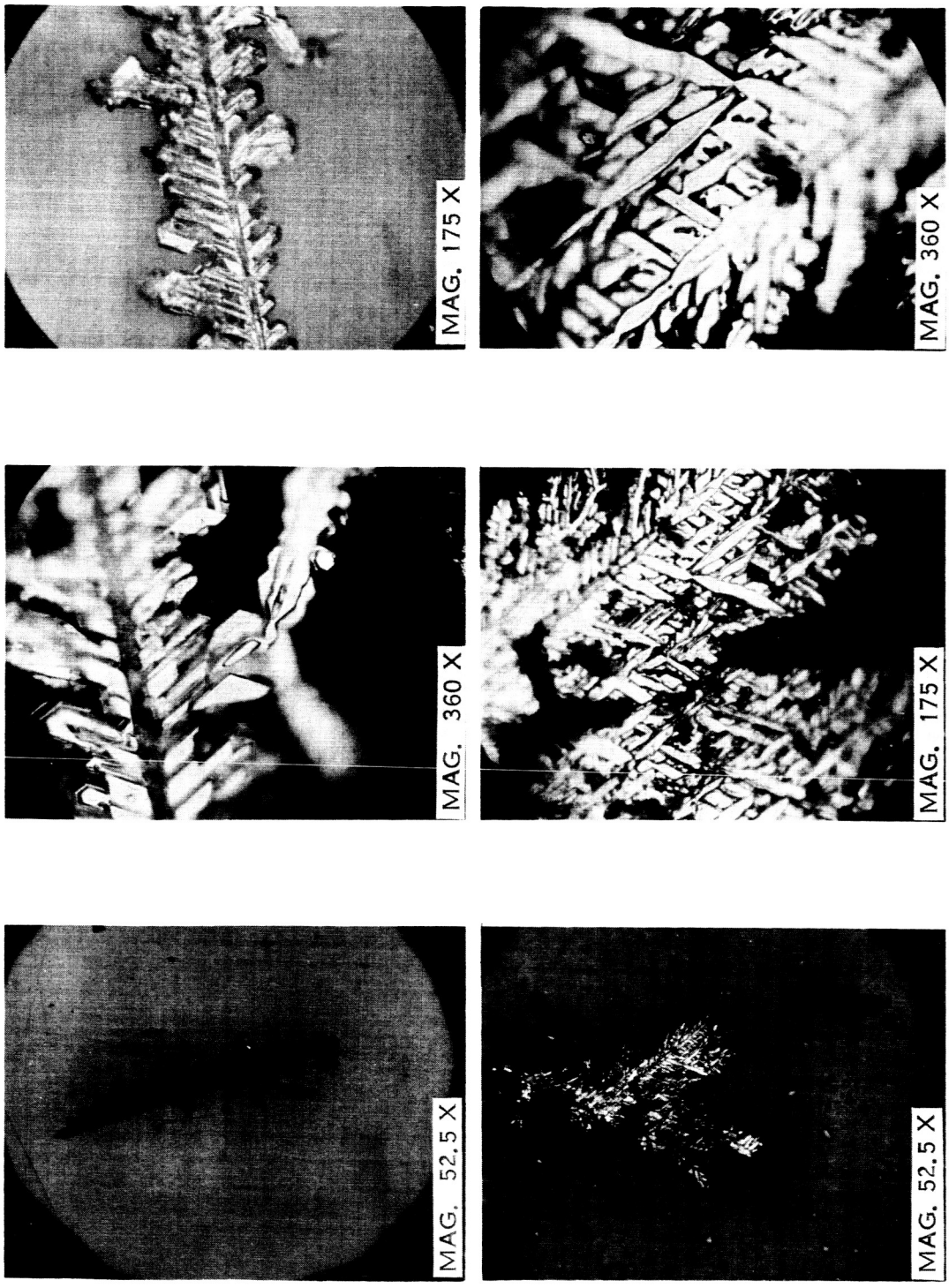

FIGURE 5-9 COBALT METAL DEPOSITS

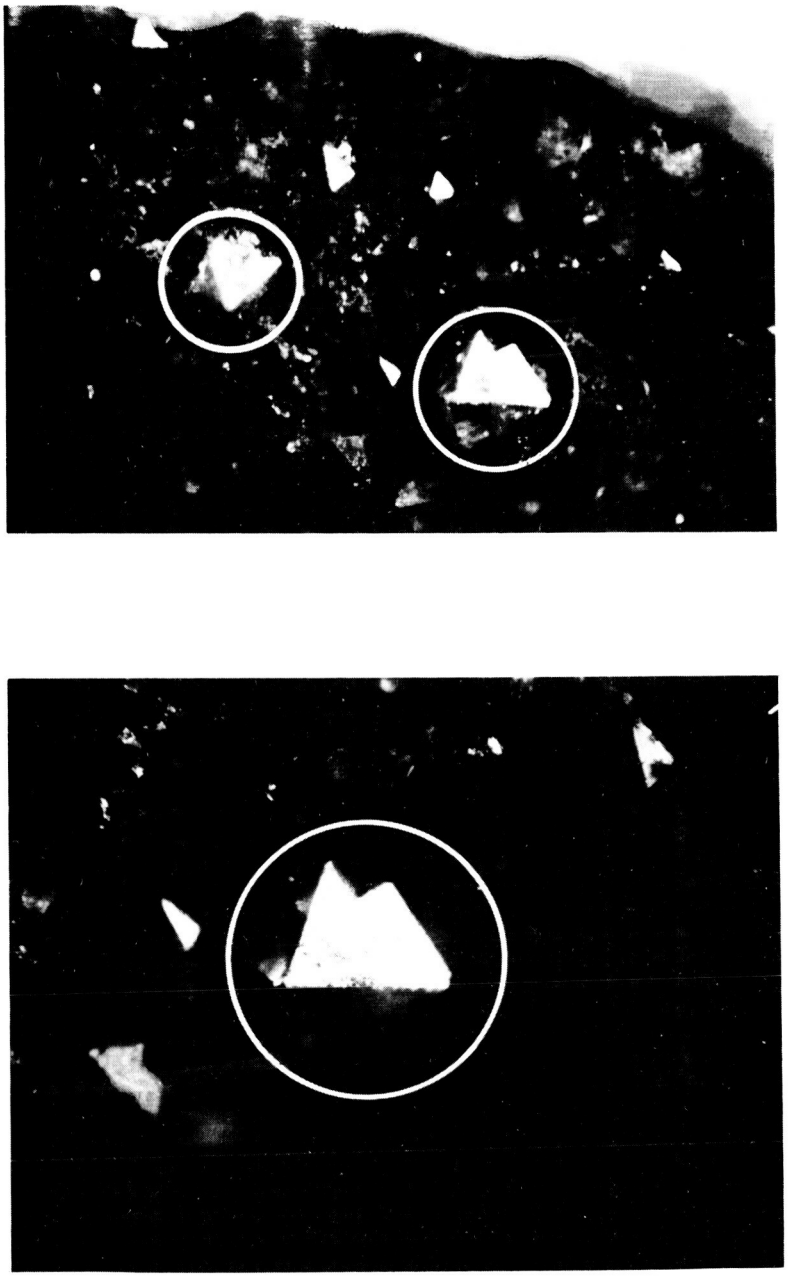

FIGURE 5-10 CATHODIC SALT CRYSTAL FORMATION

CATHODE NO.	MATERIAL	CURRENT DENSITY AMPS CM^2	DURATION HRS:MIN	CASE DEPTH IN
C–44	HS204	0.01	23:50	0.0028
C–45	304SS	0.01	72:00	0.006
C–94	304SS	0.50	2:00	0.0009
C–95	304SS	0.25	2:00	0.0012
C–96	304SS	0.10	2:00	TRACE
C–97	304SS	0.01	16:30	0.003

3/16 INCH DIAMETER 304SS ROD

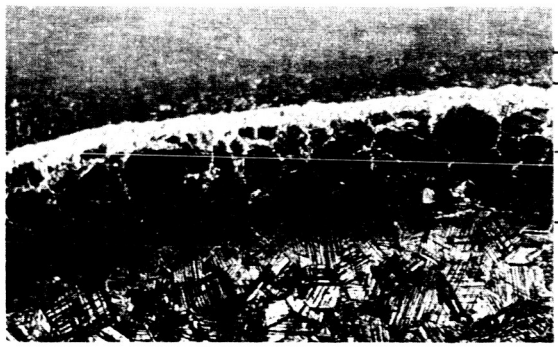

MAGNIFICATION 150 X

FIGURE 5-11 CARBURIZATION OF AISI 304 STAINLESS STEEL

Run No.	Melt Composition (moles)	Voltage E/Cell Volts	Temp. °C	Blanket Gas	Run Time Hrs.	Remarks
C55	Li_2CO_3 (1) Na_2CO_3 (1)	0.65	670	Air	16	No adherent graphite; Some nodular carbon entrained in salt
C65	Li_2CO_3 (3) KCl (3) LiF (1)	0.91	588	Air	72	Graphitic deposit
C72	$BaCO_3$ (2.5) $BaCl_2$ (6) LiCl (5) LiF (1) B_2O_3 (10 gr)	0.82	680	Air	16	Graphitic deposit
C245	Li_2CO_3 (1) LiF (1)	0.5	684	Dry CO_2	72	Graphitic deposit
C247	K_2CO_3 (1) KCl (1)	1.25	650	Wet CO_2	24	No carbon deposit
C263	K_2CO_3 (1) KCl (1) B_2O_3 (0.5% wt)	1.05	685	Wet CO_2	16	Thin graphitic film
C264	Na_2CO_3 (0.6) NaCl (0.8)	1-1.38	640	Dry Argon	16	Patchy carbon deposit
C266	Na_2CO_3 (0.6) NaCl (0.8)	1.14-.78	689	Dry CO_2	18	No carbon deposit

Current Density - 10 ma/cm^2
Cathode Material - Nickel
Anode Material - Carbon

FIGURE 5-12 EFFECT OF ALKALI METAL SPECIES ON CARBON DEPOSITION

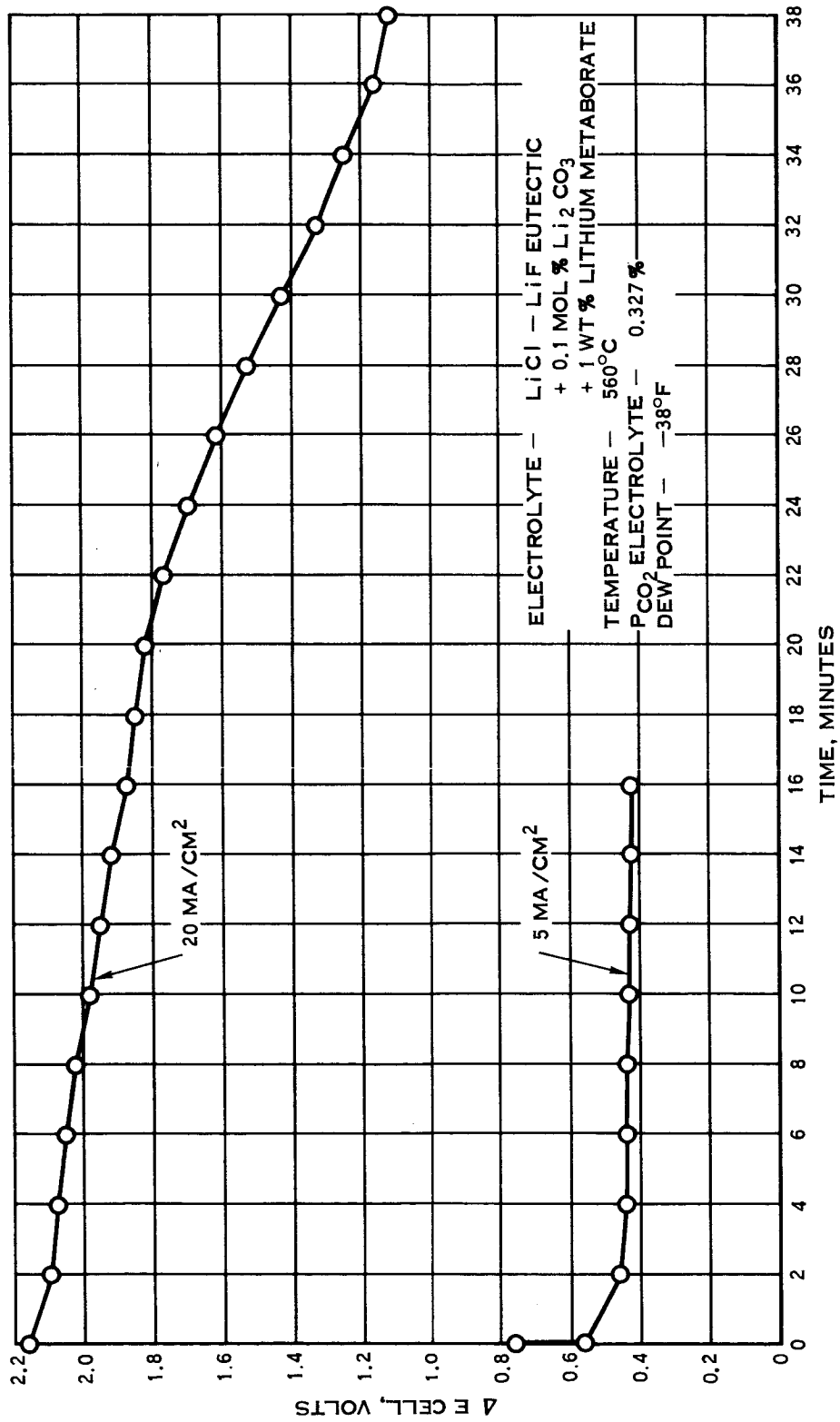

FIGURE 5-13 CELL OPEN CIRCUIT VOLTAGE DECAY RATE AFTER ELECTROLYSIS AT TWO DIFFERENT CURRENT DENSITIES

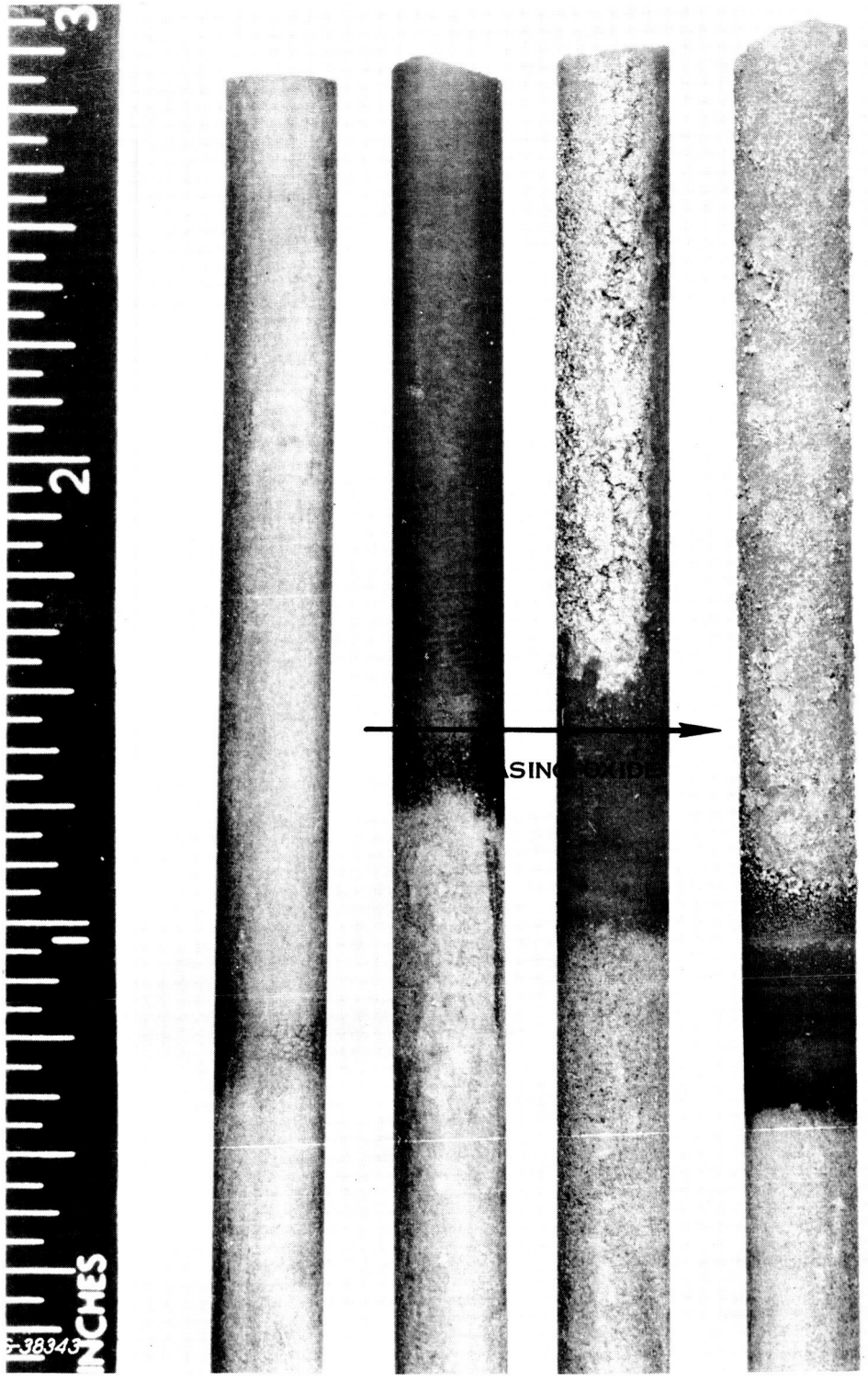

FIGURE 5-14 CATHODE DEPOSIT SHOWING EFFECT OF INCREASED OXIDE CONCENTRATION

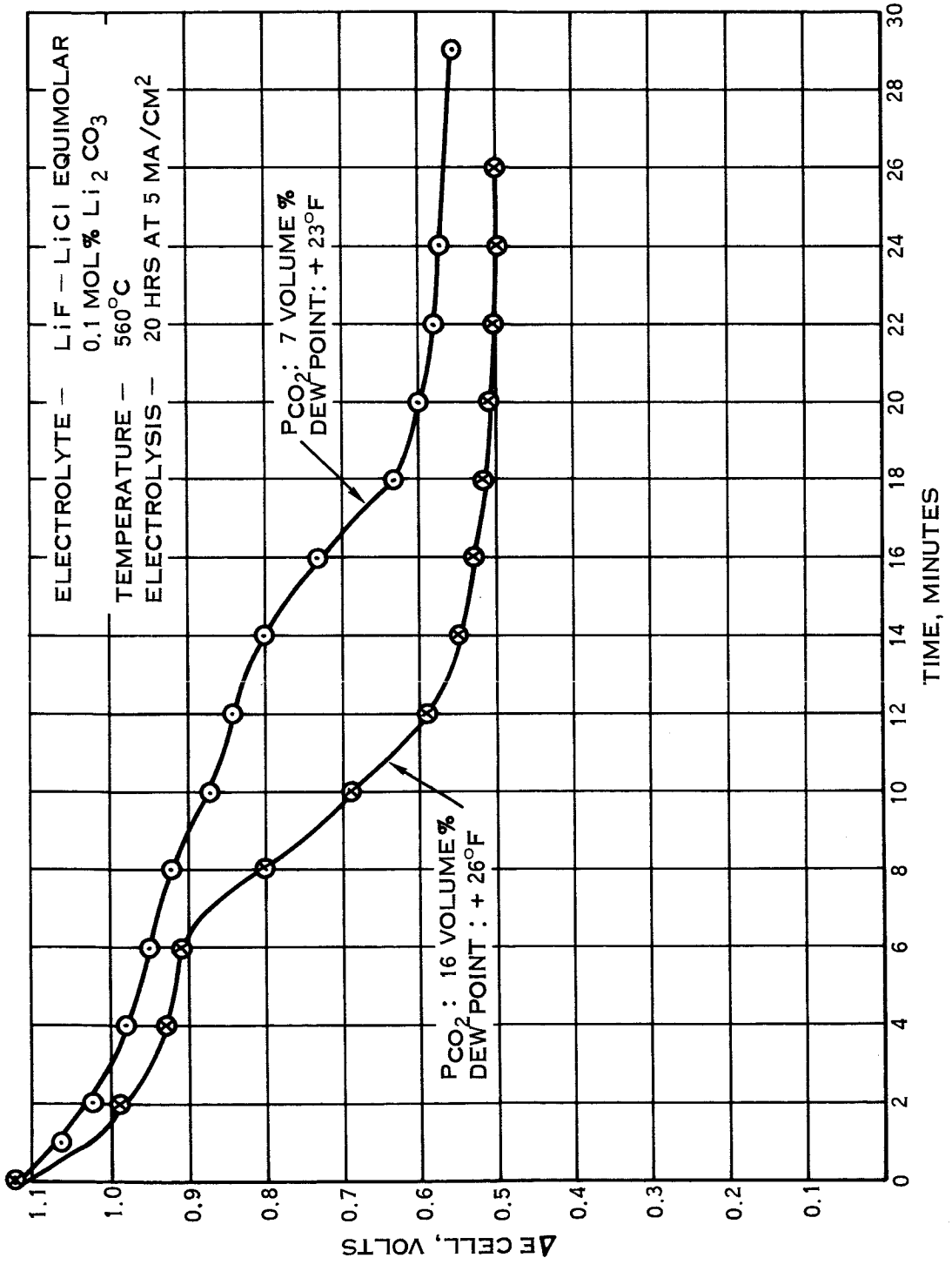

FIGURE 5-15 EFFECT OF CONSTANT P_{H_2O} AND VARIED P_{CO_2} ON OPEN CIRCUIT POTENTIAL

Number	Current Density (ma/cm^2)	Atmosphere	Percent C	Used
22-1	10	Dry	19	x
22-2*	10	Wet	32	x
22-3	100	Wet	8	
22-4	10	Wet	26	
22-5	100	Wet	9	x
22-6	10	Dry	29	
22-7	100	Dry	22	x
23-1	10	Dry	21	
23-2	100	Dry	17	
23-3*	100	Wet	27	
23-4	100	Wet	6	

Conditions: Temperature - 640°C
Melt - 60 wt % LiCl, 40 wt % Li_2CO_3
Atmosphere - 50 vol % Ar, 50 vol % CO_2
Cathode - Carbon
*Water only passed through melt for a short time before electrolysis

FIGURE 5-16 EFFECT OF ALKALI METAL SPECIES ON CARBON DEPOSITION

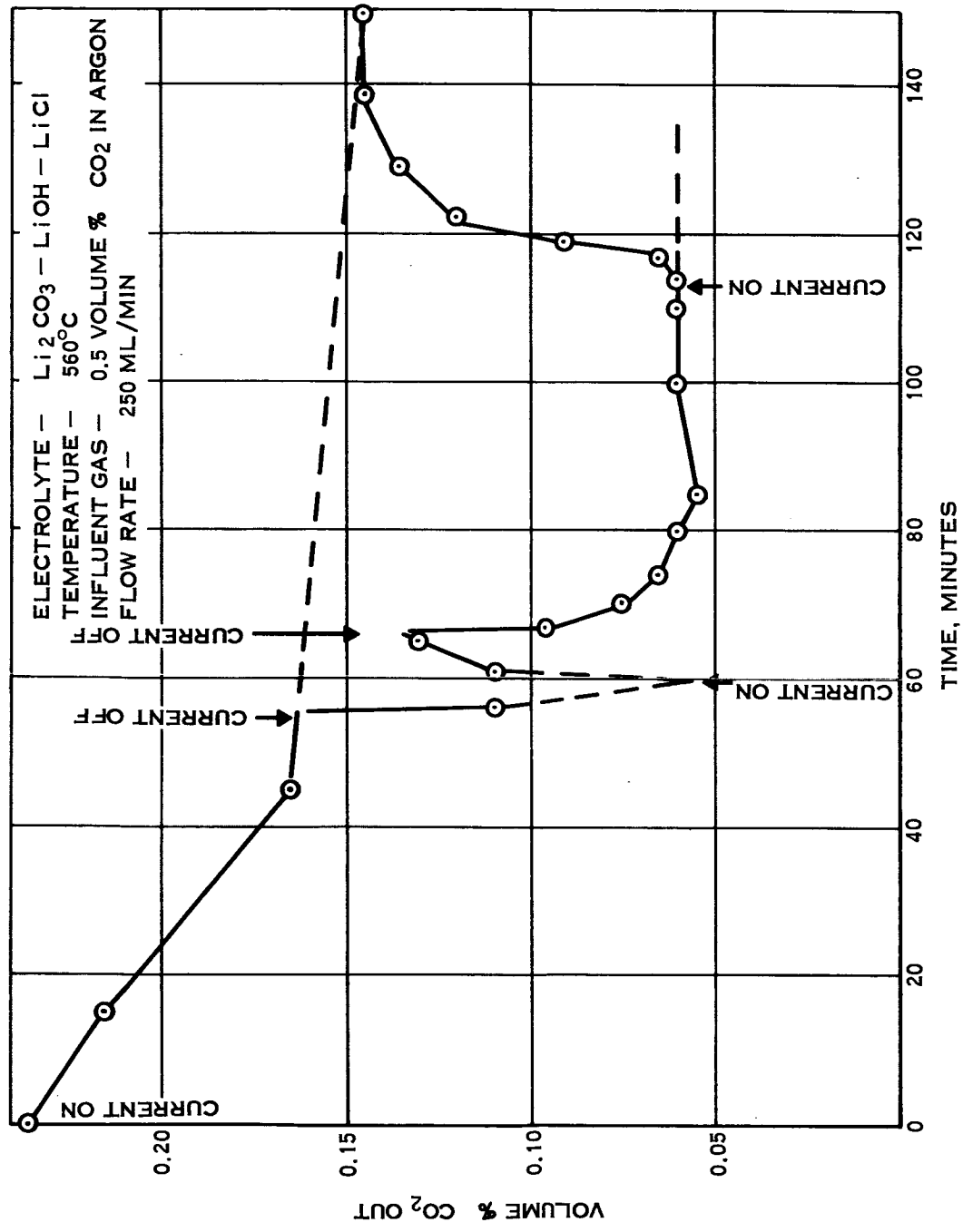

FIGURE 5-17 OXIDE RETENTION AT CATHODE DURING ELECTROLYSIS

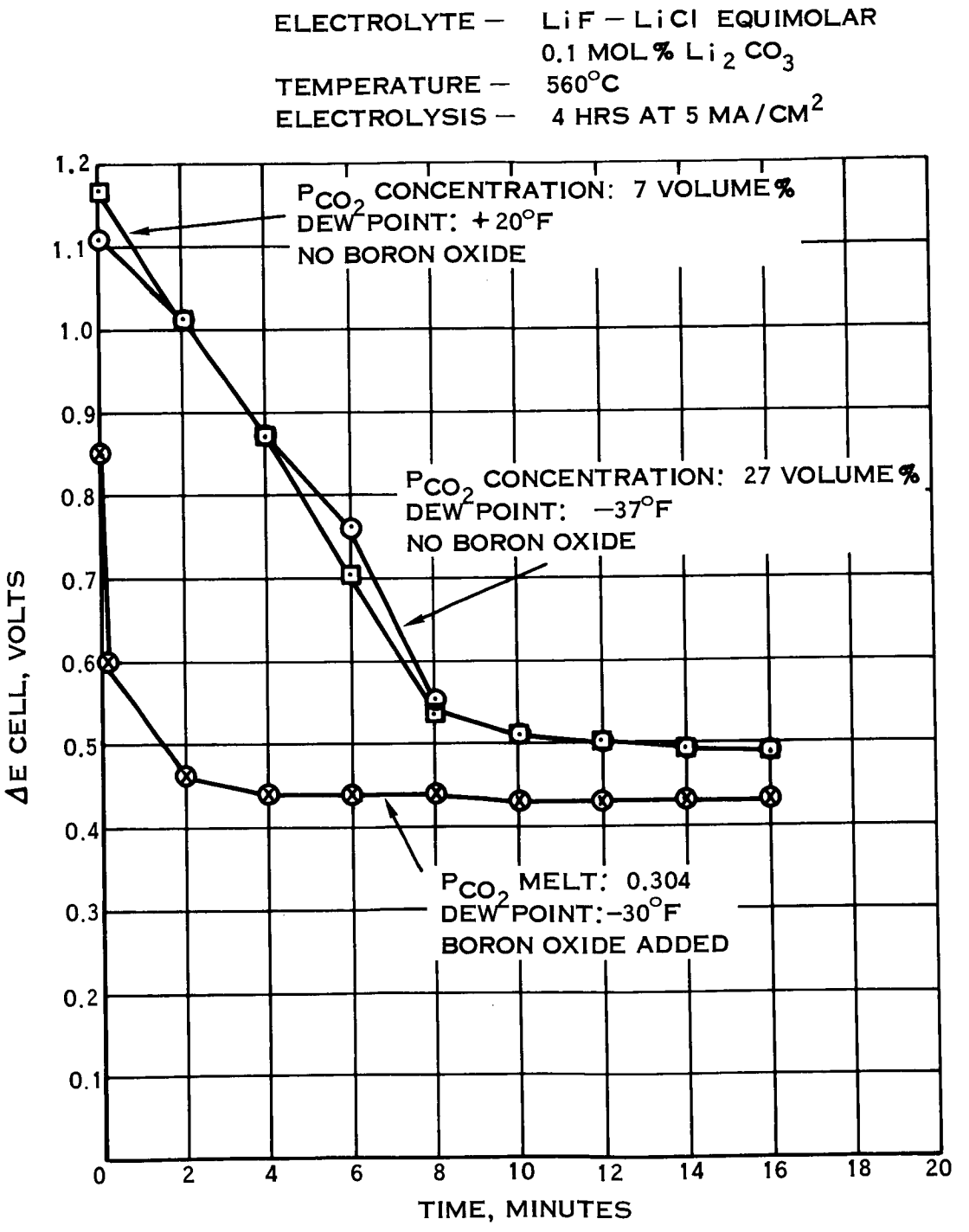

FIGURE 5-18 EFFECT OF BORON OXIDE ADDITION ON OPEN CIRCUIT POTENTIAL

Run No.	Anode	Cathode	Cathode Deposit
C276	Carbon	Carbon	Carbon coating - magnetic; no Fe or Ni by chemical analysis
C278-9	Carbon	Carbon - Ni Couple	Carbon coating on carbon; no Fe or Ni by chemical analysis
			Carbon coating on Ni; trace Fe, high Ni
C282	Nickel	Carbon	Carbon coating, no Fe or Ni
C284	304 SS	Carbon	Carbon coating, no Fe or Ni
C287	Cobalt	Carbon	No carbon coating, trace Ni, high Fe, presence of Co uncertain
C288	304 SS	Carbon	Very light carbon coating, trace Fe, high Ni
C290	304 SS	Carbon	No carbon coating, Fe present, no Ni
C291-2	Carbon	Carbon - Ni Couple	No carbon coating on carbon, large amount of Fe
			Carbon coating on Ni, Fe fringe
C294-5	Carbon	Carbon - Ni Couple	No carbon coating on carbon, large amoung of Fe
			Carbon coating on Ni, Fe fringe
C297-8	Carbon	Carbon - Ni Couple	Nodular carbon coating on both materials, Fe fringed

Li_2CO_3-LiCl equimolar + 0.2% wt B_2O_3
Temperature 670°C

FIGURE 5-19 CARBON-METAL CO-DEPOSITION STUDIES

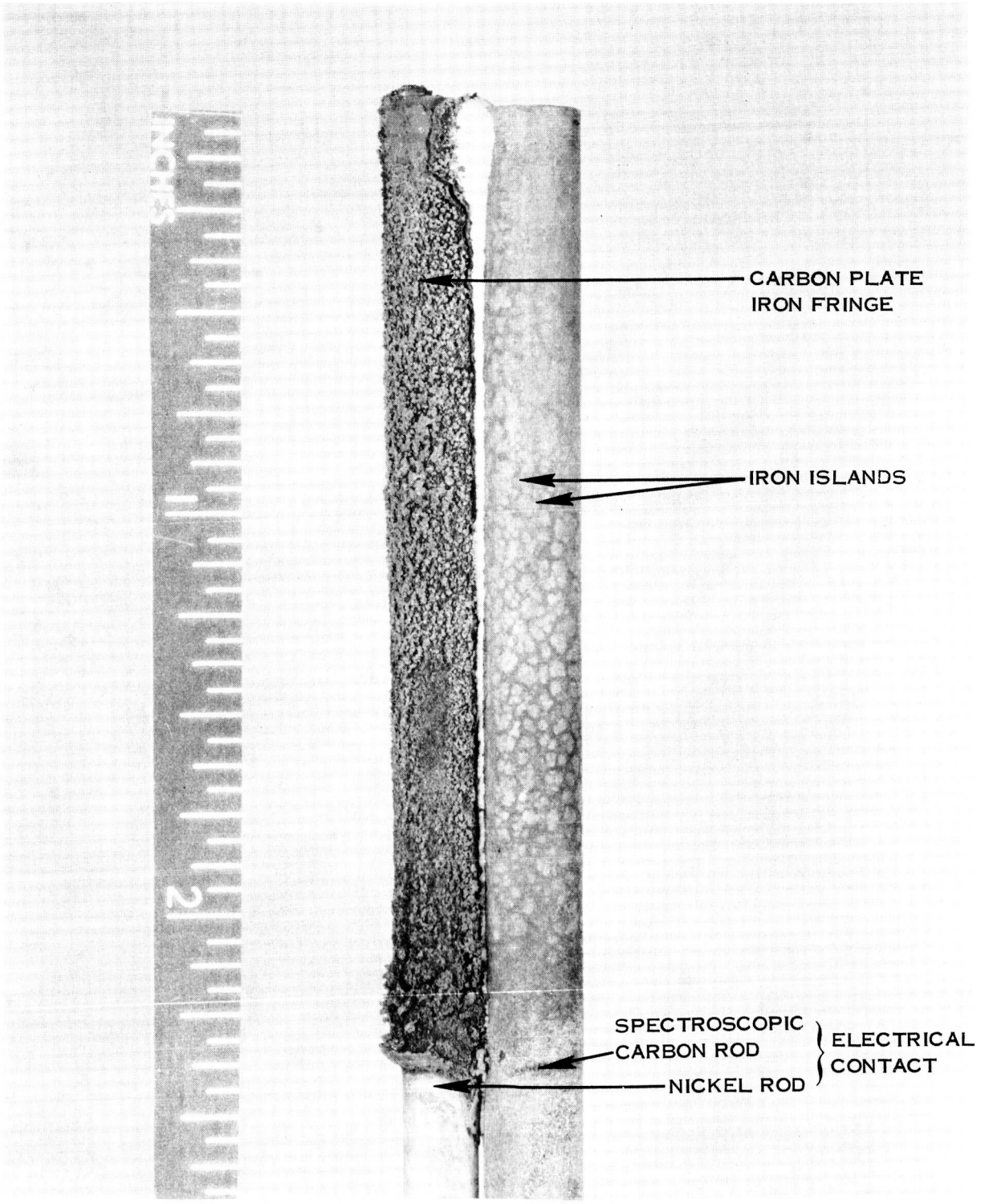

FIGURE 5-20 CATHODE, NICKEL-CARBON COUPLE

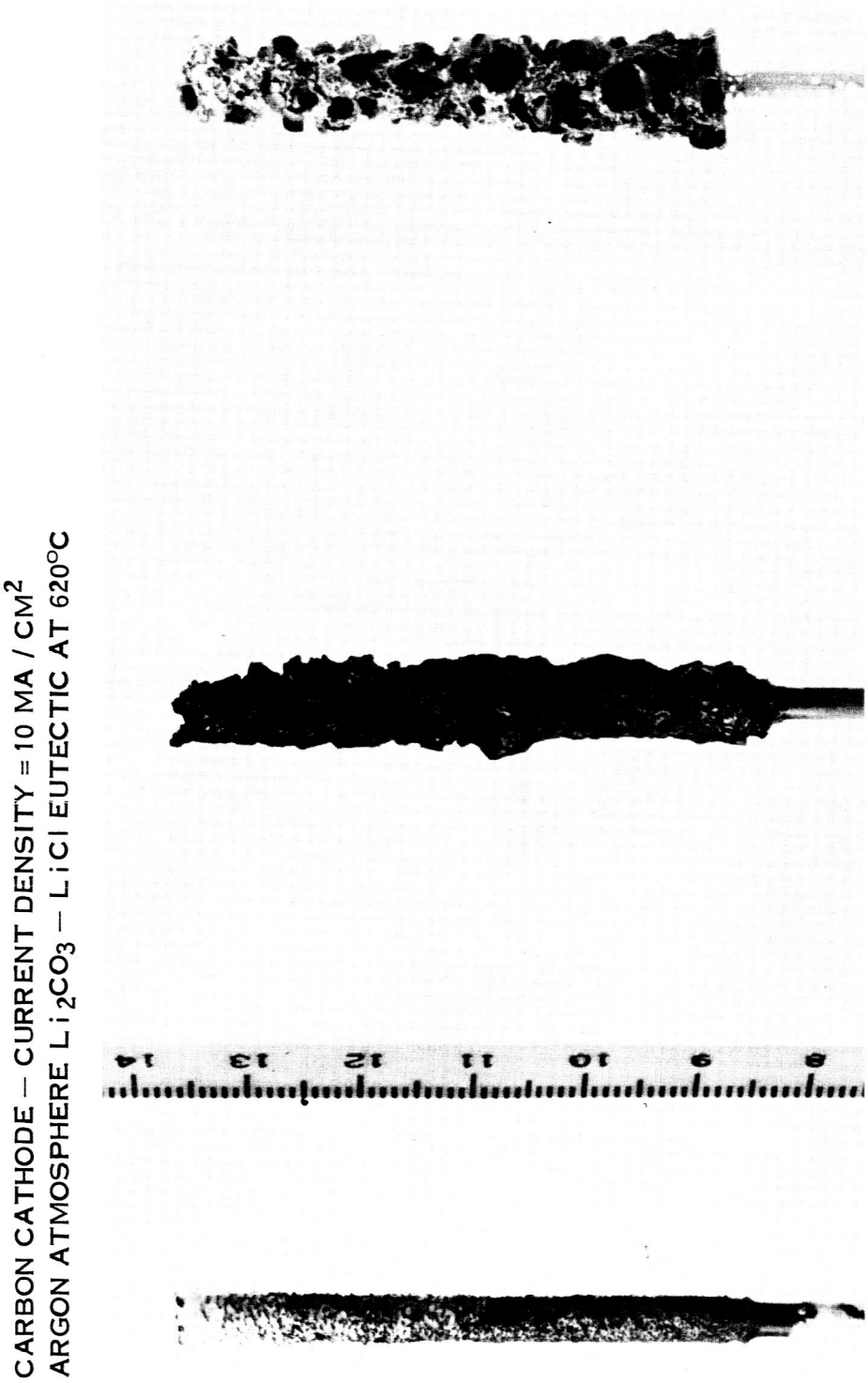

FIGURE 5-21 EFFECT OF CO-DEPOSITED METALS ON CARBON STRUCTURE

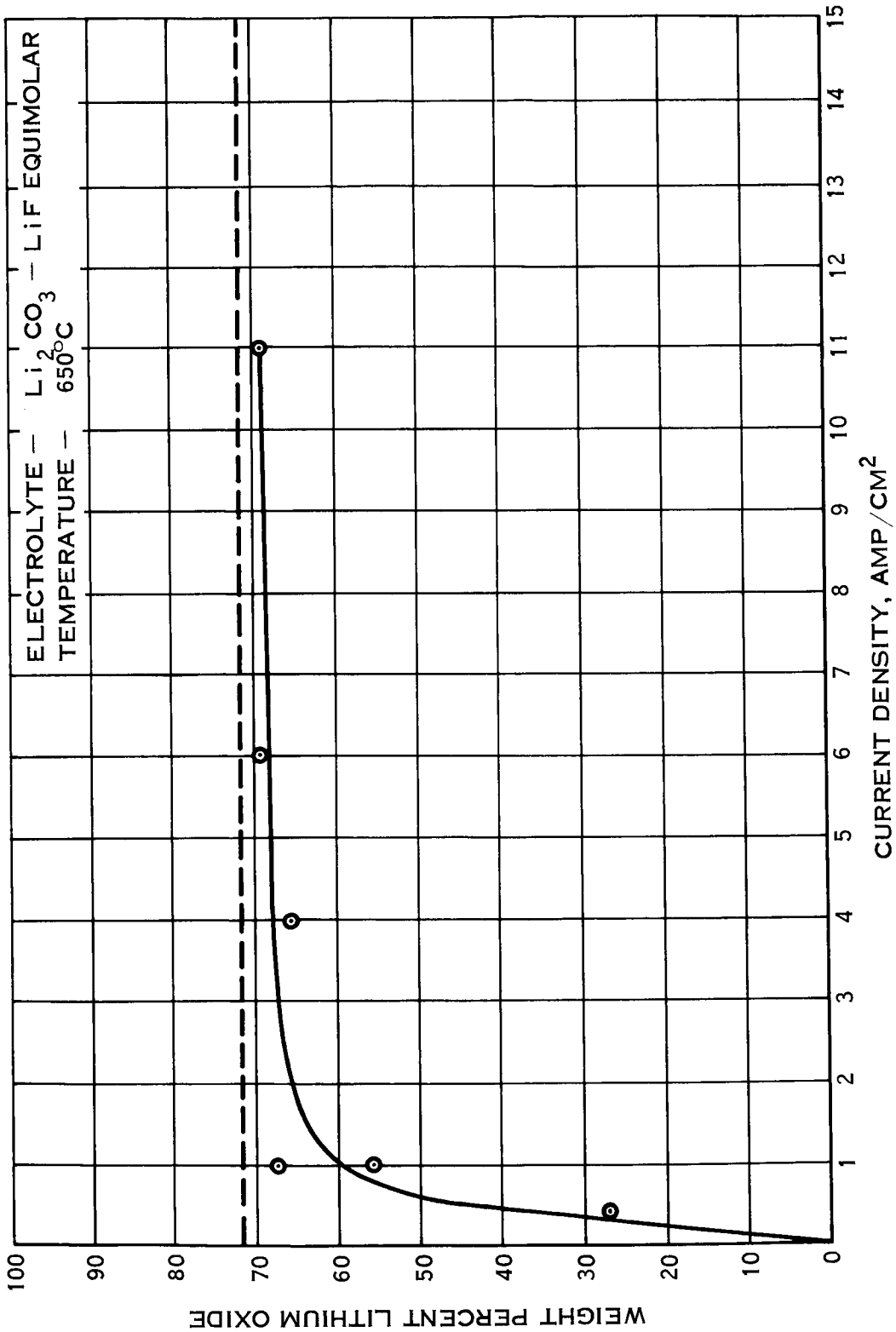

FIGURE 5-22 CATHODE LITHIUM OXIDE CONTENT SHOWING DEPENDENCE ON CURRENT DENSITY

Number	Melt	Current Density ma/cm	Cathode	Temperature °C	% C	Agitation
8-2	$LiF-Li_2CO_3$	10	C	700	4	None
8-3	$LiF-Li_2CO_3$	10	C	785	35	None
8-4	$LiF-Li_2CO_3$	10	C	700	21	Ar Bubbling
11-5	$LiCl-Li_2CO_3$	10	C	680	37	None
11-6	$LiCl-Li_2CO_3$	10	C	585	9	None
5-2	$LiF-Li_2CO_3$	10	Ni	800	8	None
U-5-1	$LiF-Li_2CO_3$	10	Ni	750	40	Rotation
U-5-2*	$LiF-Li_2CO_3$	10	Ni	750	34	Rotation

FIGURE 5-23 EFFECT OF TEMPERATURE AND AGITATION

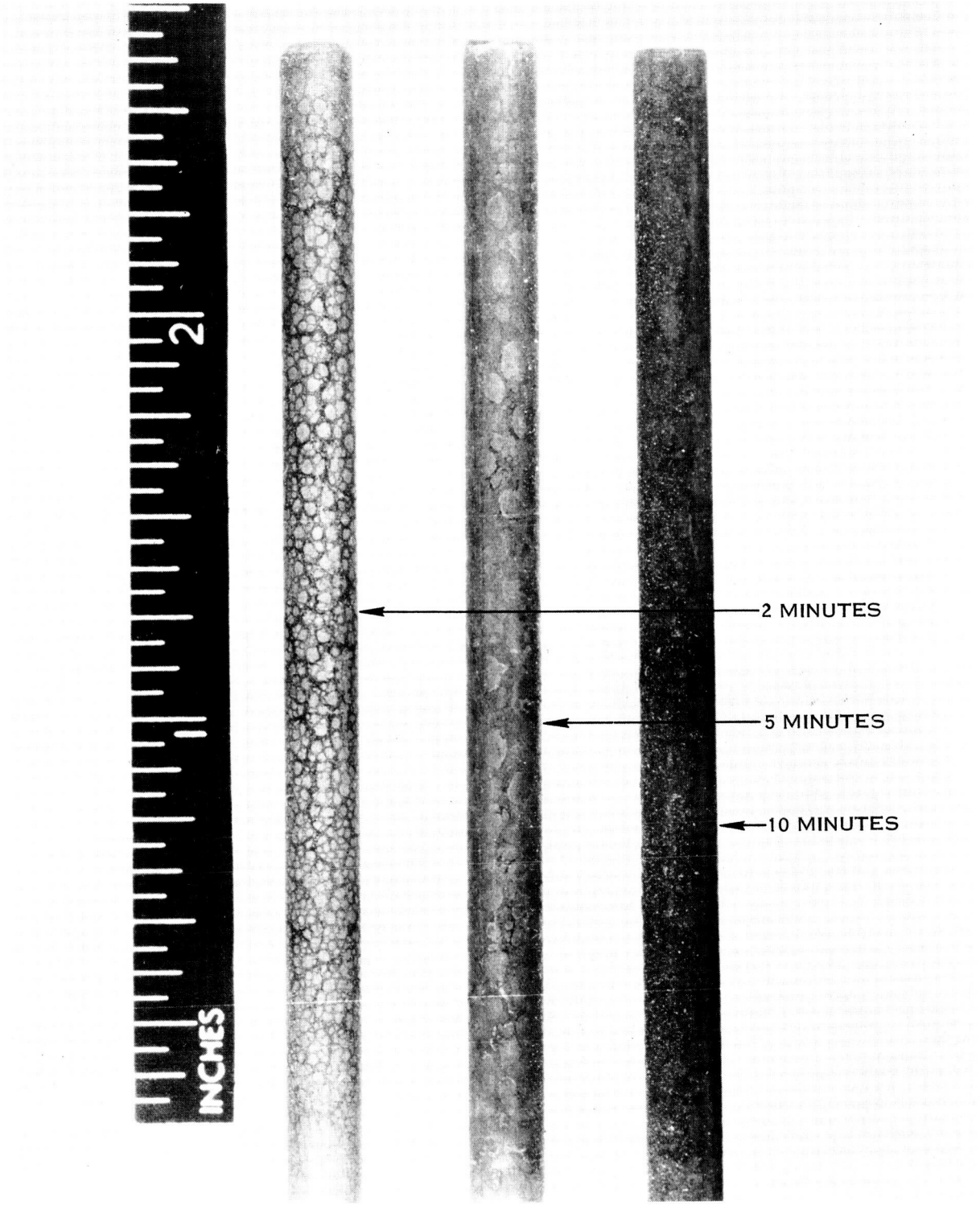

FIGURE 5-24 CARBON GROWTH PATTERN

Electrolyte: Li_2CO_3-LiCl Equimolar Mixture

Temperature: 700°C

Counter Electrode: Gold

NOTE: Arrows show direction of external current between coupled combinations.

Current Imposed on Coupled Electrode (ma)	Atmosphere: Argon	Atmosphere: Air
Anodic, 15	C ← Au	C ← Au
15	C ← Ni	C → Ni
15	C → Fe	C → Fe
0	C ← Au	C ← Au
0	C ← Ni	C → Ni
0	C → Fe	C → Fe
Cathodic, 30	-	C → Fe
30	-	C → Ni
40	-	C → Fe
40	-	C → Ni
60	C → Au	C → Au
60	C ← Fe	C ← Fe
60	C → Ni	C → Ni
100	-	C ← Fe
100	-	C ← Ni
120	-	C ← Fe
120	-	C ← Ni

FIGURE 5-25 CURRENT DIRECTION BETWEEN METAL AND CARBON COUPLES USED AS EITHER ANODE OR CATHODE

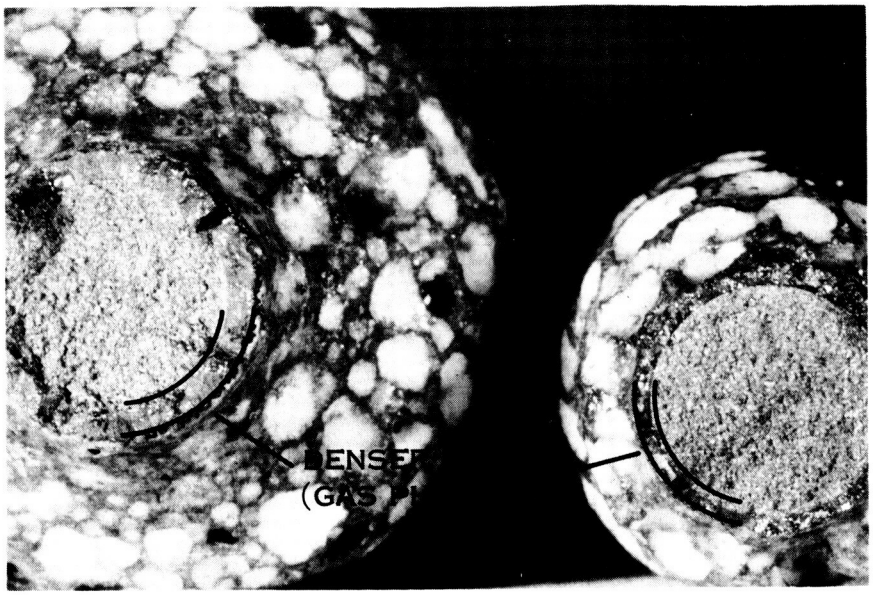

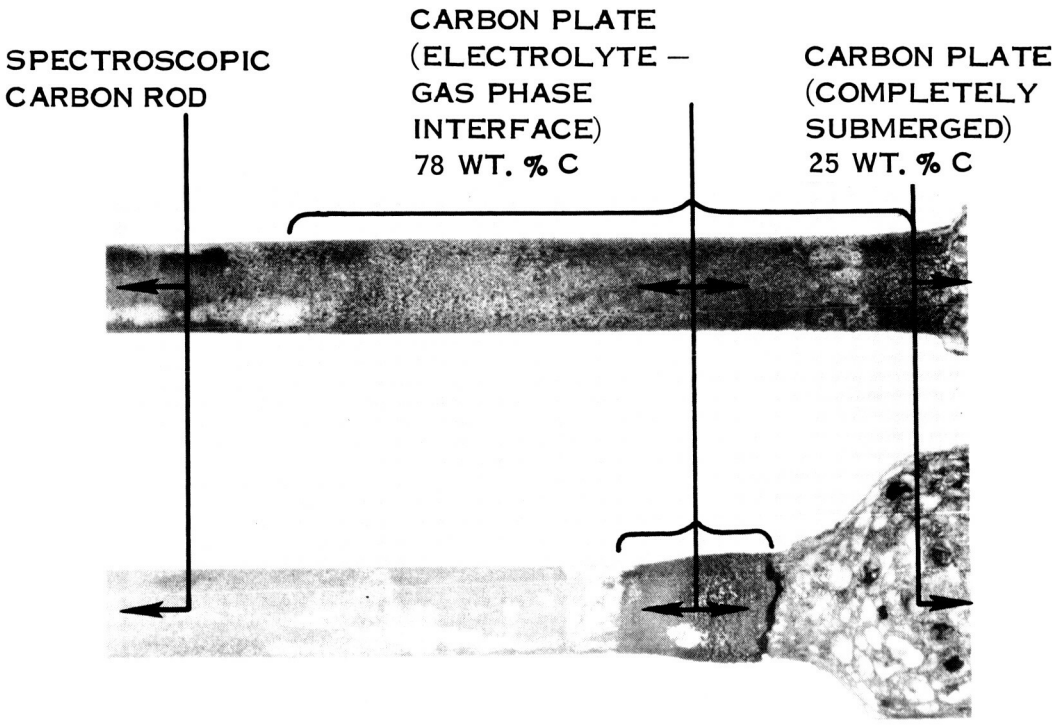

FIGURE 5-26 THIN FILM CATHOLYTE STUDIES

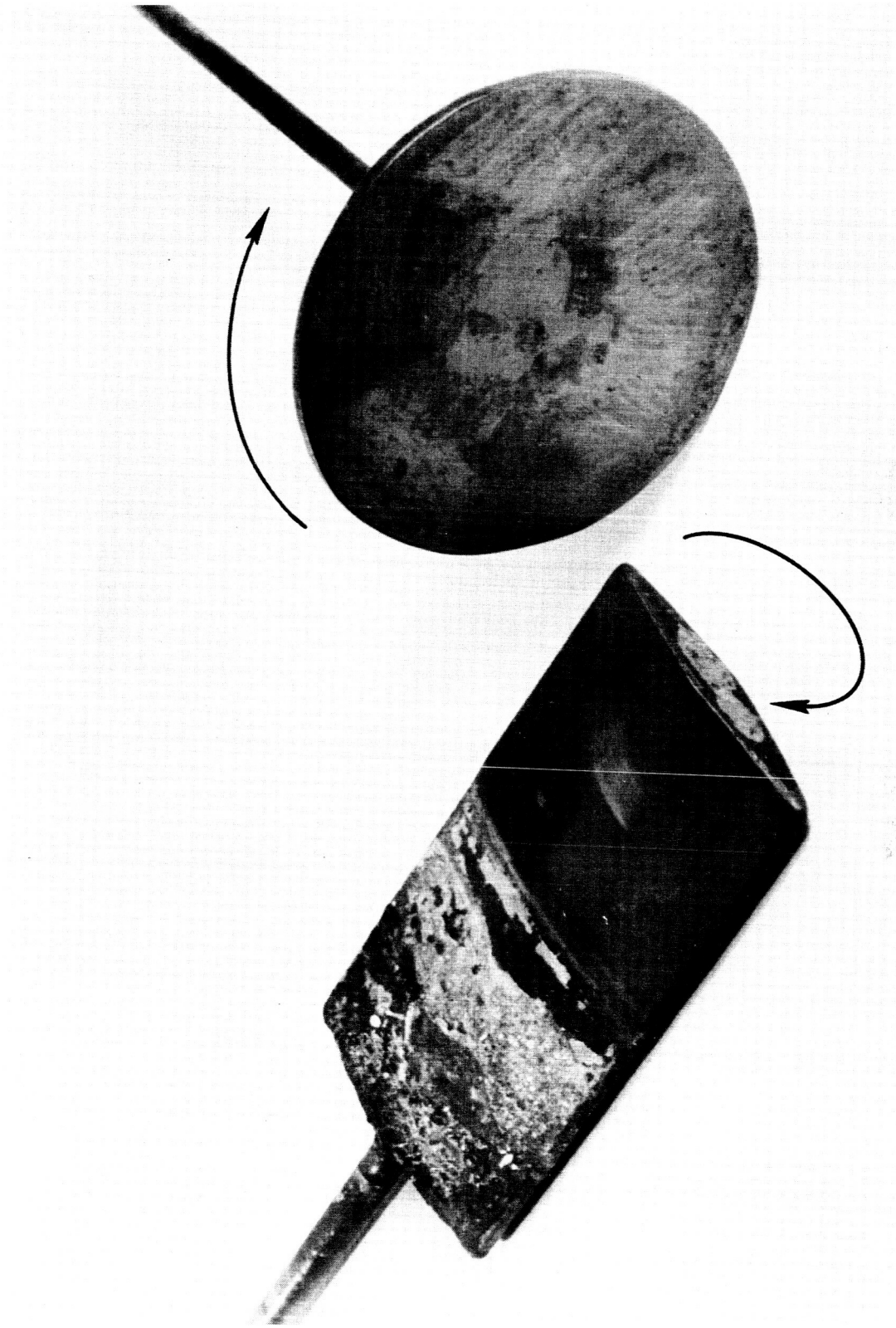

FIGURE 5-27 ROTATED CATHODES

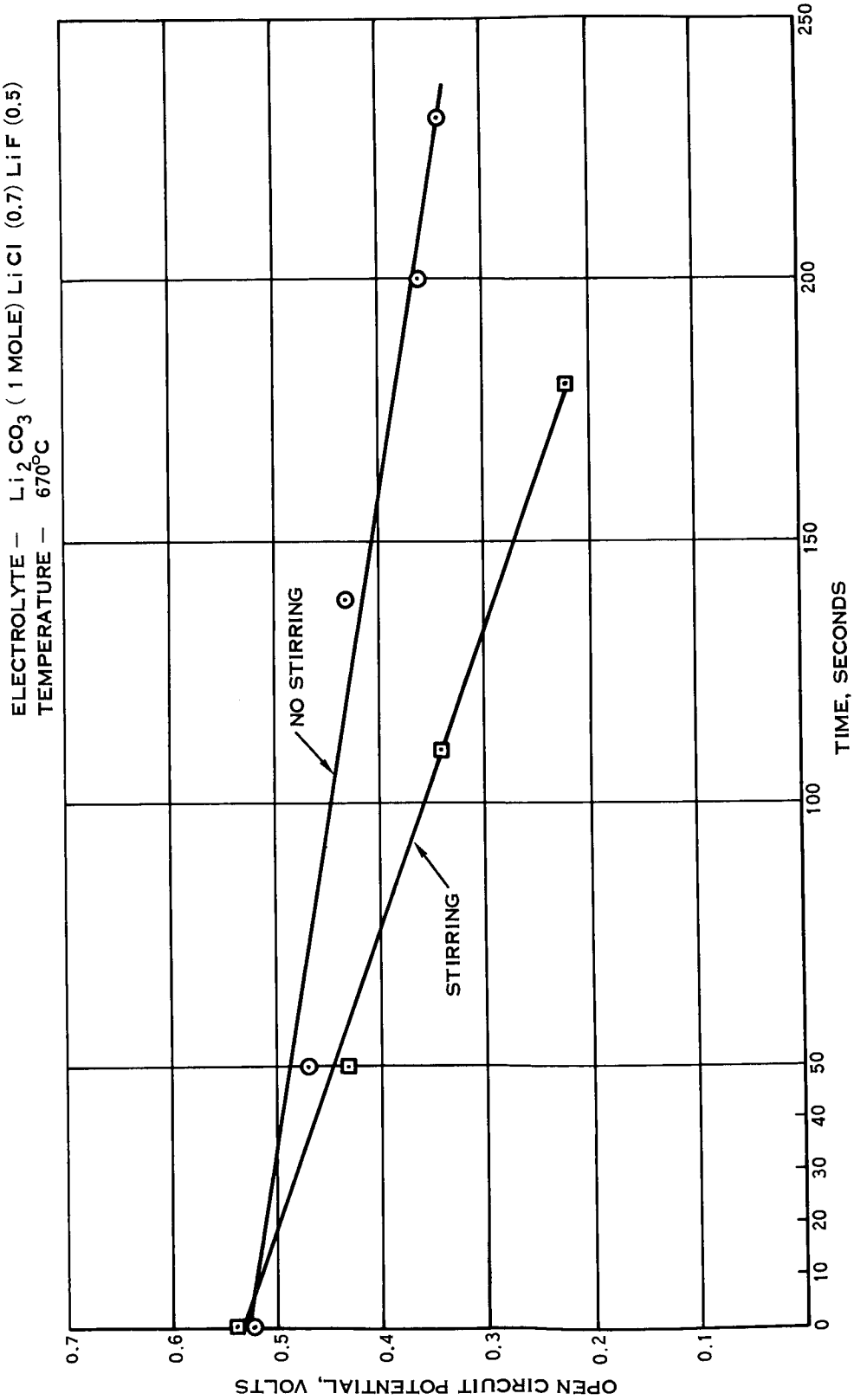

FIGURE 5-28 EFFECT OF ELECTROLYTE AGITATION ON OPEN CIRCUIT DECAY RATE

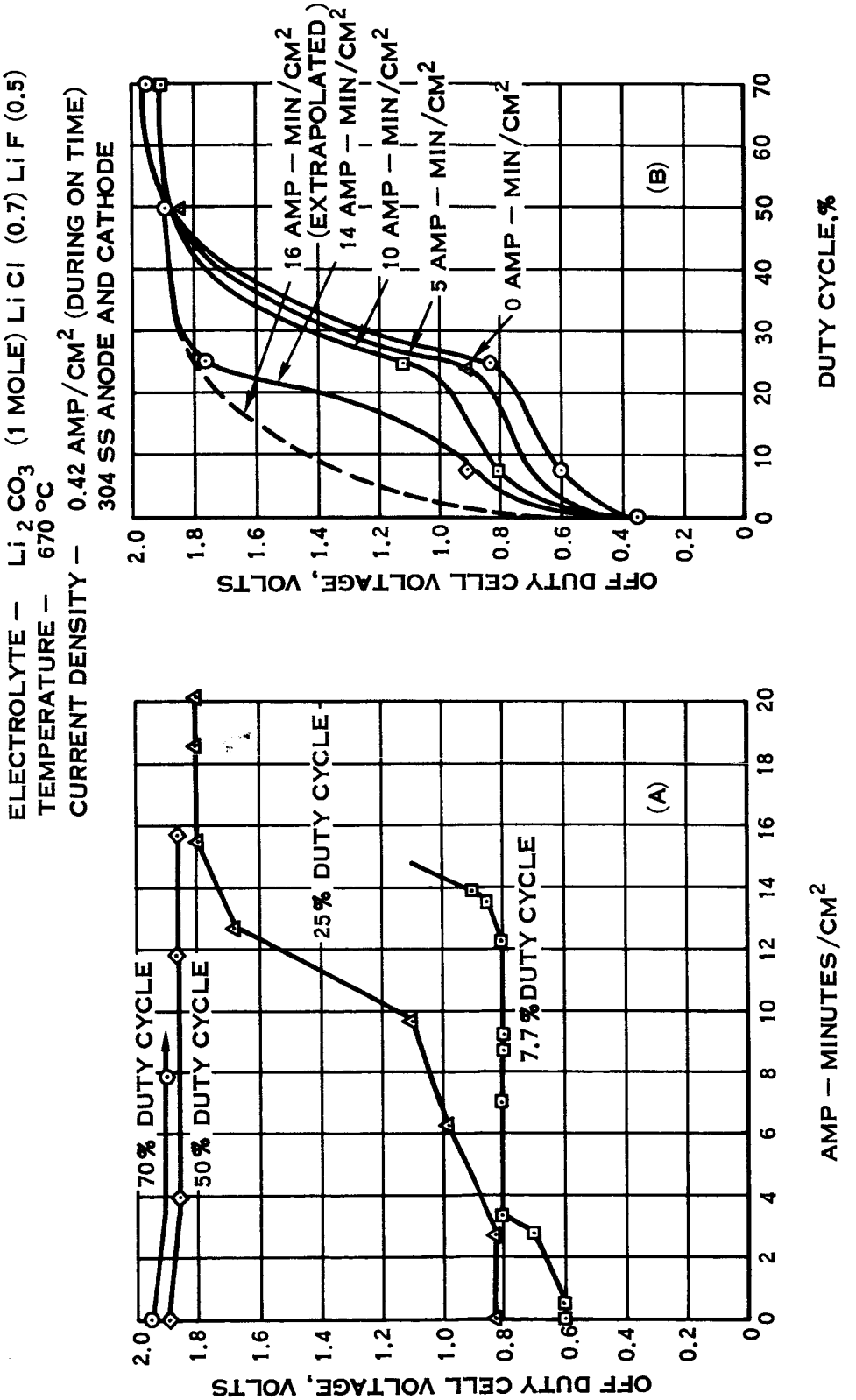

FIGURE 5-29 OPEN CIRCUIT POTENTIAL CHANGE (OXIDE ACCUMULATION) WITH DUTY CYCLE AND ACCUMULATED CURRENT

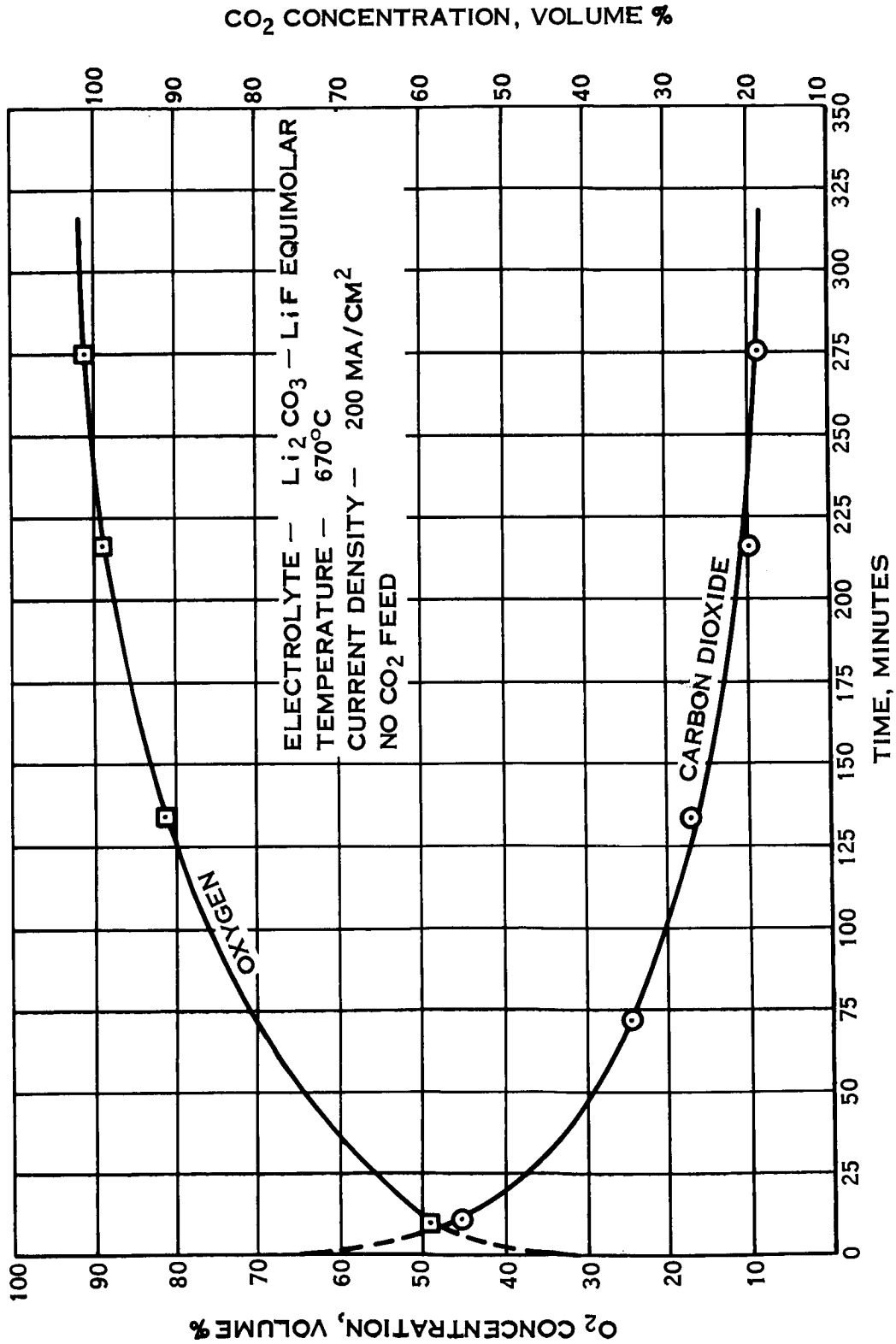

FIGURE 5-30 ANODE EFFLUENT GAS COMPOSITION FROM START OF ELECTROLYSIS

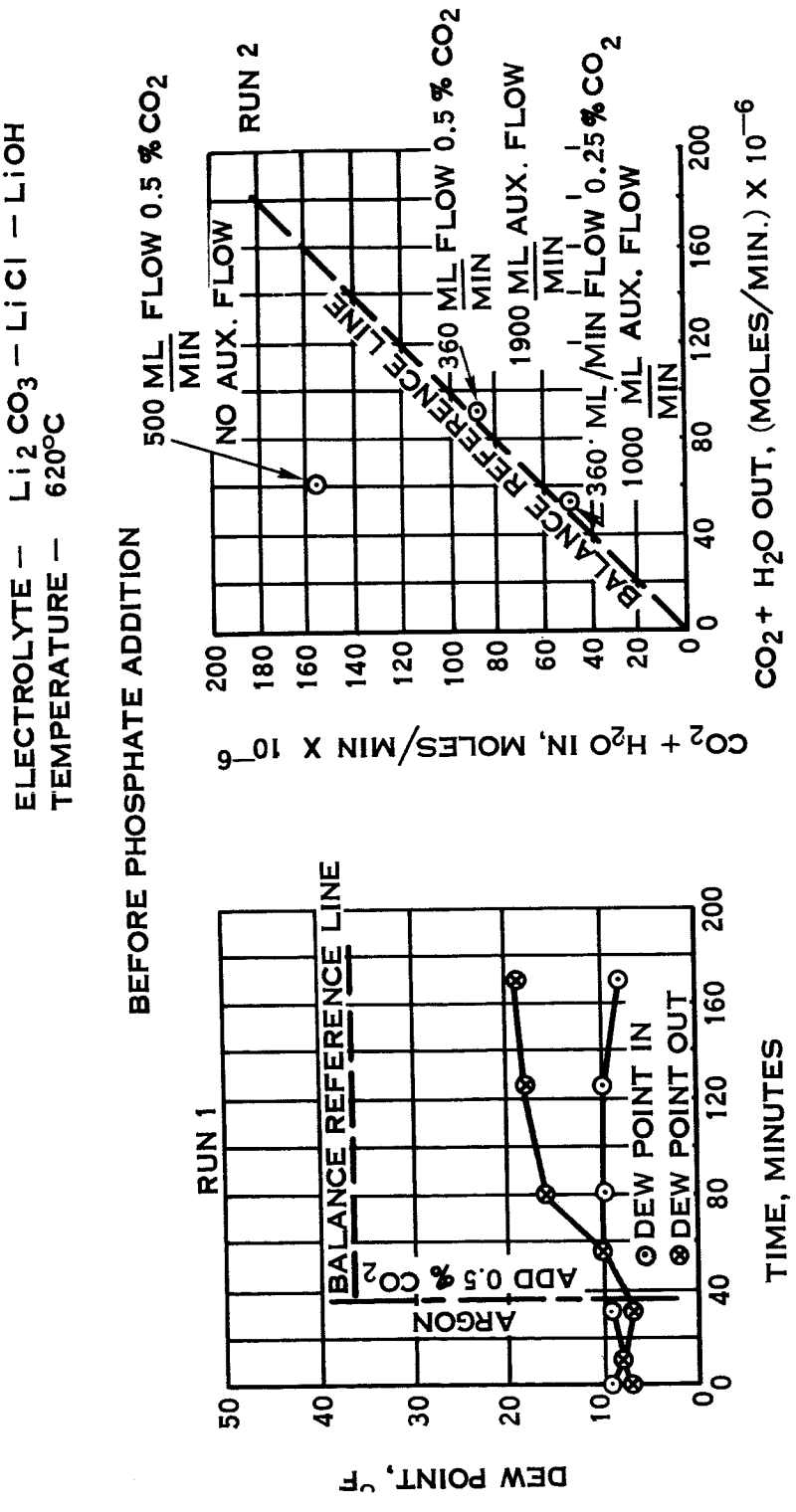

FIGURE 5-31 INPUT-OUTPUT BALANCE STUDIES BEFORE PHOSPHATE ADDITION

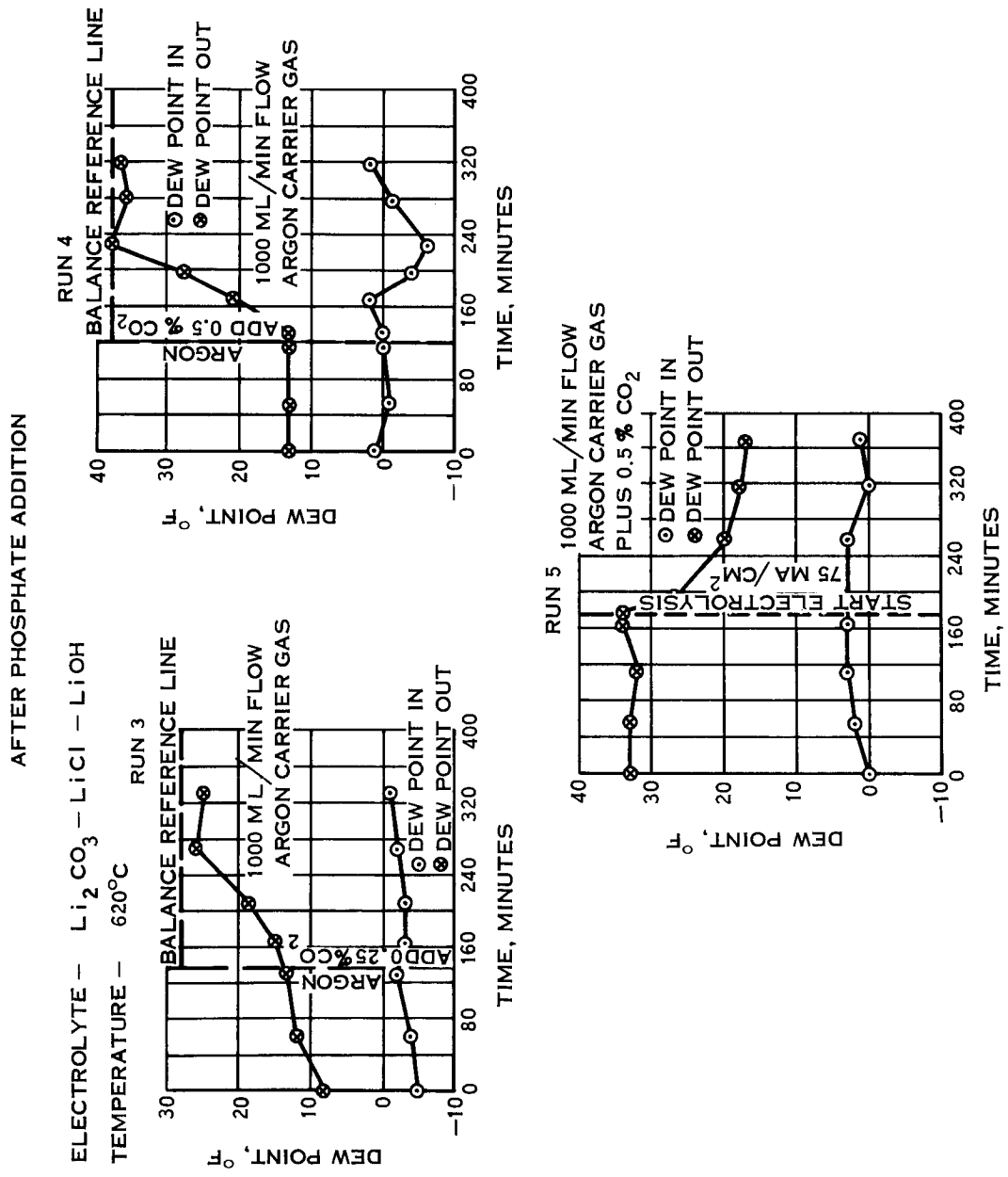

FIGURE 5-32 INPUT-OUTPUT BALANCE STUDIES AFTER PHOSPHATE ADDITION

6.0 ELECTRODE REACTION STUDIES

6.1 Steady State Current-Voltage Relationships

6.1.1 Characteristic Cell Potentials

A study of current-voltage relationships has formed a major part of the research program. These relationships were investigated to determine reduction and oxidation potentials associated with carbon deposition, oxygen discharge, and with other possible electrolysis by-products so that wanted and unwanted cell operating conditions might be sorted out, as well as to ascertain the cell voltage which will be necessary to maintain a given current in a practical electrolytic cell.

To determine steady state current-voltage relationships, voltage to the electrolytic cell was set at a given level and the current allowed to come to equilibrium. After noting the current, the voltage was reset to the next higher level, and so on. By this means, a current-voltage relationship could be plotted. In a later section, rapid potential sweep techniques will be treated.

Applied cell potentials at which the rate of increase in current rose sharply as potential was systematically increased were used to mark the occurrence of major events in the electrolysis process. Such potentials have been termed herein reduction potentials when referring to the events at the cathode, and oxidation potentials when referring to the anode processes. These two potentials have numerical significance only when they are referred to a specific and known reference potential. Where no such reference is available, as was the case in the initial experiments now to be described, the potentials at which current surges occur have been termed characteristic cell potentials, and these potentials pertain only to specific electrolysis cells and operating conditions.

The first series of current-voltage measurements were made in a LiCl+10 weight percent Li_2CO_3 electrolyte using wet and dry argon/CO_2 atmospheres and carbon electrodes. The cell current-voltage plot could be broken down into two straight line portions - as cell voltage was increased step-wise, a steady very slight current rise, then a current surge. The intersection of these lines (near the elbow of the plot) occurred at 0.8 and 1.1 v, respectively, in the wet and dry systems.

For comparison, similar studies were carried out in which wet and dry argon and argon/CO_2 atmospheres were passed over LiCl without initially added carbonate as shown in the following tabulation.

6.1.1 (Continued)

Run No.	Temp. (°C)	Melt Composition	Atmosphere	Potential at Current Surge
24-4	630	LiCl + 10 wt % Li_2CO_3	Ar(380 mm), CO_2(380 mm)	1.1 v
24-6	630	LiCl + 10 wt % Li_2CO_3	Ar(380 mm), CO_2(360 mm), H_2O(20 mm)	0.8 v
26-1	650	LiCl	Ar(760 mm)	2.9-3.1 v
26-2	650	LiCl	Ar(380 mm), CO_2(380 mm)	2.3-2.4 v
26-3	650	LiCl	Ar(380 mm), CO_2(360 mm), H_2O(20 mm)	1.5-1.7 v
26-4	650	LiCl	Ar(760 mm)	1.9-2.4 v

With dry argon above this system a single current surge was observed at 2.9-3.1 v which was attributed to lithium metal deposition. When CO_2 was added to the argon this potential decreased to 2.3-2.4 v; humidification of this mixture further reduced the potential to 1.5-1.7 v. After returning to a dry argon atmosphere (Run 26-4), the current-voltage curve indicated a current surge at 1.9 v which was associated with a limiting current followed by a second current surge at 2.6 v. The addition of one mole percent Li_2O to the electrolyte and subsequent exposure of the electrolyte to an argon/CO_2 atmosphere lowered the potential to the level noted in the 10 weight percent Li_2CO_3-LiCl mixture, about 1 v. Thus, these data indicated that in a pure lithium chloride system with carbon electrodes, lithium was discharged at a cell voltage of about 3 v. When appreciable carbonate was present, carbon was deposited at a much lower characteristic cell potential of 0.8-1.1 v. At intermediate carbonate concentrations resulting from electrolyte exposure to dry and humidified CO_2, the characteristic cell potential was seen to vary with carbonate concentration, a limiting current and higher potential being observed as concentration diminished. This latter observation is in accord with experience in aqueous system polarography for a non-reversible cell process. In the present case carbon is irreversibly deposited at the cathode. It should be noted also that in this particular system where carbon electrodes are employed, the carbon anode can be oxidized when the electrolyte contains sufficient carbonate, which would contribute to a lower cell potential.

6.1.2 Isolation of Anodic and Cathodic Components

In view of the wide shifts in characteristic cell potential with gas

6.1.2 (Continued)

phase changes as noted above it becomes necessary to observe specific effects on each electrode of changes in the experimental conditions. For example, under certain conditions the anode might be relatively unaffected by changes in P_{CO_2} or P_{H_2O}, while changes in cathode potential prove largely responsible for shifts in the overall cell potential. In order to do this it is helpful to use an auxiliary electrode as a reference potential. This electrode does not carry any current. The potential difference between this reference electrode and the cell working electrodes are measured and plotted against the current passing between the working electrodes. The sum of potential differences between reference electrode and each working electrode at all times adds up to the overall cell potential. Thus it is possible to distinguish if one working electrode, anode or cathode, is more heavily involved in overall cell potential changes by observing the fractional change in contribution to the overall cell potential.

Anodic and cathodic polarograms for $LiCl-Li_2CO_3$ and $LiF-Li_2CO_3$ eutectic electrolytes are presented in Figure 6-1.[3] The electrode potentials in this instance are referenced to a submerged graphite rod. The use of graphite as a reference has been treated earlier in Section 4.9 and is discussed further later in this section. In this case a nickel anode, permitting oxygen discharge, and a carbon cathode were utilized as working electrodes. A characteristic cell potential of about 2.2 v was observed for the chloride-carbonate eutectic where 1.4 v was associated with the anode and 0.8 v with the cathode. It is interesting to note that if the anode were carbon, the oxygen would oxidize the carbon to form carbon dioxide rather than be discharged and thereby reduce the observed anode voltage by about a volt. Reducing the observed 2.2 v cell potential by one volt would give a value of 1.2 volts which is in fair agreement with that obtained in the all carbon electrode system previously described for a similar chloride-carbonate system. Electrode potentials proved less in the fluoride-carbonate system; cell operating temperatures, on the other hand, were much higher. Effect of temperature will be described later in this section.

6.1.2.1 Effect of Gas Phase Composition

Data on effects of gas phase composition on current voltage relationships were obtained in a cell using a small Au-Pd crucible for containing the electrolyte and Au-Pd electrodes. The working anode and cathode were fitted with Al_2O_3 sheaths for convenient control of the electrode atmospheres, and a Au-Pd wire was used as an auxiliary electrode. This electrode is not a true reference but may be used as a potential base. The difference in potential

6.1.2.1 (Continued)

between the auxiliary and the working electrode when at zero current has been used as a correction factor. It has been found that this voltage difference is stable and can be reattained after each run. The operating procedure is the same as that described in the preceding section. The physical test setup is described in Section 7.1.4.

Current-voltage curves showing the effects of a dry or wet argon/CO_2 mixture over a Li_2CO_3-LiCl eutectic mixture are shown in Figure 6-2. A large part of the potential shift observed when water is added to the system is due to a change in the cathode potential. It is not possible to tell whether this shift is caused by a change in the nature of the reacting species at the cathode or is merely a change in potential due to a shift in the concentration of the reacting species. For instance, it has already been shown that equilibrium considerations require that P_{CO_2} increase when P_{H_2O} is increased in a carbonate system; the resulting increase in P_{CO_2} at the cathode could change the cathode potential rather than P_{H_2O}.

The low current cathodic wave at -0.4 to -0.5 volts seen in Figure 6-2 is similar to one which has been attributed to direct CO_2 reduction by Janz and Ingram (Reference 8) according to:

$$CO_2 + 2e^- \longrightarrow CO + O^=$$

These authors report that electrolysis at cathodic potentials in this range does not produce carbon, indicating that the CO produced is not reduced any farther. The explanation involving direct reduction of CO_2 is probably not necessary, since partial reduction of the carbonate would be adequate to describe the process. The anode shift in this electrolyte is small.

Results upon exposure of pure LiCl electrolytes to atmospheres containing CO_2 and water are shown below.

Effect of CO_2 and H_2O on Electrode Potentials in Pure LiCl

Number	Gas	Electrode Potentials Cathode	Anode
29-1	Argon	-2.75	+0.11
29-2	Argon + P_{CO_2} = 30 mm	-2.15	+0.32
29-3	Argon + P_{CO_2} = 250 mm	-2.00	+0.26
30-1	Argon	-2.10	+0.28
30-2	Argon + P_{H_2O} = 20 mm	-1.56	+0.23

6.1.2.1 (Continued)

Conditions: Temperature - 630°C
Electrodes - Au-Pd

The sequence of Runs 29-1, 29-2 and 29-3 illustrate a decreasing cathodic potential as P_{CO_2} is increased, again with no perceptible pattern of change at the anode. It is believed that the primary anodic process in this high chloride system is the dissolution of the metal anode, even in the presence of the small amount of carbonate during CO_2 exposure which appears sufficient to affect the cathodic processes. Runs 30-1 and 30-2, illustrating the effects of moisture, were carried out in a freshly prepared electrolyte. The initial dry argon atmosphere run indicated this electrolyte to be somewhat less pure than was the case in the preceding carbon dioxide series; note potential discrepancies. A large effect on the cathodic potential is found which must be attributed to water or hydroxide since no carbonate is present in the system. An increase in anodic potential is observed, but no significance has been related to this.

Traces for the dry argon CO_2 runs are reproduced in Figure 6-3. It is interesting to compare the potential difference between Curves 2 and 3 in Figure 6-3 with the theoretical difference in potential predicted by Equation 4-18, Section 4.3, considering CO_2 pressures of 250 mm and 30 mm at 630°C. The measured difference is 150 mv, while the difference calculated from the pressure ratio is 124 mv. While better agreement has been obtained in later experiments, where shielded probe and reference electrodes permitted more precise control of electrode environments, this comparison nevertheless attests to the semi-quantitative validity of the experimental technique.

The cathodic and anodic processes in a cell can alternatively be separated by making one of the cell electrodes very large compared with the other. This means that the current density at the large electrode is very low compared with that at the smaller electrode, which is more readily polarizable and is the determining electrode in observed changes in current-potential relation.

Cathodic polarograms, where the cathode was small relative to the anode, have been obtained, showing the effects of different blanket gases. These polarograms, obtained by alternating the gas phase back and forth between dry air, dry CO_2, and dry helium are shown in Figure 6-4 for a lithium carbonate-chloride base electrolyte. Curve 3 for dry helium serves as a base line for comparing the

6.1.2.1 (Continued)

effect of the other gases. Curve 2, showing the effects of a dry CO_2 atmosphere, begins to rise in current at a lower potential than the dry helium base line curve. This has been attributed to the presence of high P_{CO_2} at the cathode which results in CO evolution at a lower CO_2 potential than for carbon deposition. Curve 1, showing the effect of a dry air atmosphere shows a current surge appreciably before the other two. This effect may be due to oxidation of the carbon deposit when present but is believed to be due more likely to direct oxidation of atomic lithium or its equivalent when highly susceptible during the postulated electrochemical reduction step for carbon deposition at the cathode.

6.1.2.2 Temperature

The technique of a small cathode and a large anode has likewise been applied to a study of the effects of temperature and the presence of metal ions in the electrolyte on observed cathode reduction potentials. The effect of temperature on the cathodic current-voltage relationship is quite pronounced, as shown for the ternary carbonate eutectic (Li, Na, K) in Figure 6-5. Curves 1 through 5 show the effect of decreasing electrolyte temperature. Carbonate decomposition potential varies from about 0.4 at 790°C all the way to about 1.8 at 470°C. It is evident from these results that different systems are not easily compared unless operating temperatures are identical. Furthermore, in systems being operated near eutectic melting temperatures, ionic activities are prone to change appreciably with relatively small temperature changes.

6.1.2.3 Metal Deposition

The effect of adding 0.5 mol percent $CoCl_2$ to a $LiCO_3$-LiCl eutectic base electrolyte on cathode current-voltage relationship is shown in Figure 6-6. Cobalt metal is found to be deposited and the deposition potential is observed to be about 0.7-0.8 v. Nickel deposition voltage, not as clearly detectable in other studies, appeared to be about 0.85 v. These values will vary with electrolyte halide-oxyanion ratio, and halide type, as would be expected from prior anion diluent discussions (Section 5.2.2) depending on the changes in ionic activities, and possibilities for complex formation.

6.2 Fast Sweep Polarography

Steady state current-voltage relationships as have been described often do not show the effects of electrolyte species present in extremely small concentrations. The use of a fast potential sweep permits a scan before diffusion rates of ionic species limit and

6.2 (Continued)

diminish the current achievable, as is the case in the steady state polarography. Thus, reactants present in small concentrations can be observed as substantial current peaks when current is observed and plotted during a fast sweep in potential. To this end an Anatrol Variable Sweep Potentiostat has been used as a power supply in conjunction with a Mosely X-Y recorder. Sweep times as low as 5 seconds can be achieved over a selected voltage range, although the data which will be presented were obtained with a sweep time of 20 seconds. All figures which are shown here are reproductions of the direct tracings.

The fast sweep studies have encompassed a wide variety of operating conditions and electrolyte compositions and have been repeated many times under each set of conditions. The data presented in this report were selected to show specific effects that can be interpreted in a qualitative manner.

The data can best be analyzed by separating the cathodic and anodic studies. Anodic and cathodic sweeps were performed using the same electrode in each case; in this way it is possible to see the removal of reaction products from the electrode when the sweep is reversed and to identify the peaks obtained, since many of them disappear after several runs.

6.2.1 Cathodic Studies

Summaries of typical cathodic curves in several different electrolytes are shown in Figures 6-7 through 6-12. The data were chosen to show the effect of the cations present in the melt, the relationship of the atmosphere above the melt to the behavior of the cathode, and the structure in the cathodic curves in the light of some of the observations made in the equilibrium current-voltage studies.

6.2.1.1 Effect of Cationic Species on Carbonate Reduction Potential

The effect of the cations present in the melt can be seen by comparing the cathodic traces in Figures 6-7 through 6-11. In systems where lithium is the only cation the curves show structure similar to that obtained in the equilibrium studies (Figure 6-7, Curve 1).

The $NaCl-Na_2CO_3$ system (Figure 6-8) shows essentially the same polarographic behavior as the lithium system when P_{CO_2} pressure is low (Curve 1): at a higher P_{CO_2} pressure (Curve 3) an initial reduction potential is observed starting at 0.5 v which has been attributed to carbonate reduction to CO. A limiting current is

6.2.1.1 (Continued)

reached at 1.75 ma, as the cathode potential shifts toward the voltage for solid carbon deposition. At a still higher P_{CO_2} no limiting current is observed and CO production appears to be the predominant cathodic process.

When potassium cations are added to lithium cation systems, the cathodic curve remains substantially the same, Figure 6-9, as for the all lithium system. In an all potassium system, however, as shown in Figure 6-10, curves resembling the sodium system with CO production are again observed.

6.2.1.2 Effect of P_{CO_2} on Carbonate Reduction Potential

Some effects of gas CO_2 partial pressure on carbonate reduction potential in a sodium system were shown in Figure 6-8 . These showed a lowering of reduction potential which was attributed to CO being produced rather than carbon. A similar decrease in potential for a lithium carbonate-chloride eutectic as a result of increasing P_{CO_2} is shown in Figure 6-11, again attributed to reduction of CO_2 carbonate partially to CO, though not nearly to as great an extent as was observed with the sodium system.

In this latter lithium system where carbonate content of the electrolyte is relatively high, effects caused by increase in P_{CO_2} were less than that which was evident in low carbonate systems such as was shown in Figure 6-3 for a LiCl system where only small amounts of carbonate were formed on exposure to CO_2. This would be expected since when initial carbonate content of the electrolyte is high it would be anticipated that overall system equilibria involving species other than carbonate would not be changed so readily with comparable increases in P_{CO_2}.

6.2.1.3 Current-Voltage Peaks Not Associated with Carbonate Reduction

In several instance peaks were obtained in the cathode curves which were not related to carbonate reduction. A peak at 0.4 volts was observed in the LiCl-KCl eutectic mixture containing low carbonate where a potential of about 1.4 was assigned to carbonate reduction. This peak increased when oxide was added or when P_{CO_2} was lowered. The peak was usually present as a broad bulge, as shown in Curve 1, Figure 6-12, and decreased after several cathodic sweeps were made. Lowering the CO_2 pressure accentuated this peak as shown in Curve 3, of that same figure. When the CO_2 pressure was held at this level the peak height was stabilized.

A peak at nearly the same potential is also apparent in the Li_2CO_3-

6.2.1.3 (Continued)

LiCl eutectic (Figure 6-7, Curve 1). This peak has been found to be present in most of the lithium containing melts used, but it is seen only after a series of anodic runs and then disappears. It appears to be associated with the removal of an oxide layer from the surface of the electrode before the deposition of carbon at 1.5 v. Oxide formation may be possible during a cathodic sweep, since the initial potential is almost always an anodic one which then proceeds in the cathodic direction. Once a carbon layer is formed this lower potential peak is not evident. This is as would be expected even if sweeps are started at anodic potentials, since the reaction would involve oxidation of carbon to form CO_2 with no oxide film formation. The fact that the peak persists in the case of the KCl-LiCl system, even after several cathodic runs, may be explained on the basis of poor carbon adhesion in this system, thus leaving the electrode material exposed for further reaction.

6.2 Anodic Studies

Polarographic studies of the anode were performed to ascertain effects of electrolyte composition and gas phase constitution on the oxygen discharge process and on anode stability. The behavior of different metals when used as anodes were also investigated.

6.2.2.1 Effect of Cationic Species and Anionic Diluents

Anodic curves for several electrolyte systems are shown in Figure 6-13. The tracings in general show, as anodic potential increases, a typical anode dissolution region, followed by a passive region, and then a final transpassive region where current surges off scale. These regions are so noted in the figure. Anode passivity is generally achieved at a little over 1 v. No passive region is evident in the all sodium system, Curve 4. The LiF-Li_2CO_3 system, Curve 3 seems to exhibit a more discernable passive region than does the LiCl-Li_2CO_3 system. However, further tracings of the chloride-carbonate system, such as in Figure 6-14, show a more obvious passive region which compares more favorably with the fluoride system. The sequence of tracings shown in Figure 6-14 for the LiCl-Li_2CO_3 system show what is believed to be the buildup of a passive oxide coating on the anode, since the anode dissolution peak is seen to get progressively smaller. Oxide coatings found on working anodes were noted in an earlier discussion of anode process experiments, Section 5.2.2.

6.2.2.2 Anode Substrate Materials

Relative effects of electrode materials on anodic current-voltage

6.2.2.2 (Continued)

relationships are shown in Figure 6-15 for a Li_2CO_3-LiF eutectic mixture. The tracings are quite similar, although platinum shows less of an anode dissolution peak and a more flat passive region than either the gold or gold-palladium. Platinum operated in the passive region would probably be the preferred choice of these three materials in this particular electrolyte system.

A similar tracing for a nickel anode in the same electrolyte is shown in Figure 6-16. Again a passive region is noted in the curve at a slightly lower anodic potential range than was seen for the other metals. Nickel has in practice proved long lived when operated in systemssuch as this at appropriate current densities.

6.2.2.3 Peak for Oxidation of Cathodic Deposit

It is interesting to note that when an anodic run is made after a series of cathodic runs a peak is noted prior to the anode dissolution peak. After one or two anodic sweeps this curve disappears. Such a peak is shown in Figure 6-17, Curve 1, at about 0.2 v for a LiCl-KCl eutectic containing 1 mol percent Li_2CO_3. It is not found in the second anodic sweep in this case, Curve 2.[3] This peak has alternately been ascribed to oxidation of deposited carbon and to oxidation of alkali metal which has alloyed with the electrode. Curve 1 in Figure 6-14 for instance showing the large peak at 0.2 v showed some carbon before the first anodic run which was no longer present after Run 3.

6.2.3 Implications of Fast Sweep Studies

The cathodic process is shown to be a function of oxide ion and CO_2 levels in the electrolyte and is greatly influenced by humidity and the presence of oxygen gas (air). Systems with predominantly lithium cations are shown to be less prone to CO formation than are sodium and potassium systems. The choice of a cathode material has made little difference in observed current-voltage relationships.

The anode reaction appears straightforward at moderate current densities (below 200 ma/cm^2). Selection of an anode material which may be used for sustained periods should be possible in an electrolyte system containing a substantial amount of carbonate.

6.3 Reference and Probe Electrode Studies

Because a finite range of oxide ion concentration at the cathode appears to be conducive to the deposition of high density carbon,

6.3 (Continued)

a means for measuring oxide ion concentration at the cathode and elsewhere in the electrolyte has been sought. It had been frequently observed that a carbon deposit with occluded oxide exhibited a potential different from that of a pure carbon rod. However, a carbon rod just immersed in the melt and used as a reference was subject to potential shifts depending on the atmosphere above the melt, and the reference base line shifted each time the melt composition was altered. Thus a more constant reference electrode proved the object of initial investigations. To this end metal oxide-oxygen gas references were studied and later a carbon rod with a controlled P_{CO_2}-oxide-carbonate environment.

6.3.1 Metal Oxide/Oxygen Reference

The voltage differential between a metal probe electrode and an oxygen reference electrode comprising nickel, platinum or gold metal over which oxygen gas was bubbled was initially evaluated as a technique for measuring oxide ion concentration in the electrolyte. Figure 6-18 shows a typical plot of the potential between the nickel and gold experimental oxygen reference electrodes and separate probe electrodes when CO_2 in argon was flushed over the probe electrodes to change their local electrolyte environment. A positive and predictable response to P_{CO_2} changes at the variable P_{CO_2} electrode was noted. However these oxygen reference electrodes did not prove stable or free from potential fluctuations caused by changing electrolyte composition, although each did prove satisfactory for temporary usage under restricted environmental changes. Nickel behavior depended upon the presence or absence of a stable oxide coating, but it was not possible to insure that one or the other condition persisted. Gold exhibited a potential which was independent of oxygen pressure and different by about 0.4 v from nickel (of which the potential was dependent on oxygen gas partial pressure, Figure 6-19) leading to the supposition that the gold was really a gold-gold chloride reference. Platinum, when evaluated as a reference with oxygen gas, exhibited abrupt shifts in potential which have not been explained.

In spite of the shortcomings of these reference electrodes attempts were made to measure and estimate the effects of oxide ion concentration at a test electrode (carbon or nickel) when it was passing cathodic or anodic currents. This was done by using the nickel-oxygen gas reference and measuring potential difference between reference and test electrode. With a LiCl-KCl eutectic to which 6 mole percent Li_2CO_3 had been added, probe, test and reference electrodes were installed as shown in Figure 6-20. Electrodes B and D are carbon working electrodes; current density

6.3.1 (Continued)

at each was generally held at 60 ma/cm^2. Electrode C is a nickel tipped test electrode to which current is varied by trickling some off from the working electrodes. It was possible to flush the nickel tip with different gas mixtures when this was desired. Electrode A is a carbon tipped probed electrode through which gas could be bubbled also when desired. Electrode E is the nickel-oxygen gas reference to which the potentials of the other electrodes could be referred, particularly those changes occurring at the test electrode when cathodic and anodic currents to it were varied. It was observed that, when the nickel test electrode was made anodic, it became indistinguishable in potential difference from the nickel oxygen reference when anodic current density was increased beyond a few milliamperes per square centimeter. This indicated possible use of the anode itself as an oxygen reference. In test, it proved possible also to utilize the working cathode D as a reference, for here oxide and carbon appeared to achieve unit activities. Such a cathode condition was obtained in this electrolyte at current densities above 50 ma/cm^2. Data presented in Figure 6-21 show the potential difference between the nickel test electrode and the working cathode (60 ma/cm^2) as a function of small anodic and cathodic currents through the test electrode. The plateaus in the curves which were obtained with differing oxide ion concentrations added to the melt have been attributed to differences in oxide diffusion rate from the test electrode. It was also observed that the isolated carbon electrode immersed in the melt showed a wide difference in potential with respect to the nickel-oxygen and working cathode references depending upon the concentration of oxide ion in the melt, indicating the good possibility of using carbon as a probe electrode.

6.3.2 Carbon/CO_2 Reference

Continued testing and theorizing has led to a carbon/CO_2 electrode for use as a reference. Initial tests involved the use of two identical electrodes, each comprising a 1/8 inch diameter graphite rod encased in a close-fitting alumina tube. A CO_2/argon mixture was passed through the tube and flushed over the graphite tip which was submerged in the electrolyte. The CO_2/argon mixture was held constant at one electrode and varied in the other. A number of experiments were run which showed potential difference was readily related to the varied CO_2 pressures. By isolating the gas bubbling electrodes in small separate alumina wells containing a minimum of melt and allowing ionic continuity to the bulk melt via pinholes in the alumina only, response time to P_{CO_2} changes at the variable electrode were made fairly rapid. It has proved desirable that the carbon-constant P_{CO_2} reference electrode be maintained at a

6.3.2 (Continued)

P_{CO_2} greater than melt P_{CO_2} for satisfactory results, since when CO_2 pressures are lower, equilibrium is more difficult to achieve due to the ready supply of CO_2 from the bulk electrolyte. P_{H_2O} of the gas stream past the two carbon tips has been maintained near equivalent since it was desired that potential difference be attributable only to the oxide/carbonate/CO_2 equilibria. Also, it was necessary to maintain near equal flow through the electrodes so as to minimize potential differences due to flow and/or temperature gradients.

For a number of experimental conditions, it was found that the potential difference is linearly related to log P_{CO_2},

$$E_1 - E_2 = \frac{3RT}{4F} \ln \frac{P_1}{P_2}$$

and therefore to local oxide concentration in accordance with the equilibrium,

$$CO_3^{=} \leftrightharpoons CO_2 + O^{=}$$

Theoretical justification and derivation of this relationship is presented in Section 4.3 . A slope of 3RT/4F is believed to indicate no oxide accumulation or gas formation and is therefore believed to be a necessary condition for the growth of dense cathodic carbon. Figures 6-22 and 6-23 show data with the characteristic 3RT/4F slope.

Further testing showed that the 3RT/4F slope for potential versus log P_{CO_2} was not achieved in all experiments with the reference-probe technique and that a transition in slope to RT/4F commonly occurred when P_{CO_2} was decreased below some limit. Figure 6-24 shows an example of such a transition. It was shown subsequently that further control of moisture was required to extend the P_{CO_2} range for achievement of the 3RT/4F slope (see Section 4.6).

Reproducible slopes of 4RT/4F were consistently obtained over a wide range of probe P_{CO_2} from 0.05-100 percent in argon in a $LiCl-LiF-Li_2CO_3$ mixture at 595°C, Figure 6-25. When this system was purged with dry argon and CO_2, and then lithium oxide added until the moisture content of the outlet gas stream was substantially reduced, a 3RT/4F slope was obtained. It is believed that the 4RT/4F slope is characteristic when gas evolution at the electrode is a prominant feature of the processes going on there, but adequate theoretical justification has not been established.

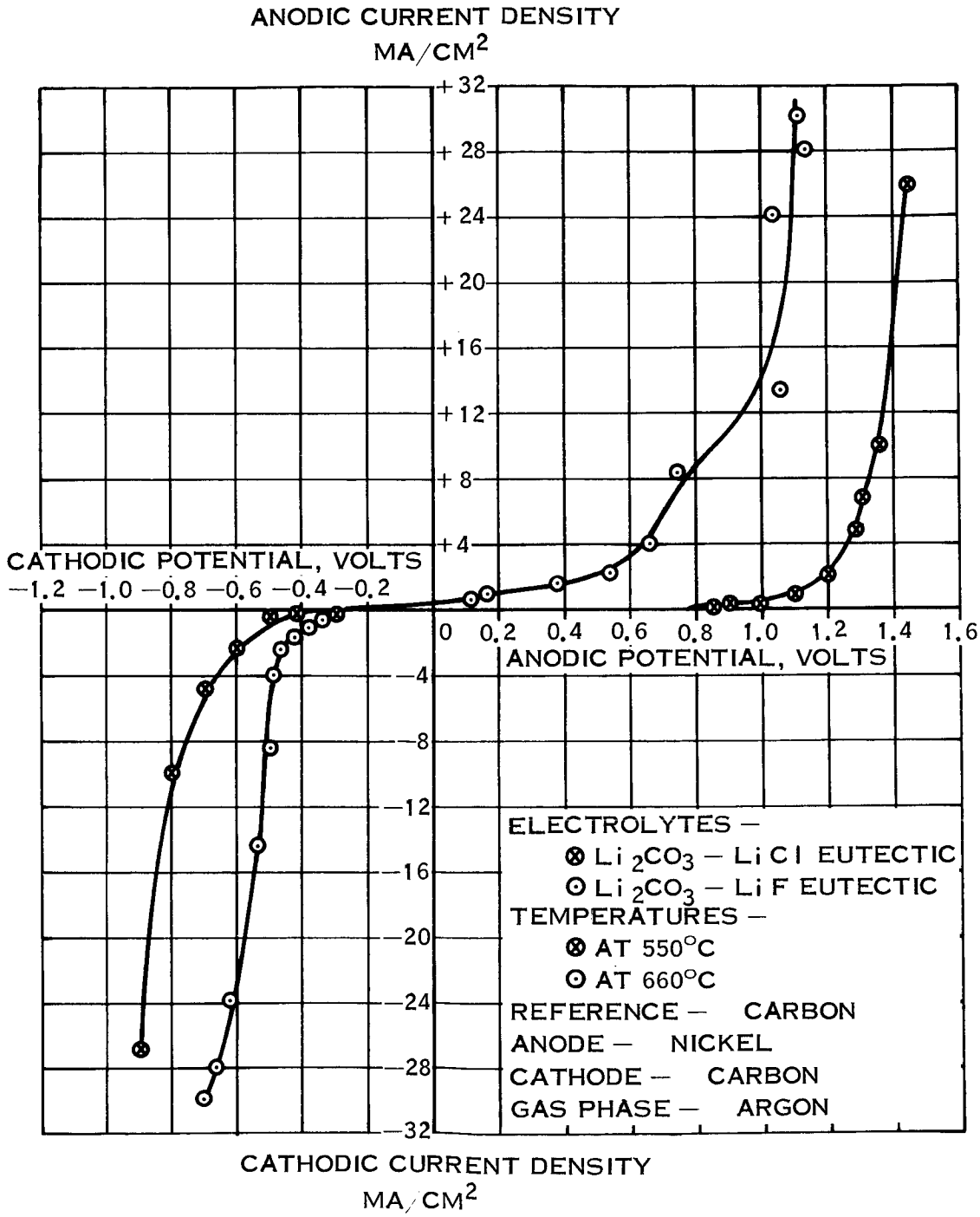

FIGURE 6-1 CURRENT-VOLTAGE TRACES IN Li_2CO_3-LiFl AND Li_2CO_3-LiF EUTECTICS

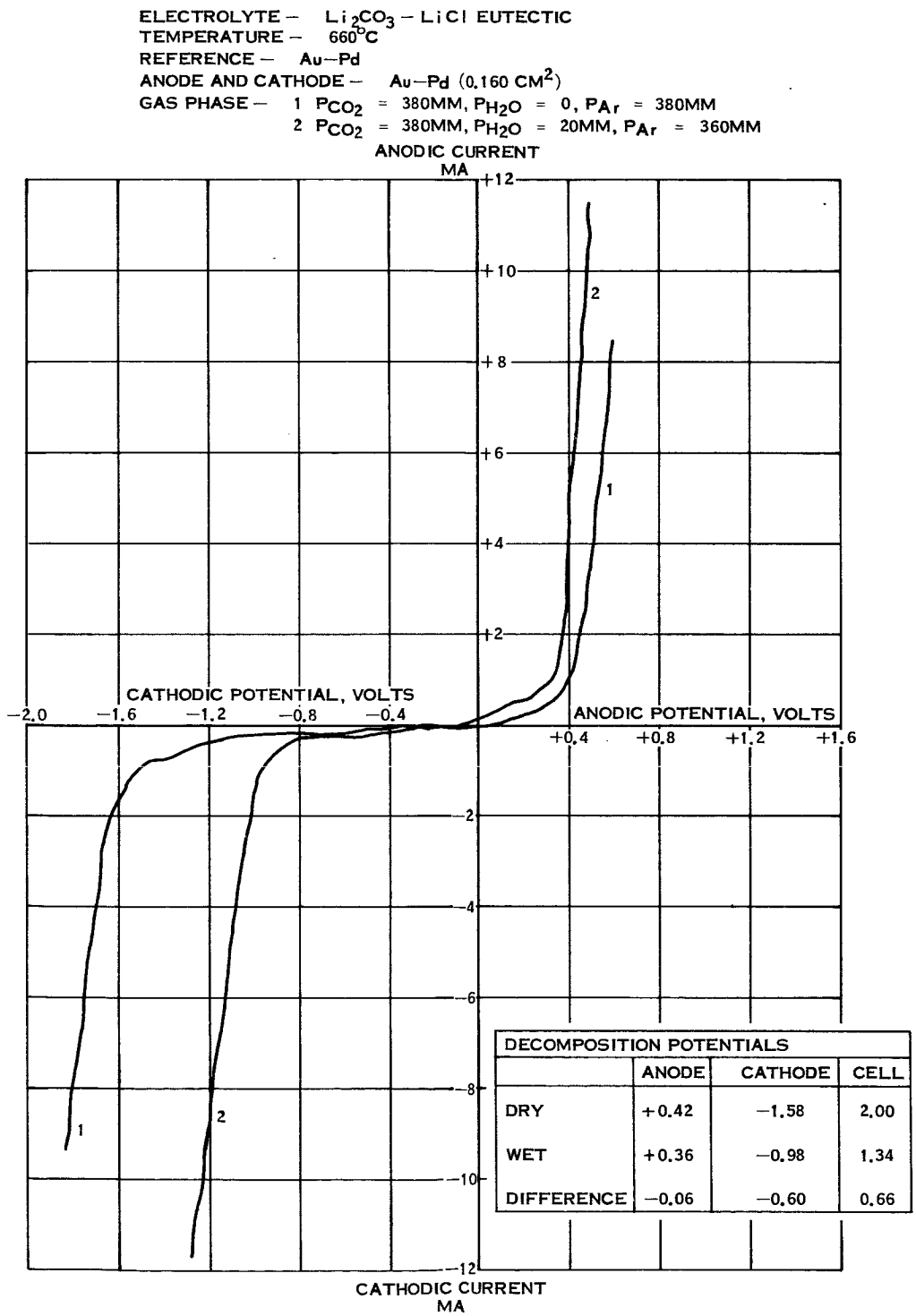

FIGURE 6-2 CURRENT-VOLTAGE TRACES IN Li_2CO_3-LiCl EUTECTICS

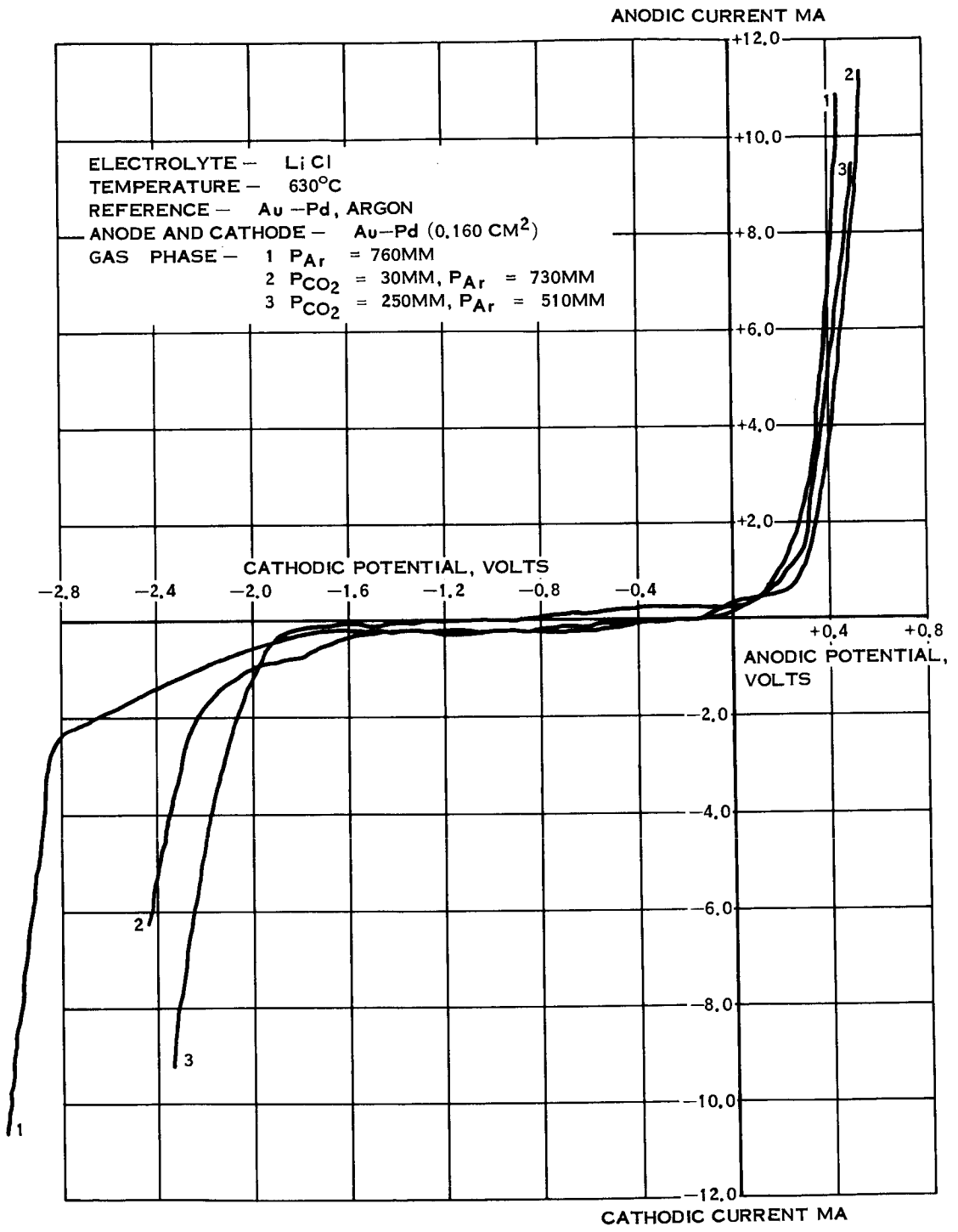

FIGURE 6-3 CURRENT-VOLTAGE TRACES IN LiCl

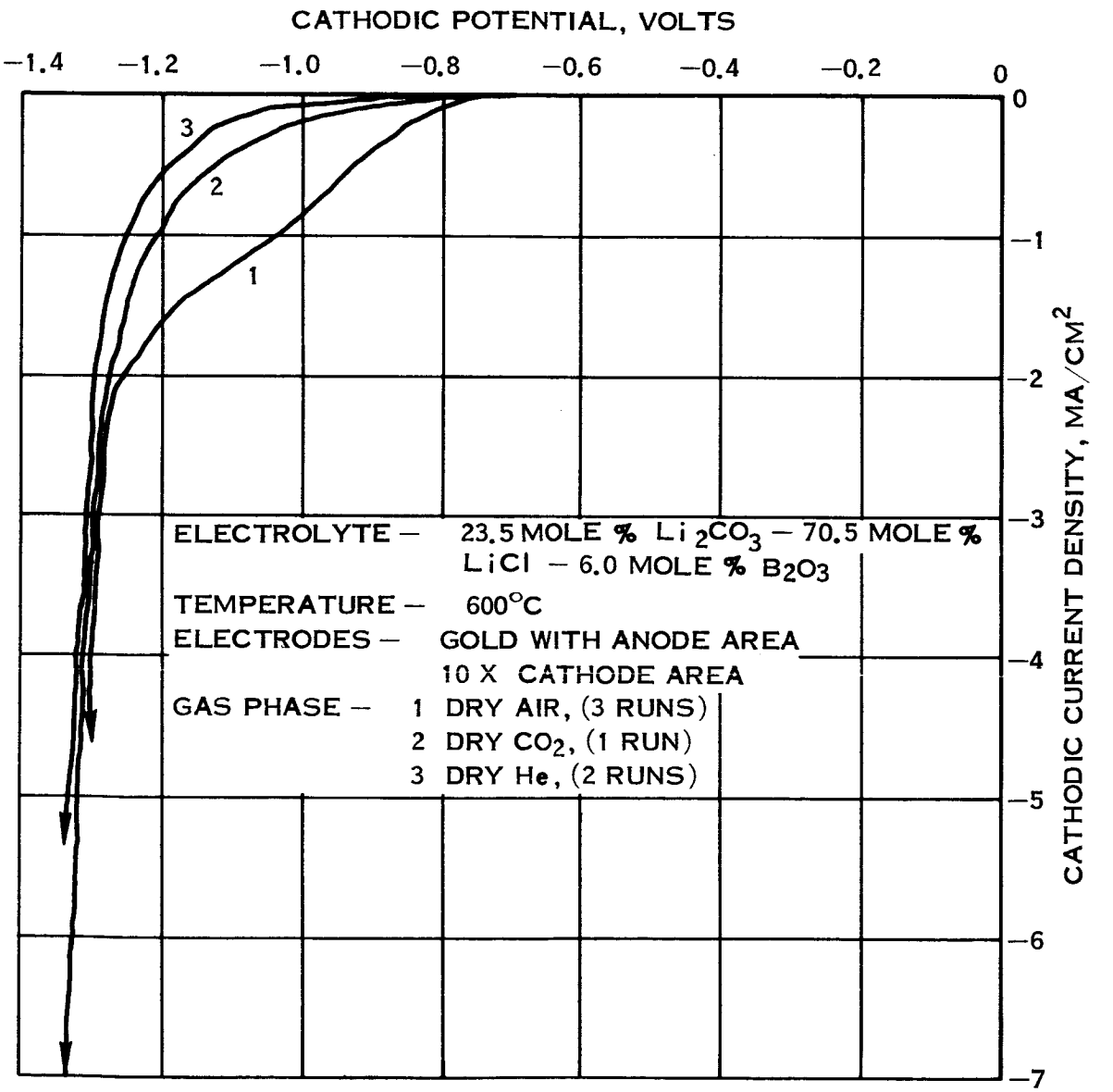

FIGURE 6-4 EFFECT OF GAS PHASE COMPOSITIONS ON CATHODIC CURRENT-VOLTAGE TRACES

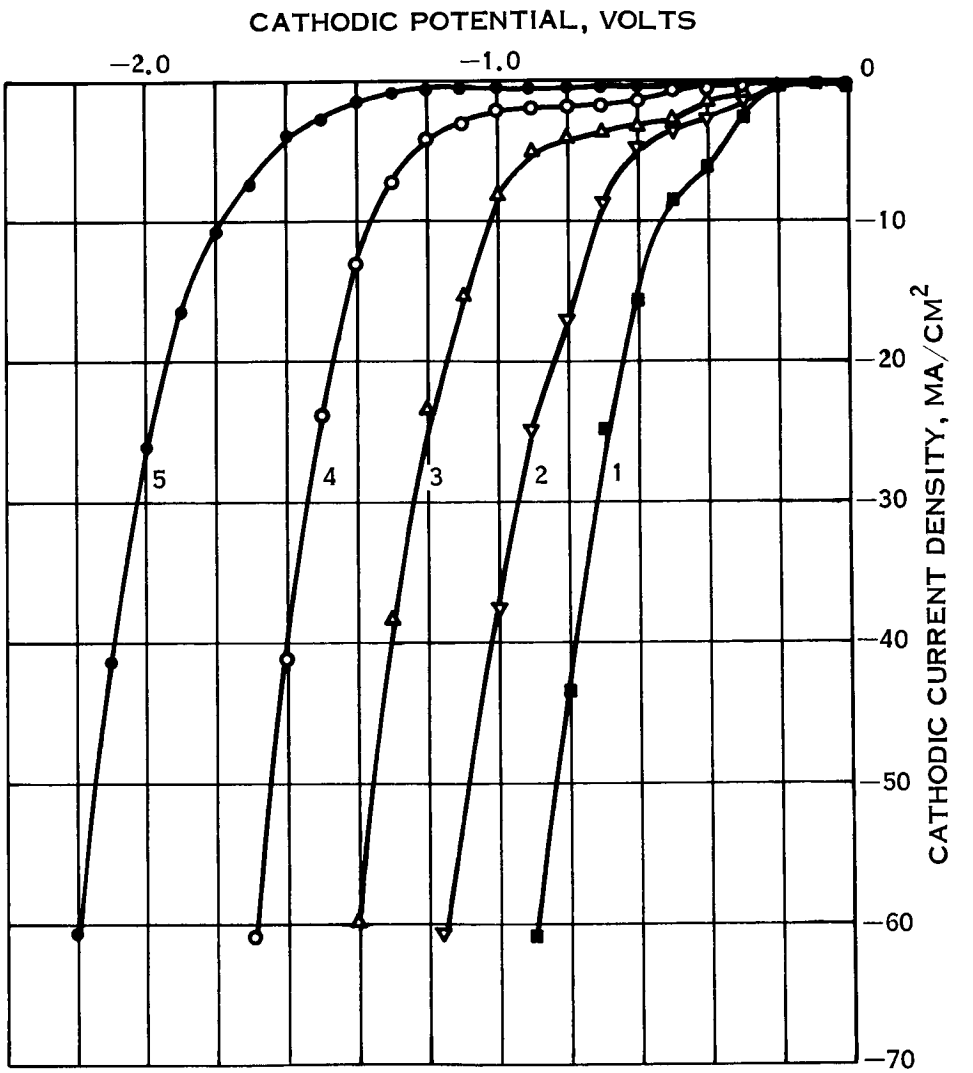

ELECTROLYTE — 40 MOLE % Li_2CO_3 — 30 MOLE % K_2CO_3 — 30 MOLE % Na_2CO_3
TEMPERATURE — 1 790°C
2 725°C
3 670°C
4 550°C
5 470°C
ELECTRODES — CARBON WITH ANODE AREA 10 X CATHODE AREA
GAS PHASE — ARGON

FIGURE 6-5 EFFECT OF TEMPERATURE ON CATHODIC CURRENT-VOLTAGE TRACE IN TERNARY CARBONATE MELT

ELECTROLYTES – 1 Li_2CO_3 – LiCl EUTECTIC + 5 MOLE % B_2O_3
2 Li_2CO_3 – LiCl EUTECTIC + 5 MOLE % B_2O_3
+0.5 MOLE % $CoCl_2$

TEMPERATURE – 600°C
ELECTRODES – GOLD WITH ANODE AREA
10X CATHODE AREA
GAS PHASE – ARGON

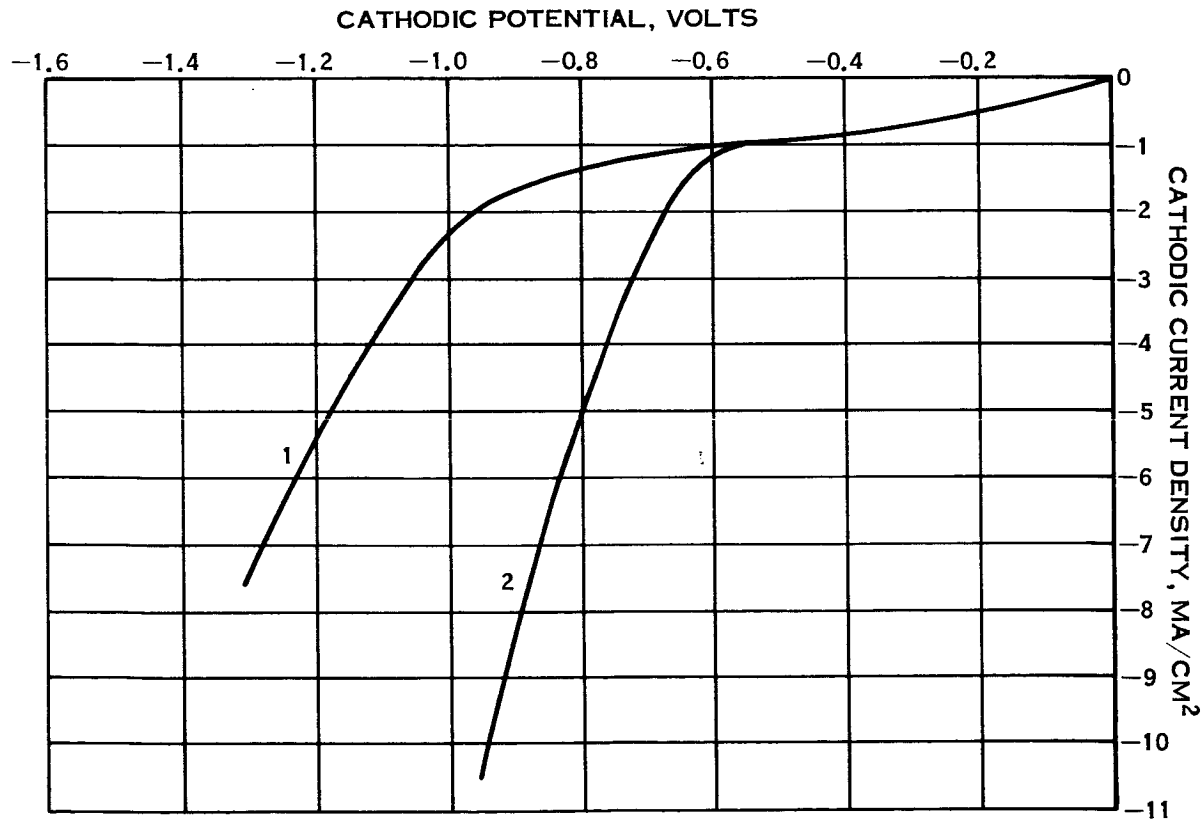

FIGURE 6-6 EFFECT OF COBALT ADDITION ON CATHODIC CURRENT-VOLTAGE TRACE

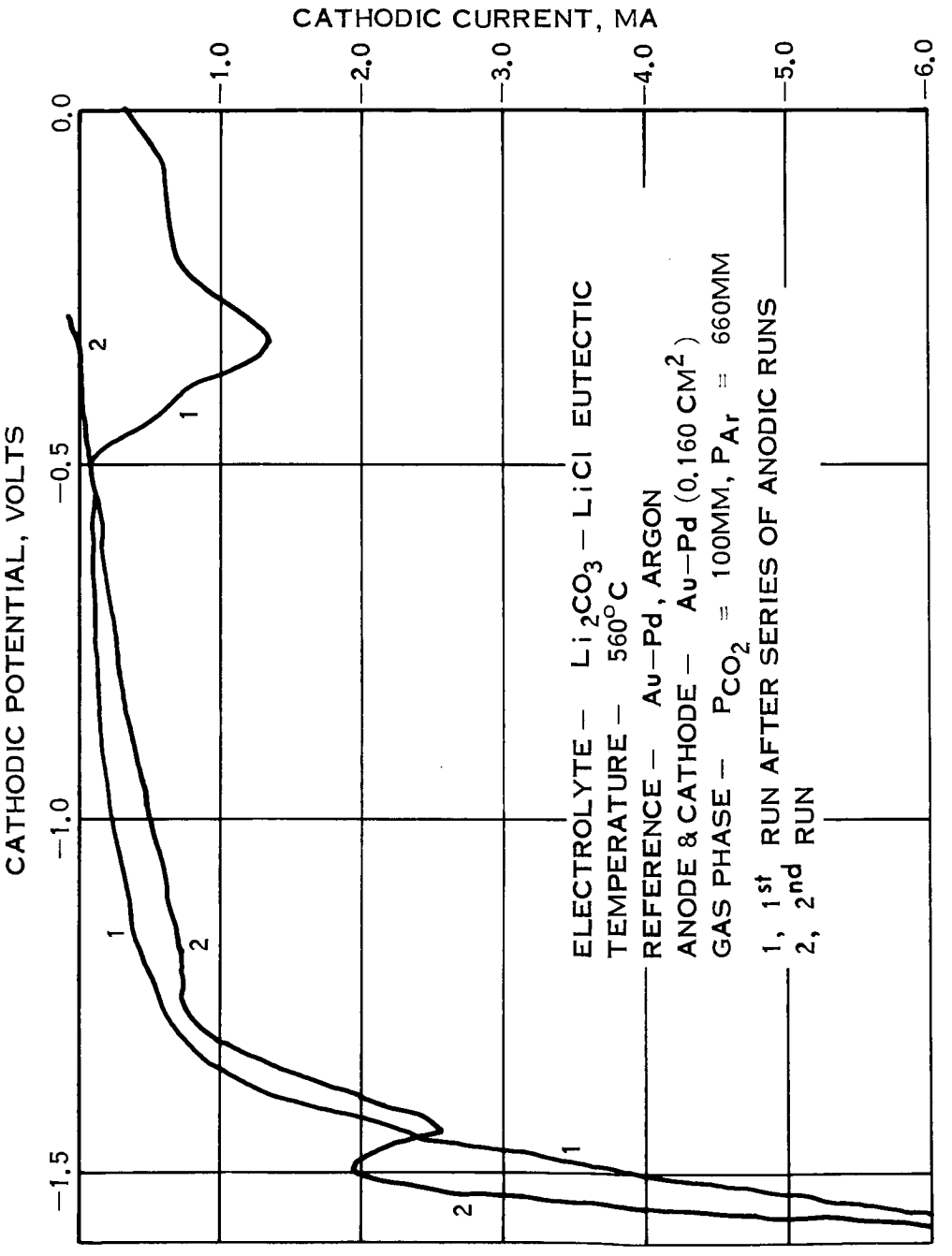

FIGURE 6-7 CATHODIC TRACES IN Li_2CO_3-LiCl EUTECTIC

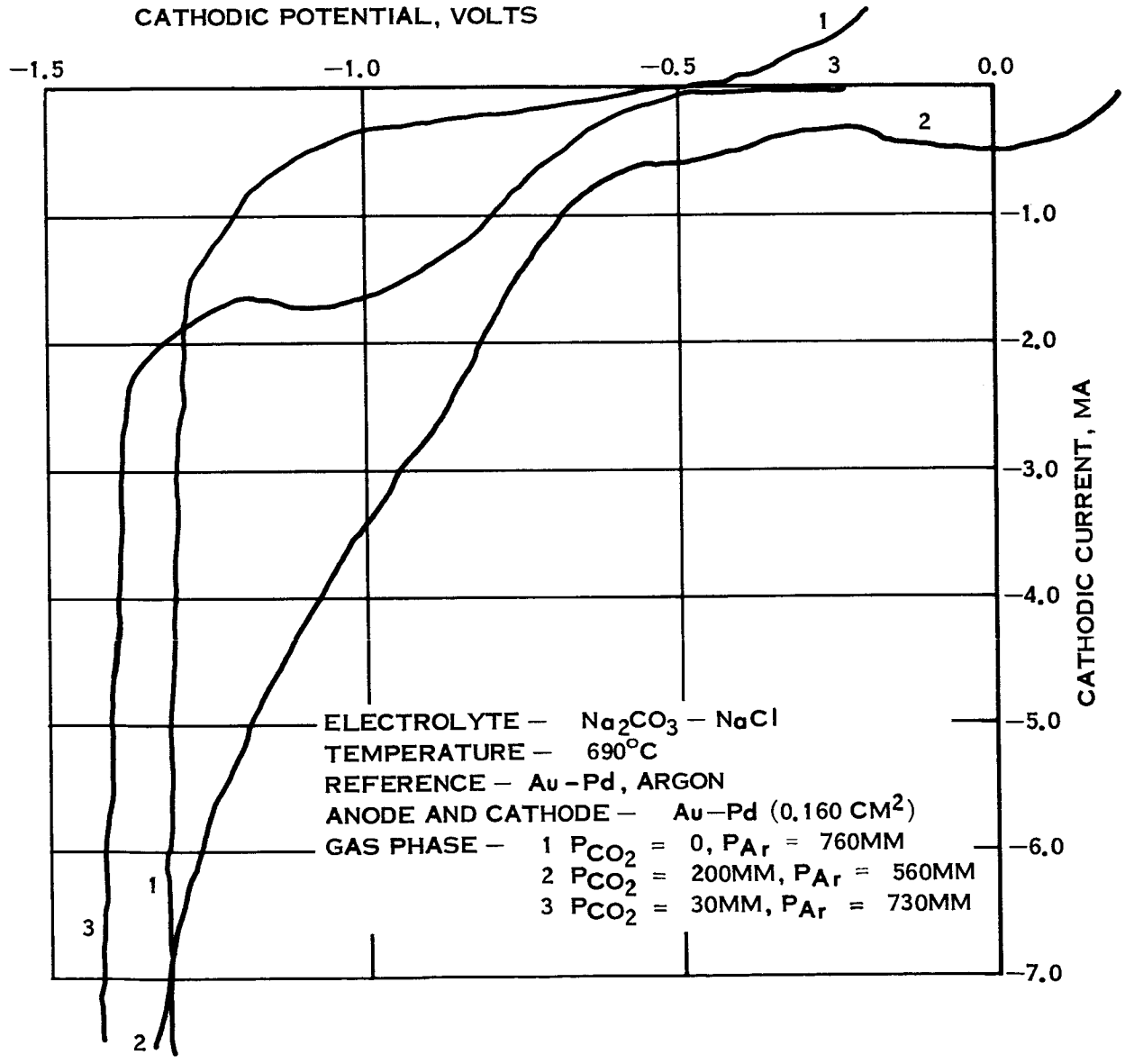

FIGURE 6-8 CATHODIC TRACES IN Na_2CO_3-NaCl EUTECTIC

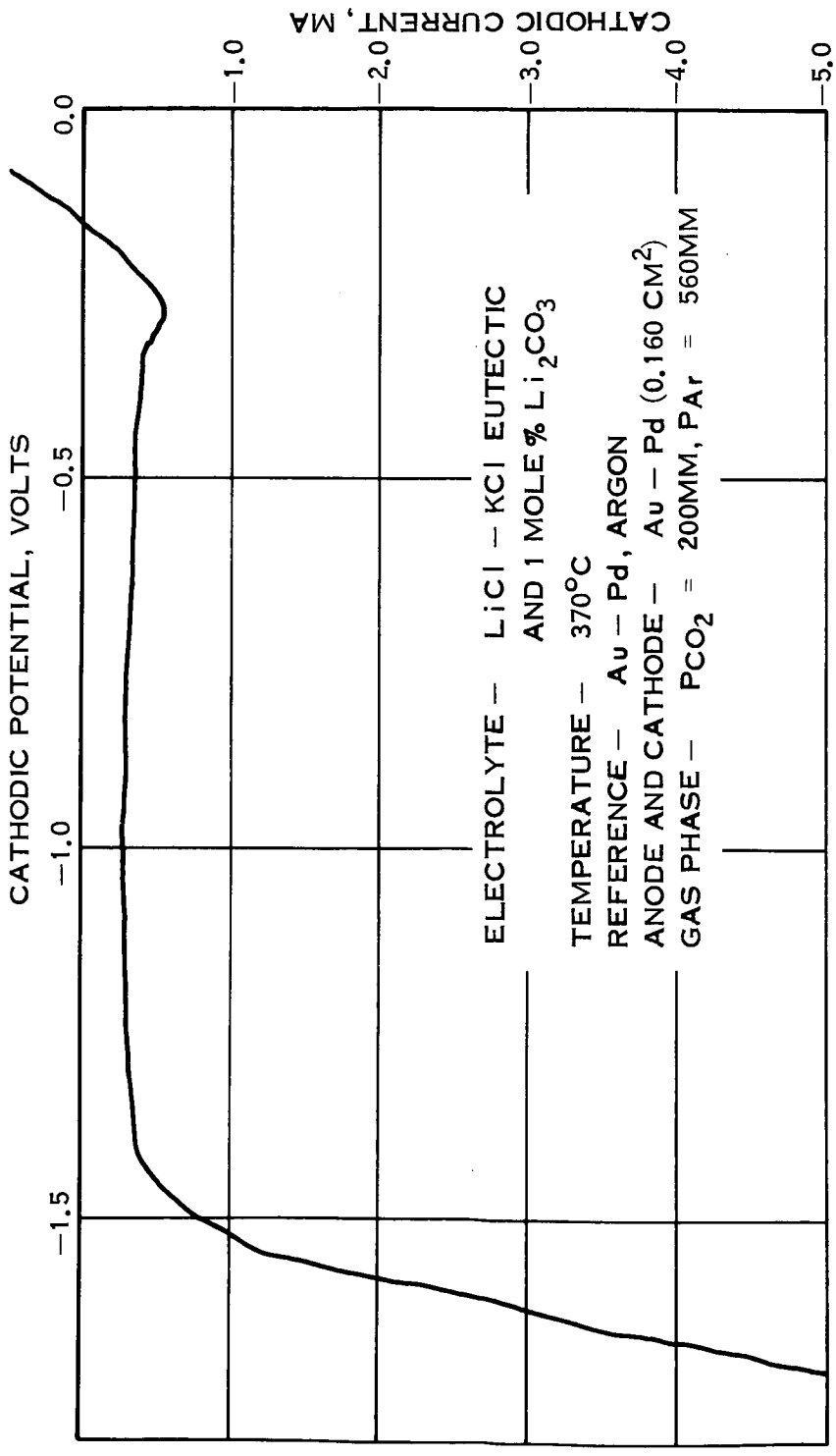

FIGURE 6-9 CATHODIC TRACE IN LiCl-KCl EUTECTIC AND 1 MOLE PERCENT Li_2CO_3

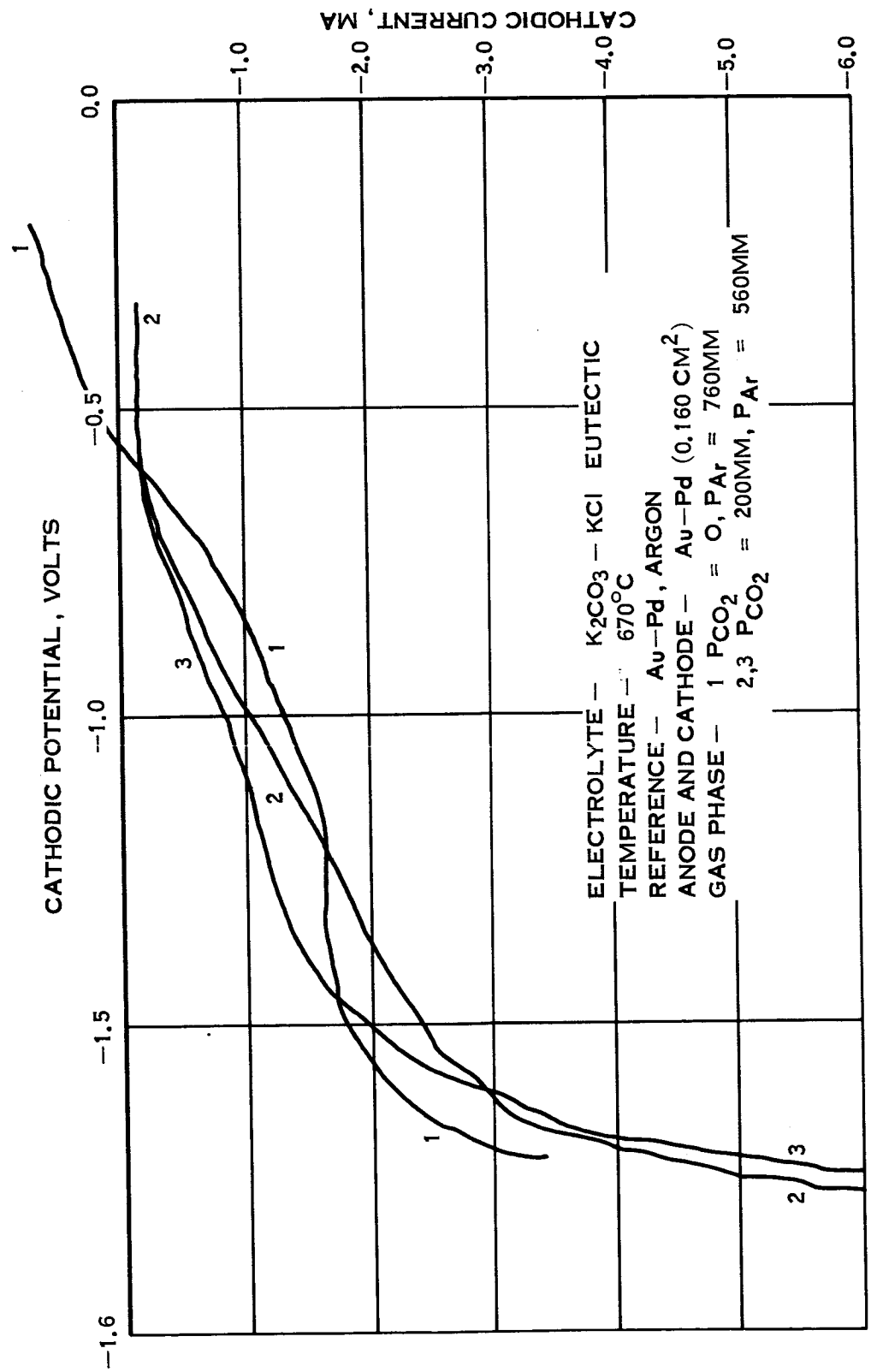

FIGURE 6-10 CATHODIC TRACES IN K_2CO_3-KCl EUTECTIC

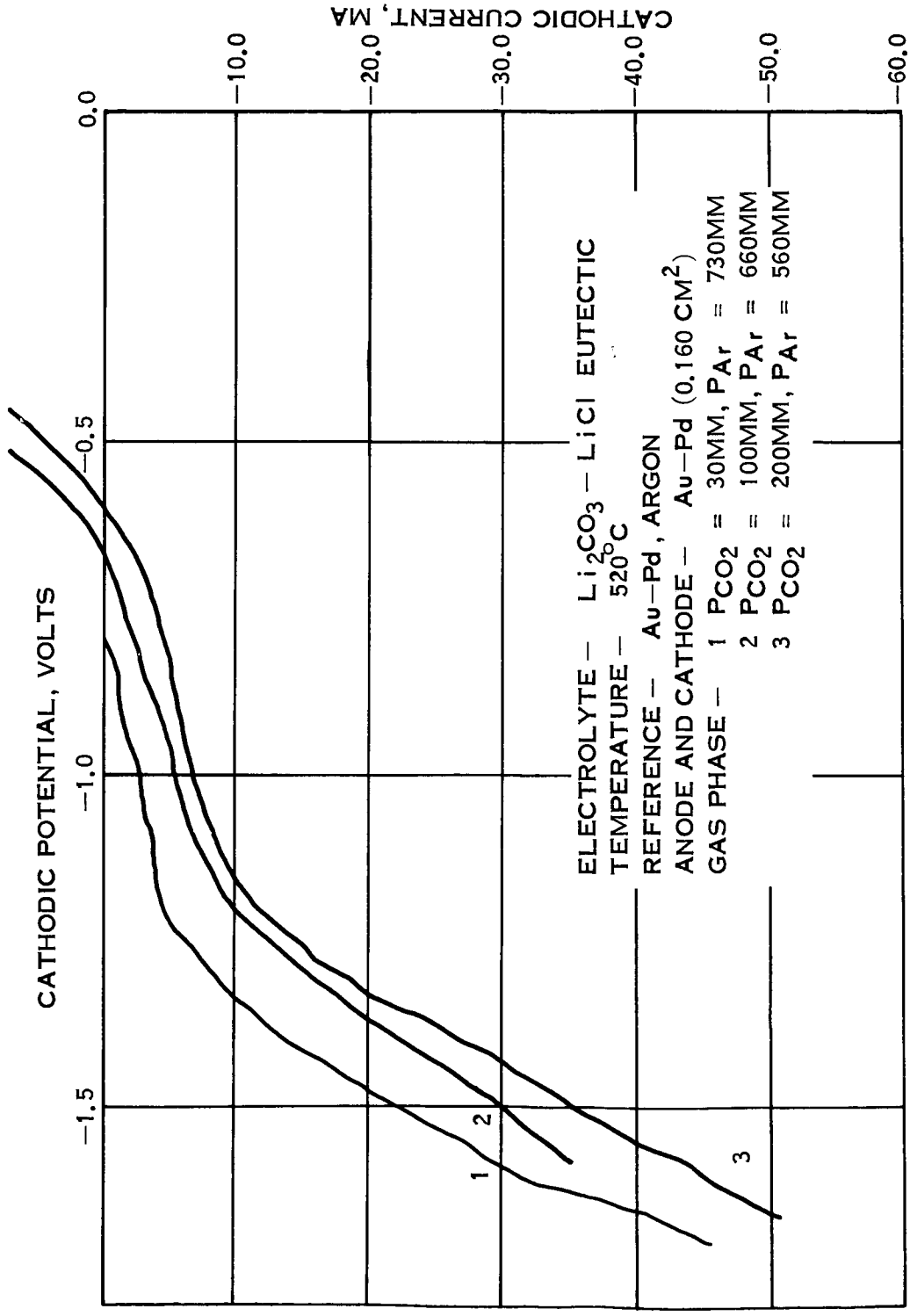

FIGURE 6-11 CATHODIC TRACES IN Li_2CO_3-LiCl EUTECTIC (VARIED P_{CO_2})

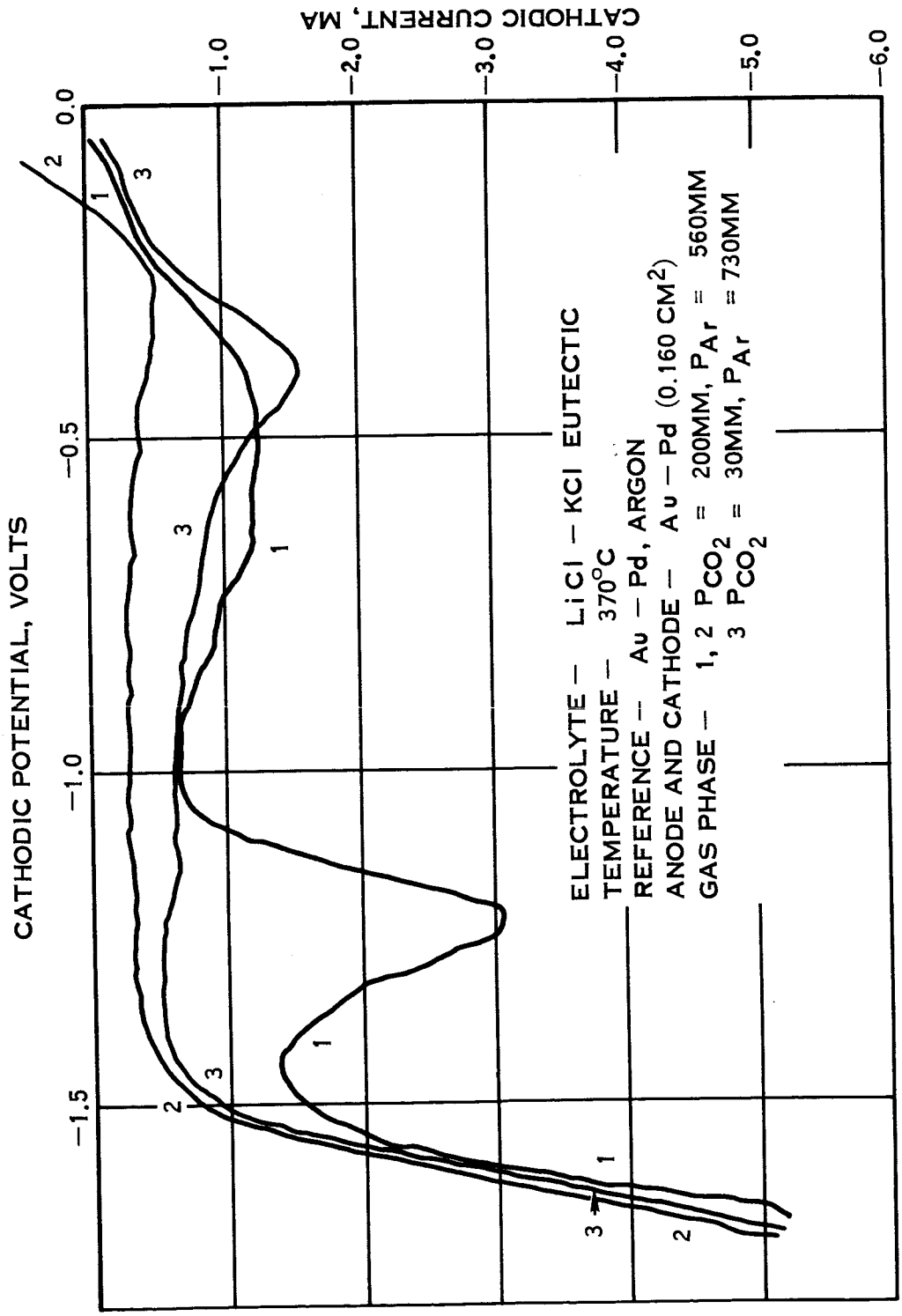

FIGURE 6-12 CATHODIC TRACES IN LiCl-KCl EUTECTIC

ELECTROLYTE — K_2CO_3 — KCl EUTECTIC
1 TEMPERATURE — 670°C
REFERENCE — Au — Pd, ARGON
ANODE AND CATHODE — Au — Pd (0.160 CM^2)
GAS PHASE — P_{CO_2} = 200MM, P_{Ar} = 560MM

ELECTROLYTE — Li_2CO_3 — LiCl EUTECTIC
TEMPERATURE — 570°C
2 REFERENCE — Au — Pd ARGON
ANODE AND CATHODE — Au — Pd (0.160 CM^2)
GAS PHASE — P_{CO_2} = 40MM, P_{Ar} = 720MM

ELECTROLYTE — Li_2CO_3 — LiF EUTECTIC
TEMPERATURE — 750°C
3 REFERENCE — Au — Pd (P_{CO_2} = 200MM, P_{Ar} = 560MM)
GAS PHASE — P_{CO_2} = 200MM, P_{Ar} = 560MM
CATHODE — Ni
ANODE — Au — Pd (0.160 CM^2)

ELECTROLYTE — Na_2CO_3 — NaCl EUTECTIC
TEMPERATURE — 690°C
4 REFERENCE — Au — Pd, ARGON
GAS PHASE — P_{CO_2} = 30MM, P_{Ar} = 730MM
ANODE AND CATHODE — Au — Pd (0.160 CM^2)

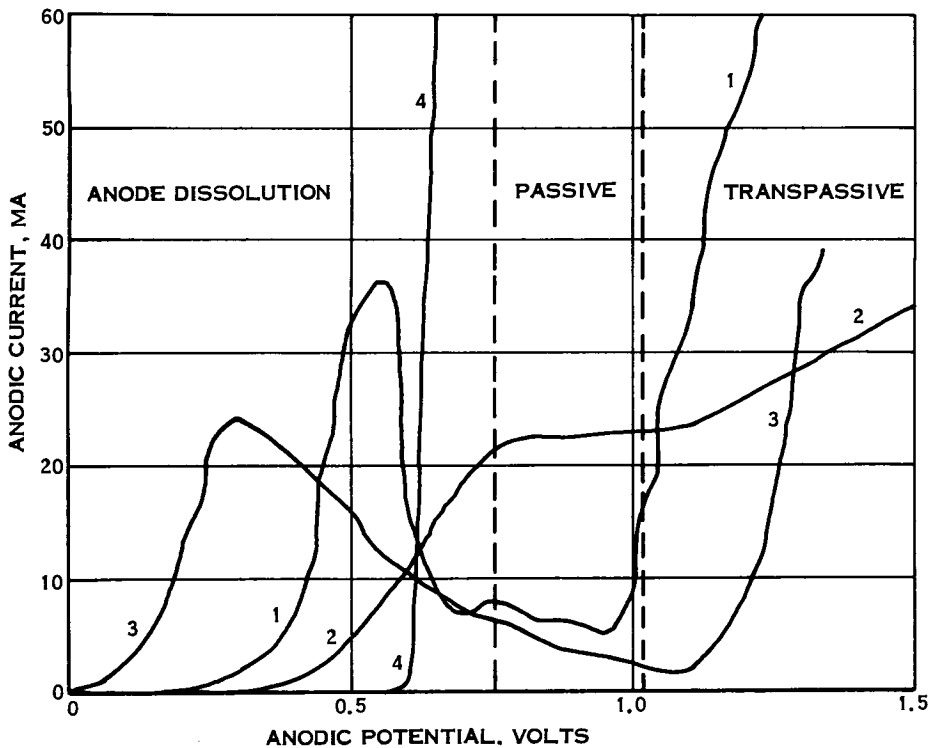

FIGURE 6-13 ANODIC TRACES IN MISCELLANEOUS ELECTROLYTES

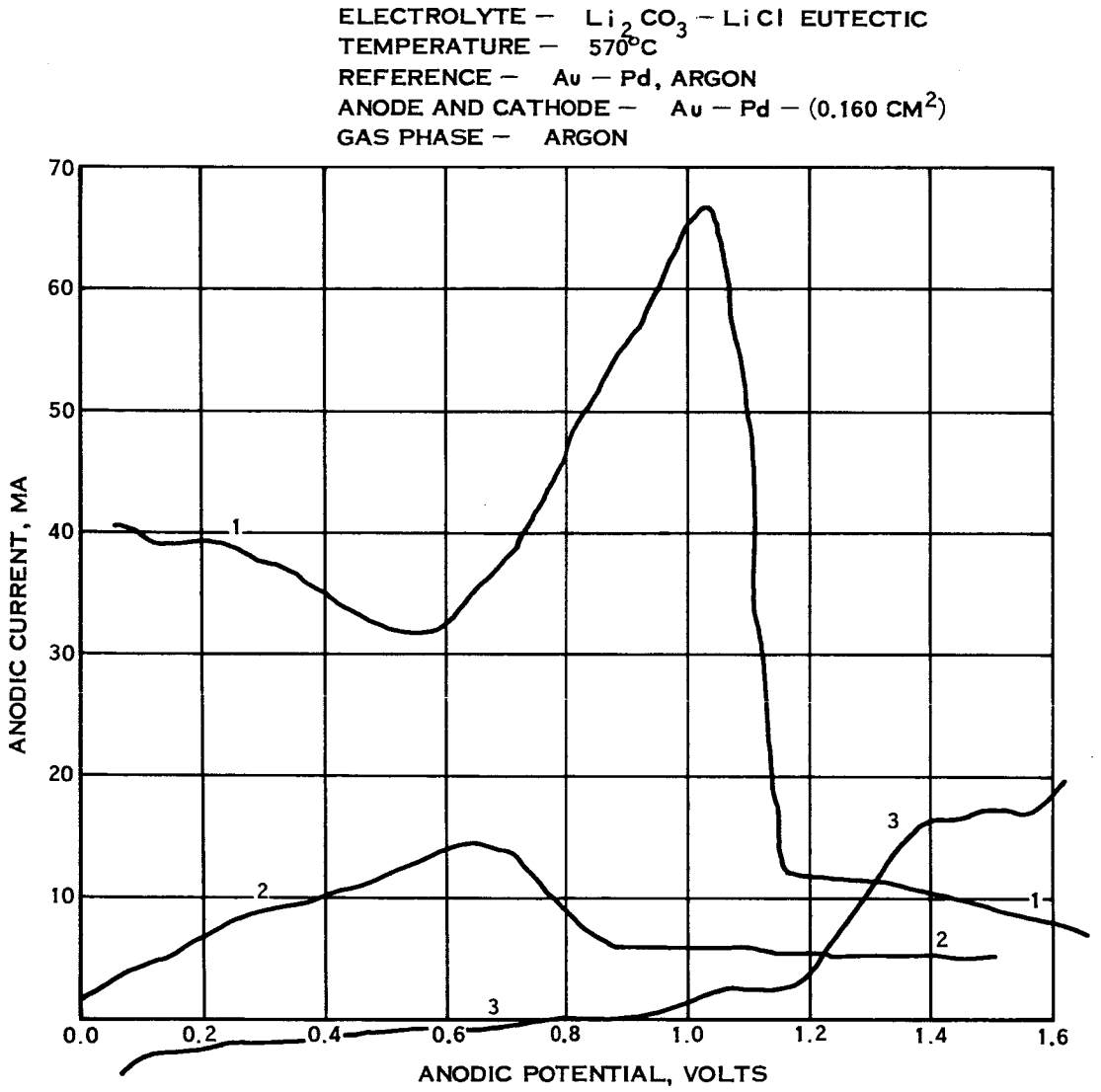

FIGURE 6-14 ANODIC TRACES IN Li_2CO_3-LiCl EUTECTIC

ELECTROLYTE — Li_2CO_3 — LiF EUTECTIC
TEMPERATURE — 750°C
REFERENCE — Au — Pd, (P_{CO_2} = 200MM, P_{Ar} = 560MM)
CATHODE — Ni
ANODE — 1 AuPd (0.160 CM^2)
2 Au (0.160 CM^2)
3 Pt (0.160 CM^2)
GAS PHASE — P_{CO_2} = 200MM, P_{Ar} = 560MM

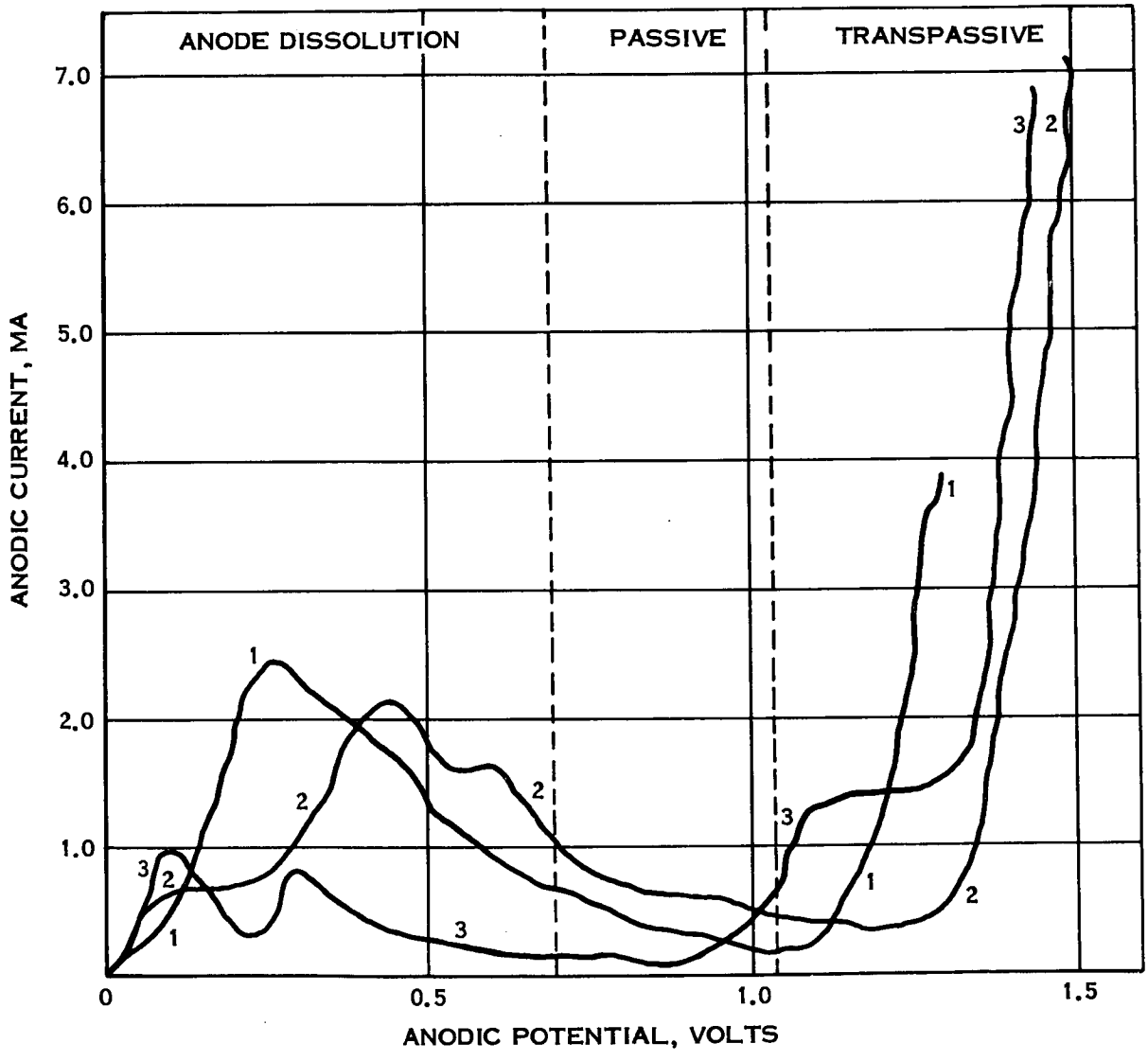

FIGURE 6-15 ANODIC TRACES IN Li_2CO_3-LiF EUTECTIC VARIOUS METAL ANODES

ELECTROLYTE — $Li_2CO_3 - LiF$ EUTECTIC
TEMPERATURE — 750 °C
REFERENCE — Au — Pd (P_{CO_2} = 200MM, P_{Ar} = 560MM)
CATHODE — Ni
ANODE — Ni (0.160 CM^2)
GAS PHASE — P_{CO_2} = 200MM, P_{Ar} = 560MM

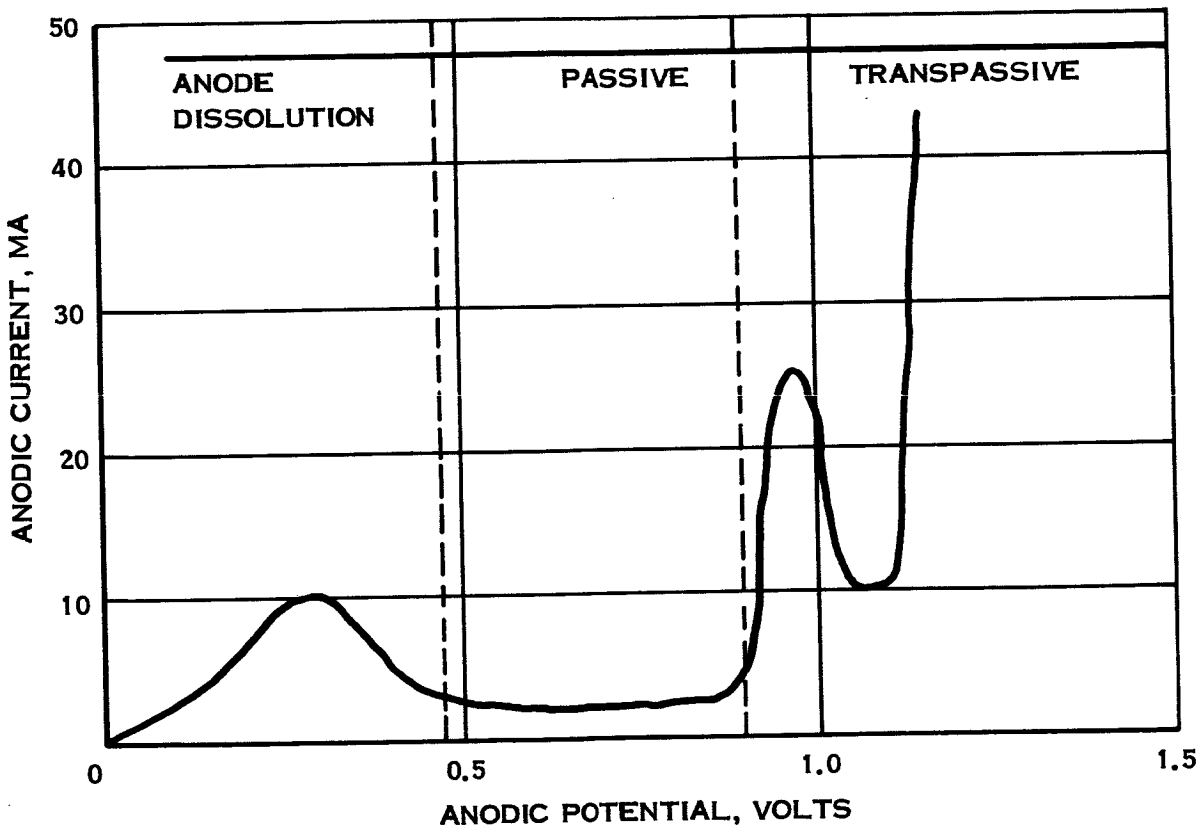

FIGURE 6-16 ANODIC TRACES IN Li_2CO_3-LiF EUTECTIC

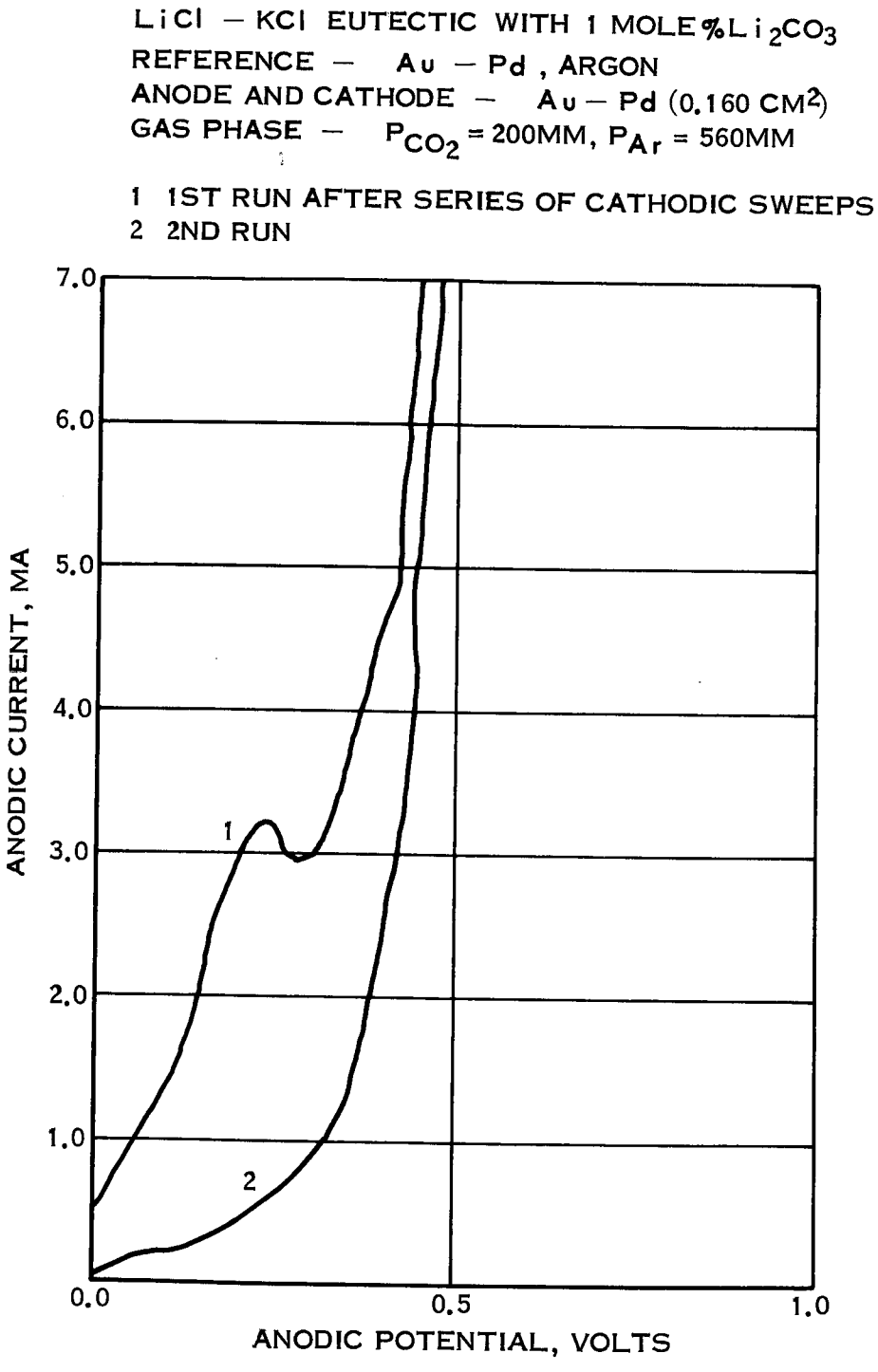

FIGURE 6-17 ANODIC TRACES, CATHODE DEPOSIT OXIDATION

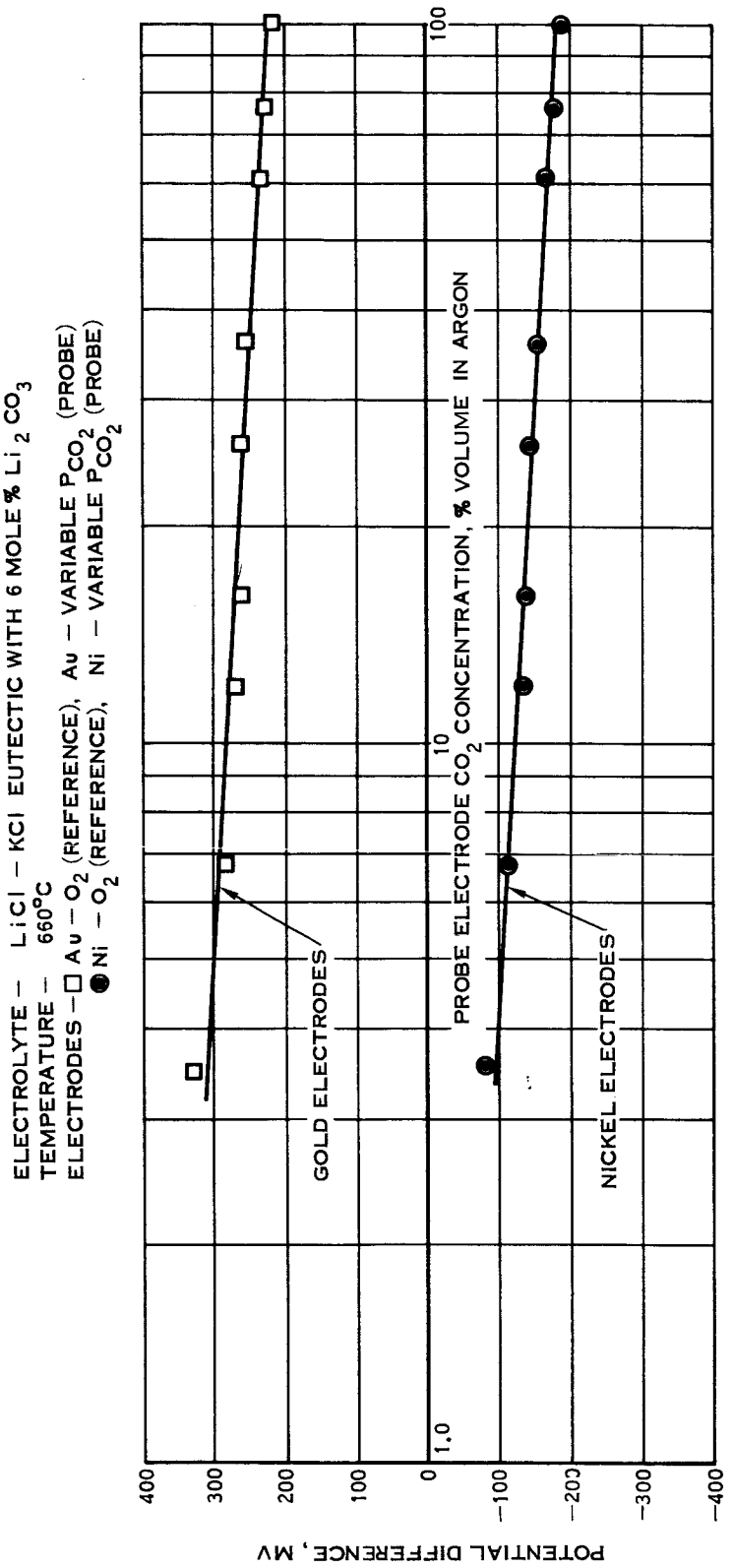

FIGURE 6-18 SENSITIVITY OF METAL PROBES TO CARBON DIOXIDE PARTIAL PRESSURE

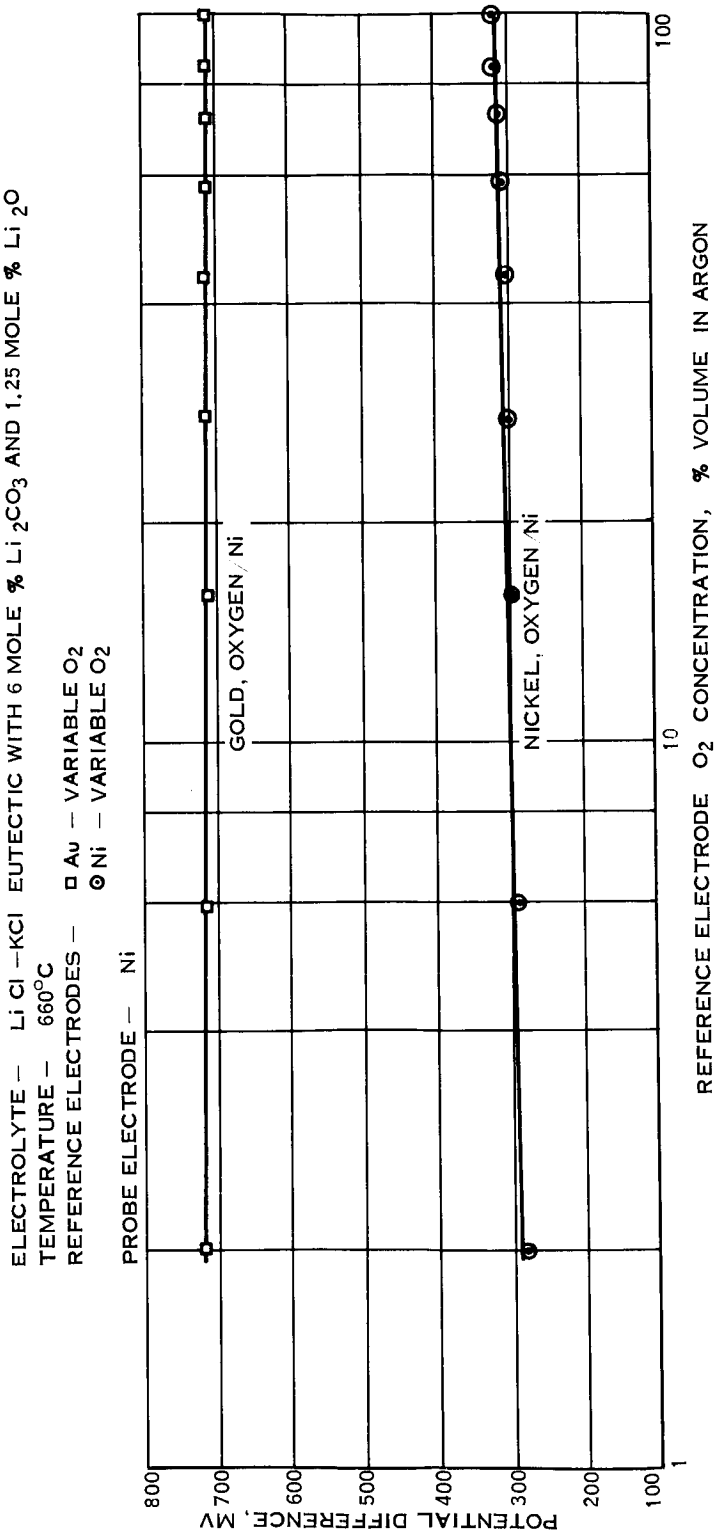

FIGURE 6-19 SENSITIVITY OF REFERENCE TO OXYGEN PARTIAL PRESSURE

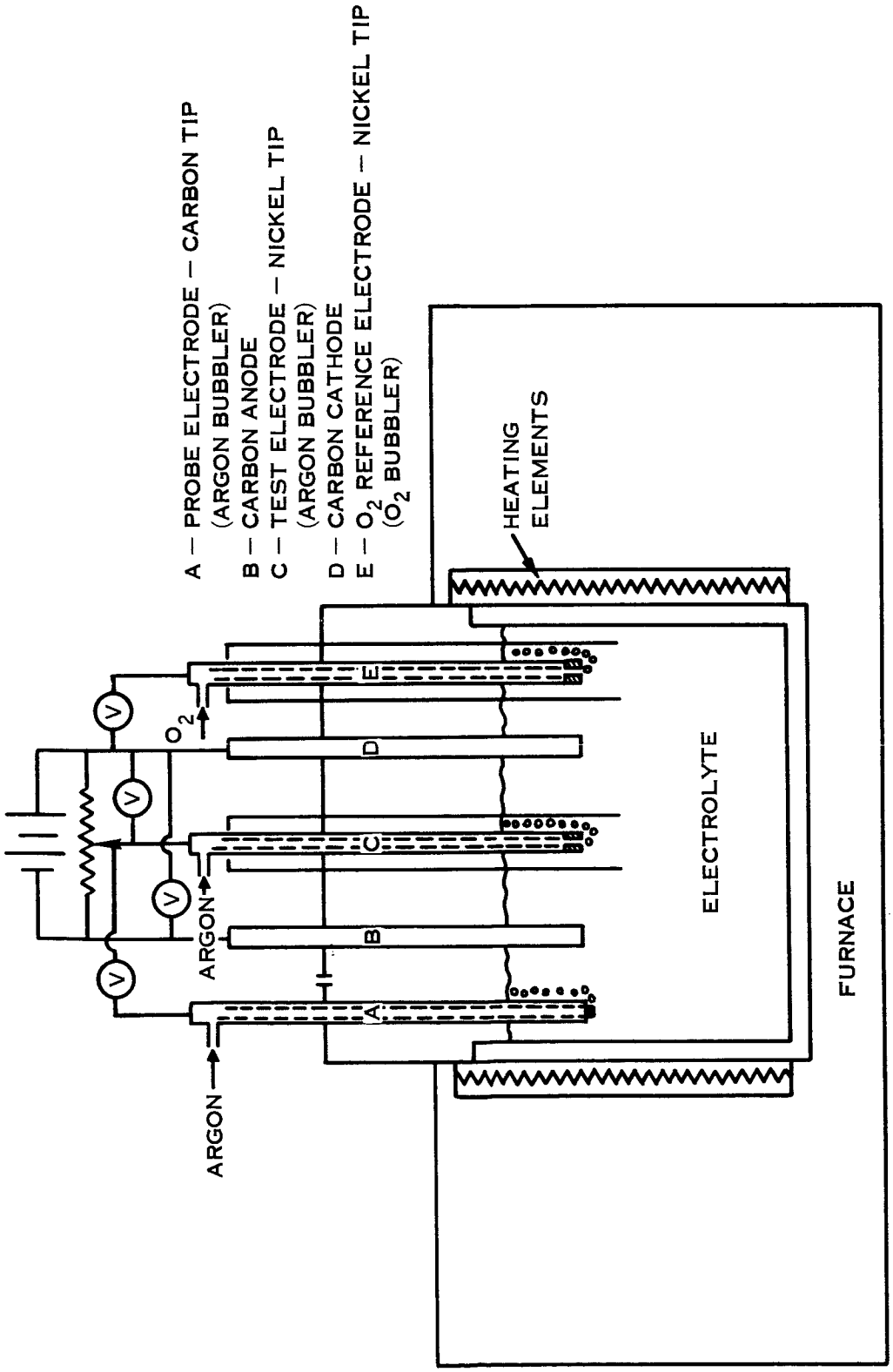

FIGURE 6-20 SKETCH; REFERENCE AND PROBE STUDIES

ELECTROLYTES –
1 Li Cl –KCl EUTECTIC WITH 6 MOLE % Li_2CO_3
2 Li Cl –KCl EUTECTIC WITH 6 MOLE % Li_2CO_3 + 1 MOLE % Li_2O
3 Li Cl –KCl EUTECTIC WITH 6 MOLE % Li_2CO_3 + 2 MOLE % Li_2O
TEMPERATURE – 521°C
WORKING ELECTRODES – CARBON AT 60 MA/CM^2,
STEADY STATE POTENTIAL = 1.85 VOLTS
TEST ELECTRODE – NICKEL
GAS PHASE – ARGON

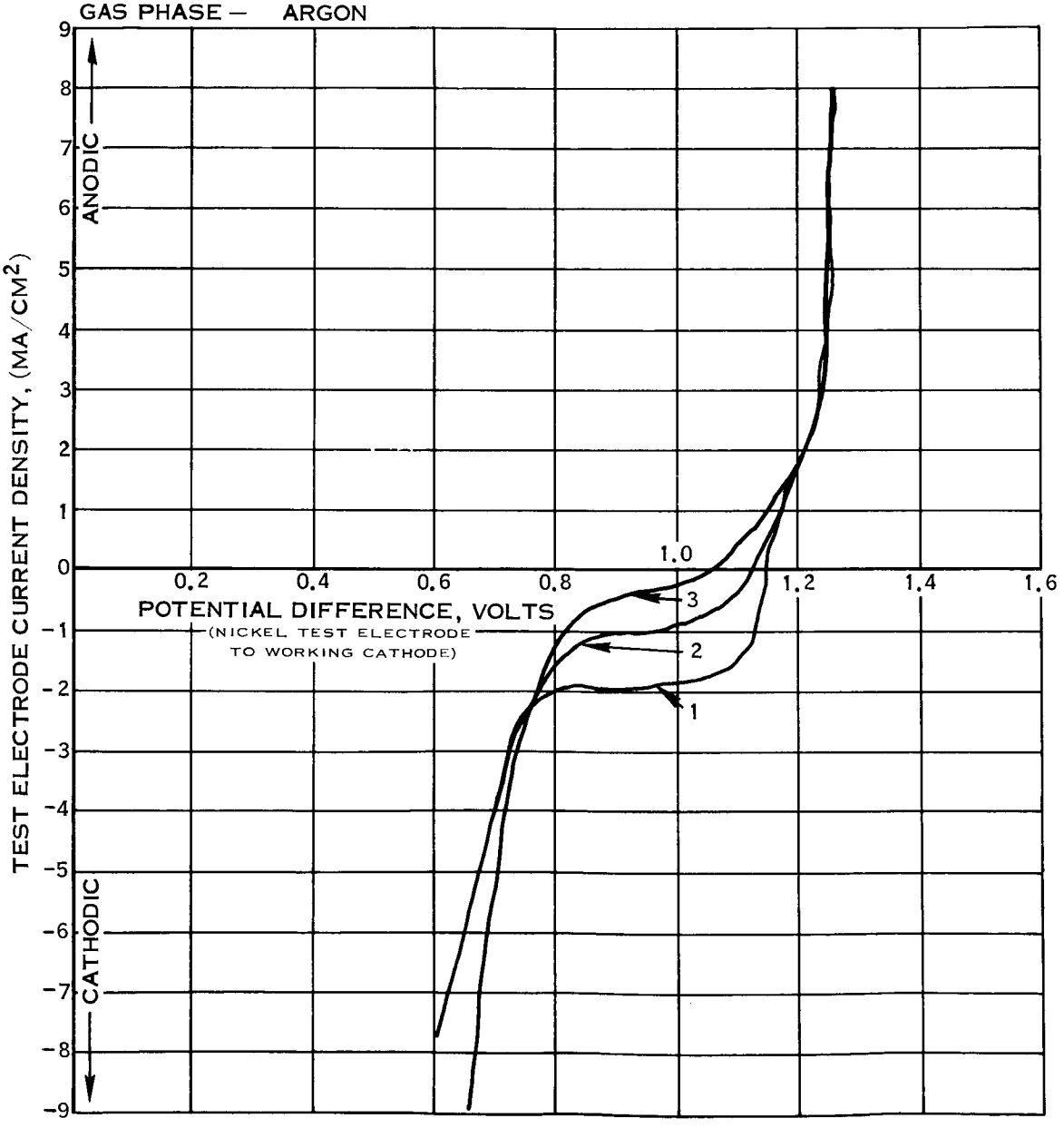

FIGURE 6-21 REFERENCE ELECTRODE STUDIES, Li_2O SENSITIVITY

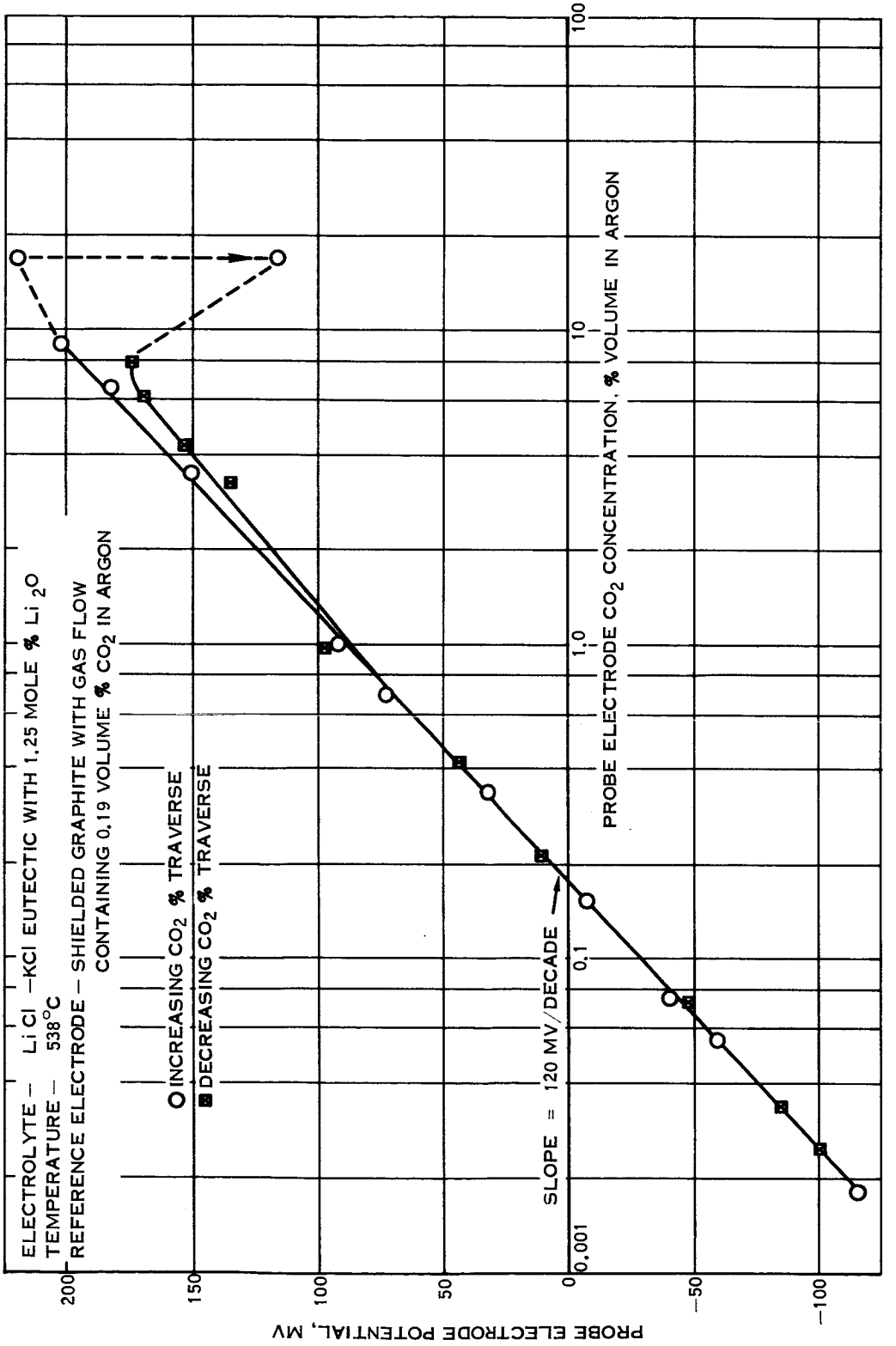

FIGURE 6-22 CARBON PROBE SENSITIVITY TO CARBON DIOXIDE PARTIAL PRESSURE, LiCl-KCl BASE ELECTROLYTE

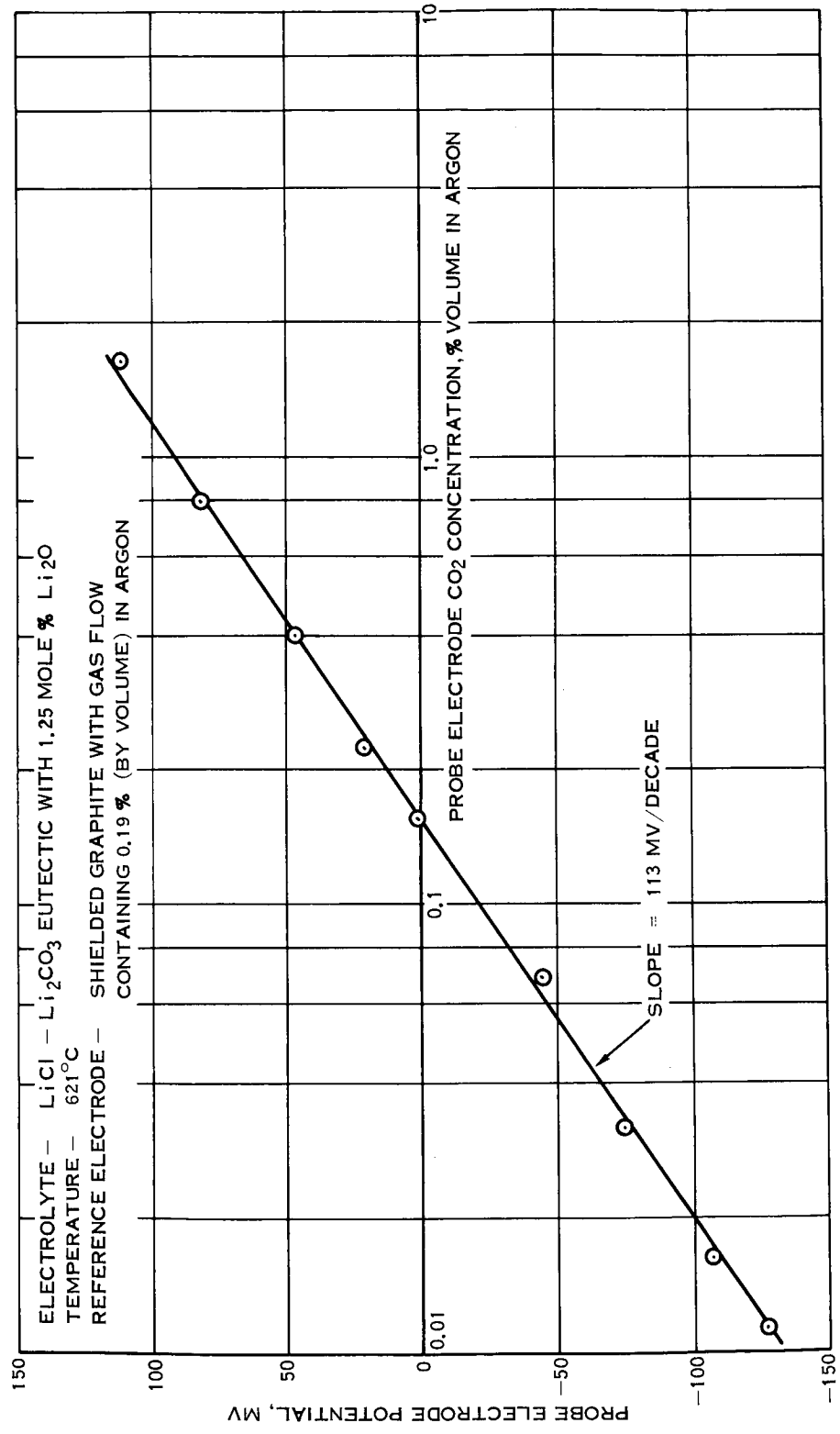

FIGURE 6-23 CARBON PROBE SENSITIVITY TO CARBON DIOXIDE PARTIAL PRESSURE, Li_2CO_3-LiCl BASE ELECTROLYTE

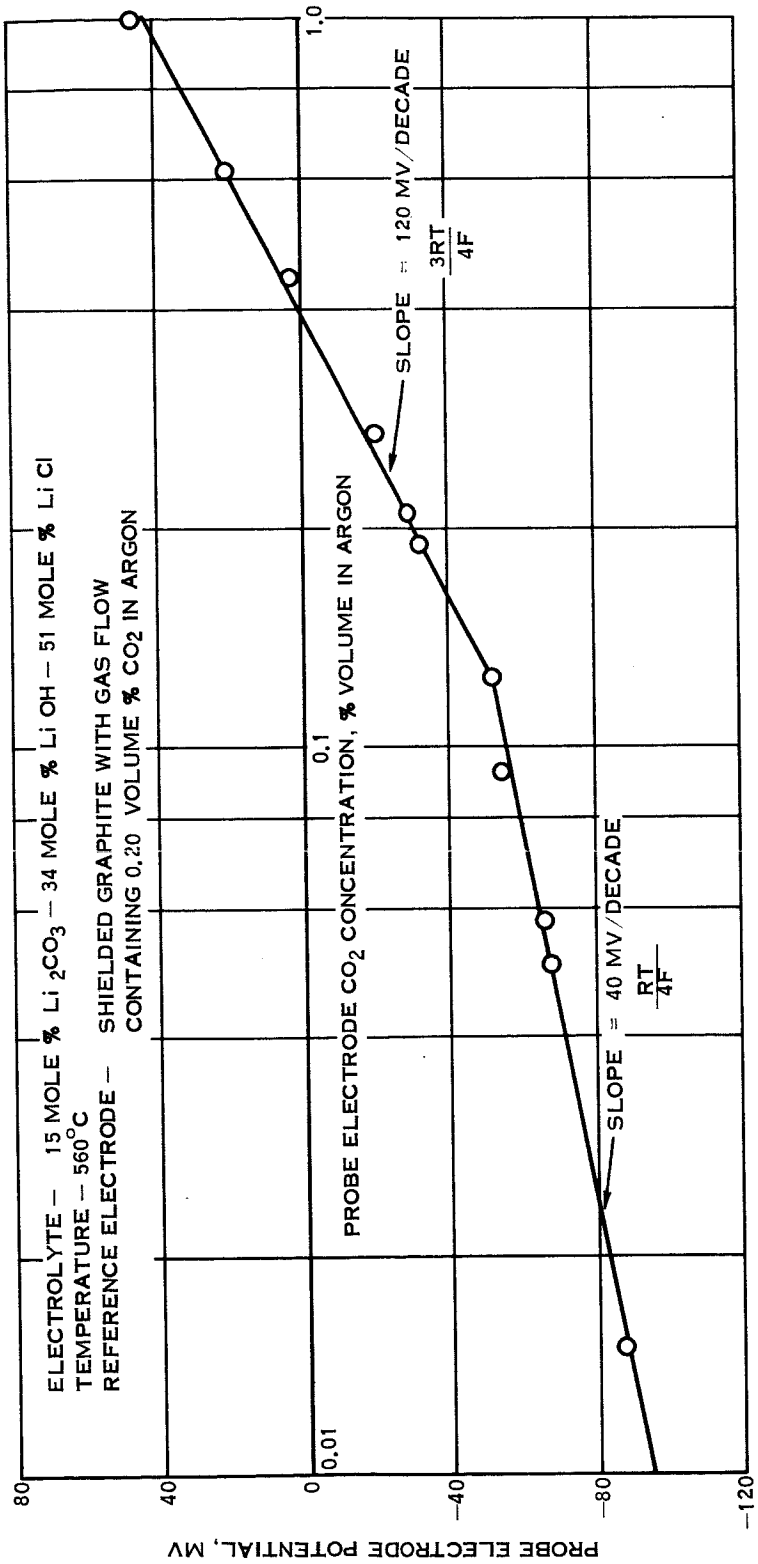

FIGURE 6-24 CARBON PROBE CO_2 SENSITIVITY IN ELECTROLYTE WITH ADDED HYDROXIDE

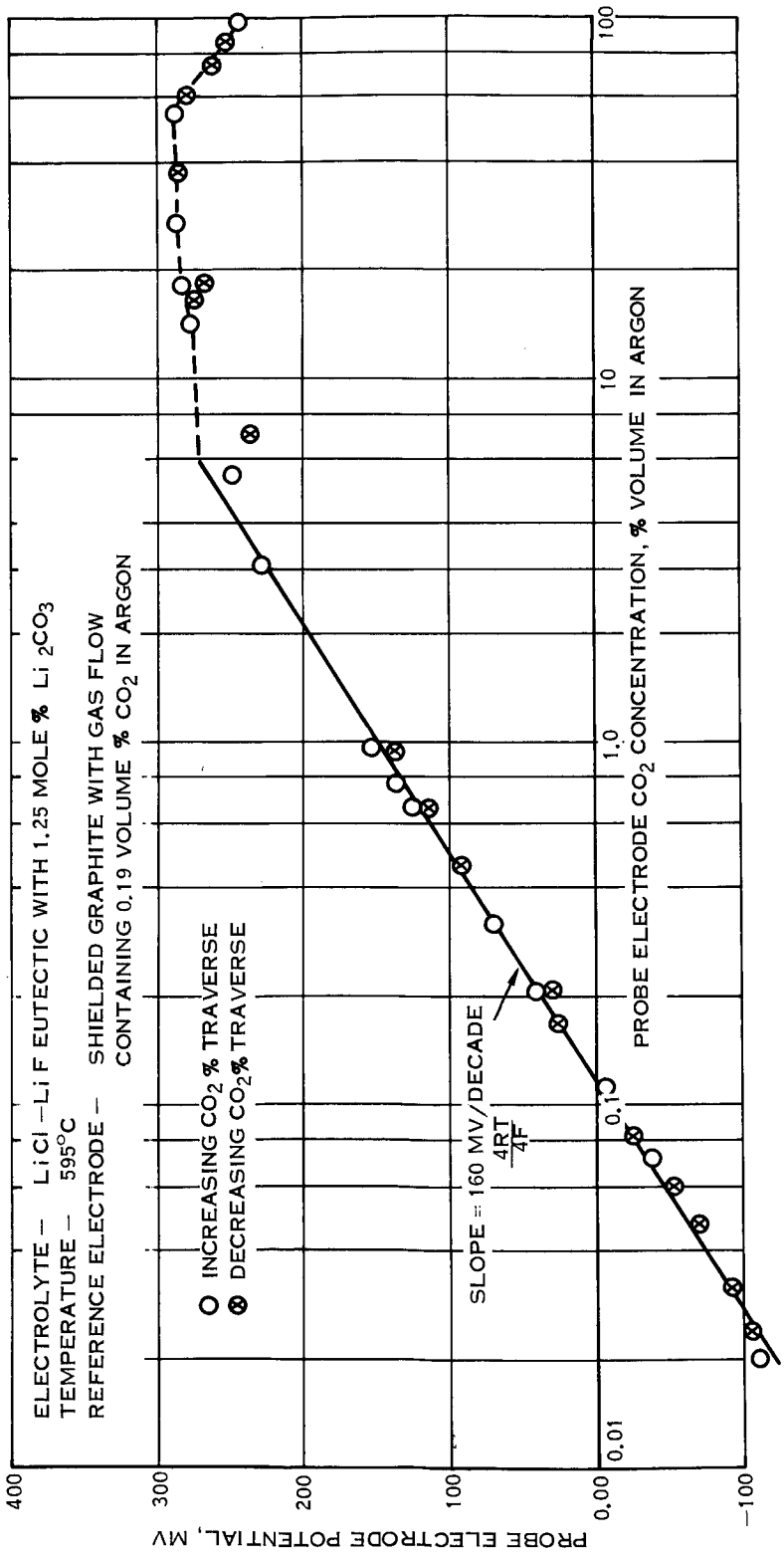

FIGURE 6-25 CARBON PROBE CO_2 SENSITIVITY IN WET ELECTROLYTE

7.0 EXPERIMENTAL SETUP AND PROCEDURES

Experimental activities have been carried out at two autonomous research facilities. It has been proven desirable at times to provide for some overlap of investigation, such as in cathode deposit studies and current-voltage studies. When such has been the case, both independent test setups are described with appropriate notation as to the location of the activity, Product Research Laboratory or Chemical Sciences Laboratory. Description of experimental hardware is limited to the following major areas of study:

Cathode Deposit Morphology
Anode Efficiency Studies
Carbon Dioxide Absorption
Polarography and Reference Electrodes
Phase Diagrams
Carbonate Decomposition Pressures

Also, some discussion of electrolyte preparation and analytical equipment and procedures is presented.

7.1 Equipment

7.1.1 Cathode Deposit Morphology

7.1.1.1 Product Research Laboratory

Three independent electrolytic cells have been employed. A photograph of the test facility is shown in Figure 7-1. A schematic of an individual cell unit is presented in Figure 7-2. The furnace assembly consists of ceramic encased heater elements enclosed by several inches of perlite insulation contained within an aluminum outer shell. Internal to the heater core is a AISI 304 steel liner implemented for appropriate temperature sensing. Temperature is controlled by a Minneapolis-Honeywell Pyrovane, while a Minneapolis-Honeywell Protectovane provides for over-temperature cutout. The electrolyte is contained in either a graphite or alumina crucible 4.5 inches O.D., which is set into a protective alumina coated nickel canister - the combined assembly being readily inserted into and removed from the furnace assembly. A cover fabricated from insulating material abuts the metal canister and supports electrodes, gas, bubblers, an electrolyte thermocouple well, and provides for exit gas ports.

The gas phase composition within the cell may be established prior to initiation of electrolysis with the system completely protected from the ambient atmosphere. Dry argon and nitrogen, less than 7 ppm H_2O, was supplied from the plant's tank farm as required.

7.1.1.1 (Continued)

Carbon dioxide was added through suitable metering and flow control devices. Humidity was controlled by bypassing an appropriate portion of the gas stream through a humidifier. Cell out-gases were vented through overhead "elephant trunk" vent hoods. Specific methods for gas phase monitoring and analysis of cell out-gases will be covered in the separate general section on analytical equipment and procedures.

Power for electrolysis was supplied by a model 809A Harrison Laboratories power supply which was readily modified for constant current or constant voltage operation. Upon completion of electrolysis, the cathode could be removed through a small port in the cover for examination of the deposit with little disturbance of the overall system. At times, devices have been provided for rotating or axially oscillating the cathode.

7.1.1.2 Chemical Sciences Laboratories

Cathode deposition studies were performed using a graphite crucible as the melt container. The crucible also served as the anode of the electrolytic cell. The cell container consisted of an Inconel tube which was closed at both ends with threaded fittings of the same material. The bottom fitting served as a holder for an adjustable pedestal which supported the graphite crucible and also served as the anodic electrical terminal. A "T" connection to the anode assembly served as a gas inlet to the cell. The top fitting was used to hold the cathode by means of a nylon swagelock connector which was bored through to allow a vertical adjustment of the cathode position in the melt. The entire assembly was supported in a Marshall tube type furnace which has heating coils provided with taps for shunting certain portions of the coils in order to minimize temperature gradients. The furnace temperature was controlled by a Barber-Colman proportional unit using a chromel-alumel thermocouple. It was found that the temperature could be held to $\pm 2^{\circ}C$ in the center zone of the furnace in the temperature range of 400°-$800^{\circ}C$. A photograph of a typical furnace assembly is shown in Figure 7-3, and a schematic drawing of the internal cell configuration is shown in Figure 7-4.

7.1.2 Anode Efficiency Studies

The cell configuration used in determining anode efficiencies is illustrated in Figure 7-5. It consists of a shielded nickel anode and a nickel cathode. A regulated flow of helium gas continually purges the anode chamber. Flow rate through the chamber is regulated and monitored by observing the rate of displacement of

7.1.2 (Continued)

bubbles through a volumetrically calibrated burette. Oxygen content of the purge gas leaving the anode and its flow rate allow a determination of the volume of oxygen being produced at the anode under electrolysis. The flow rate of the purge gas is periodically altered to ensure that readings are not being affected by system leaks. Volume of anode oxygen determined with varying purge gas flow rate has been consistently repeatable. The experimentally determined volume of oxygen compared to that predicted by Faraday's law is used as a measure of anodic efficiency.

7.1.3 Carbon Dioxide Absorption

A cell configuration such as has been illustrated in Figure 7-2 has been employed in carbon dioxide scrubbing experiments. Requirements for controlled carbon deposition have required monitoring of cell inlet and outlet carbon dioxide and have thereby provided scrubbing performance information. At specific times, however, cell modifications have been made to permit larger anode and cathode surface areas, and changes in sparger configuration and depth of submergence. Higher gas flows have required that a means of pressure regulation be provided so as not to force electrolyte to too high a level in the reference electrode, where it freezes and stops flow of the reference mixture. At all times carbon when in the system or at the cathode is protected from exposure to anodically produced oxygen or atmosphere by use of inert purge gases such as argon and protective metallic or ceramic shields.

7.1.4 Polarography and Reference Electrode Studies

7.1.4.1 Product Research Laboratory

Voltage was set and maintained by a constant voltage Model 809A Harrison Laboratories power supply. The corresponding current usually achieved steady state within 30 seconds. Voltages were determined by a Hewlett Packard Model 412A vacuum tube voltmeter and currents were monitored by a Triplet Model 800 V-O-M.

A schematic of a typical carbon reference and probe assembly is shown in Figure 4-8. The assembly consists of a 1/8 inch diameter graphite rod enclosed in a close fitting alumina tube through which controlled flows of CO_2-H_2O argon mixtures are passed and directed over a pointed end of the graphite submerged in the electrolyte. Isolation of the gas bubbling electrode by placing it within another alumina tube containing a minimum of melt and allowing ionic continuity to the bulk melt via pinholes in the shield has permitted fairly rapid response time with respect to controlled P_{CO_2} environments. A Hewlett Packard Model 412A VTVM was used to measure probe to reference potential differences.

7.1.4 (Continued)

7.1.4.2 Chemical Sciences Laboratories

Photographs of the experimental setup and an internal view of the cell for the current-voltage studies are shown in Figures 7-6 and 7-7. A sketch of the cell is shown in Figure 7-8. The power supply is a Wenking Potentiostat which electronically maintains a constant potential between the working and auxiliary electrodes.

The crucible and electrodes were constructed from an alloy of gold and palladium alloy. Alumina tubes were fitted over the working anode and cathode for convenient control of the electrode atmospheres. An Au-Pd wire was used as an auxiliary electrode. This electrode although not a true reference was used as a potential base. The difference in potential between the auxiliary and working electrode at zero current adjusts potentials to a true reference.

A photograph of the equipment used in the fast sweep polarography studies is shown in Figure 7-9 along with a typical cell and furnace configuration. The cell configuration is similar to that described in the preceding paragraphs. An Anatrol variable sweep potentiostat is used for the power supply in conjunction with a Mosley X-Y recorder. Sweep times as low as 5 seconds can be achieved over the selected voltage range.

7.1.5 Phase Diagrams

The phase diagram studies were performed using gold-palladium crucibles in the same type of furnace configuration as was shown in Figure 7-8 with the exception of the electrode sheaths. For the phase studies the top was fitted with stainless steel tubes joined at the bottom with 80 percent gold-20 percent palladium alloy tubing which penetrated the melt. A closed end tube was used as a well for a Pt-Pt 10 percent Rh thermocouple, and an open end tube was used as an argon bubbler for melt agitation. Accurate temperature measurement was achieved using Pt-Pt 10 wt % Rh thermocouples calibrated against a standard thermocouple certified by the National Bureau of Standards. The major portion of the thermocouple emf was balanced with a Leeds and Northrup Type K Potentiometer, and the remainder (less than 200 microvolts) was amplified with a Leeds and Northrup microvolt amplifier. This amplified signal was fed to a Varian 10 microvolts strip chart recorder. In this manner full-scale deflection of the recorder corresponds to $5.0^{\circ}C$, using the most sensitive amplifier range (50 microvolts). The accuracy of the temperature measurements is limited only by the thermocouple calibration, which is $\pm 0.2^{\circ}C$.

7.1.6 Carbonate Decomposition Pressures

CO_2 vapor pressure studies were performed using the apparatus shown in Figure 7-10. The melts were contained in an Au-Pd crucible 1.0 inch in diameter by 2.5 inches long. The crucible was suspended from a Mettler model H16 semi-micro balance by means of a 0.020 inch Au-Pd wire. The furnace and furnace control were the same as those previously described with the exception that the Barber-Colman furnace control unit was supplemented by a model 2000 program controller. A series of cams were used so that the furnace could be heated at a linear rate of about 1.0°C/minute. The flow rates of each gas was measured with Matheson series 600 calibrated flow meters.

7.2 Electrolyte Preparation

7.2.1 Product Research Laboratory

Commercially available salts, ACS and reagent grade have generally been used without any further chemical purification. Occasionally salts were partially dried by heating in a vacuum furnace; in nearly all instances salts were dried within the electrolytic cell by prolonged heating and the use of dry inert purge gas stream such as argon. Measurements of the concentration of water vapor in the effluent argon purge and of hydrogen served as a reliable indicator of residual water with the melt. Mixtures containing LiCl stubbornly retained water which was extremely difficult to remove. Displacement of water by CO_2 has been one method used but extremely slow water removal rates were experienced if very low moisture levels were to be obtained. Chlorine gas has been used as described by Maricle and Hume (Reference 9) to purge the melt of water and hydroxide in accord with the reaction:

$$LiOH + Cl_2 \longrightarrow LiCl + HCl + 1/2O_2$$

which resulted in a drier melt. This reaction was verified by measurement of O_2 in the outgas.

7.2.2 Chemical Sciences Laboratories

All salts were dried before use by heating under vacuum at room temperature until the pressure in the system was less than 10^{-4} mm Hg. The temperature was then raised and the process repeated. This procedure was continued to temperatures of 500°C in the case of the alkali halides and lithium oxide. Lithium carbonate was dried under vacuum at room temperature only. Subsequent drying to 450°C was accomplished with the salt exposed to a dry atmosphere of CO_2 (< 20 ppm H_2O). It was found that Li_2O and LiF could be

7.2.2 (Continued)

readily dried; however, LiCl required 7-8 days to dry at a maximum temperature of 500°C. Removal of the bulk of the water from this salt at low temperatures has been found to minimize the hydrolysis (Reference 10).

Although lithium carbonate does not pick up moisture as readily as lithium chloride, it became apparent from these studies that the reagent grade carbonate contained more water than the same purity lithium chloride, and that the rate of water removal from the carbonate was much slower under the same conditions of temperature and pressure so that it required even longer drying periods. In most cases the hydrolysis of the carbonate was less than 0.1 percent; the LiCl was found to contain as much as 1.5 percent hydroxide.

7.3 Analytical Equipment and Procedures

In the course of the program, it has been necessary to rely upon an assortment of analytical techniques for establishing the composition and structure of electrolysis products. X-ray diffraction, optical microscopy, and electron microscopy have been widely utilized for structure determinations on cathodic deposits. A Beckman D-2 paramagnetic oxygen analyzer is used for oxygen analysis. Two Beckman D-2, an MSA LIRA infrared analyzer and a Consolidated Electrodynamics Model 21-620A mass spectrometer have been used for carbon dioxide measurements, and a General Electric, Type H-1, halide detector for halogen gases. A Jarrell-Ash N-700 gas chromatograph equipped with an argon ionization detector was used for trace analysis of hydrogen, methane, carbon dioxide, acetylene, etc. A Baird Atomic 3 meter spectrograph was employed for trace analysis of nickel, iron, boron, and other elements found at times in the melts and deposits. Wet chemistry techniques for oxide, carbonate, chloride, etc., analyses are used extensively. The oxide-carbonate analysis has been so frequently employed that it is briefly described below. Chemical detection tubes which change color have been employed for carbon monoxide, nitrogen oxides, hydrogen sulfide identification when appropriate. In controlled humidity studies, Beckman electrolytic hygrometers and an Alnor (Type 7300) dew pointer were utilized.

The determination of the Li_2O concentration in the carbonate halide mixtures was based on the acid titration of the carbonate-hydroxide mixture resulting from the dissolution of the sample in pure water under an inert atmosphere. A pH meter was used to indicate the two end points in the titration, the first corresponding to the hydroxide content plus one-half the carbonate, and the second to one-half the carbonate. The difference between the first and second end points corresponds to the amount of oxide originally in the sample.

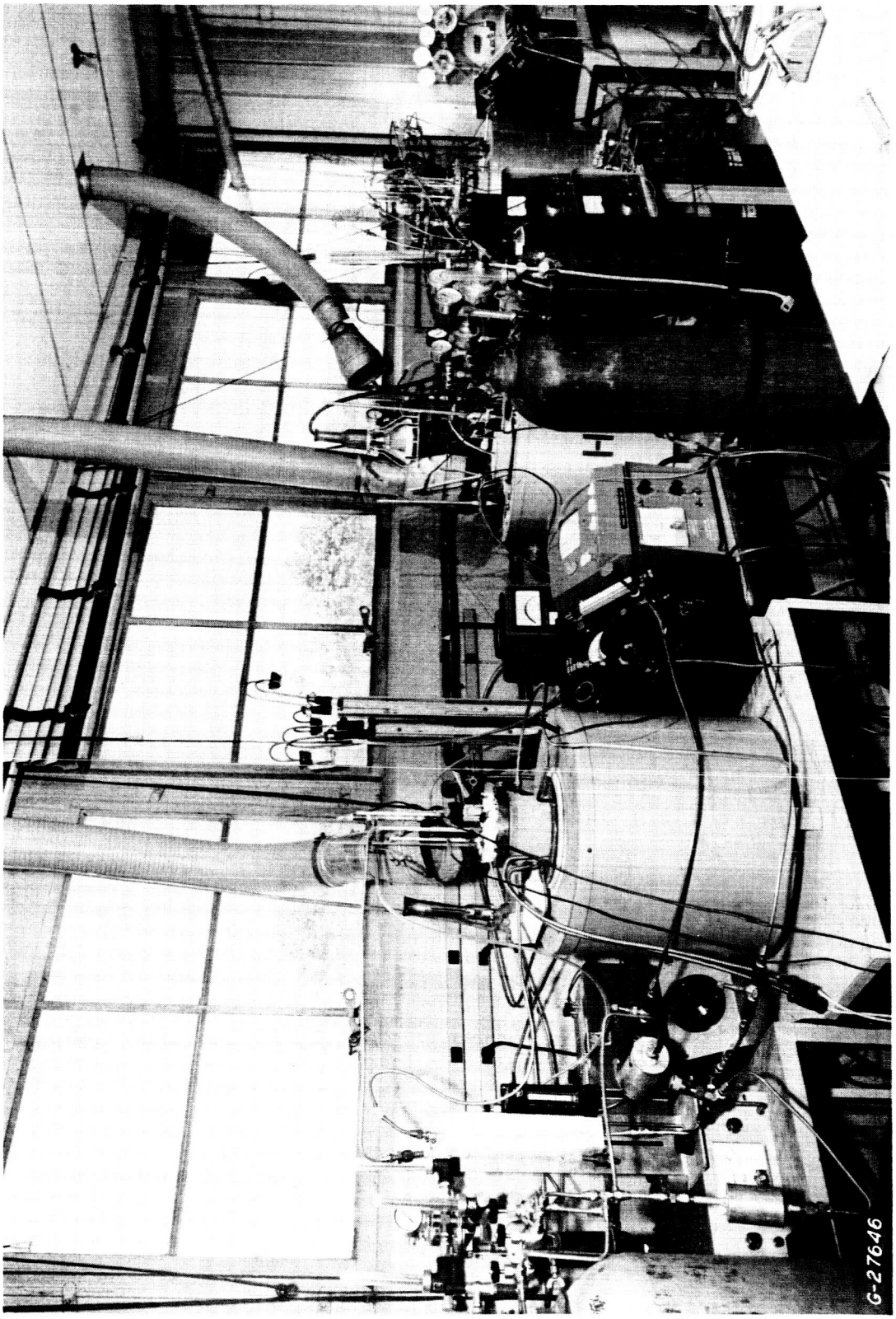

FIGURE 7-1 PHOTOGRAPH SHOWING THREE ELECTROLYSIS CELLS (PRODUCT RESEARCH LABORATORY)

THIS IS A BLANK PAGE

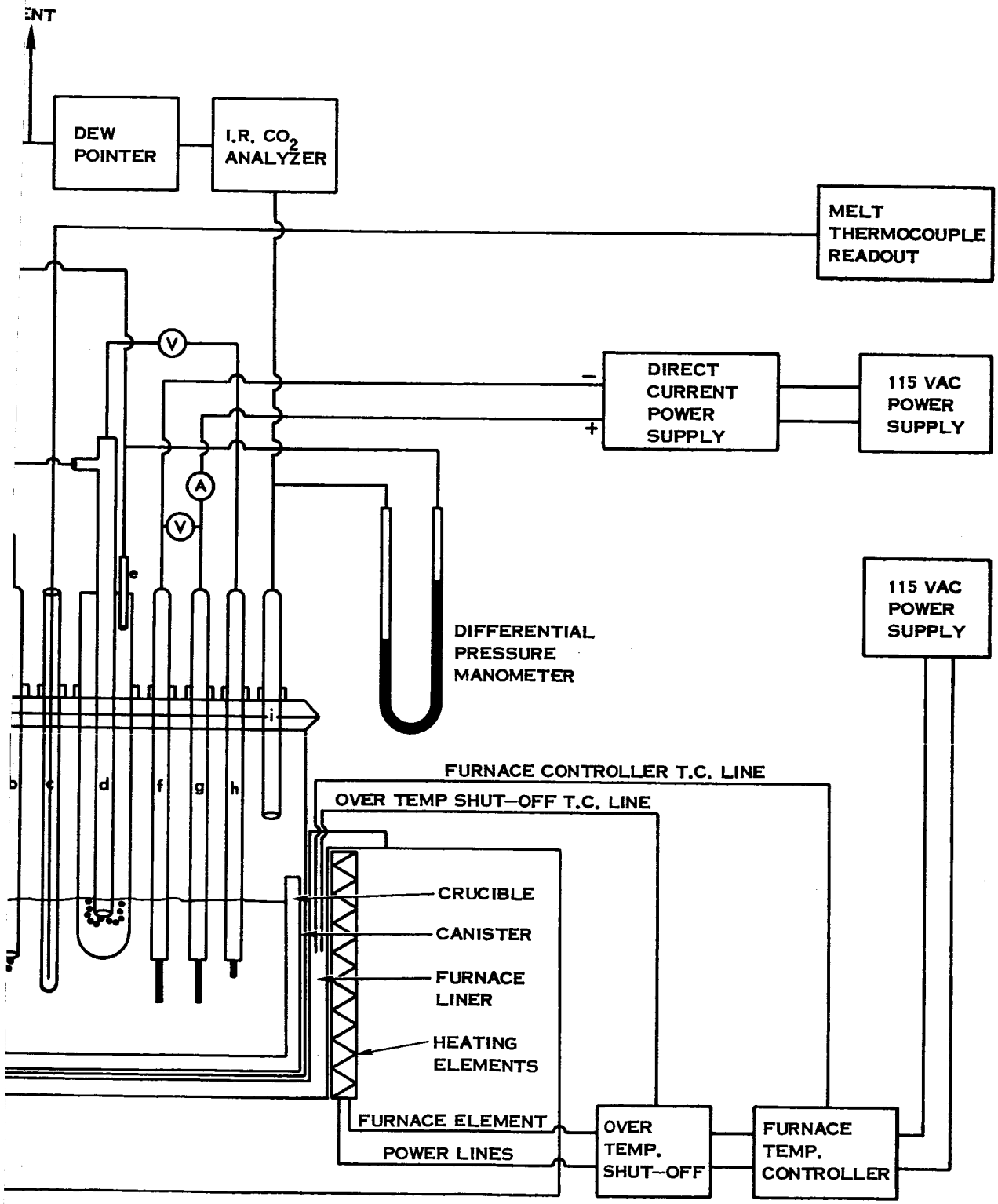

FIGURE 7-2
SCHEMATIC: ELECTROLYSIS CELL
(PRODUCT RESEARCH LABORATORY)

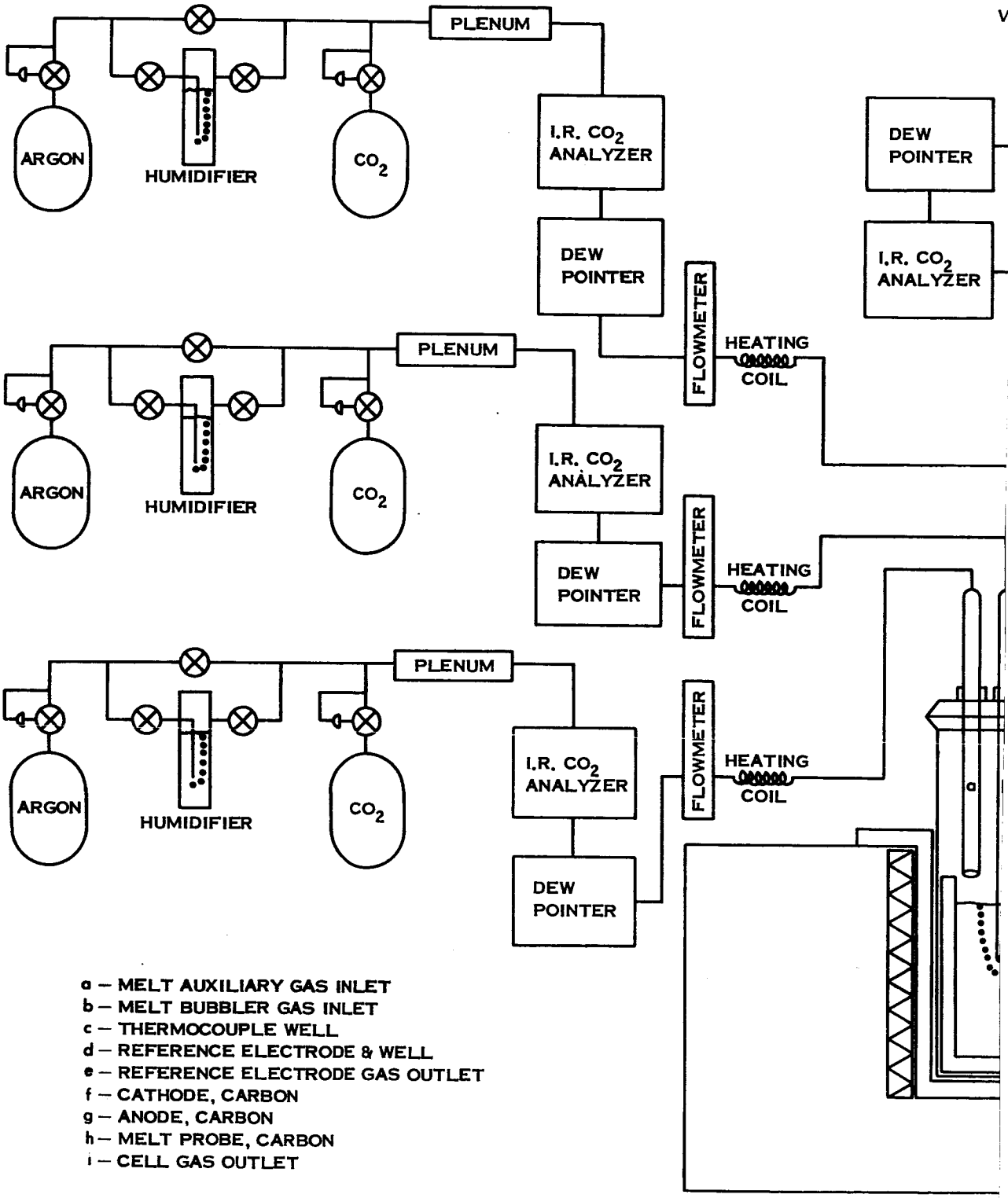
PLENUM
ARGON
HUMIDIFIER
CO_2
I.R. CO_2 ANALYZER
DEW POINTER
FLOWMETER
HEATING COIL
DEW POINTER
I.R. CO_2 ANALYZER
PLENUM
ARGON
HUMIDIFIER
CO_2
I.R. CO_2 ANALYZER
DEW POINTER
FLOWMETER
HEATING COIL
PLENUM
ARGON
HUMIDIFIER
CO_2
I.R. CO_2 ANALYZER
DEW POINTER
FLOWMETER
HEATING COIL
a
a – MELT AUXILIARY GAS INLET
b – MELT BUBBLER GAS INLET
c – THERMOCOUPLE WELL
d – REFERENCE ELECTRODE & WELL
e – REFERENCE ELECTRODE GAS OUTLET
f – CATHODE, CARBON
g – ANODE, CARBON
h – MELT PROBE, CARBON
i – CELL GAS OUTLET

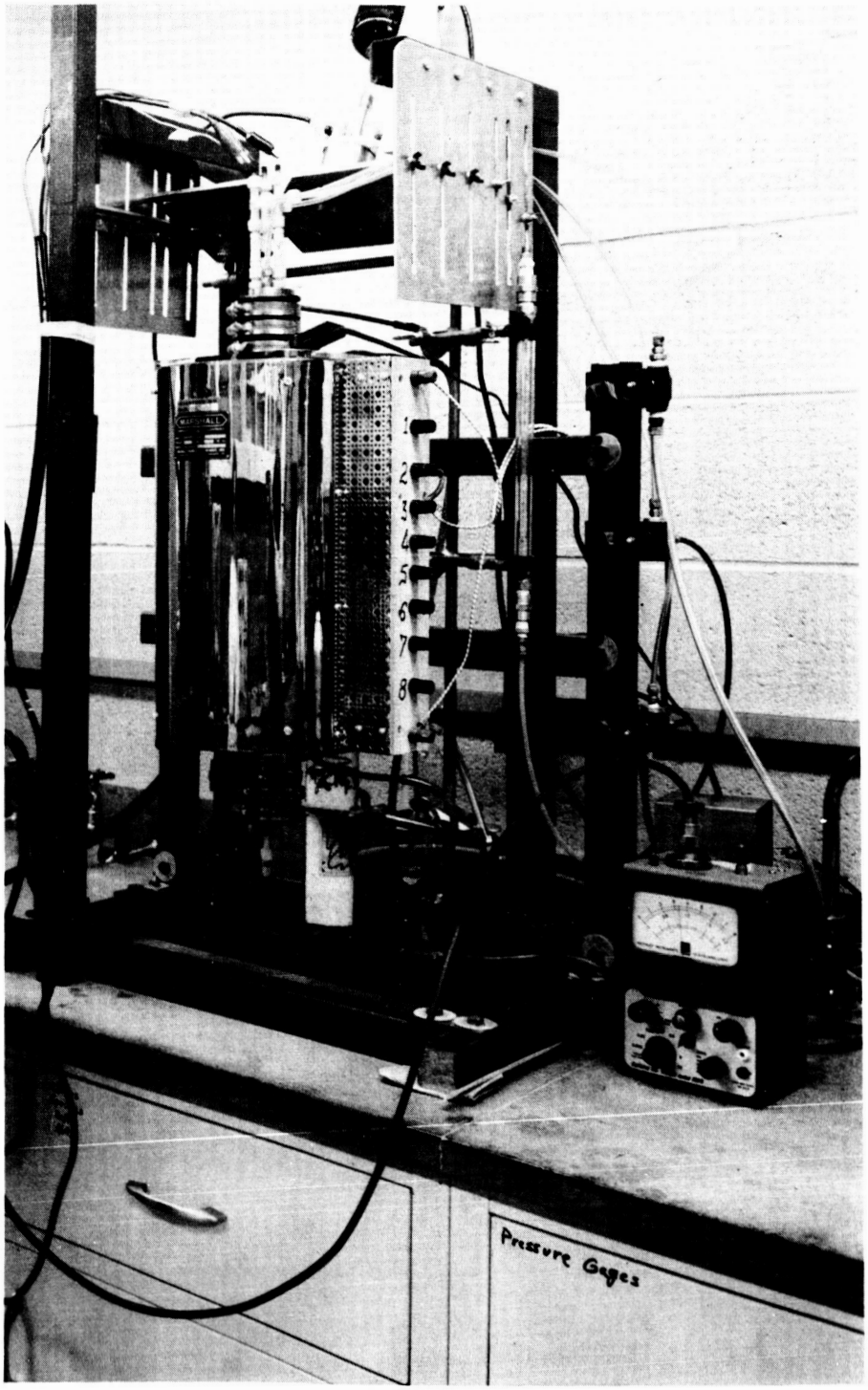

FIGURE 7-3 ELECTROLYSIS CELL (CHEMICAL SCIENCES LABORATORIES)

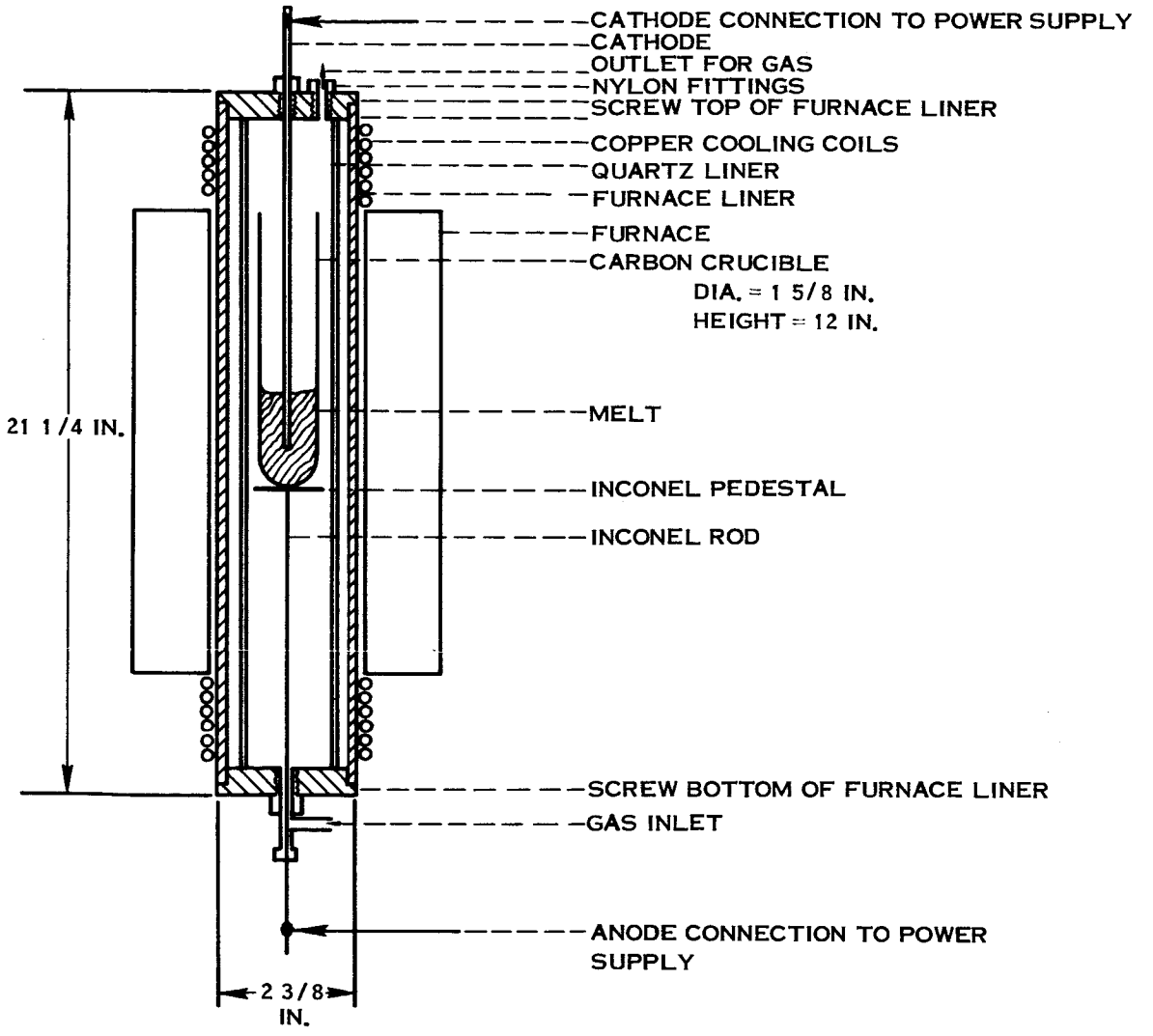

FIGURE 7-4 ELECTROLYSIS CELL FOR CARBON DEPOSIT STUDIES (CHEMICAL SCIENCES LABORATORIES)

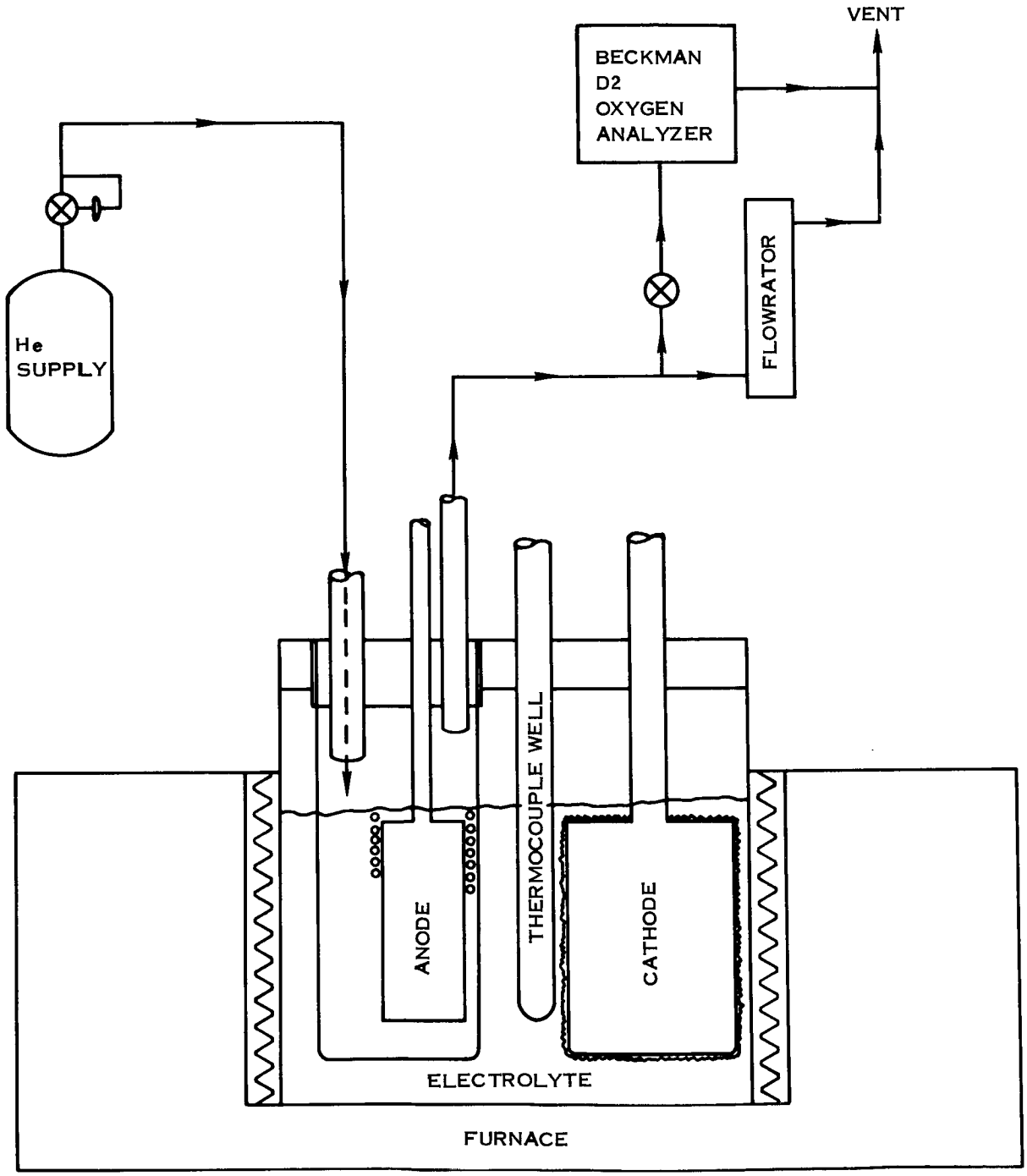

FIGURE 7-5 SCHEMATIC OF UNIT FOR ANODIC EFFICIENCY DETERMINATION

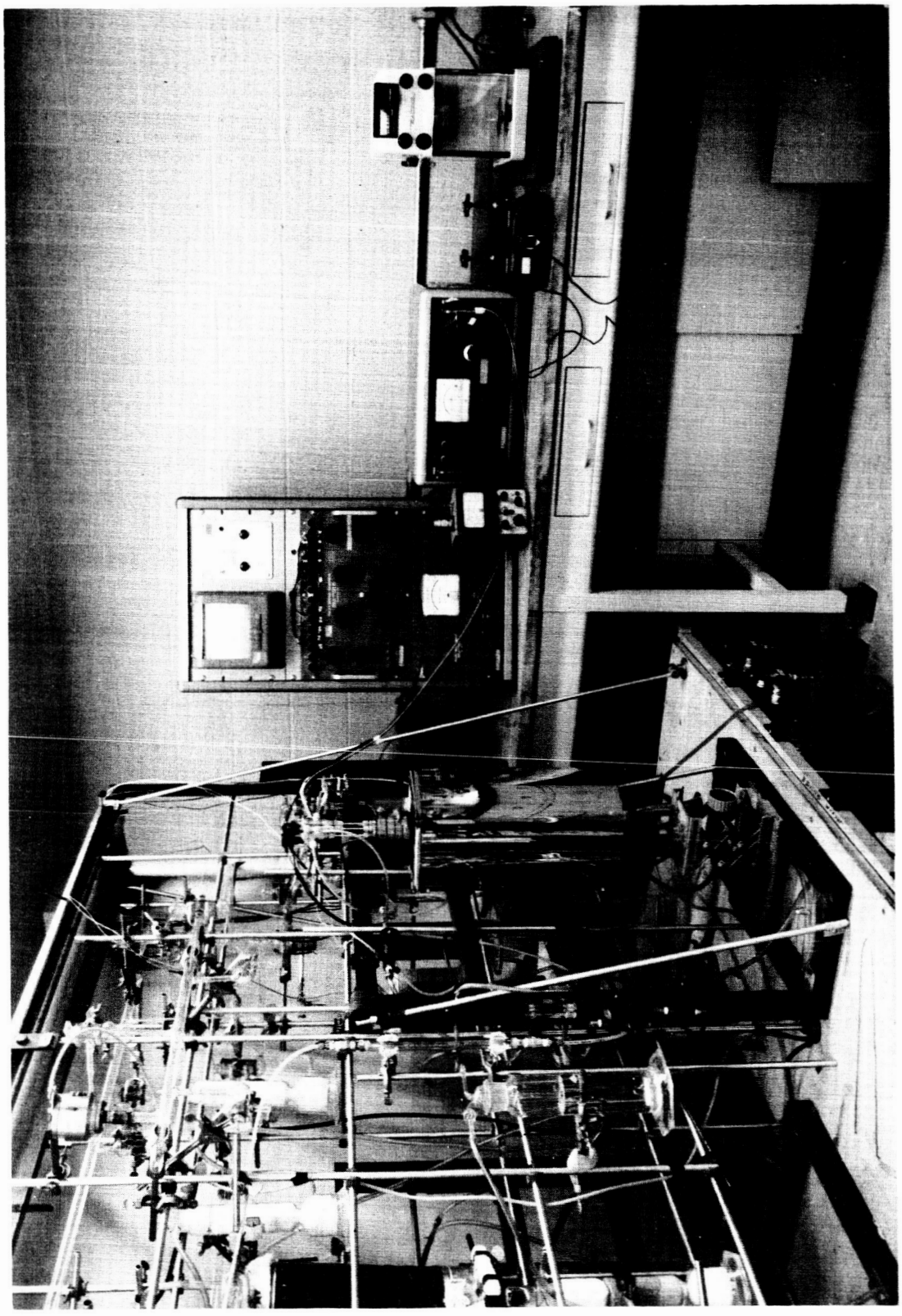

FIGURE 7-6 PHOTOGRAPH SHOWING ELECTROLYSIS CELL AND POLAROGRAPHIC EQUIPMENT (CHEMICAL SCIENCES LABORATORIES)

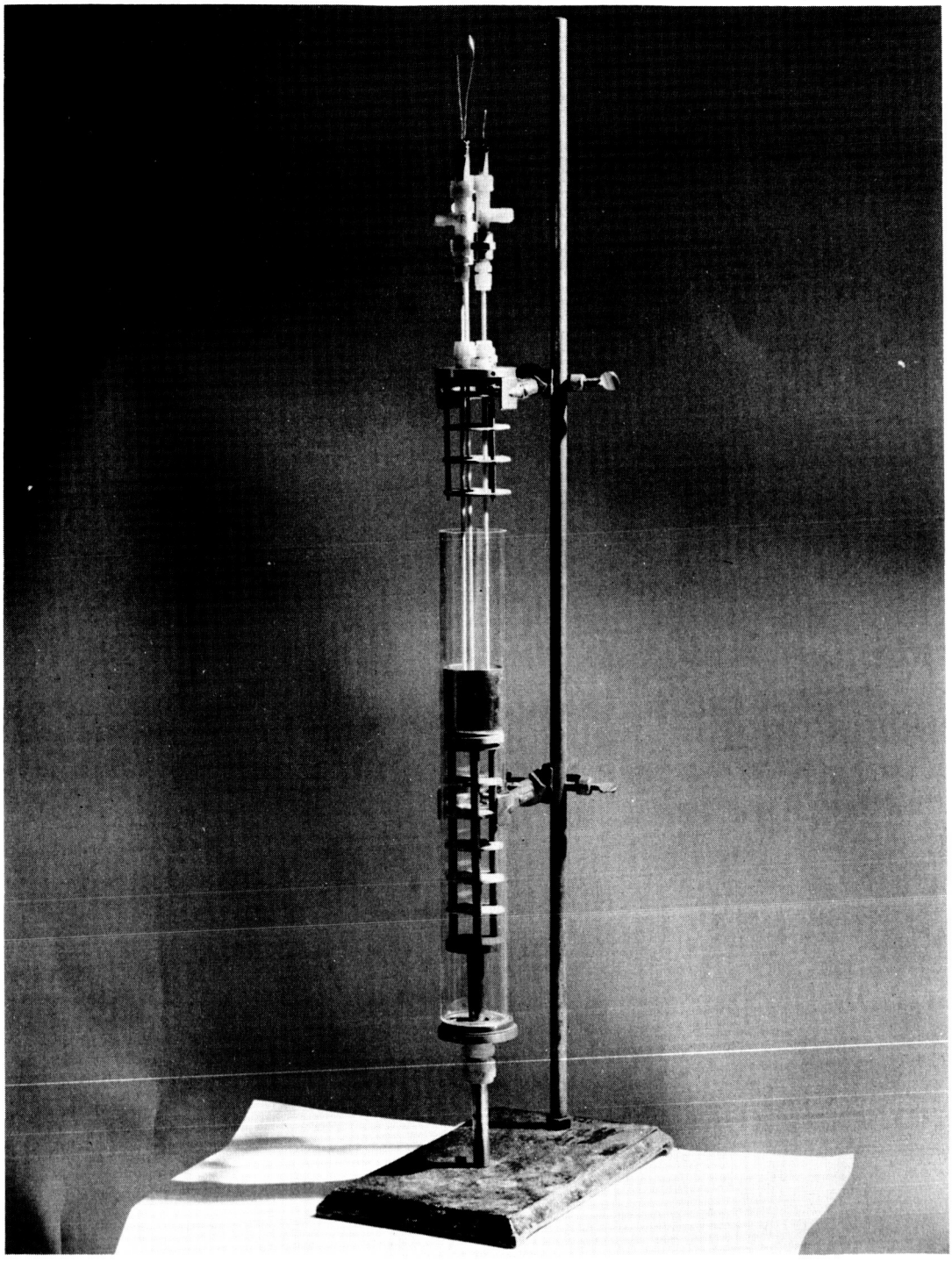

FIGURE 7-7 PHOTOGRAPH OF CELL USED FOR POLAROGRAPHIC AND PHASE DIAGRAM STUDIES (CHEMICAL SCIENCES LABORATORIES)

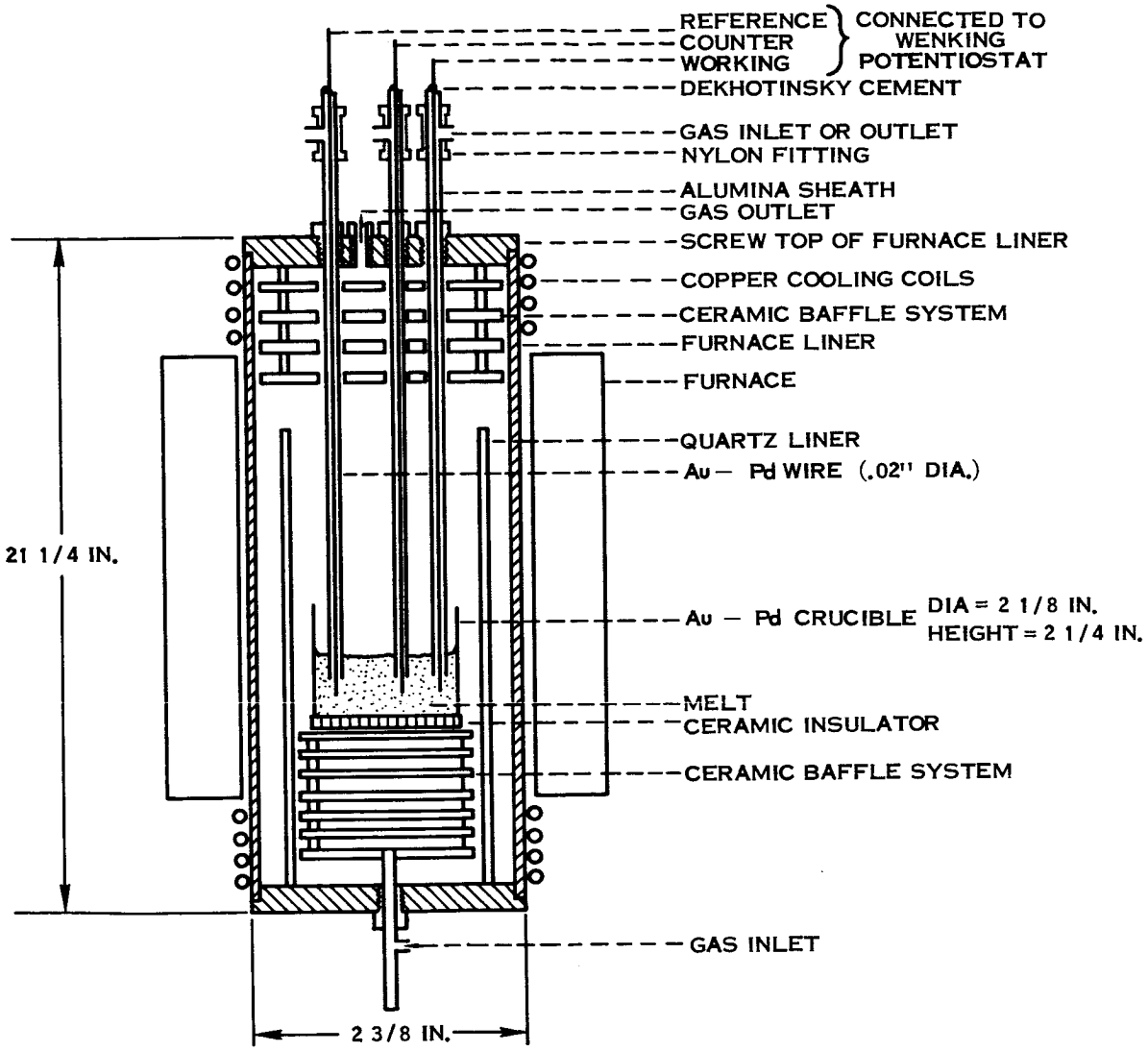

FIGURE 7-8 SCHEMATIC OF CELL USED FOR POLAROGRAPHIC AND PHASE DIAGRAM STUDIES (CHEMICAL SCIENCES LABORATORIES)

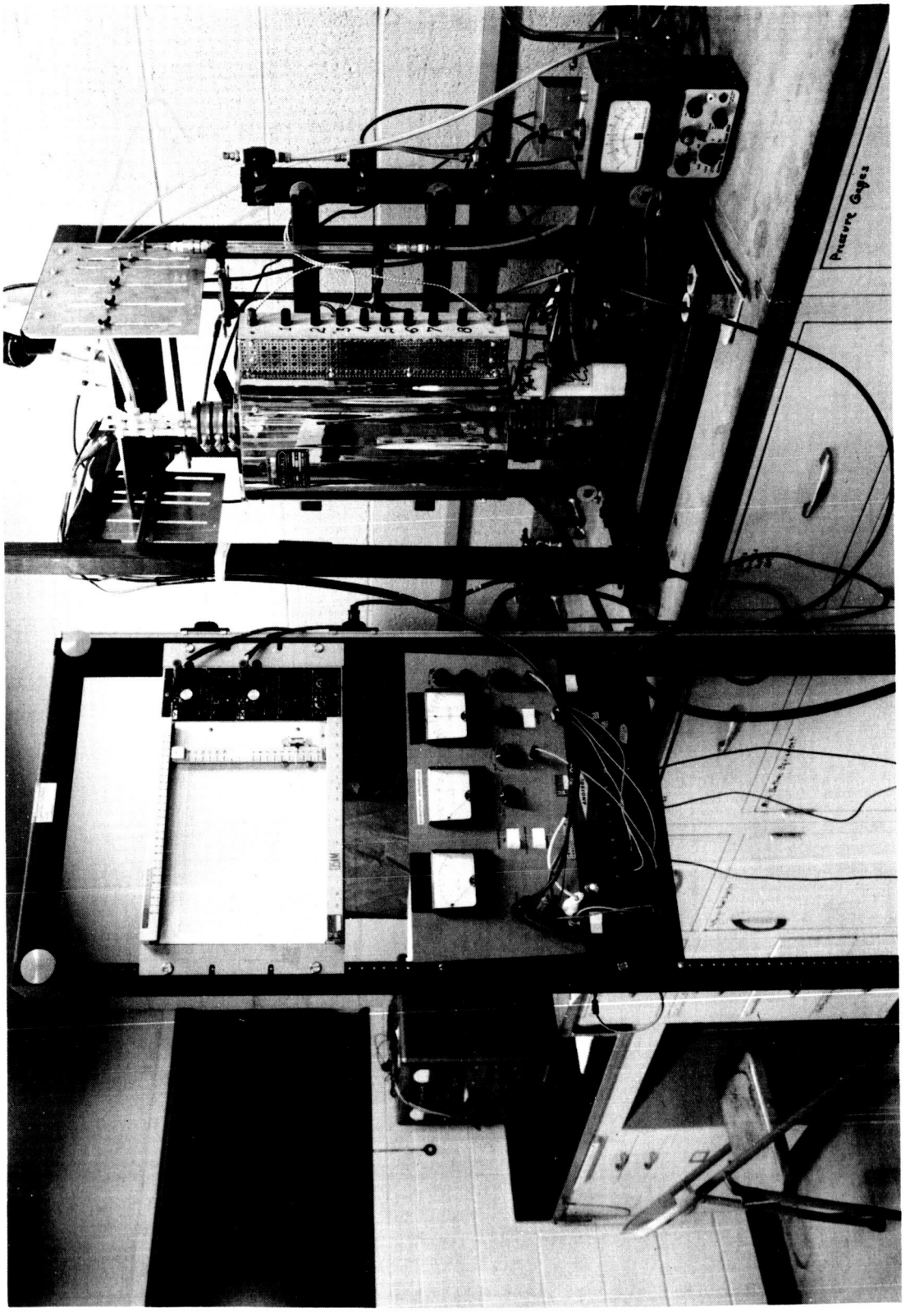

FIGURE 7-9 PHOTOGRAPH OF ELECTROLYSIS WITH A RAPID SWEEP POLAROGRAPHIC EQUIPMENT (CHEMICAL SCIENCES LABORATORIES)

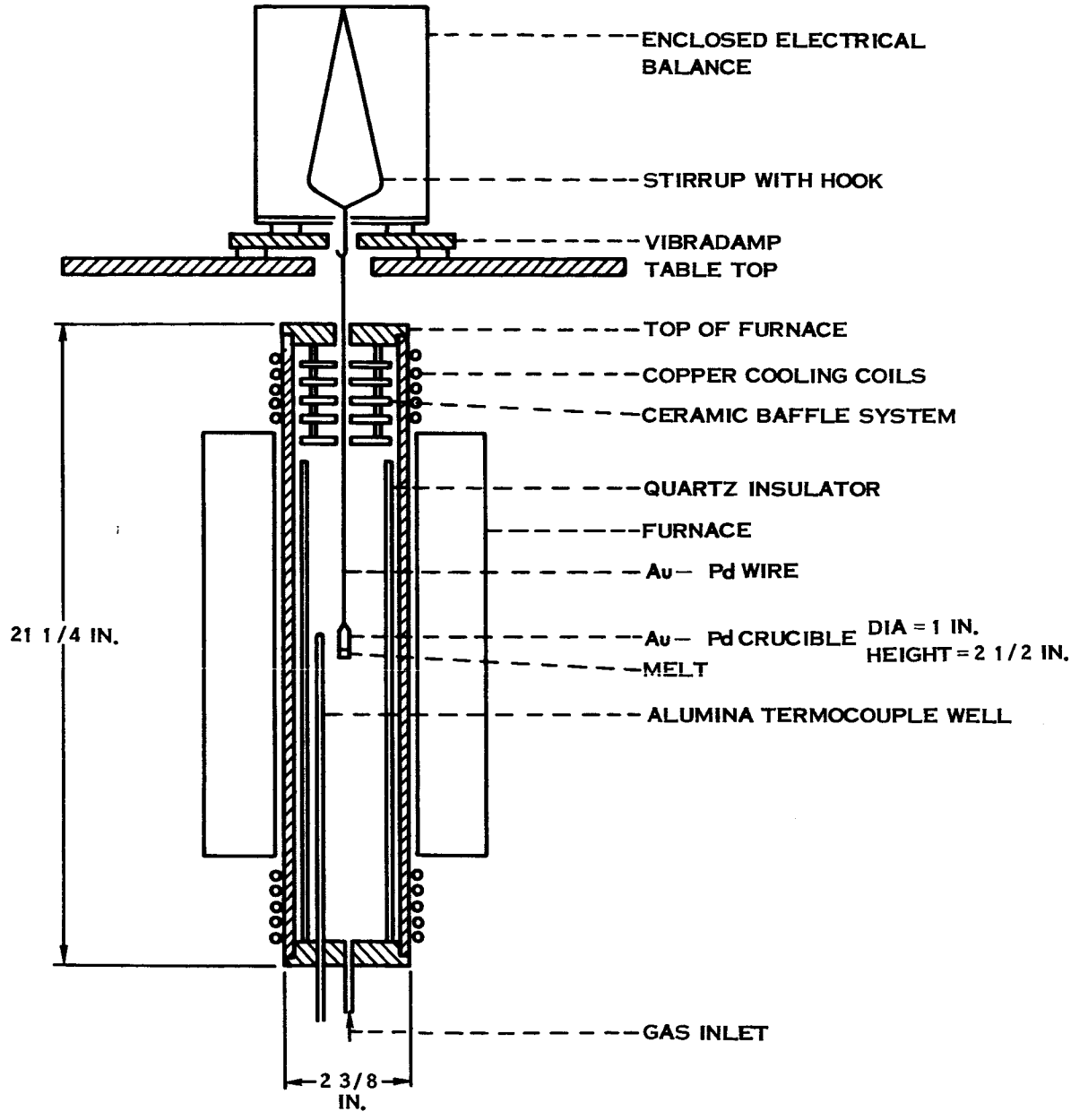

FIGURE 7-10 SCHEMATIC OF DISSOCIATION PRESSURE APPARATUS

8.0 ELECTROLYTE STUDIES

Selection of an electrolyte in which suitable P_{CO_2}, P_{H_2O}, carbonate, oxide, and hydroxide equilibria can be maintained is required for pure oxygen production over long periods of time, and formation of dense carbon at the cathode while sufficient oxide ions are provided to the electrolyte for absorbing further carbon dioxide. A primary problem is accumulation and precipitation of lithium oxide in the vicinity of the cathode during electrolysis, thus interfering with the orderly deposition of carbon and in the process the oxide becoming unavailable for CO_2 scrubbing. The accumulation of lithium oxide appears to be a function of the cathode current density; at low current densities a graphitic carbon deposit can be formed at the cathode for a considerable period of time before oxide accumulation upsets the process. Thus, any salt-solvent composition in which the solubility of lithium oxide is at a maximum should improve carbon deposition at the cathode and overall cell processes. For this reason phase diagram studies were performed to ascertain the relationship of Li_2O to the Li_2CO_3-LiCl and Li_2CO_3-LiF systems.

The CO_2 vapor pressure of the electrolyte is an indication of the amount of oxide present in the melt if it is assumed that the carbonate ion activity remains constant. In this case the P_{CO_2} is inversely proportional to the oxide ion concentration. Although the concentration of oxide can not be directly determined, to ascertain equilibrium constants, it is still possible to compare one system to another. For when P_{CO_2} for each system is determined as a function of temperature, it is possible to obtain a heat of decomposition from the slope of an Arrhenius plot that is in actuality the heat of the reaction:

$$CO_3^{=} \leftrightharpoons CO_2 + O^{=} \qquad 8\text{-}1$$

in the particular molten system under investigation. If ΔH for Equation 8-1 is constant over the temperature range investigated, it is then possible to estimate equilibrium constants using the Nernst approximation formula:

$$\log K_p = \frac{-\Delta H}{4.57T} + 1.75\,\Delta ng \log T + \Sigma(nc) \qquad 8\text{-}2$$

where n is the number of moles of each gaseous species participating in the reaction, Δng is the difference in the number of moles of gaseous reactants and gaseous products, and **c** is an empirical constant for each gaseous substance.

It is for this reason that a program was initiated to determine the equilibrium CO_2 partial pressures of several carbonate-containing systems as a function of temperature.

8.0 (Continued)

The corrosion of various containers and electrode materials has also been investigated as part of the electrolyte studies. Much information on corrosion in all-carbonate melts has been obtained from a series of papers by Janz and his coworkers (References 11, 12 and 13); however, the problem of anode dissolution in halide-carbonate mixtures was investigated in this laboratory.

8.1 Phase Diagram Studies

The method of analysis was based on the well-known freezing point method of thermal analysis where halts in a temperature-time plot as the melt cools is an indication of phase separation. An inflection in this plot is obtained when the first solid phase separates and a final temperature halt is obtained at a eutectic point corresponding to the final disappearance of the liquid phase. The fundamental concepts of this experimental technique are similar to those of Solomons and Janz (Reference 14).

The results of studies with the Li_2CO_3-LiF-Li_2O system are summarized in Figure 8-1. Although the freezing point depression shows a leveling off at the higher concentrations of Li_2O, visual observation indicates that the solubility limit has not been reached. Since no inflection point was noted in the cooling curve before the final solidification, it appears that the ternary system forms solid solutions rather than a ternary eutectic. This behavior may be explained on the basis of the sizes of the oxide and fluoride ions. It has been shown that most systems that form solid solutions are those which contain ions of similar size. The diameter of the oxide ion is 1.40 Angstroms and the fluoride ion, 1.36 Angstroms.

In order to provide support for this behavior the Li_2O-LiF system was studied up to 30 weight percent Li_2O (27.0 mole percent). Again, only one break was noted in the freezing point curves and the freezing point was lowered from 845°C (the freezing point of LiF) to 810°C at 30 weight percent Li_2O. A plot of freezing point against Li_2O concentration shows a slight leveling off in this curve indicating a solid solution formation. This plot also indicates a system with a minimum melting point (not to be confused with a eutectic composition). It is not possible to tell where this minimum lies without going to high Li_2O concentrations. This latter course was not possible in the present apparatus due to corrosion problems and temperature limitations (the melting point of $Li_2O \cong 1500°C$).

The solubility of Li_2O in fluoride systems seems to be high. The fact that a high degree of association exists in the melt may be beneficial but whether this presents problems of decreased mobility of oxide ions is not known.

8.1 (Continued)

The $LiCl-Li_2O$ system was investigated in the low Li_2O concentration range in order to determine if the larger difference in anion sizes had an appreciable effect on the nature of the phase diagram. The cooling curves showed two breaks in each case as shown below.

Freezing Points of the $LiCl-Li_2O$ System

Composition (wt % Li_2O)	Initial Solid Separation Temp., °C	Final Solidification Temp., °C
0.0		602
5.0	583	560
9.5	563	560
10.4	560	559
12.0	560	558
16.7	559	558

The Li_2O concentrations noted above were as added and no actual analyses were performed. It was noted that solids were present in the bottom of the Au-Pd crucible at Li_2O concentrations above the nominal 10.4 weight percent. It would appear that a solubility limit is reached at this point since raising the melt temperature to 750°C did not cause the solids (probably Li_2O) to go into solution. It appears that the eutectic point is near 10 weight percent Li_2O at 560°C but that there is a sharp rise in the solid-liquidus curve above that concentration. In any event, it does appear that the Li_2O-LiCl system acts in a regular manner at low Li_2O concentrations, rather than forming solid solutions.

In view of these encouraging results a series of experiments were performed on the Li_2CO_3-LiCl-Li_2O system. Freezing point determinations were made on Li_2CO_3-LiCl mixtures containing 20, 30, 40, 50 and 60 weight percent Li_2CO_3. The change in the freezing point in each one of these mixtures was measured as a function of Li_2O concentration. In this manner it was hoped that a three-component phase diagram at low Li_2O concentrations could be mapped out. The binary eutectic point for the Li_2CO_3-LiCl system was found to be 513°C at 37 weight percent Li_2CO_3. The data for the addition of Li_2O to the various Li_2CO_3-LiCl mixtures is summarized in Figure 8-2. In most cases only two breaks were noted in the cooling curves; however, three breaks are sometimes present. Typical cooling curves for these two cases are shown in Figure 8-3. The latter observation would be expected in a ternary system if the initial temperature of the cooling curve were high enough to ensure a homogeneous liquid phase. The three

8.1 (Continued)

breaks in this case correspond to (1) initial separation of a solid phase, (2) the separation of a second solid at a binary eutectic line, and (3) final solidification of the ternary melt.

The second solidification point is sometimes quite pronounced and other times just a change of slope in the cooling curve (shown in brackets with a question mark). This behavior does not seem to be a function of Li_2O concentration. It may be that when the first and second solidification points are close to one another they show up at one inflection point in the cooling curve, or that the separation of a second solid is not accompanied by a long enough isothermal period as compared to the cooling rates used in these experiments.

Since there were so many uncertainties in the cooling curves, the difference between the first solidification and final solidification points was used to determine the proximity of the original homogeneous liquid composition to the ternary eutectic point. When this data is coupled with that for the LiCl-Li_2O and Li_2CO_3-LiCl systems it is possible to draw the binary eutectic lines for this part of the system. The result of these approximations are shown in the diagram in Figure 8-4. It appears that the ternary eutectic lies somewhere near the composition 30 weight percent Li_2CO_3 and 5 weight percent Li_2O.

A series of experiments were also carried out in the Li_2CO_3-Li_2O system at Li_2O concentrations up to 12 weight percent. The cooling curves were similar to those of the Li_2O-LiCl system but the limit of solubility of Li_2O, and thus the eutectic point, was about 6 weight percent. The postulated binary tie line for this part of the system is also shown in Figure 8-4.

The problem of the solubility of Li_2O is not really solved. The fact that Li_2O does not appear to go into solution at the higher temperatures when it is present in excess of 5-10 weight percent may be due to very slow solubility or to some compound formation that is as yet not understood. From a practical standpoint the temperature of this system cannot be raised much above 700°C because of LiCl vaporization. Therefore, a limit of about 5 weight percent Li_2O in compositions near the Li_2CO_3-LiCl eutectic point must be imposed on the CO_2 reduction system if this electrolyte is used.

In summary, it would appear that the solubility of Li_2O is enhanced in the presence of fluoride ions. The reduction in the melting point of the Li_2CO_3-LiF system is greater than that in the Li_2CO_3-LiCl system at a given Li_2O concentration even though there is no evidence of a eutectic point in the former electrolyte. The fluoride system also has the advantage of being thermally stable. No

8.1 (Continued)

volatilization of LiF is noted at temperatures up to 900°C.

8.2 Carbonate Dissociation Pressures

The atmosphere over the melt was controlled by mixing argon and CO_2, dried over magnesium perchlorate, in the proportion desired. The total flow rate of gas through the cell was held at 100 cubic centimeters/minute and each gas mixture was analyzed by mass spectrometry. At very low P_{CO_2} values the CO_2 was introduced into the argon stream by passing the argon over $CaCO_3$ heated to the desired temperature in a combustion tube furnace. Again, the gas mixture was analyzed by mass spectrometry.

The vapor pressure measurements were made by holding the P_{CO_2} constant over the melt and slowly changing the temperature. A chromel-alumel thermocouple, placed near the suspended crucible, was used to measure the temperature. At these slow rates of temperature change the measured temperature should be the same as that of the melt. When the vapor pressure of the melt exceeds the P_{CO_2} in the system, the sample should lose weight. The weight of the samples is recorded as a function of temperature and the point at which the weight loss was noted was taken as the decomposition temperature at that pressure.

The buoyancy effect was studied by determining the change in weight of the empty crucible over the temperature range 250-650°C. The weight was found to be constant within ±0.2 milligrams.

After each run the furnace was cooled to a temperature just above the melting point of the system under study, and the P_{CO_2} was raised to one atmosphere. The sample was kept under those conditions until the original sample weight was achieved. In this manner the amount of oxide present at the beginning of each run was constant and very small, even though the original carbonate purity is not known. This method also served as a check on halide volatility when carbonate-halide mixtures were studied since the halide loss is not reversible.

The results of these measurements on three electrolyte systems are summarized in Figure 8-5. The data obtained with "pure" Li_2CO_3 dried at 600°C under a CO_2 atmosphere, was found to be in good agreement with that of Lorenz and Janz (Reference 15). The absolute pressures were slightly lower than those reported in Reference 15, but the slope of a log P_{CO_2} vs 1/T plot was the same. These plots are based on the integrated form of the Clausius-Clapeyron equation:

8.2 (Continued)

$$\log P = -\frac{\Delta H}{2.303R}(1/T) + \text{constant} \qquad 8\text{-}3$$

where, in this case, ΔH can be taken as the heat of dissociation of the carbonate and is calculated from the slope of the plot $\left(-\frac{\Delta H}{2.303R}\right)$.

The log P_{CO_2} vs 1/T plots, for Li_2CO_3, the Li_2CO_3-LiF eutectic mixture and the LiCl-KCl eutectic containing 10 weight percent Li_2CO_3, are shown in Figure 8-6. These plots represent the best straight line for each system as calculated by the method of least squares. In the temperature-pressure range where these systems can be compared, the Li_2CO_3 system shows the lowest dissociation pressure, the Li_2CO_3-LiF eutectic, slightly higher pressures, and the LiCl-KCl + 10 wt % Li_2CO_3, the highest. These observations are supported by the heats of dissociation for the reaction:

$$CO_3^{=} \leftrightharpoons CO_2 + O^{=}$$

as shown below.

Electrolyte	ΔH, (K cal/mole)
Li_2CO_3	76.9
Li_2CO_3-LiF eutectic	37.0
LiCl-KCl + 10 wt % Li_2CO_3	16.5

Using the equation 8-2

$$\log K_p = \frac{-\Delta H}{4.57T} + 1.75\,\Delta ng \log T + \Sigma(nc)$$

and assuming that ΔH is an average value over the temperature range studied in such case, T may be selected as the average temperature in °K. Taking $c = 3.2$ for CO_2 and $\Delta ng = 1$, $n = 1$, the following values for K_p are obtained at the average temperatures of 800°K for the KCl-LiCl and 10 wt % Li_2CO_3 system, 1100°K for the Li_2CO_3-LiF eutectic and Li_2CO_3 systems:

Electrolyte	K_p	Average Temperature
Li_2CO_3	1.0×10^{-7}	1100°K

8.2 (Continued)

Li_2CO_3-LiF eutectic	8.9×10^0	1100°K
LiCl-KCl + 10 wt % Li_2CO_3	6.0×10^3	800°K

the large difference in the equilibrium constants for these three systems indicates that the halide plays an important role in the dissociation of the carbonate ion. The equilibrium constant estimations can be used to calculate relationships in the melt when CO_2 and H_2O are added to the system.

The LiCl-Li_2CO_3 system could not be studied since the halide was volatile in the temperature range of interest, as evidenced by the failure to achieve the original sample weight after a run. This irreversible loss in weight was very pronounced above 600°C. Using the criterion of irreversible weight loss as a basis for halide stability, it was found that pure KCl was very volatile at 800°C (10°C above its melting point), but that the Li_2CO_3-LiF eutectic system was stable up to 900°C, the maximum temperature studied. LiCl-KCl + 10 wt % Li_2CO_3 (melting point 340°C) was found to be stable up to 650°C.

The halide volatility is a problem which must be taken into consideration when choosing an electrolyte for the CO_2 reduction system. On the basis of volatility, a fluoride system would appear to be preferred. However, operating temperatures tend to be high. The presence of sodium and potassium in fluoride systems has proved detrimental to the carbon deposition process, so that to lower operating temperature other cations with reducing properties similar to lithium may be required, such as barium.

8.3 Corrosion of Materials

As noted in the preceding sections, it was found that many materials were attacked by the electrolyte. During the earlier phase diagram work nickel crucibles were used and it was found that a black deposit formed on the inside of the crucible above the melt level. This deposit was NiO, but evidently it did not form a protective coat and the top of the crucible gradually deteriorated. Gold-palladium alloy has been used extensively as the melt container and the anode. Although this alloy is very satisfactory in pure carbonate melts, it was found to dissolve to some extent in chloride-containing melts, and melts with a high oxide content (>10 weight percent). The corrosion behavior of this alloy in chloride-containing melts can be explained by considering the tendency for the transition metals to form anionic chloride complexes of the type $(MX_2)^-$ or $(MX_4)^-$. The complexes $(AuCl_2)^-$ and $(AuCl_4)^-$ are common and

8.3 (Continued)

the complexes $(PdCl_6)^{=}$ and $(PdCl_4)^{=}$ are also well known. The most probable oxidation states for these two metals are +3 for Au and +2 for Pd. The standard oxidation potential at room temperature for the formations of these complexes are:

	$Au + 4Cl^-$	$(AuCl_4)^- + 3e^-$	+1.00 v
	$Pd + 4Cl^-$	$(PdC/4)^{=} + 2e^-$	+0.64 v
and	$(PdCl_4)^{=} + 2Cl^-$	$(PdCl_6)^{=} + 2e^-$	1.29 v

Although it is not possible to make direct comparisons of potentials from room temperature to the actual potentials observed in our systems, it would appear that the palladium would be dissolved first. This behavior is supported by visual observations when the silver colored alloy takes on a gold color after use as an anode for an extended period of time.

One could expect this dissolution to be reduced if a protective oxide coat was formed on the metal due to oxide ion oxidation when the material is used as an anode. However, aurous oxide (Au_2O) decomposes at 205°C, and auric oxide (Au_2O_3) decomposes at 250°C, temperatures considerably below those normally encountered in these studies. Palladium dioxide (PdO_2) decomposes at 877°C and should be formed on the Au-Pd electrodes.

In view of the possible protection of the anode by oxide formation, a series of anodic dissolution experiments were run both at constant anodic current and at constant anodic potential. The data from these experiments are summarized in Figure 8-7. In the case of the constant potential experiments an average current was assumed when the current was found to fluctuate during the runs. The percent efficiency for dissolution was based on the number of Faradays passed compared to the weight loss of the electrode, and indicates the percent of the total current that was involved in metal dissolution. The remaining current is assumed to be used in oxygen generation.

Melts 43-1 and 43-2 show the effect of electrolysis at constant potential at -0.2 and -0.9 v. In the latter case oxygen evolution is known to occur. At the lower anodic potential some other oxidizable species is involved. In the case of Run 43-2 at -0.9 v, a black PdO coat was formed on the anode, as confirmed by x-ray analysis.

The constant current Runs 43-3, 44-1 and 46-1 show the effect of running for an extended period of time at an anode potential above

8.3 (Continued)

that necessary for oxygen evolution, and the relative effects in the ternary carbonate and Li_2CO_3-LiF melt. The conclusions to be drawn here are that the presence of oxygen at the anode partially protects it, and that the removal of chloride ions from the melt essentially eliminates anode dissolution. It is also interesting to note that the black oxide film was not present in Runs 44-1 and 46-1.

Although anode dissolution is inhibited when oxygen is evolved, it is desirable to greatly reduce the chloride ion content of the melt for improved anode protection. The fact that the best results were achieved in the Li_2CO_3-LiF system even at the higher temperatures indicates a lesser tendency for soluble complex formation and is a favorable argument for the use of this latter electrolyte.

The corrosion studies of Janz and Conte (References 11, 12, 13) in pure carbonate melts indicate that nickel is poorly protected by passivation and has been found to be worse than silver in this respect. Type 304 and 347 stainless steels passivated in the molten carbonates and this passivity conferred by anodic electrolysis made the properties of these steels comparable to gold-palladium alloy and platinum. The corrosion potentials for the series of metals studied at 600°C were:

80% Au - 20% Pd	- 430 mv
Au	- 470 mv
Pt	- 475 mv
304 and 347 stainless steel	- 525 mv
Ag	- 680 mv
Ni	-1166 mv

The potentials for 80 percent Au - 20 percent Pd, Au, and Pt are strikingly similar to those obtained during the anodic studies in the Li_2CO_3-LiF eutectic melt as shown in Figure 8-23, Section IV-17. Our experience shows, however, that in electrolytes containing substantial amounts of carbonate, nickel may be used as an anode with negligible dissolution. The same is the case for cobalt. On the other hand, when a 304 stainless steel anode has been used, sufficient iron is introduced to the system to affect the carbon deposition process at the cathode. Ostroushka (Reference 16) claims that lithium oxide does not attack nickel below 1000°C. Littlewood (Reference 17) and De Zubay (Reference 18) suggest that nickel will corrode under the combined influence of a molten carbonate and an oxidant such as air. In the light of this assortment of information it is apparent that it still remains to provide adequate theory to predict electrolyte circumstances

8.3 (Continued)

where nickel or other metal passivity will be assured. The selection of electrical insulating materials which may be safely exposed to the electrolytes also remains very narrow. Aluminum oxide has been found generally acceptable except when boron oxide was present or when fluoride concentration was high relative to electrolyte oxide concentration. Experiments by Janz (Reference 12) indicate that magnesium oxide is only slightly affected by fused carbonate at temperatures up to 1000°C, although such material was not evaluated in the studies being reported here. Other oxides, such as zirconium oxide, have also found use in other molten salt studies.

Experience has shown that it is possible to provide a measure of protection for metallic structural elements in contact with the electrolyte by maintaining them with a trickle of cathodic current. Under this condition, in addition to the anticipated cathodic type protection, a further order of protection is provided by the graphitic coating produced by the electrolysis. In instances where the melt has been contaminated with metallic impurities, application of cathodic current to the metal container (when such as used) resulted in removal of these impurities, usually evidenced by electrolyte color change.

Graphite generally proved to be a satisfactory crucible material. However, since it is easily oxidized when in contact with several gases, appropriate precautions had to be taken. Use of graphite in electrode construction has been common; protection from gas phase oxidation has generally been provided by use of alumina shields.

Li_2CO_3 grams	LiF grams	Li_2O grams	Weight % Li_2O	Freezing Point °C	ΔT_f
37.50	12.50	-	-	611.0	-
37.50	12.50	0.50	1	607.5	3.5
37.50	12.50	2.50	5	598.9	12.1
37.50	12.50	3.00	6	598.6	12.4
37.50	12.50	3.50	7	598.2	12.8

FIGURE 8-1 FREEZING POINT STUDIES ON THE Li_2CO_3-LiF EUTECTIC MELT

Melt Analysis (wt %) Li_2CO_3	LiCl	Li_2O	Thermal Analysis (°C) 1st Break Point	2nd Break Point	Final Solidification Point	** Δ T°C
14.5	85.5	-	562	-	514	-
18.4	78.4	3.2	538	512	494	44
22.5	74.1	3.4	530		492	38
27.6	72.4	-	534	- *	512	-
23.2	71.9	4.9	505	501 *	492	13
26.5	68.6	4.9	496	493 *	487	9
34.6	63.8	1.6	498	494	490	8
32.0	64.3	3.7	493	-	488	5
32.7	59.1	8.2	496	492	489	7
31.4	68.2	0.4	522	-	516	-
37.5	58.3	4.2	519	-	497	22
34.5	57.2	8.3	520	-	494	26
35.8	56.9	7.3	521	-	494	27
39.5	49.0	11.5	520	-	489	31
39.4	60.1	0.5	559	-	512	-
56.1	38.3	5.6	551	-	485	66
45.2	49.4	5.4	553	523 *	482	71
49.2	41.9	8.9	551	-	478	73
47.2	46	6.8	558	-	469	89
49.8	50.2	-	-	-	514	-
52.1	44	3.9	591	-	492	99
37.2	55.9	6.9	600	-	487	113
32.2	58	9.8	606	-	477	129
35.7	57.7	6.6	586	-	469	117
53.6	46.1	0.3	608	-	513	-

*2nd break point may not have occurred
** Δ T for ternary systems (1st break point-final solidification point)

Our binary (Li_2CO_3-LiCl) eutectic temp. = 513 ± 2°C
Our ternary (Li_2CO_3-LiCl-Li_2O) eutectic temp. = 486 ± 7°C

FIGURE 8-2 FREEZING POINT DETERMINATIONS,
Li_2CO_3-LiCl-Li_2O SYSTEM

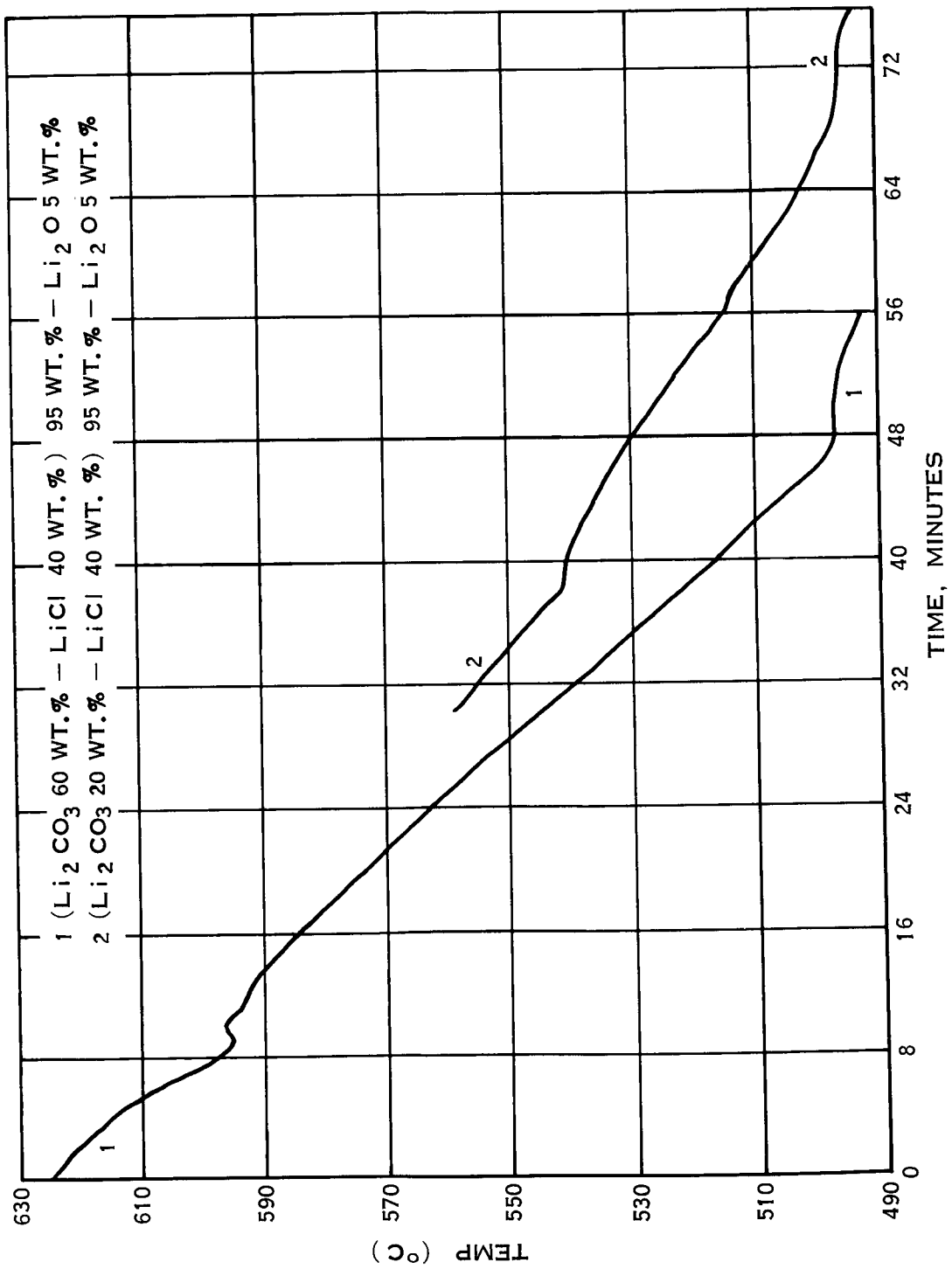

FIGURE 8-3 COOLING CURVES FOR Li_2CO_3, LiCl, Li_2O SYSTEM

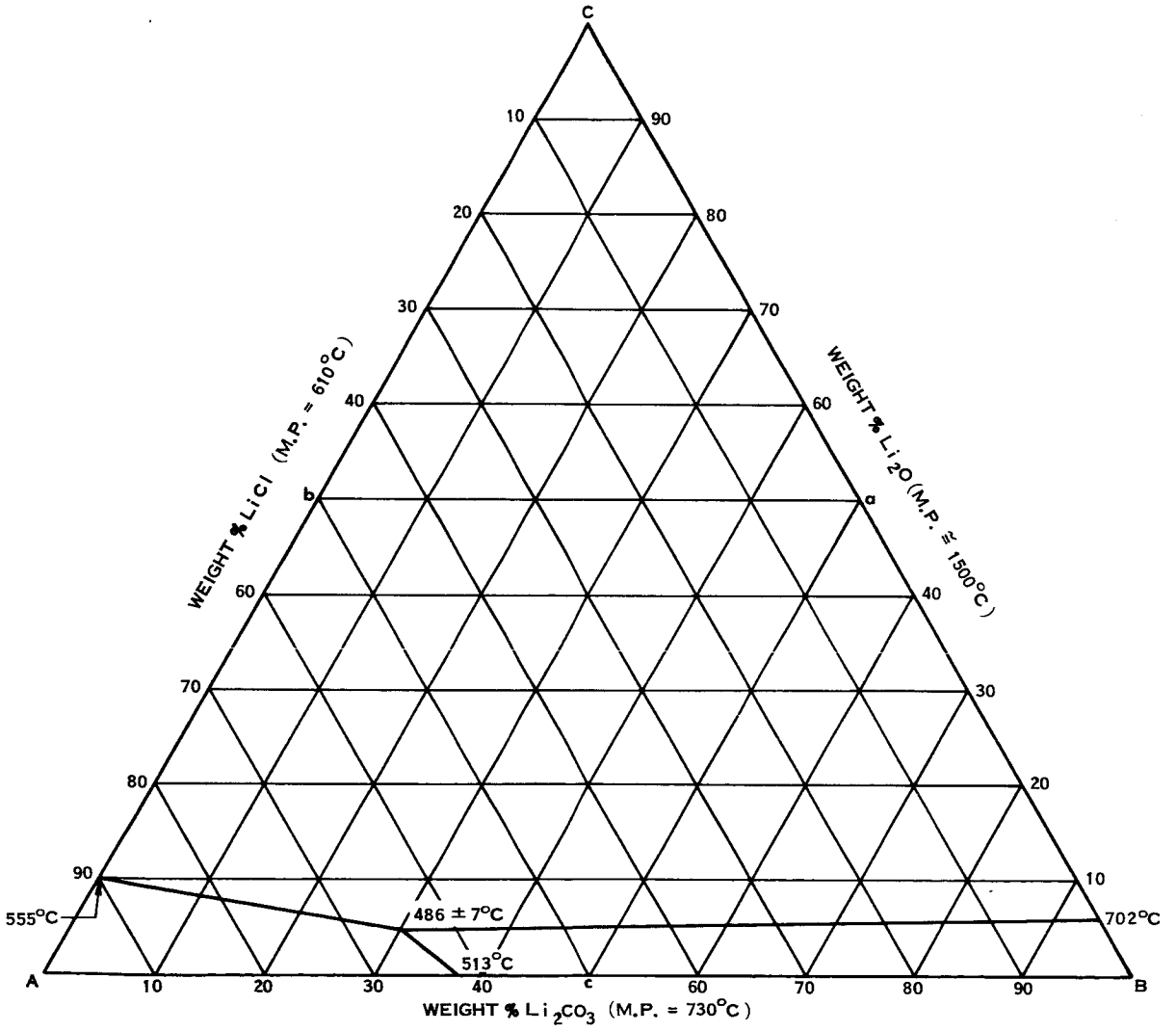

FIGURE 8-4 PHASE DIAGRAM; Li_2CO_3, LiCl, Li_2O

Li_2CO_3		Li_2CO_3-LiF Eutectic		KCl-LiCl Eutectic +10 wt % Li_2CO_3	
P_{CO_2} mm	Temp. °C	P_{CO_2} mm	Temp. °C	P_{CO_2} mm	Temp. °C
23	758	43.7	739	2.0	449
100	807	97.3	782	7.0	520
100	810	188	810	7.0	558
150	815	253	861	8.1	550
286	815	381	864	9.6	590
700	859			10.4	560
700	838			13.8	612
700	879			30.0	666

FIGURE 8-5 CO_2 DISSOCIATION PRESSURES

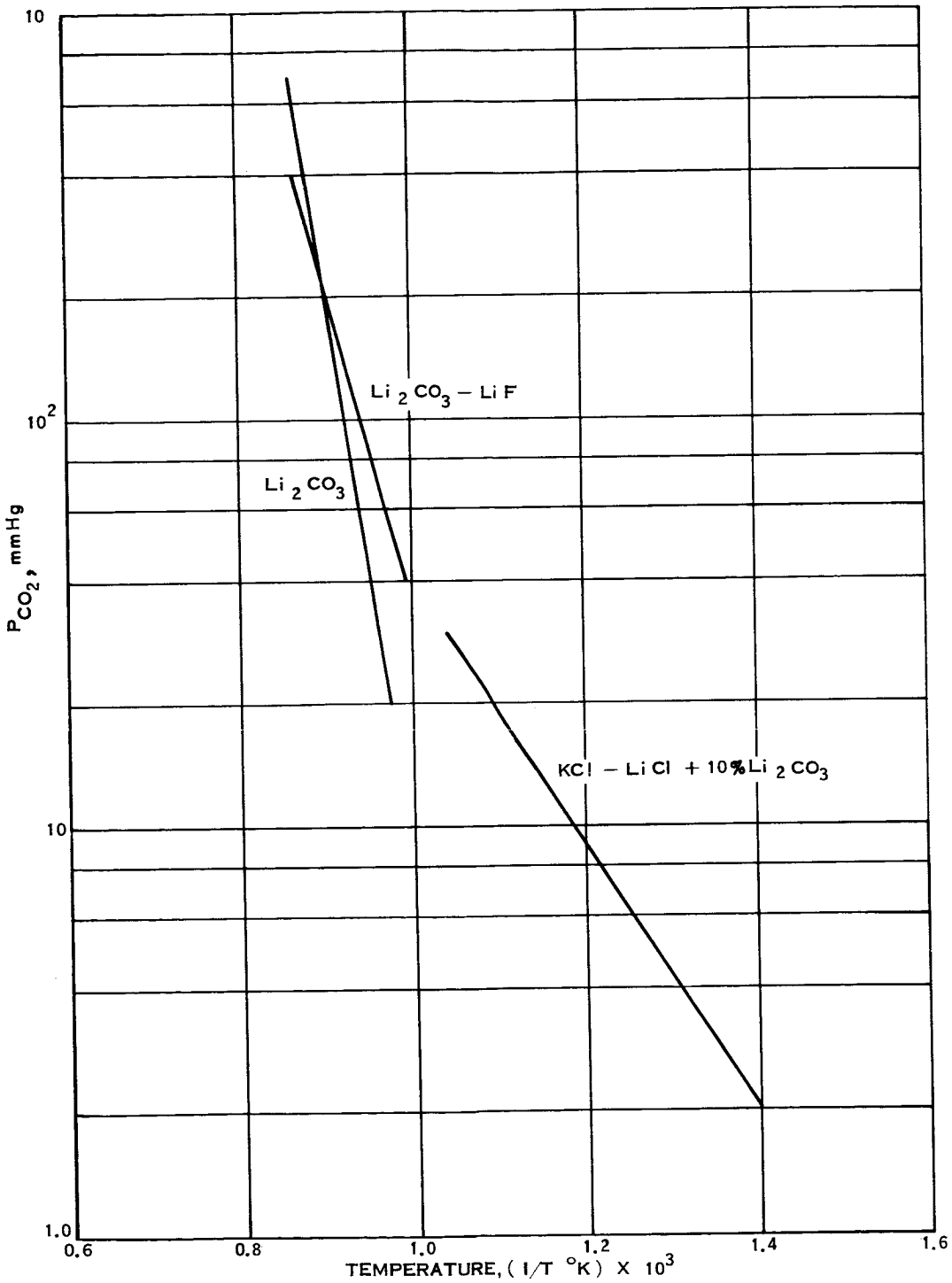

FIGURE 8-6 DECOMPOSITION PRESSURES OF CARBONATE CONTAINING MELTS

Melt No.	Eutectic Melt Composition	Temp. (°C)	Current (ma)	Time (hr)	Anode Potential	Wt. Loss (mg)	Anode Reaction	% Efficiency for Dissolution
43-1	Li_2CO_3-LiCl 190 mm CO_2	520	10	1.1	-0.2 v (constant)	0.1	$Pd \rightarrow Pd^{+2}$ $Au \rightarrow Au^{+3}$	15.5 12.6
43-2	Li_2CO_3-LiCl 190 mm CO_2	520	varied	2.5	-0.9 v (constant)	1.1	$Pd \rightarrow Pd^{+2}$ $Au \rightarrow Au^{+3}$	8.2 7.2
43-3	Li_2CO_3-LiCl 190 mm CO_2	520	10	21	-1.0 v	16.8	$Pd \rightarrow Pd^{+2}$ $Au \rightarrow Au^{+3}$	4.0 3.1
44-1	Li_2CO_3-K_2CO_3-Na_2CO_3 760 mm CO_2	476	30	4	-3.0 v	0.5	$Pd \rightarrow Pd^{+2}$ $Au \rightarrow Au^{+3}$	0.2 0.2
46-1	Li_2CO_3-LiF 190 mm CO_2	750	30	4	-1.1 v	0.05	$Pd \rightarrow Pd^{+2}$ $Au \rightarrow Au^{+3}$	0.02 0.02

FIGURE 8-7 DISSOLUTION OF Au-Pd ANODES

PART II

DESIGN STUDIES

9.0 INTRODUCTION TO DESIGN STUDIES

Prior to the start of Phase I of this contract, a company-funded test program had conclusively demonstrated that the molten salt system would not only decompose CO_2 into elemental carbon and oxygen but will also absorb dilute CO_2 directly from cabin air. The potential savings of this system, such as providing an integral CO_2 scrubbing system and the reliability inherent in a simpler system, created the desire to investigate the molten salt system more thoroughly for application to future manned space flights.

Several approaches are presently under consideration both by industry and by governmental agencies for spacecraft CO_2 control and reduction systems. Section 12.0 of this report presents an analysis of integrated CO_2 management systems that include removal, transfer, and reduction subsystems. Also included in this analysis are provisions for supplying makeup oxygen to account for total metabolic oxygen requirements of the crew not available from CO_2 alone.

In response to the eventual requirement for applicability to a flight system, a preliminary investigation of the more obvious zero gravity problem areas was initiated; namely, positive control of the liquid electrolyte, disposal of carbon formed by the process, and control of the process gases, in order to evaluate better the magnitude of these problems for operation in a zero gravity environment. To this end, a design study program concurrent with the research effort was started.

The primary objective of the design study program was to define conceptually a flight prototype unit configuration appropriate for cell operation under a condition of weightlessness. To accomplish this task required the definition of process and engineering problem areas and the subsequent investigation of potential solutions to these problems. Since answers to many of the process-oriented problems were not available and because concurrent research was not addressed to the feasibility of particular flight concept configurations, it was necessary to impose certain ground rules or make assumptions and estimates in those areas where basic electrochemical processes have an influence on equipment size.

The program undertaken was therefore limited to process "state of the art" with regard to optimizing operating parameters. This, however, did not necessarily limit the investigation of gross concepts devoted to applying the system to zero gravity operation. An outline and general description of each concept is presented in Section 13.0 of this report. These concepts, with regard to melt containment, carbon recovery, and CO_2 scrubbing were evaluated on a pro/con basis in order to narrow the scope of the investigation and to exert meaningful effort toward problem definition and possible solutions. This was necessary in order

9.0 (Continued)

to meet the commitment to demonstrate a concept for separation of the three phases (solid, liquid and gas) in an early stage of the Phase I contract period. The resultant product of this effort, the three phase separator demonstration model, is discussed in Section 14.0 of this report.

Upon completion of the design effort required to define the three phase separator model, the program scope was again broadened to allow for another review of candidate concepts prior to selecting the most promising system concept for evaluation and discussion in this report.

Because firm design data upon which to base a final recommended configuration for a flight prototype unit are presently unavailable, the decision was made to evaluate that system which offered the greatest potential with regard to weight, power, volume, and simplicity of operation. The concept selected for this evaluation includes a porous matrix to control the gas/liquid interface at the anode and would be classified as a "passive" system due to elimination of high power consuming equipment necessary to provide dynamic control of the liquid in an artificial gravity field. The investigation of this concept is presented in Section 15.0.

10.0 CONCLUSIONS

While the design study conducted during Phase I to determine applicability of the molten salt concept to a flight prototype unit accomplished many of the objectives intended with regard to problem definitions, system design criteria, and the evolution of possible solutions, it should be recognized that to recommend a firm configuration for weightless operation requires relatively complete theoretical and experimental background that provides the engineering data necessary to effect a design. The state of the program with regard to the overall objective, i.e., the fabrication and system evaluation of a four man flight prototype unit, is as follows:

1. Theoretical hypotheses for the basic process reaction mechanisms have, in many cases, been experimentally substantiated. However, adequate refinement for process repeatability, definition of control tolerances, melt composition selection, and complete understanding of the interaction of system variables has not been achieved.

2. A comparison of the oxygen reclamation systems presently envisioned as candidates for future space craft has shown a significant weight savings could be achieved using the molten carbonate system for long duration missions.

3. The three phase separator demonstration model reflects one potentially feasible configuration for solving the three phase interface problem in a zero gravity environment.

4. A firm concept, adequate for starting a flight prototype design and development program cannot be proposed at this time. Process knowledge and feasibility testing of proposed concepts sufficient for concept selection have not been experimentally demonstrated.

5. All the phase control concepts presently considered for weightless operation have significant problems from both an engineering and process viewpoint.

6. Should the matrix concept studied in this report prove feasible, a relatively simple system for the molten carbonate process can be foreseen that would compete with stored oxygen systems for the 60 day or longer missions in the 1972-74 period.

11.0 RECOMMENDATIONS

It is recommended that a feasibility test program be conducted concurrently with the research program proposed in Section 3.0 of this report. This program would be directed toward the practical solutions of engineering problems associated with zero gravity application of the proposed system. This advanced development effort will be addressed toward problem identification and provide a preliminary evaluation of the feasibility of design concepts resulting from the studies of Phase I.

It is also recommended that the laboratory demonstration model, constructed as part of Phase I, remain at Hamilton Standard to provide the capability for initial advanced development testing at the start of the proposed next phase of this program. This model will facilitate conduction of experimental evaluations of process variables to provide requisite design data beyond the requirements for basic process control and understanding. These experiments would include appraisals of electrode life, effects of electrode geometric configuration, and physical characteristics of zero gravity devices.

12.1.2 (Continued)

functions.

12.1.3 Comparison Basis of Oxygen Reclamation Systems

Three carbon dioxide reclamation and reduction systems in addition to molten carbonate, were investigated. These systems were chosen as being the most competitive of those covered in the "MARS" (Reference 20) and "MOSS" (Reference 21) studies conducted by Hamilton Standard. As a yardstick for comparison, the penalty for stored oxygen and a combined stored oxygen/water electrolysis system is presented. The comparison is based on a vehicle usage rate of 9.5 lbs. oxygen per day plus whatever is chargeable to the recovery - reduction system. Oxygen for airlock repressurization is assumed to be supplied from a separate source. Any subsystem (such as water reclamation) common to all methods are not shown in the penalty comparisons. It is assumed that penalty for electrical power, including heat rejection system weight is 300 lbs. per kilowatt.

This section gives a brief description and simplified schematic flow charts of the systems compared. They are:

- Sabatier with methane dump
- Sabatier with methane decomposition
- Solid electrolyte and water electrolysis
- Cryogen oxygen
- Cryogenic oxygen with water electrolysis
- Molten carbonate with water electrolysis

12.1.4 CO_2 Removal and Concentration

For all systems, except molten carbonate, carbon dioxide scrubbing is done by means of regenerable solid absorbents. This subsystem was chosen after comparison with:

- Liquid absorption
- Electrodialysis
- Freeze out
- Membrane diffusion

12.1.4.1 CO_2 Concentrator System Description

Figure 12-1 shows a schematic of this subsystem. Process air is drawn into the solid adsorption CO_2 removal system from the environmental control system recirculation stream at a point downstream of the water separator where the minimum moisture concentration exists. The CO_2 is desorbed and delivered to the reduction system by heating

12.0 COMPARISON OF OXYGEN RECLAMATION SYSTEMS

12.1 Discussion

12.1.1 Metabolic Oxygen Balance

The human metabolic process reacts oxygen and food to produce energy, carbon dioxide and water. The amount of oxygen consumed is dependent on the metabolic rate. The ratio of water to carbon dioxide produced is dependent on the percentage of fat, protein, and carbohydrates in the diet. The following table taken from the proceedings of the Conference on Nutrition in Space and Related Waste Problems (Reference 19) shows a partial metabolic balance for an average metabolic load.

Intake - lbs/day		Output - lbs/day	
Oxygen	2.0	CO_2	2.30
Protein	.15	H_2O	.87
Fat	.38		
Carbo-hydrate	.64		
TOTAL	3.17		3.17

The amount of oxygen that can potentially be recovered is:

from CO_2 = 1.67
H_2O = .77
TOTAL 2.44 #/man day

The amount of oxygen coming from food being .44 lbs/man day

12.1.2 Oxygen Requirements for a Four-Man Vehicle

The normal oxygen usage in a spacecraft will be for metabolic use, leakage, vehicle and airlock repressurization, and backpack recharge. It is assumed that stored oxygen will be used for repressurization and recharge. The system comparison discussed in this section are based on supplying metabolic and leakage oxygen as follows:

Metabolic	8.0
Leakage	1.5
TOTAL	9.5 lbs/day

Since the amount of oxygen which can be reclaimed from CO_2 only is $4 \times 1.67 = 6.68$ lbs/day, it becomes evident that a mission which requires oxygen reclamation from CO_2 will also require supplemental oxygen, most readily obtained via reclamation from metabolic water. Any oxygen reclamation system must therefore combine both of these

12.1.4.1 (Continued)

up the zeolite canister, thus driving off the CO_2 at a higher partial pressure than that at which it was adsorbed. A heat transfer fluid receives this heat from a waste heat source and delivers it to the bed through imbedded coils. A compressor is used to deliver the CO_2 to an accumulator at pressures up to 40 psig. Silica gel beds are used to dry the process air before it goes to the CO_2 removal beds. CO_2 is delivered at 95 percent purity. Cooling fluid at a maximum temperature of $60^{\circ}F$ and heating fluid at $375^{\circ}F$ are required.

One of the assumptions for the comparison is that waste heat is available for CO_2 concentration. If it is necessary to provide electrical heat for this purpose an additional 1200 watts or 360 lbs. of penalty must be added to all systems with the exception of molten carbonate and cryogenic storage.

Power and weight for the CO_2 concentrator are based on actual designs of flight type hardware.

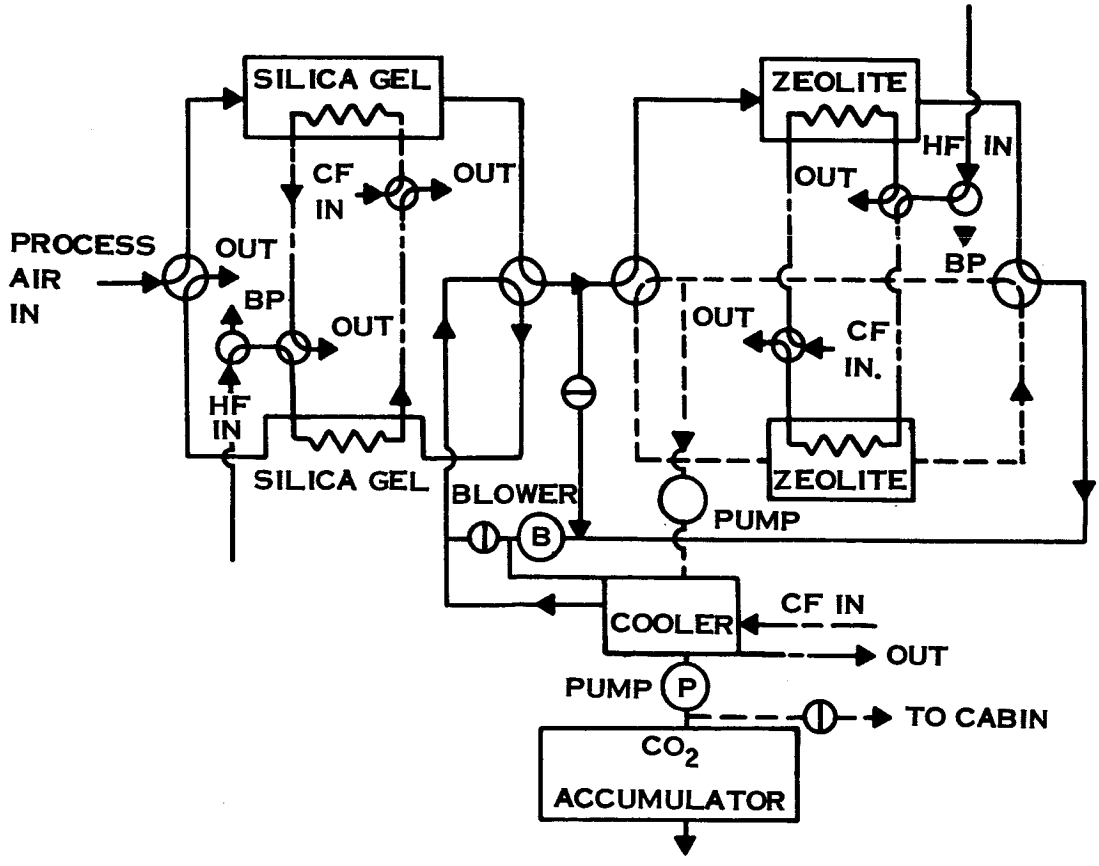

FIGURE 12-1 CO_2 CONCENTRATOR SCHEMATIC

12.1.5 Water Electrolysis Unit

All of the systems compared utilize an electrolysis cell for producing a portion or all of the oxygen. The electrolysis unit weights and powers used in this study are based on a Pratt & Whitney Aircraft redesign of a compact fuel cell. Efficiencies are based on actual test data. Other concepts were also considered but found to be either less desirable or lacking in design data. In any case, the penalty difference between the various concepts is not significant.

12.1.5.1 Description of the Electrolysis Unit

The electrolysis system is built of modular single cells that can be put together by stacking all cells in series.

A simplified schematic of the water electrolysis unit is shown below in Figure 12-2.

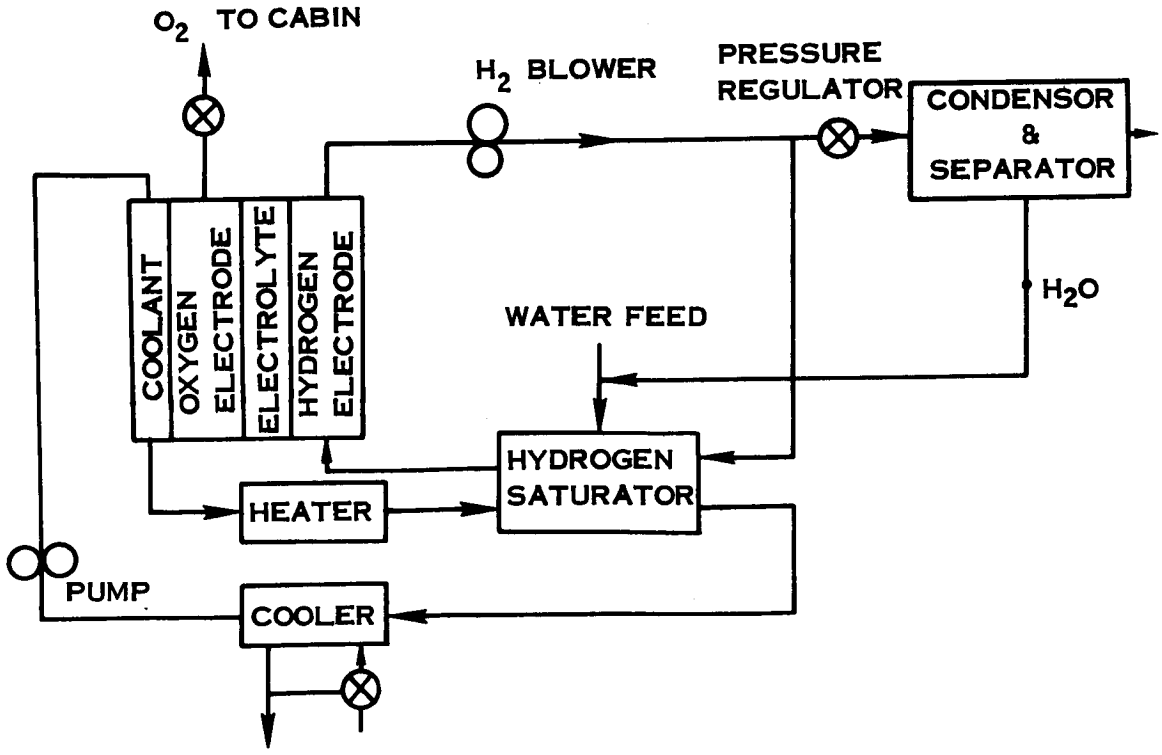

FIGURE 12-2 WATER ELECTROLYSIS SCHEMATIC

12.1.5.1 (Continued)

The water to be electrolyzed is delivered to the cell in a recirculating stream of moist hydrogen. A portion of the hydrogen initially produced in the cell is used as the carrier for the water vapor. The water vapor is picked up by the hydrogen stream as it passes through a saturator. Make-up water is fed to the saturator where it is evaporated into the hydrogen stream. The moist hydrogen stream then flows from the saturator to the cell where the water vapor enters the porous, hydrogen electrode and is electrolyzed. After leaving the cell, a portion of the hydrogen is removed from the recirculating stream. The remainder of the hydrogen is recirculated to the saturator. Moist oxygen flows from the cell through flow control valves and is delivered to the cabin. The cell is cooled by recirculating coolant. Major components in the electrolysis unit includes the Compact Cell, saturator, water pumps, hydrogen blower, and temperature control system. The Compact Cell and saturator are described below.

Compact Cell: The Compact Cell consists of two catalyzed screen electrodes pressed against a matrix impregnated with an aqueous solution of potassium hydroxide. Each cell is separated from the next, in an assembly, by a hollow cooling plate, as shown in Figure 12-3. This plate serves the role of current collector and gas-housing as well as providing a passage for circulating a coolant through the cell assembly.

The cooling plate, which also serves as current dissipator and gas-housing consists of two nickel sheets brazed together with a channel of the coolant between the plates. Each plate is formed to provide a large number of dimples which press against the electrodes in the assembly. The space around the dimples provides a gas-housing for the hydrogen on one side of the cooling plate and a housing for the oxygen on the other side of the cooling plate.

Saturator: Saturators utilizing porous-stainless steel, water transport plates have been developed for space fuel-cell operation. The saturator consists of water and gas chambers separated by the porous plate. The pressure and temperature of the water are controlled so that the pores of the plate are filled with water which evaporates into the hydrogen; evaporation continues until the partial pressure of water in the gas equals the vapor pressure of the water.

The compact cell design is particularly suited for operation in a zero-gravity environment since it does not require the use of a mechanical liquid-gas separator to separate the gas evolved at the electrodes from the liquid electrolyte. In fact, the electrolyte is completely separated from the gases by the nature of the electrodes. In the compact cell design, the gas evolved at the electrodes never mixes with the electrolyte. This occurs because the electrolyte is trapped in the pores of a fiberous matrix and held there by capillary action. The gas evolved at the electrodes is able to move away freely from the electrode without having to bubble through the electrolyte.

12.1.5.1 (Continued)

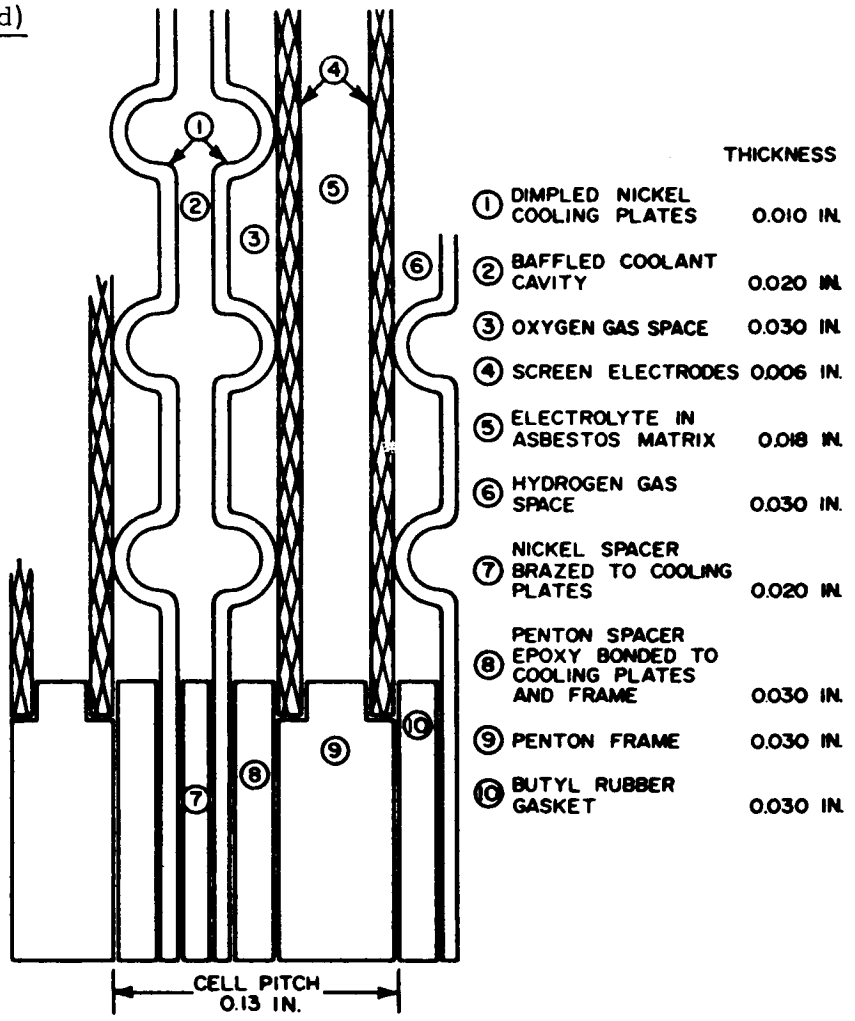

FIGURE 12-3 COMPACT CELL FOR WATER ELECTROLYSIS

12.2 Sabatier

12.2.1 Sabatier With Methane Dump

A simplified flow chart of this system is shown in Figure 12-4. Carbon dioxide is delivered by the concentrator described previously.

CO_2 and H_2 are reacted in the presence of a catalyst to form methane (CH_4) and water. The process is not 100 percent efficient and there are small amounts of both H_2 and CO_2 leaving the reactor. The water is condensed and delivered to the electrolysis cell. The non-condensable gases are dumped overboard.

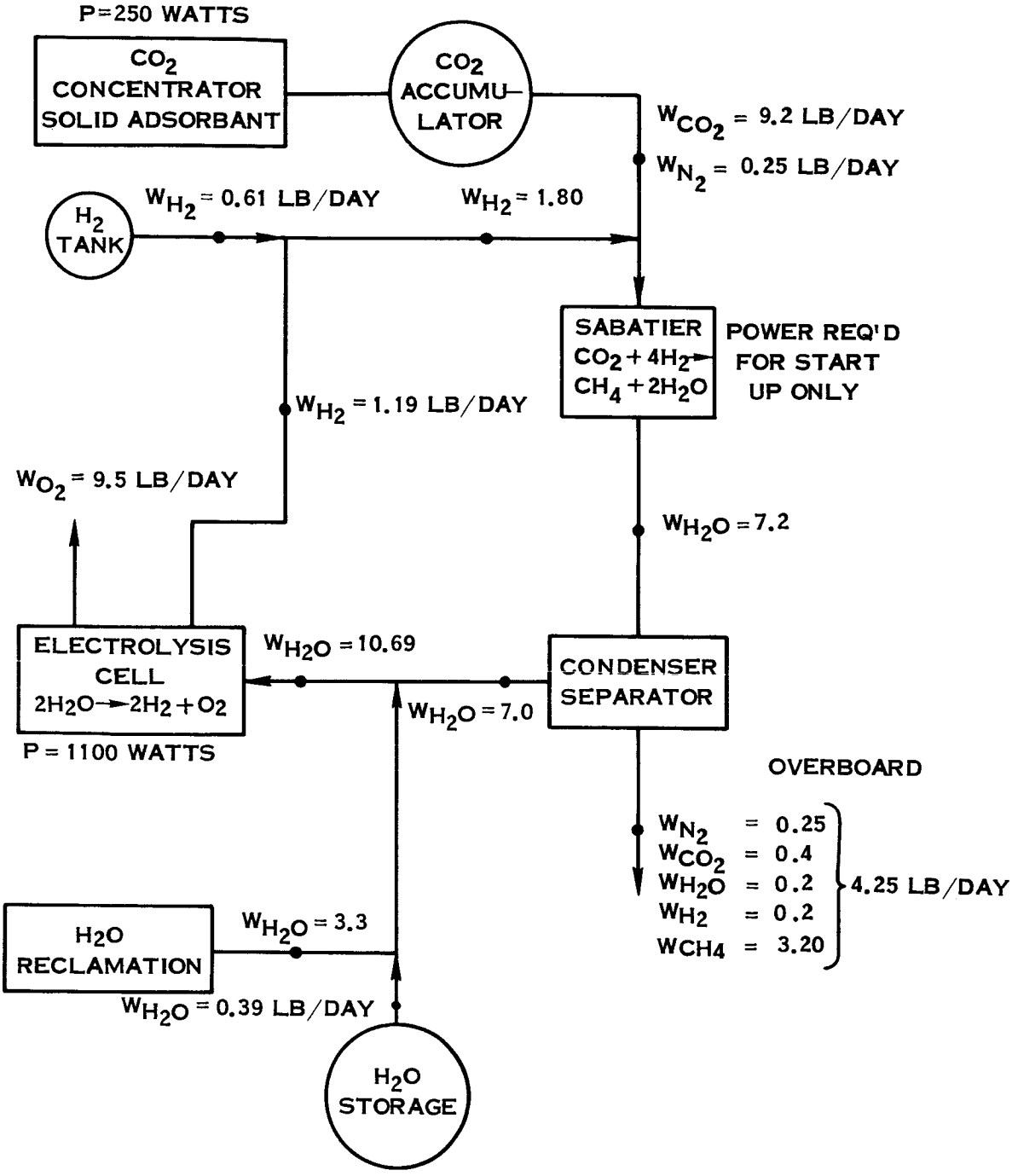

FIGURE 12-4 SABATIER WITH METHANE DUMP

12.2.1 (Continued)

Electrolysis of water produces both oxygen and hydrogen. The hydrogen is delivered to the sabatier reactor and the oxygen to the cabin. Because oxygen is dumped overboard in the form of CO_2 and H_2O, makeup water in addition to the amount reclaimed is required. Makeup hydrogen is also required for the normal metabolic balance of carbon dioxide to water recovered.

Sabatier System Penalty

Basic Equivalent Weight Less Expendables

Fixed Weight		
CO_2 Concentrator	250.0	
Sabatier Reactor	18.0	
Electrolysis Subsystem	70.0	
		338
Power Penalty		
1350 watts @ 300# Kw =		405
Spares		
Assume one redundant unit		338
Support Equipment		
Heat rejection equipment, heating fluid supply, etc.		50
	TOTAL	1131 lbs
Expendables - lbs/day		
H_2 + tank	1.81	
H_2O + tank	.43	
N_2 + tank	.32	
	TOTAL	2.56 lbs/day

12.2.2 Sabatier With Methane Decomposition

An undesirable feature of the methane dump system is the 2.56 lbs. per day of expendables required. These can be nearly eliminated by reclaiming hydrogen from methane.

The CO_2 concentrator and electrolysis cell remain unchanged from Figure 12-4. The CO_2 reduction-CH_4 decomposition loop is shown on Figure 12-5. A catalyst and power are used to decompose CH_4 to carbon and H_2. Since this process is inefficient, a recirculation loop is required rather than a single pass through. Periodically the concentration of gases other than CO_2 and H_2 will require the loop be purged. This can be done back to the cabin perhaps into a catalytic burner.

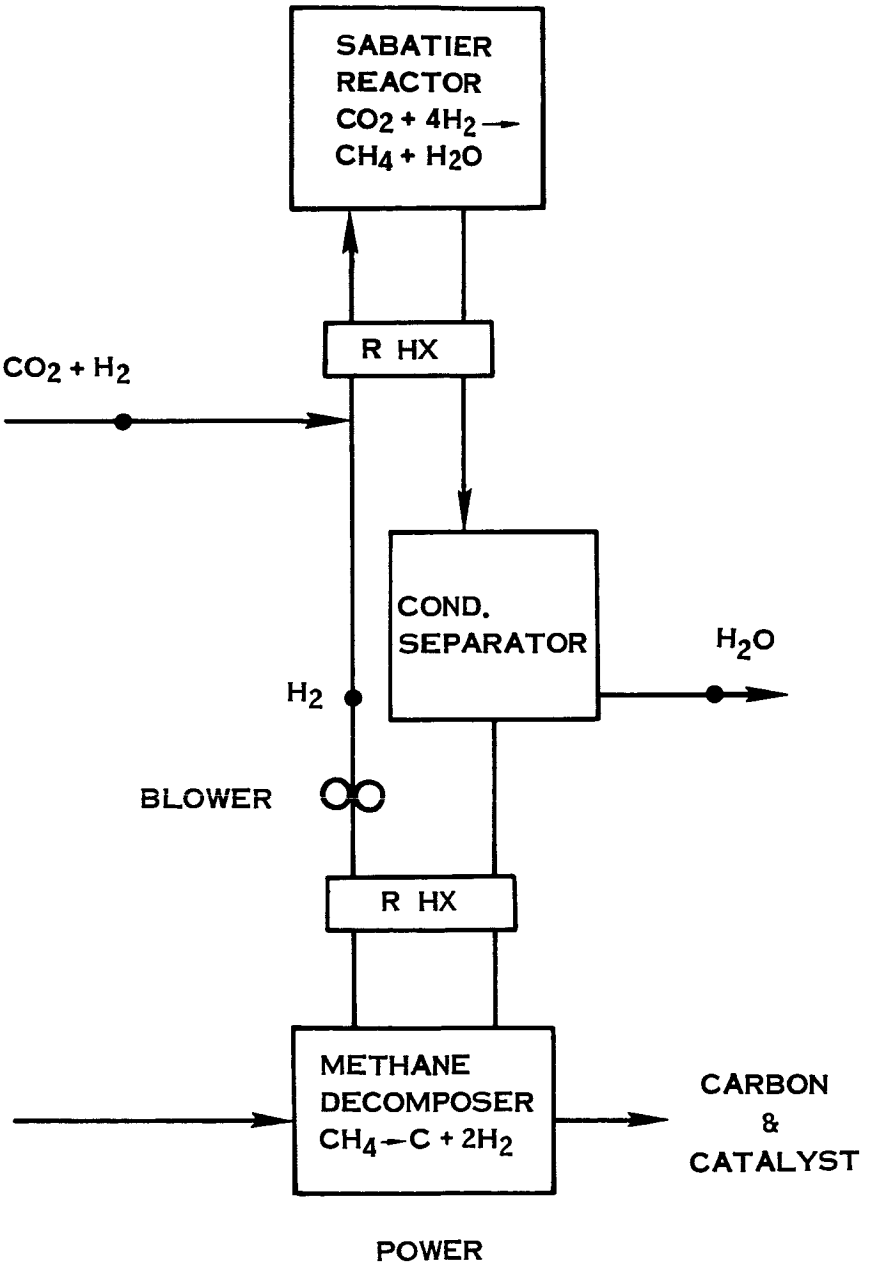

FIGURE 12-5 SABATIER WITH METHANE DECOMPOSITION

12.2.2 (Continued)

Penalty for Sabatier with Methane Decomposition

There is very limited data on the recirculation rates, heat losses, and power requirements for this system. A reasonable assumption is that the initial penalty for this system is 300 lbs. greater than the basic Sabatier system. However, this system will cross over with the Sabatier - methane dump at about 100 days as expendables are theoretically minor.

12.3 Solid Electrolyte CO_2 Reduction

This system also utilizes the solid adsorption CO_2 concentrator described earlier. A schematic of the system is shown in Figure 12-6.

The process converts CO_2 to carbon and oxygen without producing water as an intermediate step. The solid electrolyte reactor consists of ceramic tubes of a special mixed oxide composition. Electrodes are applied to the inner and outer surfaces of the tube walls and the tubes are heated internally by an auxiliary heating coil. CO_2 flows around the outside of the tube and the O_2 is liberated inside the tube. It is felt that the oxygen comes from a thermal decomposition of CO_2 to CO and nascent oxygen at the cathode surface where the oxygen atom is ionized. This oxygen ion then migrates under the influence of a potential field through vacancies in the crystal lattice of the solid electrolyte material. Upon reaching the anode, the oxygen ion is converted back to an oxygen atom.

A mixture of CO_2 and CO containing about 80-90 percent CO_2 is fed to the cell and oxygen is generated. The composition of the circulating gas varies with time as the catalyst in the catalytic reactor declines in activity. The gas flow to the cells, which are arranged in parallel, is evenly distributed. A composition sensor on the cell gas effluent determines the composition of the effluent recycle gas, and, when the concentration of CO in this effluent rises above 70 percent, automatically shuts down the cell. If the concentration of the CO is allowed to rise above this level, there is a possibility that the electrolyte will decompose. This switch then acts to protect the cell.

The power consumption in the cell is split between energy required to decompose the CO_2 and I^2R heating of the solid electrolyte material. The circulating gas stream will be cooled to provide temperature control in the loop. As the predicted cell efficiency is thought to be good and the operating temperature high, this unit must be well insulated to prevent excessive heat leak which would decrease unit performance. The auxiliary heaters, one in each tube, can be designed to bring the system to temperature ($1830^{\circ}F$) in four hours

12.3 (Continued)

with the normal operating power. No expendable weight is required for the operation of the solid electrolyte cells.

Upon leaving the electrolytic cell, the gases pass through a regenerative heat exchanger where the temperature is reduced to 932°F which is the operation temperature of the catalytic reactor. In the catalytic reactor, the carbon monoxide formed in the reduction cell is combined to form carbon and carbon dioxide over a nickel catalyst which is deposited on a light fibrous substrate. When the carbon has built up to high level, a pressure switch will sense the increasing ΔP and signal for a change of catalyst bed. The reaction occurring is exothermic in nature and no heating of this unit is necessary once the system has reached operating temperature. The gases leave the catalytic reactor and go to a cooler where the excess power put into the electrolytic cell is removed. Since the reduction of CO_2 will not produce all of the O_2 necessary, an electrolysis cell is shown supplying the remainder of the required oxygen from reclaimed metabolic water.

Solid Electrolyte System Penalty

Basic Equivalent Weight Less Expendables

Fixed Weight		
CO_2 Concentrator	250	
Electrolysis System	35	
Solid Electrolyte System	90	
		375
Power Penalty		
1512 watts @ 300#/Kw		454
Spares		
One Redundant System		375
Support Equipment		50
	TOTAL	1254 lbs

Expendables

The only expendable required is the catalyst which is dumped with the carbon. A ratio of carbon to catalyst weight of 50:1 is indicated feasible by tests.

12.4 Stored Oxygen

12.4.1 Stored Oxygen Only

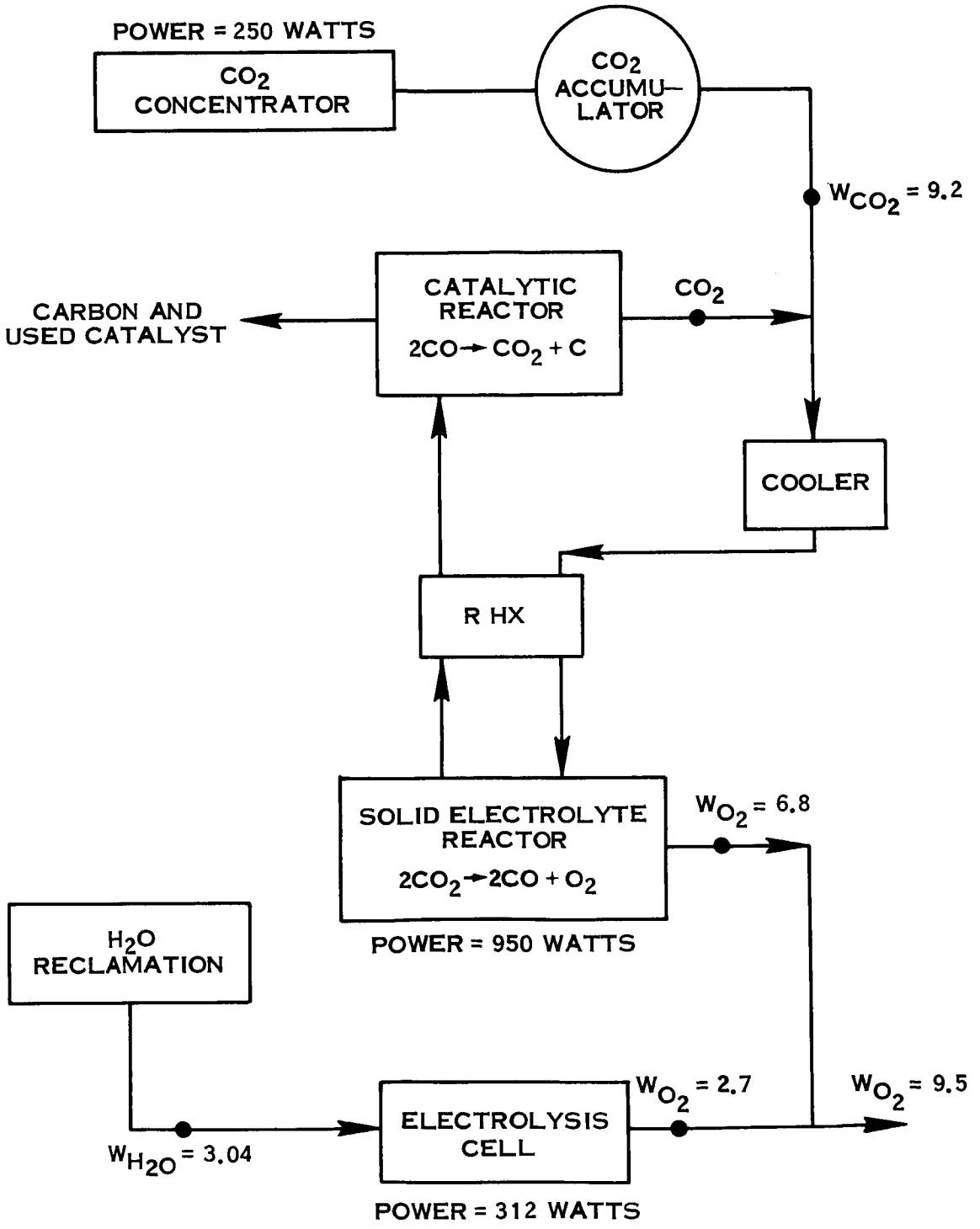

FIGURE 12-6 SOLID ELECTROLYTE SYSTEM SCHEMATIC

12.4.1 (Continued)

The stored oxygen will be in cryogenic form. Tankage and insulation are calculated to be 15 percent of oxygen weight. A CO_2 removal system is necessary and the penalty shown for this study is based on a solid adsorbent system which desorbs CO_2 to space.

Penalty for Stored O_2 System

Basic Equivalent Weight Less Expendables

CO_2 Removal System with Redundancy	130.0#
Power Penalty	15.0#
TOTAL	145.0

Expendables - lbs/day

CO_2 Unit N_2 Ullage	.35
O_2 Tankage	9.85
	1.50
TOTAL	11.70 lbs/day

The above table is based on no reclamation of oxygen from metabolic water.

12.4.2 Stored Oxygen With Water Electrolysis

For comparative purposes, a system which recovers oxygen from metabolic water only was investigated. This system is shown in Figure 12-7. Since only 2.9 lbs. per day of oxygen are available from metabolic water, 6.9 lbs. must be stored. A CO_2 removal unit is also required as before.

12.4.2 (Continued)

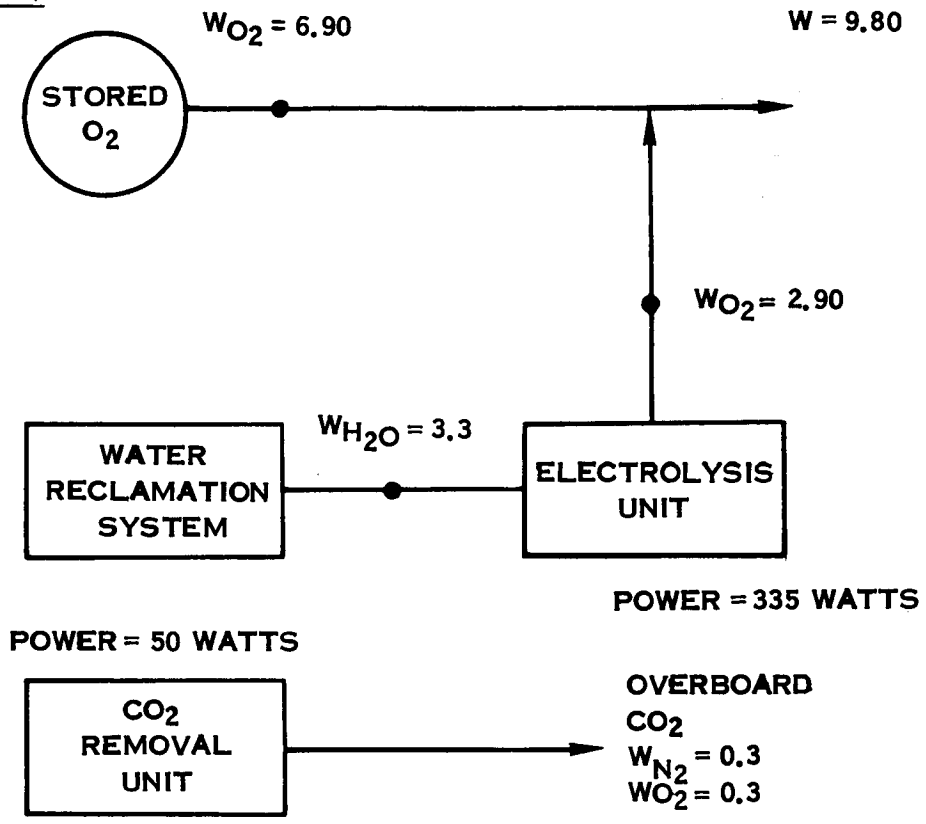

FIGURE 12-7 STORED O_2 WITH H_2O ELECTROLYSIS

Penalty

Basic Fixed Equivalent Weight - lbs

Fixed Weight		
Electrolysis System	35	
CO_2 Removal System	65	
		100
Power Equivalent Weight		
385 watts @ 300#/Kw		115
Spares		100
	TOTAL	315

Expendables - lbs/day		
N_2 + tank	.35	
O_2 + tank	7.95	
	TOTAL	8.30

12.5 Molten Carbonate System

The molten carbonate system is described in detail in Section 15.0 of this report. In order to make a valid comparison with the other systems discussed, it is necessary to provide a water electrolysis unit as shown in Figure 12-2. The penalty for the water electrolysis unit is included in the weight comparison.

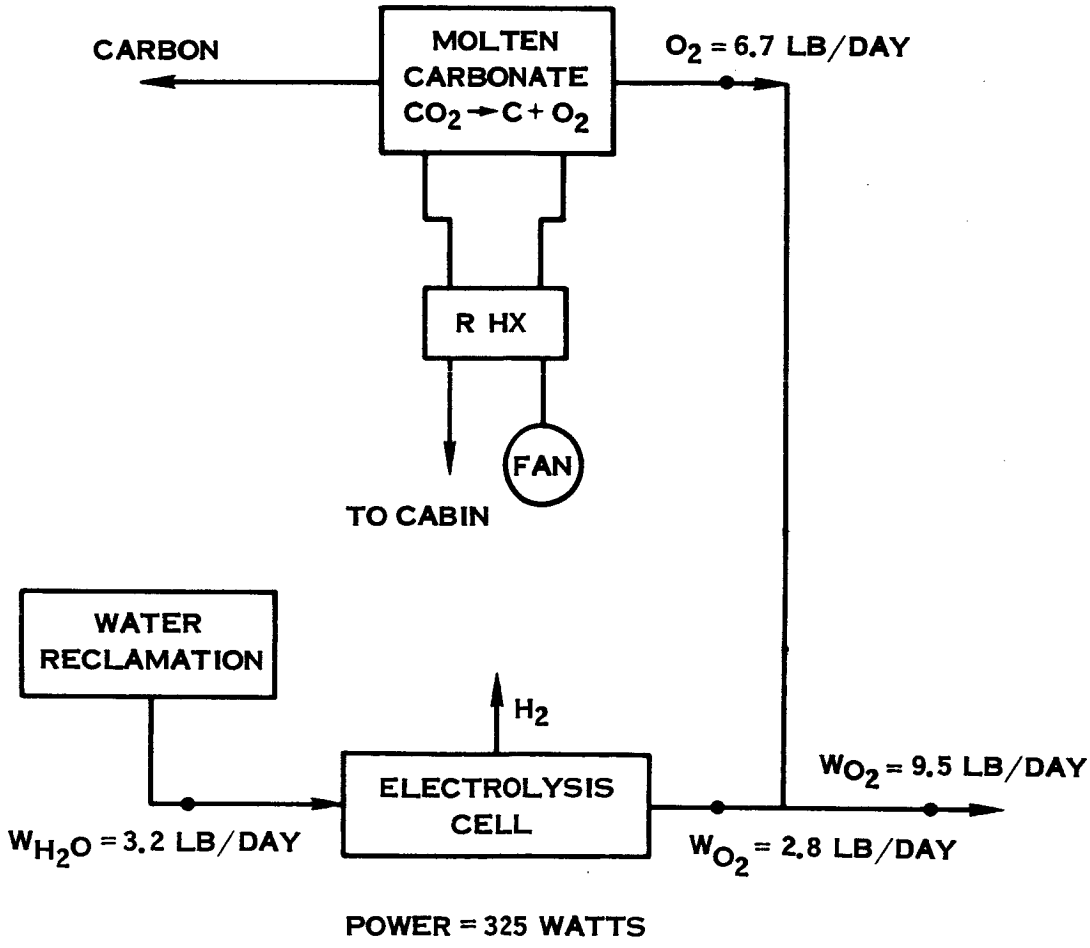

FIGURE 12-8 MOLTEN CARBONATE SYSTEMS SCHEMATIC

12.5.1 Molten Carbonate Penalty - 60 Days

The molten carbonate system weight is a variable dependent on design mission duration. The following table is for a 60-day mission.

Fixed Weight		
Water Electrolysis System	35	
Molten Carbonate System	77	
		112
Power Penalty		
Water Electrolysis System	98	
Molten Carbonate System	435	
		533
Spares		112
Support Equipment		50
Expendables		
Cells (2)		73
	TOTAL	880

12.6 System Penalty Comparison

The systems discussed in this section are compared on an equivalent weight basis in Figure 12-9. For missions of up to 60 days, stored cryogenic oxygen only is optimum. Beyond 60 days it becomes desirable to reclaim oxygen from metabolic water to supplement cryogenic stored oxygen. Based on the assumed ground rules, molten carbonate has the lowest weight of the systems compared and has the potential of becoming competitive after 70 days. The CO_2 concentrator accounts for the major portion of the weight increase of the other CO_2 reduction system as compared with molten carbonate.

Of the systems compared, the Sabatier with methane dump is at the highest state of development and hence its availability for flight in the near future and its calculated equivalent weight have high confidence factors. The other systems are scarcely beyond the feasibility stage and could possibly have equivalent weights substantially greater than those shown on Figure 12-9.

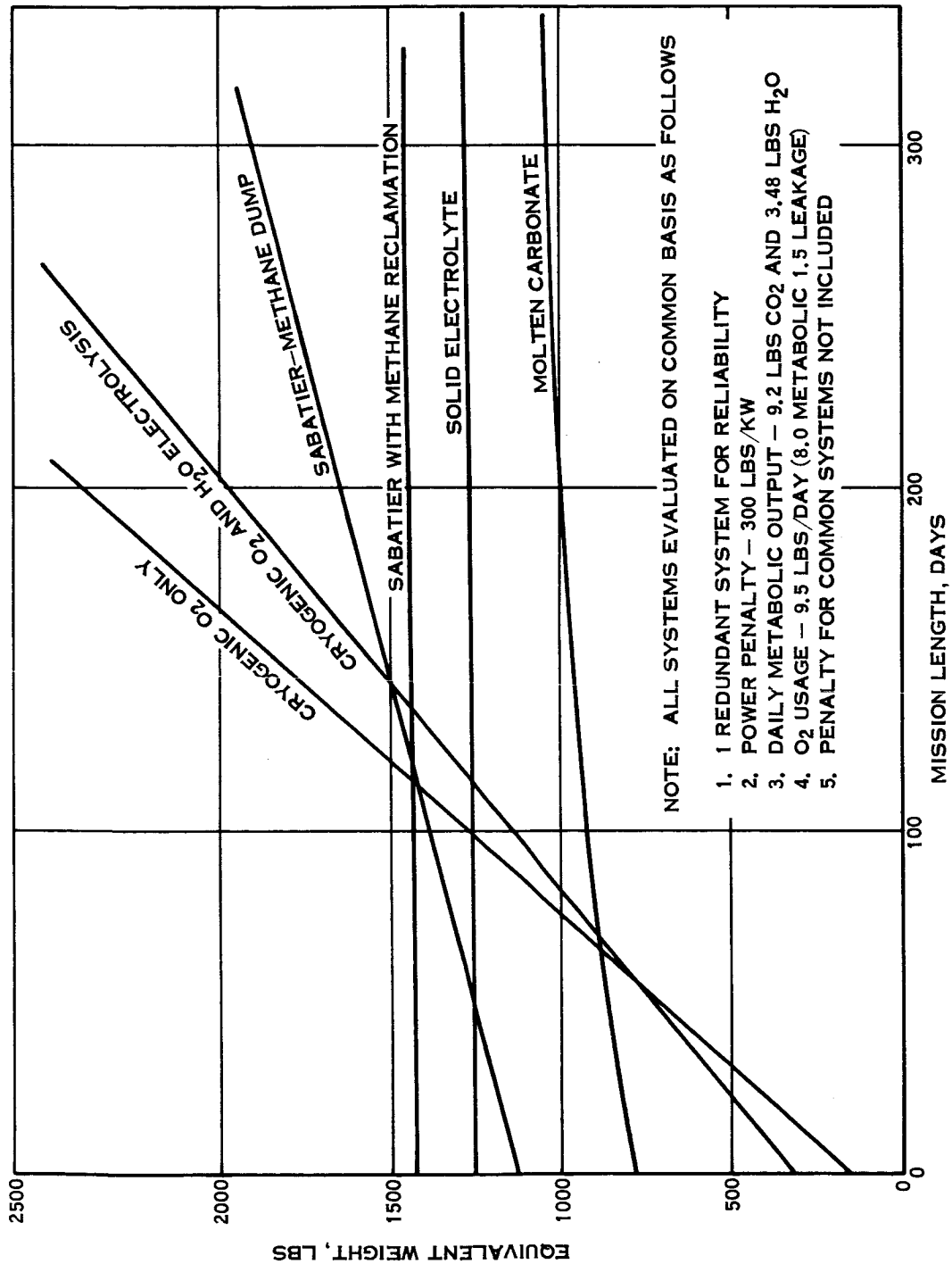

FIGURE 12-9 COMPARISON OF OXYGEN RECLAMATION SYSTEMS

13.0 BASIC CONCEPTS REVIEW

It was recognized in the early stages of process conception that application of the molten salt concept to manned space flight vehicles would require practical engineering solutions to three basic problems in addition to those concerned with definition and understanding of the process. The problems of melt containment, carbon management, and the control of process gases to effect CO_2 removal must be resolved if the objectives of this program are to be ultimately achieved. Within the known limits imposed by process requirements, potentially applicable engineering concepts were formulated for evaluation on a gross pro/con basis and provided a starting point for the design studies investigation.

This section will be concerned with presenting and describing the concepts considered as potential solutions in each of the three general problem areas.

13.1 Melt Containment

The salts used for the electrolytic decomposition of CO_2 form a molten liquid in the temperature range at which this system is operated. A liquid in a weightless environment must be positively positioned to provide a composite substance that retains all the properties of a liquid. This is necessary from a process point of view to provide a constant electrode/electrolyte interface needed for controlled current densities and subsequent controlled carbon deposition and oxygen evolution as well as a positive gas/liquid interface. Two basic physical methods for accomplishing this task are to impose an artificial gravity field on the liquid or to utilize the surface tension properties of a liquid in a capillary system. Configurations for implementing these basic concepts are described in the outline below.

13.1.1 Artificial Gravity Concepts

13.1.1.1 Centrifugal Cell

In the centrifugal cell concept, all components including the melt container, electrodes, carbon recovery and gas control devices, are rotated about a fixed point at a constant angular velocity. A gradient gravity field results, varying from zero at the axis to some finite gravity multiple at the cell extremities, imposing the forces necessary for location of the gas/liquid interface.

13.1.1.2 Free Vortex

The free vortex, identified by the classic $V = k/r$ relationship, is accomplished by tangentially injecting the melt into the periphery of a cylindrically shaped container at a sufficient velocity and mass flow

13.1.1.2 (Continued)

rate to create a stable vortex. The only moving components of this concept would be the melt and the pump for melt circulation.

13.1.1.3 Forced Vortex

The forced vortex utilizes a series of radial vanes that are angularly spaced and rotated about an axis within a cylindrically shaped container. This impeller is driven at a constant angular velocity imparting a gravity gradient throughout the fluid, and creating the required interface provisions.

13.1.2 Melt Immobilization Concepts

13.1.2.1 Porous Matrix

This concept utilizes the surface tension properties of a liquid which, when subjected to controlled pressure differential across a porous matrix, creates a physical barrier that locates the gas/liquid interface.

13.1.2.2 Paste Electrolyte

By mixing proportional amounts (approximately 50-50) of an inert substance such as magnesium oxide to the molten electrolyte, a thick paste is formed that has the integrity of a solid and will still function as an electrolyte.

13.2 Carbon Management

Carbon, formed as a solid in the cell when CO_2 is electrolytically decomposed, will grow on the cathode surfaces and displace electrolyte in the process. Since between 30 to 35 cubic inches of carbon, representing the daily accumulation of four men, is formed from the process, provisions for handling this carbon must be incorporated in a flight unit. Several considerations may be related here with regard to the physical characteristics of the carbon deposited. The purity of the deposit is a prime objective of our research program for two basic reasons. First, any impurities would be in the form of occluded salts that would penalize the system on a weight basis because they would have to be replaced. Secondly, the salts which are entrapped are done so selectively i.e., Li_2O which is formed at the cathode when Li_2CO_3 is decomposed is the predominant constituent of the occluded deposit. Since Li_2O is required for CO_2 adsorption, the depletion of this constituent will eventually stop the process reaction. For these reasons, the recovery of pure carbon is a system objective.

The physical concepts considered with regard to this objective are based on two process methods. The obvious method is to control the process

13.2 (Continued)

such that the initial deposit results in the required purity. An alternative is to purify the deposit externally to the cell. The concepts outlined below may include either or both of these methods for carbon purification.

13.2.1 Reusable Cathode

13.2.1.1 Removable Electrode

The cathode with an adherent deposit of carbon is mechanically withdrawn from the electrolyte into an inert atmosphere to prevent the carbon from recombining with oxygen at the elevated temperatures. Carbon is then sheared or scraped from the electrode surface and transported to a storage area by either mechanically displacing it or exposing it to an inert recirculating gas stream. The cathode is then reinserted in the electrolyte and a new growth of carbon is deposited.

13.2.1.2 Stationary Electrode

13.2.1.2.1 Melt Removal

The melt is pumped to an accumulator external to the cell exposing the electrodes. Carbon is then mechanically removed and transported to a storage area. Melt is then pumped back into the cell and electrolysis resumed.

13.2.1.2.2 Melt Filtration

The deposit is either mechanically scraped from the electrode or the process is controlled so that nonadherent carbon is formed at the electrode and is dispersed in the melt. The melt is circulated through an external loop to a filter and compacting device where the carbon particles are removed, purified and stored. The filtered melt is then returned to the cell.

13.2.2 Disposable Cathode

This concept utilizes a light weight cathode structure (< 10 percent of deposit weight) which is withdrawn from the melt and stored in situ at predetermined periods. A new electrode unit is then installed.

13.2.3 Disposable Cell

Carbon is allowed to form on the cathode until the cell is essentially filled. The cell is designed to include a minimum of systems components to keep down the total cell weight. At predetermined intervals, the entire cell is discarded and replaced with a new one. Melt could be conserved by allowing the carbon to displace the melt which is collected

13.2.3 (Continued)

in an accumulator for reinjection in the next cell. The cell could also be designed with expansion provisions so that carbon growth would be accommodated by expanding the cell.

13.3 Carbon Dioxide Removal

When carbon dioxide gas, either pure or in dilute concentrations (2 to 5 mm P_{CO_2}) in ambient air, is physically contacted with the electrolytes being considered for the molten salt process, essentially all of it is absorbed or scrubbed as is the case of lower concentrations. This phenomenon has been experimentally demonstrated on numerous occasions for extended periods of time in conjunction with simultaneous electrolytic decomposition of the CO_2. A more detailed discussion of process variables and efficiency can be formed in Section 5.3 of this report.

The method or technique of introduction for the gas and liquid phases in the system will be dependent on its applicability to integrate with the selected melt containment and carbon management concepts. It should be pointed out that consideration must also be given to certain process requirements such as providing shielding of the cathode region from oxygen which is either contained in the ambient gas stream or evolved at the anode.

Since the volume of process air, assuming a fixed metabolic CO_2 production rate, is inversely proportional to removal efficiency, it is necessary that the scrubber design be optimized to achieve a maximum CO_2 absorption rate. Lower flow rates, approaching 11 SCFM @ 3.8 mm P_{CO_2} as a lower limit, would result in significant system weight saving by reducing fan power and size and probably a smaller quantity of electrolyte. Techniques which may be utilized for scrubbing are common to already developed processes in the chemical industry. The primary prerequisite for adoption of these concepts to the flight molten carbonate system is a finite gas/liquid interface.

13.3.1 Sparging

The simplest method of dispensing a gas in a liquid is to introduce the gas through an open ended tube, a perforated tube or a perforated plate submerged in the liquid. This technique is presently used for process investigations being conducted in conjunction with the basic research portion of this study.

13.3.2 Surface Absorption

Process gas is passed over the liquid defined surface and depends upon diffusion of CO_2 molecules through the gas stream and adequate diffusion

13.3.2 (Continued)

of Li_2O ions from the cathode region to effect scrubbing at the gas/liquid interface.

14.0 THREE PHASE SEPARATOR DEMONSTRATION MODEL

The three phase separator, constructed and delivered as an end item requirement under this contract, was created to demonstrate a system configuration for phase separation which is applicable to zero gravity operation. The principles selected for the separation of solids and gases from liquids represent potentially feasible, but not necessarily experimentally proven concepts which can be directly related to process requirements.

The design study of a flight unit started with the evolution of gross concepts for melt containment, carbon management and CO_2 scrubbing. Each problem area was initially investigated for possible solutions without particular attention toward integrating that solution with possible solutions conceived for the other problem areas. It was felt that this procedure would produce a greater number of candidate configurations and thereby increase the potential number of candidate systems from which to choose. By allowing the flow time necessary for preparation of design sketches, component fabrication, and assembly and testing of the finished model, a date for selection of a system concept was determined in regard to delivery commitments. This commitment necessarily limited the total scope of effort. On this basis, ground rules were imposed early in the study to assure a meaningful system concept.

14.1 Concept Selection

A review of the concepts in each of the three basic problem areas resulted in the following imposed ground rules and design criteria:

- The model will utilize an artificial gravity field for control of the gas/liquid interface.
- Solid phase removal must take place without system shutdown.
- Model must clearly show separation of gases and solids from the liquid.
- Simplicity of model essential - cost to be kept to a minimum.
- Sizing of the model will not be required with regard to any man rated capacity.
- Model concept should have a minimum of moving parts.
- Water to be used to simulate electrolyte.
- Model to simulate a process (or principle) which is applicable to a flight unit.

14.1 (Continued)

Within the framework of this criteria, the concepts selected were a free vortex for melt containment, filtering for recovery of carbon and sparging for the introduction of gas into the system. The advantages of this system configuration may be stated as follows:

- Positive positioning of electrolyte
- Location of a gas/liquid interface
- Minimizes number of moving parts
- Good mixing of electrolyte constituents from process viewpoint
- Minimizes foaming effects
- Not dependent on dense, adherent carbon deposit
- Lends itself to multicell configurations

It was understood at the time this selection of concepts was made that improved understanding of the basic processes may have some effect on the ultimate selection of the system that would finally be recommended. Figure 14-1 shows the model in the final configuration.

14.2 Problem Definition

It was determined that any of the potential system configurations which may have been selected involved difficult problems requiring solutions. However, they would also have many problems in common with regard to required components and process control as well as those specific problems that were unique to that particular concept.

As a result, the problem defined for the selected configurations on a system basis are not necessarily confined to this concept. Problem definition was determined on a component and process oriented basis. The problems listed should be considered as being of a preliminary nature since it is recognized that as potential problem solutions evolve, additional problems may be revealed.

14.2.1 Component Oriented Problems

Figure 14-2 lists the major components for a system using the free-vortex-melt filtration principles for phase separation. Also listed, by component, are problems that are associated with that component. It should be noted that many of the problems shown for a particular component are of a generic nature and that solutions will be arrived at

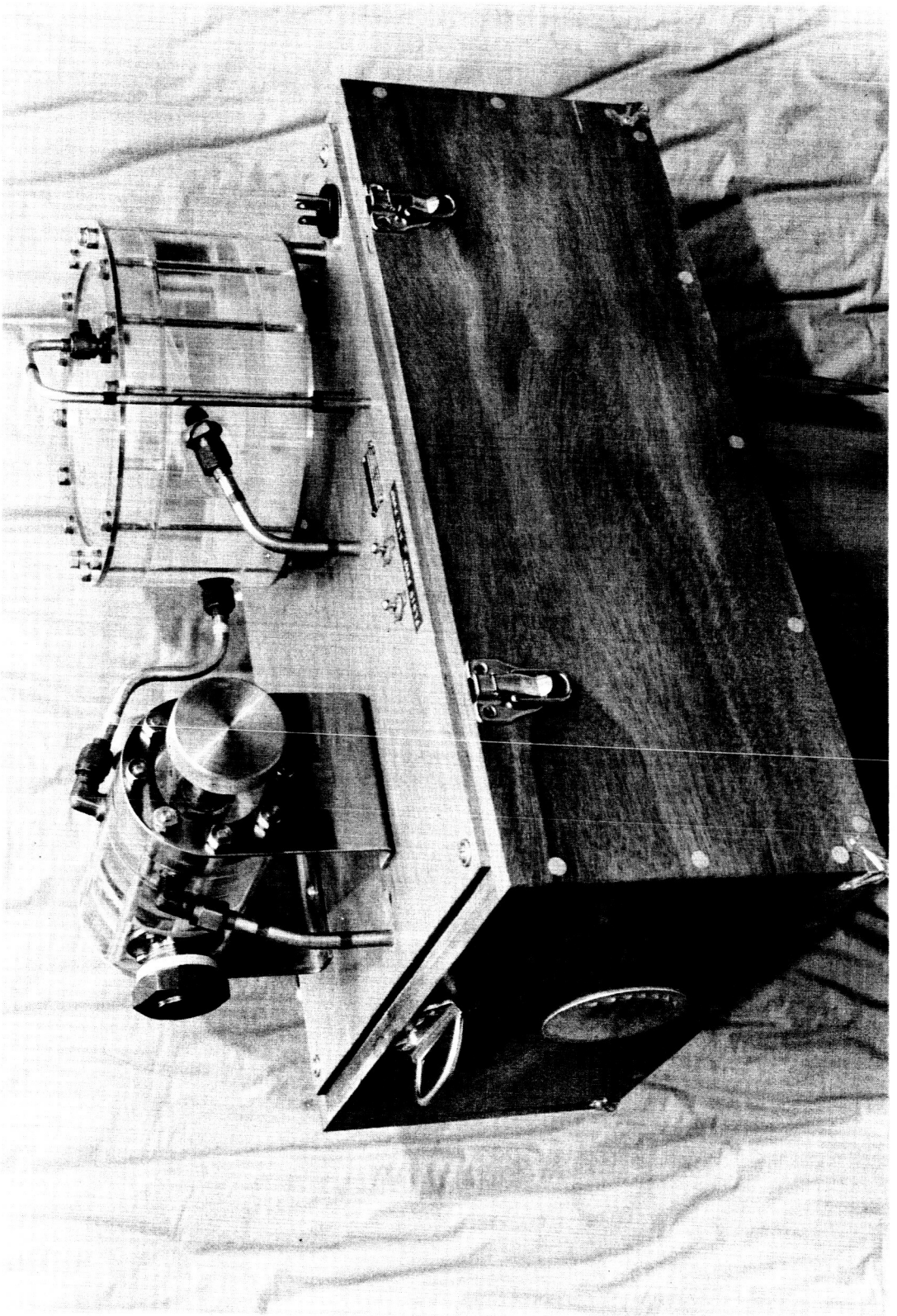

FIGURE 14-1 THE THREE PHASE SEPARATOR DEMONSTRATION MODEL

14.2.1 (Continued)

on a component integrated basis for system optimization. The remainder of the problems may require extensive development and research effort to arrive at practical solutions.

14.2.2 Process Oriented Problems

Also listed on Figure 14-2 are process oriented problems that are presently being researched under this contract. Solutions to these problems will have a direct bearing on the system components as well as on process parameters and control. The problems listed are primarily for reference only and more detailed discussion concerning research status in these areas will be found in Part I of this report.

14.3 Operational Description

The three phase separator model consists of four major components in addition to the carrying case. These components, a solid/liquid separator, a gas/liquid separator, a fluid pump, and air pump constitute the system. The components are all mounted to a common plate which is an integral part of the carrying case. Figure 14-1 shows the gas/liquid and solid/liquid separators in their mounted position. The pumps are located in an inverted position on the opposite side of the plate.

Figure 14-3 is the system schematic. The gas/liquid separator simulates the cell where electrolytic decomposition of CO_2 would take place. An interface between the two phases (gas and liquid) is achieved by tangentially injecting the liquid through an orifice, located on the smaller of two cylindrical bodies, with a sufficient velocity head to create a stable gas core or vortex within the cylinders. Air, injected into the resultant gradient force field created by the vortex, is forced to the surface or gas/liquid interface and released from the cell through an opening which is concentric with the gas core. This simulates the scrubbing of CO_2 rich air in the actual process. Water, simulating the electrolyte in the molten salt system, exits the cell tangentially on the periphery of the larger cylinder. Figure 14-4 shows the model operating with the axis of the gas core horizontal. This would be the most severe mode of operation under a gravity environment.

On either end of the larger cylinder and concentric with the smaller cylinder are located the electrodes as shown on the system schematic. The electrode location was simulated on the model with a dashed outline which is visible in Figure 14-4. Oxygen evolution at the anode was not specifically accounted for in the model but it would become part of the effluent air being bubbled through the cell.

Carbon formation at the cathode is simulated by injecting plastic pellets

REQUIRED COMPONENTS

1. Air Pump
2. Heat Exchanger
3. Bubbler
4. Cathode
5. Anode
6. Gas Shield
7. Trim Heater
8. Insulation
9. Retort
10. Temperature Control

11
12
13
14

COMPONENT ORIENTED PROBLEMS

1. AIR PUMP

   a) Power
   b) Weight
   c) Volume
   d) Efficiency
   e) Head-Flow Optimization
   f) Life

2. HEAT EXCHANGER

   a) Efficiency
   b) Weight
   c) Volume
   d) Pressure Drop

3.

8. INSULATION

   a) Thermal
      1) Weight
      2) Volume
      3) Deterioration
      4) Toxicity
   b) Electrical
      1) Dielectric strength
      2) Deterioration

9. RETORT

   a) Corrosion
   b) Sealing
   c) Thermal Expansion & Contraction of Relative Components
   e) Start and Stop Procedures

10.

PROCESS ORIENTED PROBLEMS

1. CATHODIC REACTION

   a) Determine Current Efficiency
   b) Gas Formation & Control
   c) Optimum Current Density
   d) Cathode Material
   e) Shielding Required
   f) Shield Geometry
   g) Cathode Life
   h) Agitation Effect

Electrolyte
Carbon Filter
Electrolyte Pump
Carbon Collector

BUBBLER

a) Pressure Drop
b) Flow Balance
c) High Temperature Sealing (if required)
d) Corrosion
e) Geometry
f) Effectiveness

4. CATHODE

a) Electrical Conf.
b) Corrosion
c) Current Density
d) Carbon Removal (if required)
e) Geometry
f) Life (Replacement)

5.

TEMPERATURE CONTROL

a) Power
b) Weight
c) Volume
d) Accuracy
e) Reliability

11. ELECTROLYTE

a) Agitation
b) Viscosity
c) Lubricity
d) Specific Gravity
e) Frothing
f) Wetting Properties

2. ANODIC REACTION

a) Current Density
b) Anode Material
c) Reabsorption of CO_2
d) Anode Life
e) Agitation Effects
f) O_2 Purity

3

RTEX CONCEPT

ANODE

a) Electrical Conf.
b) Corrosion
c) Current Density
d) Orientation Relative to cathode
e) Life (Replacement)
f) Geometry
g) O_2 Recovery

6. GAS SHIELD

a) Corrosion
b) Geometry

7. TRIM HEATER

a) Sizing
b) Configuration
c) Power
d) Weight
e) Life

12. CARBON FILTER

a) Grid Size & Area
b) Corrosion
c) Material
d) Geometry
e) Life
f) Pressure Drop
g) High Temperature

13. ELECTROLYTE PUMP

a) Configuration
b) Sealing
c) Bearings
d) Corrosion
e) Auxiliary Power
f) Life

14. CARBON COLLECTOR

a) Carbon Purity
b) Carbon Density
c) Geometry
d) Auxiliary Power
e) Seals

ELECTROLYTE (MELT)

a) Composition
b) Operating Temperature
c) CO_2 Scrubbing Efficiency
d) Frothing Control
e) Electrical Conductivity
f) Effect of Contaminants
g) Reaction Control
h) Melting Point
i) Instrumentation Techniques
j) Wetting Properties

4. FILTERING PROCESS

a) Carbon Purity
b) Particle Size
c) Carbon Density

FIGURE 14-2 SYSTEM PROBLEMS DEFINITION

3

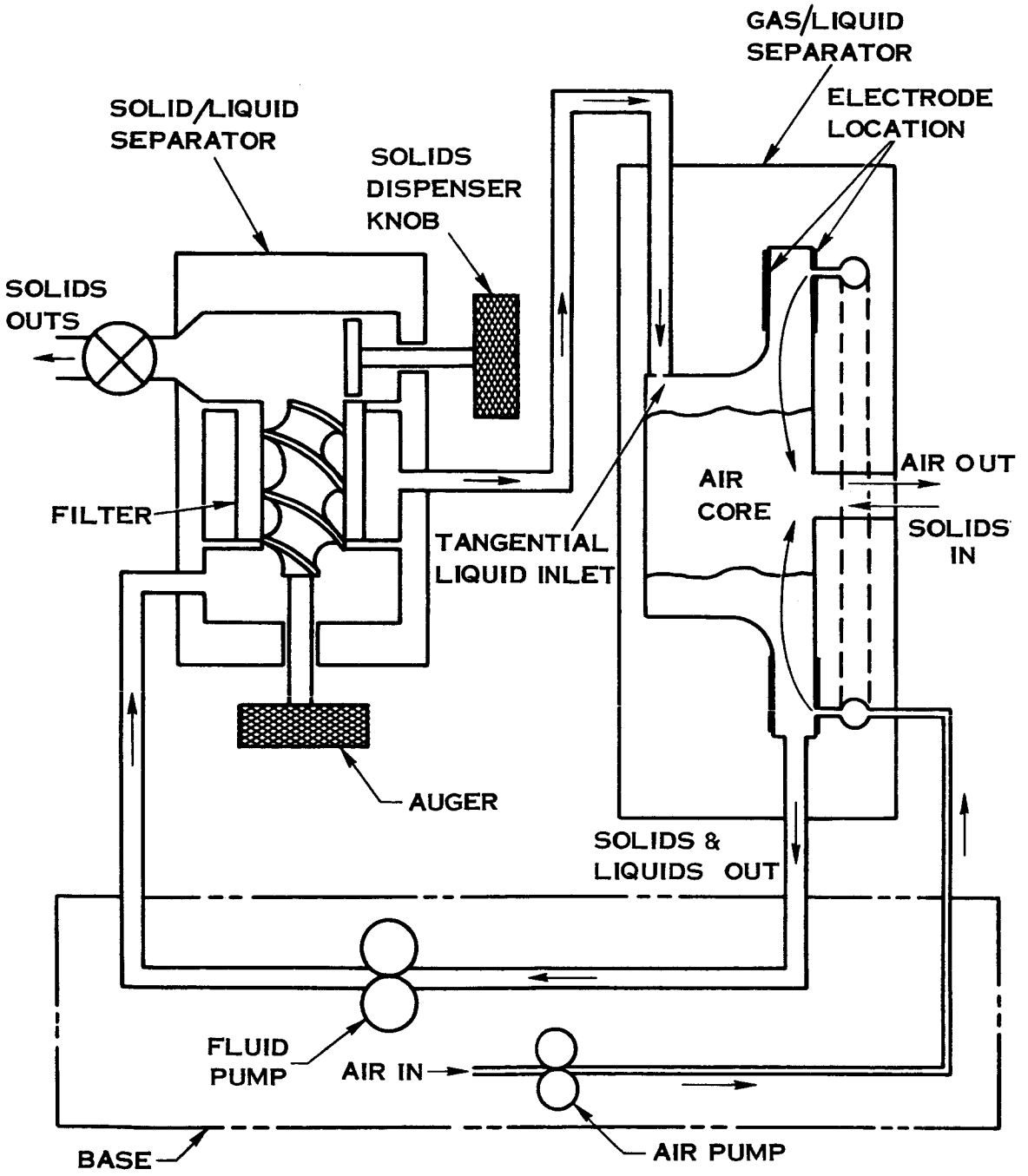

FIGURE 14-3 THREE PHASE SEPARATOR SYSTEMS SCHEMATIC

14.3 (Continued)

into the vortex. This procedure is based on the fact that with certain electrolyte compositions nonadherent carbon has been observed to form in actual practice. The solids are then picked up by the liquid which flows radially outward and are transported by the effluent fluid stream to the solid/liquid separator where the solids are separated from the liquid by a filter. The filtered liquid then returns to the gas/liquid separator for reinjection through the orifice.

Periodically, the accumulation of solids are removed from the inner surface of the filter by a scraper in the form of an auger which transports the solids into an adjacent chamber. Here a solids dispenser compresses the solids forcing the liquid back into the system through a check valve which is not shown on the schematic. The solids may now be recovered through the solids outlet port as shown in Figure 14-5.

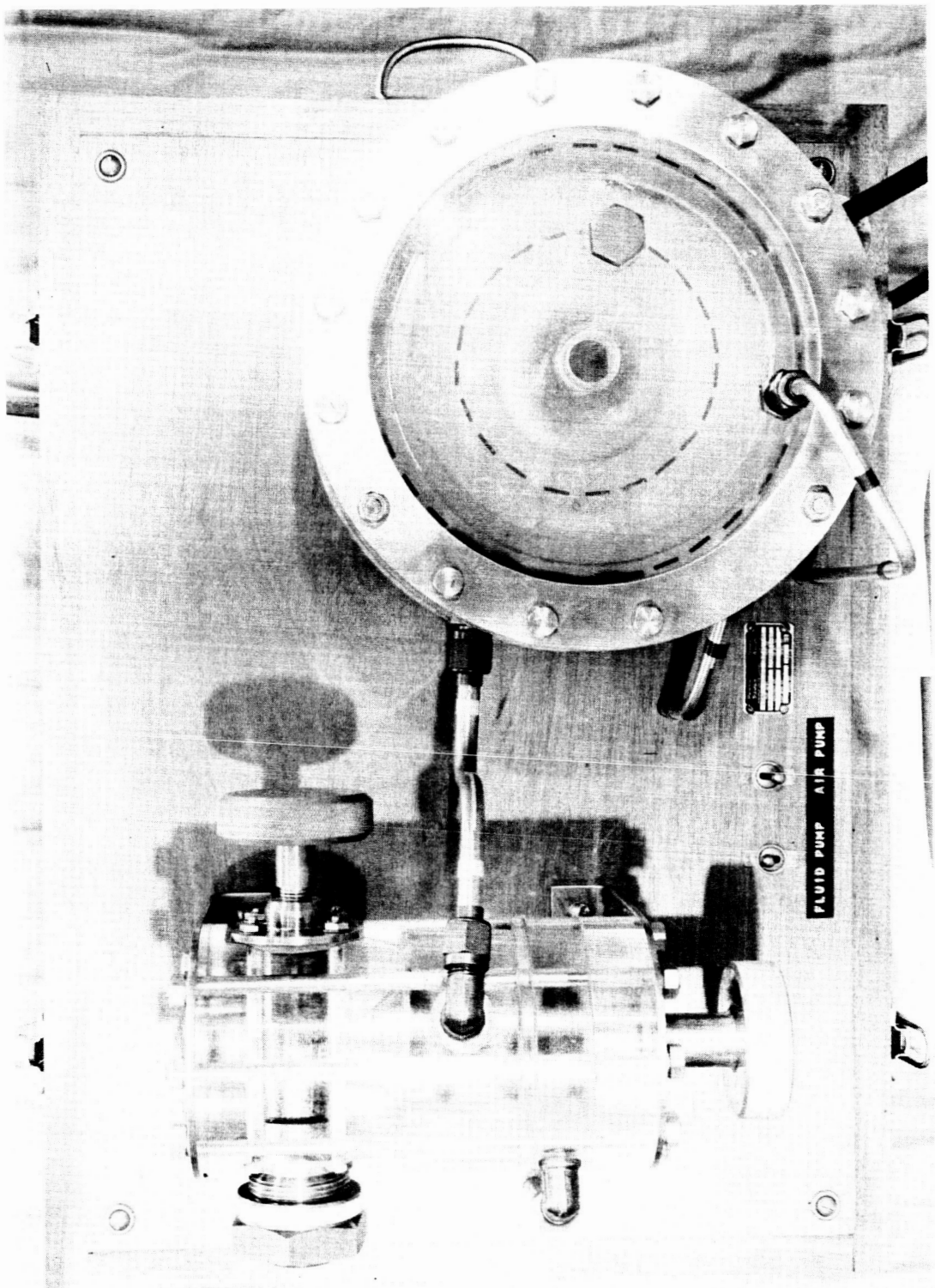

FIGURE 14-4 SYSTEM OPERATING WITH VORTEX AXIS HORIZONTAL

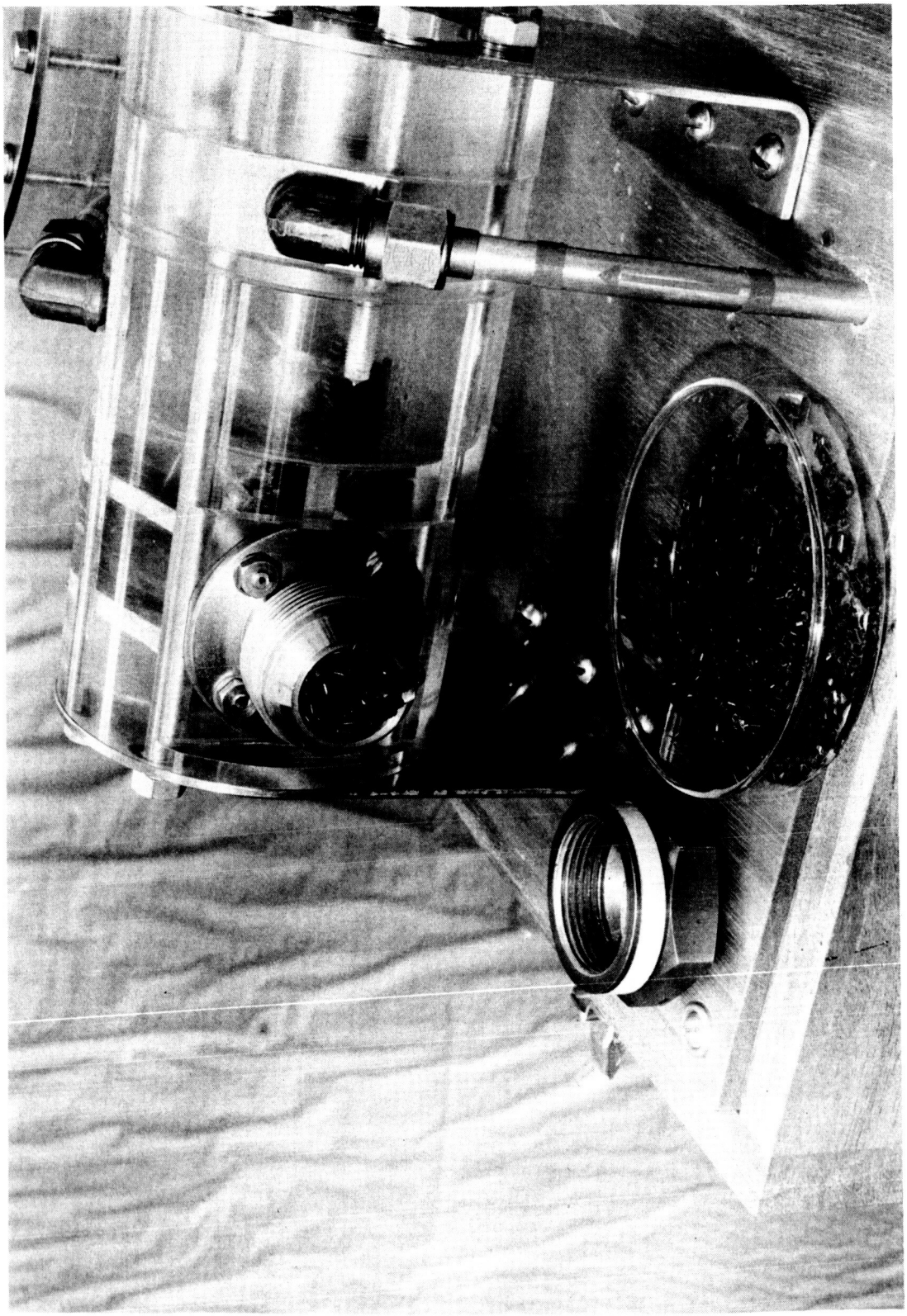

FIGURE 14-5 SOLIDS REMOVAL FROM THREE PHASE SEPARATOR

15.0 SYSTEM CONCEPT DESIGN STUDY

15.1 Discussion

Several approaches to the integration of the basic absorption and decomposition process concepts into a workable system were studied, considering a four-man unit handling nine lbs. of carbon dioxide per day. The basic schematic diagram of Figure 15-1 is common to all systems studied. A detailed example of the interface between the molten carbonate reduction system and a complete environmental control system is described in Reference 20.

Common system functions include preheating inlet air to cell operating temperature, control of electrolytic current, and control of operating temperature. Functions within the cell itself are discussed in Section 13.0 in relation to various internal configurations, hence this section will be concerned primarily with the significance of the several configurations to the achievement of minimum weight and power penalties consistent with reliability, safety of operation, and development cost. Two approaches which appear to have greatest potential will be described in some detail.

15.2 Common Basic System Components

15.2.1 Regenerative Heat Exchanger

All system requirements require the use of a regenerative heat exchanger to bring inlet air up to process temperature, tentatively 1200°F, before contacting the melt, and then to cool the outlet air sufficiently for delivery to the cabin or to the primary cabin cooling system. Air to air heat exchangers with unity mass flow ratio will normally be limited to an effectiveness of .80 to .85, hence outlet air will leave at elevated temperature and will constitute a system heat loss. Even with maximum heat exchanger effectiveness and minimum air flow rate, this loss will amount to about 400 watts, therefore maximum heat exchanger effectiveness is critically important for high system efficiency and low equivalent weight.

At least part of this heat loss will be supplied by losses inherent in the electrolytic process; supplying the entire loss by this means may be possible by increasing the operating voltage of the cell, with the concomitant benefit in cell size through increase of current density. Correspondingly, all heat losses, including those through insulation, supports, and ducting will contribute materially to the optimization of operating voltage, hence power, weight, and size, of the cell.

15.2.2 Current Control

15.2.2 (Continued)

Space cabin carbon dioxide concentration will be variable unless carbon dioxide removal rate is continuously matched to the rate of generation, which will vary with changes in metabolic rates associated with activity or diurnal cycles. Since CO_2 removal rate is determined by air processing rate and by oxide ion concentration within the cell, and the latter is determined by rate of CO_2 decomposition, or electrolytic current, all of these factors will require appropriate regulation in order to hold cabin CO_2 concentration within specified limits while simultaneously maintaining suitable electrolytic conditions for the cell process.

Current density, rather than total current, is related to cell voltage, as shown by Figure 15-2, and, since cathode area and cell geometry change with accumulation of the carbon deposit, current control through voltage regulation is not sufficient if oxide ion concentration in the cell is to be held within limits. It is expected that oxide ion sensing will be necessary and will be used to bias the schedule of operating voltage as a function of cabin air CO_2 concentration.

15.2.3 Temperature Control

The operating temperature of the electrolyte must be controlled to prevent freezing of the melt, evolution of secondary gases, and impairment of carbon purity. Since heat generated in the electrolytic process is determined by current and by the difference between operating voltage and open-circuit cell voltage, variations in this heat load will arise from regulation of cell voltage in response to cabin CO_2 and oxide ion concentration. To hold operating temperature with limits, therefore, external heat rejection will need to be correspondingly varied. The simplest concepts for this function are to bypass a variable part of the inlet air around the heat exchanger to control the temperature of mixed air entering the cell or to regulate air mass flow by inlet throttling. The bypass technique is preferred for reaons of simplicity and to avoid fan reliability problems arising from variable back pressure.

15.2.4 Insulation

The temperature differential between the cell and the ambient atmosphere makes optimum thermal insulation essential, since heat losses for the purposes of this study have been compensated at a power penalty of 300 lb/kw. Optimum insulation, however, will be determined in part by fabrication and packaging considerations, size of cell, and accessibility requirements, all of which will differ with the type of insulation used. Nonload bearing super-insulations, as used in cryogenic systems, would result in minimum insulation weight and

15.2.4 (Continued)

volume, but considerable heat loss could occur through mounting fixtures. The high vacuum required is a disadvantage in view of sealing problems in a system subject to large temperature changes, as in start-up.

An alternative is the use of a load bearing type based upon reflective radiation shields, which would eliminate the vacuum requirement and losses through mounting brackets and should provide improved rigidity for easy access in maintenance of minor components.

15.2.5 Heater

Both for purposes of electrolyte melting during start-up and to provide against melt solidification in the event of a temporary shutdown or decrease in process load, the system will require heaters, although these should be inactive during operation at design conditions. Band type heaters, as used in the laboratory demonstration model, are durable and effective at minimum weight penalty. Concepts for carbon removal or maintenance which require periodic cooling of part of the system will require considerable heater power to minimize downtime.

15.2.6 Fan

A low flow, low pressure rise fan will be required at the inlet to circulate the process air through the system. Ambient temperature at the inlet is conducive to high reliability, through improved bearing life, and lowest operating power. Low specific speed fans of the type required are in common use in the aerospace industry, and no critical problems are expected with this unit.

15.3 Molten Carbonate Cell Concepts

15.3.1 Design Criteria

The most difficult problem area in the design of a molten carbonate system to operate at zero gravity will be interface control of the three phases. Two operations involve the contact of liquid and vapor. Cabin air containing carbon dioxide must contact the molten carbonate melt, where the carbon dioxide is removed by reacting with oxide ions, and then be returned to the cabin. At the anode, oxide ions in the melt are discharged and are liberated as oxygen gas to join the outlet airstream. In both of these liquid/gas contact operations carryover of melt in the return stream to the cabin cannot be permitted. Melt carryover will result in plugging of downstream equipment, deterioration of performance, and a consequent system weight penalty. Still another phase separation problem arises in the disposal of the carbon

15.3.1 (Continued)

deposit. Any foreign materials disposed with the carbon represent an expended weight penalty to the system unless recovered and reused.

Other significant design problems arise from the following considerations:

- The operating temperature is high (1200°F)
- The melt is corrosive to common materials
- Anodic oxygen and process air must not contact the cathodic carbon

All of the foregoing considerations enter into evaluation of proposed designs based upon the following criteria:

- Weight penalties (fixed weight, power, expendable materials)
- Flexibility (adaptability, packaging)
- Maintainability (access to components, replacement of expendable components)
- Complexity
- Reliability

The three phase separator demonstration model discussed in Section 14.0 is one example of a cell. Other potential configurations include the following:

15.3.2 Forced Vortex Cell

In this concept the liquid-vapor interface is established by rotating the melt in the cell either by stirring or by rotating the cell. Carbon dioxide absorption may be accomplished either by injecting the gas directly into the melt or passing gas over the melt surface. Of the two gas absorption methods, injection into the melt is advantageous over surface absorption in obtaining the large required surface area without major size penalty. The cathode may be disposable or the carbon may be scraped from it. The power required to develop the liquid interface should be small. However, units of this type will be complex and of dubious merit relative to other methods considered. No major effort was directed to these concepts.

15.3.3 Artificial Gravity

15.3.3 (Continued)

The entire molten carbonate unit may be rotated to develop an artificial gravity field through centrifugal force. In this case, any process developed under normal gravity conditions is applicable. However, the complexity attendant to controls, maintenance, and carbon disposal, as well as the potential size of such a system, eliminated this concept from the studies here reported.

15.3.4 Porous Matrix

This concept of melt containment is presently being investigated for use in high temperature carbonate fuel cells and has performed satisfactorily in electrolysis experiments lasting several weeks (Reference 22). A porous sintered matrix of magnesium oxide powder is formed. This material is wetted by melt and forms a stable interface in the porous matrix due to capillary surface tensions. The matrix must be dense enough to hold the electrolyte in place under all anticipated forces, yet porous enough to allow sufficient ion mobility to permit an efficient process.

The anode consists of a screen or perforated plate which is held against the electrolyte-filled matrix. Oxygen is evolved at the anode-melt-matrix interface and is free to pass through the anode and into a collection passage. Carbon dioxide in the inlet air is removed by contact with oxide ions in the melt after diffusing to the walls of the gas passage and then through the porous anodes. The carbon can be handled in many ways, some of which are as follows:

- The cathode may be disposable
- The cathode may be scraped clean and carbon collected either by filtration or by direct removal from the cell
- The entire unit may be disposable

The disposable cell has been tentatively chosen as the preferred method for carbon removal in the porous matrix concept. This selection was made primarily because:

- Hardware complexity is minimized, thereby facilitating development and feasibility testing
- Operational procedures are simplified, and no exposure of the internal portions of the cell is required, favoring safer operation
- Reliability of hardware associated with the disposable cell concept is inherently greater

15.3.4 (Continued)

The disposable cell concept does not result in the lightest system, although the expendable weight is minimized for this concept by the growth of pure, compact carbon. Progress in this direction continues to be the primary goal of the research effort. Although selection of the disposable cell method for carbon removal is the most realistic choice at this time, it is possible, if not probable, that future research and development experience will result in a more sophisticated solution to the carbon removal problem, such as a light weight disposable cathode. However, the success of the concept does not depend upon such refinements, and the next steps toward development of hardware based on the matrix concept need not be complicated by carbon removal considerations.

15.4 Description of Selected Concepts

15.4.1 Basic Cell Module

Two methods for incorporating a porous matrix disposable cell concept have been evaluated. Both of the molten carbonate cell concepts which were chosen for a more detailed investigation incorporate a common basic cell, using a porous ceramic matrix to provide a stable and controlled liquid vapor interface.

The configuration for a single electrolytic unit or "Basic Cell" was selected to establish a weight basis for the matrix concepts considered in this study. Figure 15-3 presents a sketch of the basic cell, comprising a cathode (both sides utilized for carbon deposition), two porous anodes, two matrices and melt chambers, a gas passage, and appropriate spacers (not shown) and closure bars. The complete cell, when sized to provide the required amount of electrode and CO_2 "scrubbing" area, will consist of a stack of the appropriate number of Basic Cells.

The anodes are .03" thick porous nickel (sintered) plates, with 25-50 percent porosity. The cathode is .02" thick solid nickel sheet, and the matrix is .06" thick magnesium oxide with 40-60 percent porosity. The matrix and electrode thicknesses were chosen after considering cell constructions discussed in Reference 22 (Chapter 6 - High Temperature Fuel Cells). Feasibility testing will clarify the applicability of the assumed matrix and electrode thicknesses while providing a basis for eventual cell fabrication techniques. The cross-section chosen for the cell is one foot by one foot square, and the gas passage is .06" wide.

The electrodes of the several Basic Cells in a stack may be connected in series or parallel, depending upon the eventual vehicle power supply. No further attention is given to electrical wiring of the cells

15.4.1 (Continued)

in this study.

The width of the melt space between the matrix and the cathode will be dependent upon the cell replacement interval, which can be optimized as a function of mission time. This size of chamber allows for carbon deposit growth on the cathode. The growth, in turn, is set by the metabolic rate and mission duration. These carbon growth factors, along with the initial charge of melt, are used in the optimization of a final cell design, for which a weight summary is given below. As the width of the melt chamber is variable, weight of melt, spacers, and closure bars are not included in this summary.

Basic Cell Weight

Matrices (2) (50 percent Porosity)	1.12
Anodes (2) (25 percent Porosity)	2.08
Cathode	.92
Closure Bars (gas passage)	.03
Closure Bars (matrix)	.11
Spacers (gas passage)	.12
Melt Contained by the Matrix (melt sp. gravity = 2)	.62
	5.00 lbs

Optimum cell size will be determined primarily by consideration of electrode area, representative of unit weight, relative to electrical power required. For the example chosen, the total current of a single equivalent cell is 416 amperes, and the power can be determined by reference to the relation between current density and voltage, illustrated by Figure 15-2. While this relationship is, in general, a function of electrolyte composition, temperature, electrode geometry, electrode surface characteristics, and other factors, it was necessary to assume that Figure 15-2 would be sufficiently representative for use in all of the configurations studied, in lieu of more detailed information for a series of experimental designs and operating conditions. Based upon this assumption, the equivalent weight of the power required was derived as a function of current density and plotted in Figure 15-4, using a power penalty of 300 lbs/kw.

Research studies have shown that the carbon dioxide partial pressure

15.4.1 (Continued)

in equilibrium with the electrolyte can be far below cabin levels. Furthermore, substantially complete carbon dioxide removal from air in contact with the melt has been demonstrated in laboratory experiments. Mass transfer calculations show that, for absorption surface area based upon electrode area requirements, removal of CO_2 is primarily dependent upon absorption and diffusion characteristics of the melt in the porous matrix and relatively insensitive to air velocity or gas passage geometry. Any deficiencies in the ability of the melt-matrix to absorb CO_2 will be reflected in an increase in partial pressure at the porous anode, which separates the gas stream from the matrix. Since simultaneous evolution of oxygen gas at the anode interface will be associated with a local increase in CO_2 partial pressure, the uncertainty of the magnitude of this effect has been recognized by assuming a conservative scrubbing efficiency of 70 percent. This assumption results in a system penalty due to the increased heat losses in the regenerative heat exchanger occasioned by the increased flow required, as well as the increased fan power required for the higher flow. In the event that the partial pressure at the anode more nearly approaches that of the melt, air flow will be reduced, with considerable saving in system penalty. This saving in flow is demonstrated in Figure 15-5, showing air flow as a function of scrubbing efficiency.

15.4.2 Expandable Cell Concept

Among the molten carbonate system concepts studied, an expandable cell seems to have the minimum potential penalty. The expandable cell stack system incorporates the features of a basic cell, except that it expands to accommodate carbon growth, thus eliminating the need for a melt accumulator. When the maximum allowable carbon thickness has been reached, this cell stack is replaced. Replacement of the cell stack requires cooling of the cell and removal from the container.

Figure 15-6 shows an expandable cell, utilizing a metal diaphragm which deflects to accommodate carbon growth. This cell would be encased in a unit similar to that illustrated in Figure 15-7, except that additional space must be provided to allow for the increase in size during expansion of the cell. At periodic intervals during a mission, a fully expanded stack would be removed from the case and replaced by a fresh stack, stored for this purpose. The number of cells in a stack was determined as follows:

- Cell weight was determined as a function of current density (Figure 15-8)
- Power penalty was determined as a function of current

15.4.2 (Continued)

density (Figure 15-4)

- A curve of total equivalent cell stack weight versus current density was generated (Figure 15-9)

Figure 15-9 shows a minimum penalty at a current density of 32 milliamps/cm^2, which was chosen as the operating current density.

The optimum number of cell stacks is determined by evaluating the equivalent penalty as a function of mission length for an integer number of stacks. As shown by Figure 15-10, the optimum number varies with mission time. For the 60-day mission considered, two cell stacks were chosen. For an expandable cell system with an installation such as shown in Figure 15-7, the weight and power breakdown shown below was determined. Those weights are the same as shown in Section 12.0. However, weight and power for a water electrolysis cell to provide supplementary oxygen from reclaimed water has not been included here. Furthermore, this system does not take advantage of waste heat to preheat cabin air prior to entering the regenerative heat exchanger.

Expandable Cell Stack
Weight and Power
60-Day Mission

Component	Weight lbs.	Power watts	Equivalent Power wt/lbs
Cell Stacks (2)	73	990	297
Regenerative heat exchanger	11		
Fan	4	90	27
Insulation	15		
Heater	5	753	226
Container	9		
Frame & Misc.	33		
	150	1833	550
		Fixed Weight	150
Power Penalty = 300 lbs/Kw		TOTAL	700 lbs

15.4.3 Rigid Cell Concept

An alternative to the solid matrix expandable cell concept is the use of a number of rigid cells. This scheme utilizes an accumulator to store melt displaced by carbon growth in the electrolytic cell. The cell is periodically replaced and discarded (or stored) when the carbon thickness reaches the limitations of the cell. At that time, the accumulator is isolated by a disconnect between it and the cell stack, and the cell stack is cooled and removed from its container. The new cell then receives its charge of melt from the accumulator. Figure 15-11 presents a schematic of the rigid cell module. As in the expended cell concept, the complete installation is illustrated in Figure 15-7.

The rigid cell stacks are assemblies of several basic cells which provide the CO_2 removal and reduction capacity required. This cell stack incorporates a manifold connecting the assembly melt chamber to an accumulator which stores the melt displaced by carbon deposited at the cathode. As in the case of the expandable cell, the optimum number of cell stacks was determined as a function of mission time and is shown in Figure 15-12.

For a 60-day mission, a breakdown of system weights is given in the table below.

Rigid Cell Stack
Weight and Power
60-Day Mission

Component	Weight lbs.	Power watts	Equivalent Power wt/lbs
Cell Stacks	143	990	297
Melt (exclusive of matrix)	36		
Regenerative Heat Exchanger	11		
Fan	4	90	27
Melt Accumulator	24		
Insulation	15		
Heater	5	750	225
Container	8		
Frame & Misc.	58		
	304	1830	549
		Fixed Weight	304
Power Penalty = 300 lbs/Kw		TOTAL	853

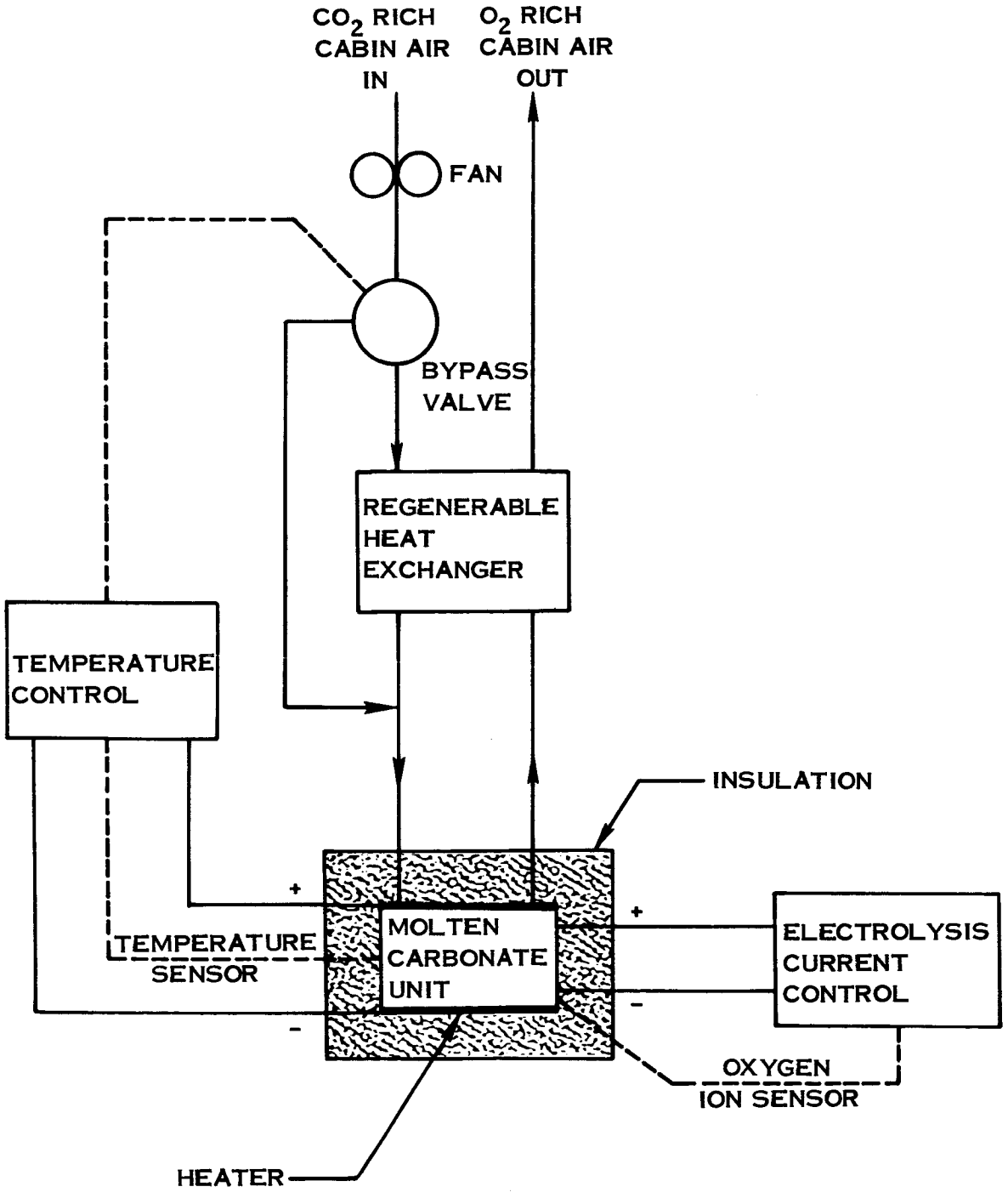

FIGURE 15-1 MOLTEN CARBONATE UNIT BASIC SCHEMATIC

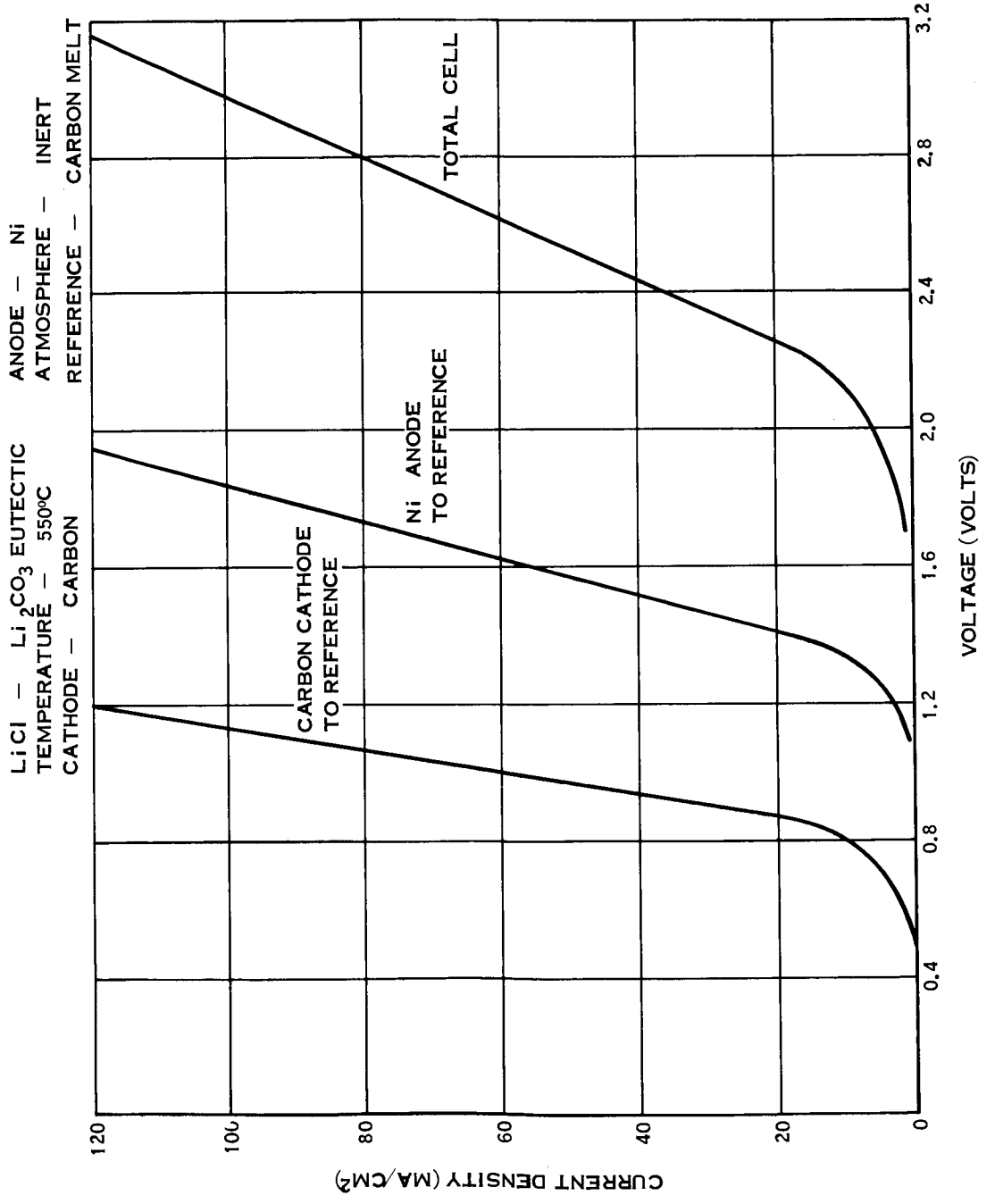

FIGURE 15-2 ELECTROLYTIC CHARACTERISTICS OF A MOLTEN CARBONATE CELL

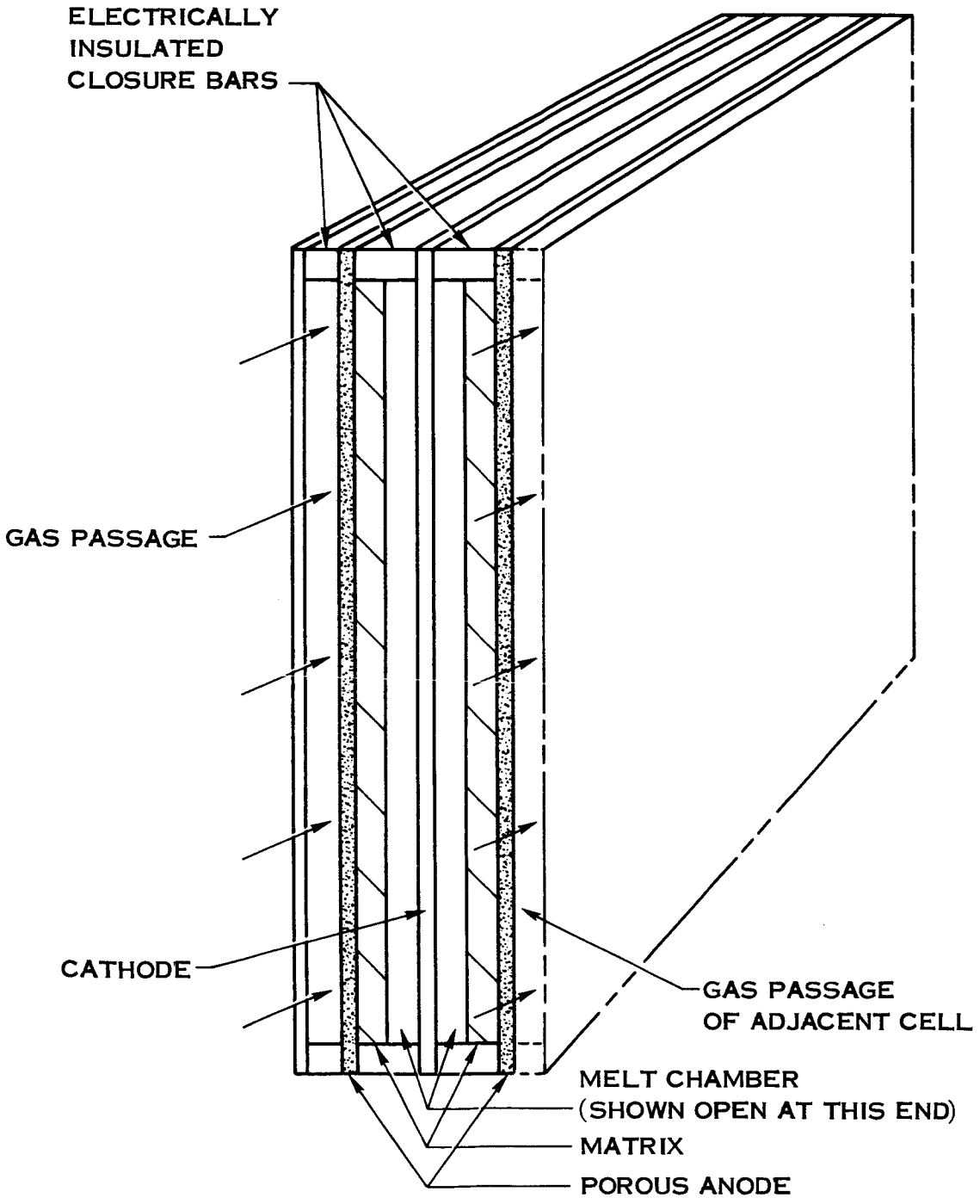

FIGURE 15-3 BASIC CELL MODULE

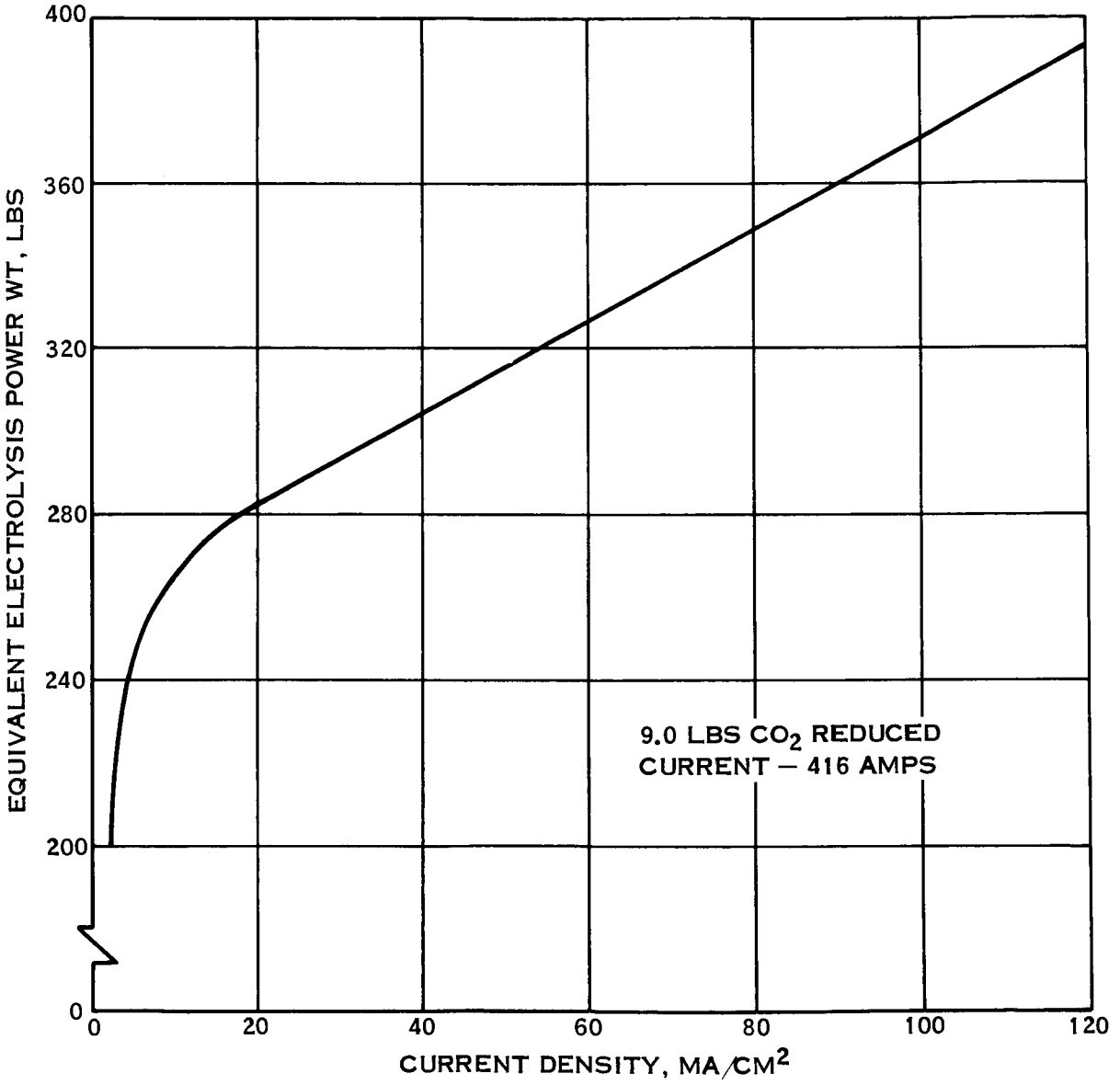

FIGURE 15-4 ELECTROLYSIS CELL POWER PENALTY

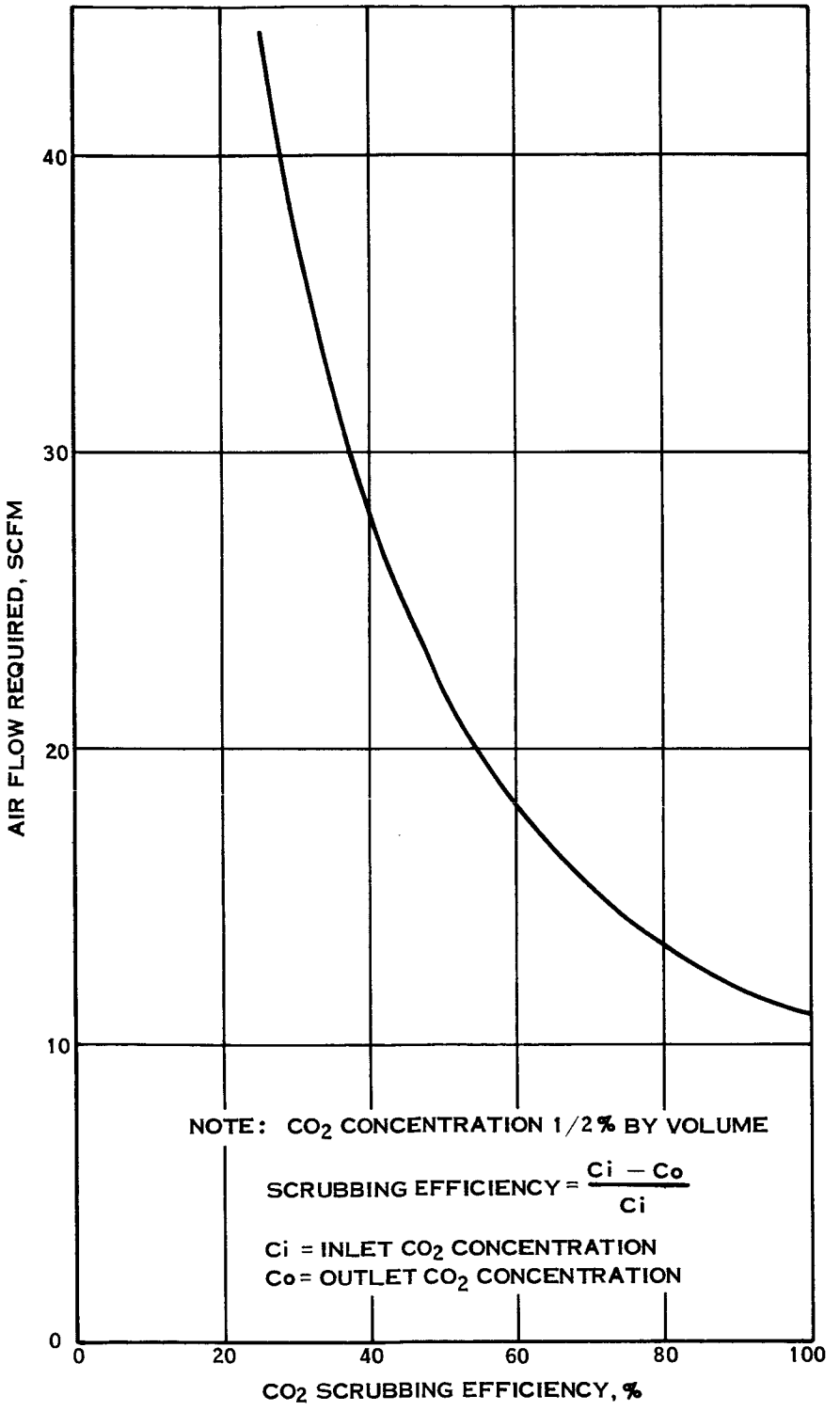

FIGURE 15-5 REQUIRED SYSTEM AIR FLOW

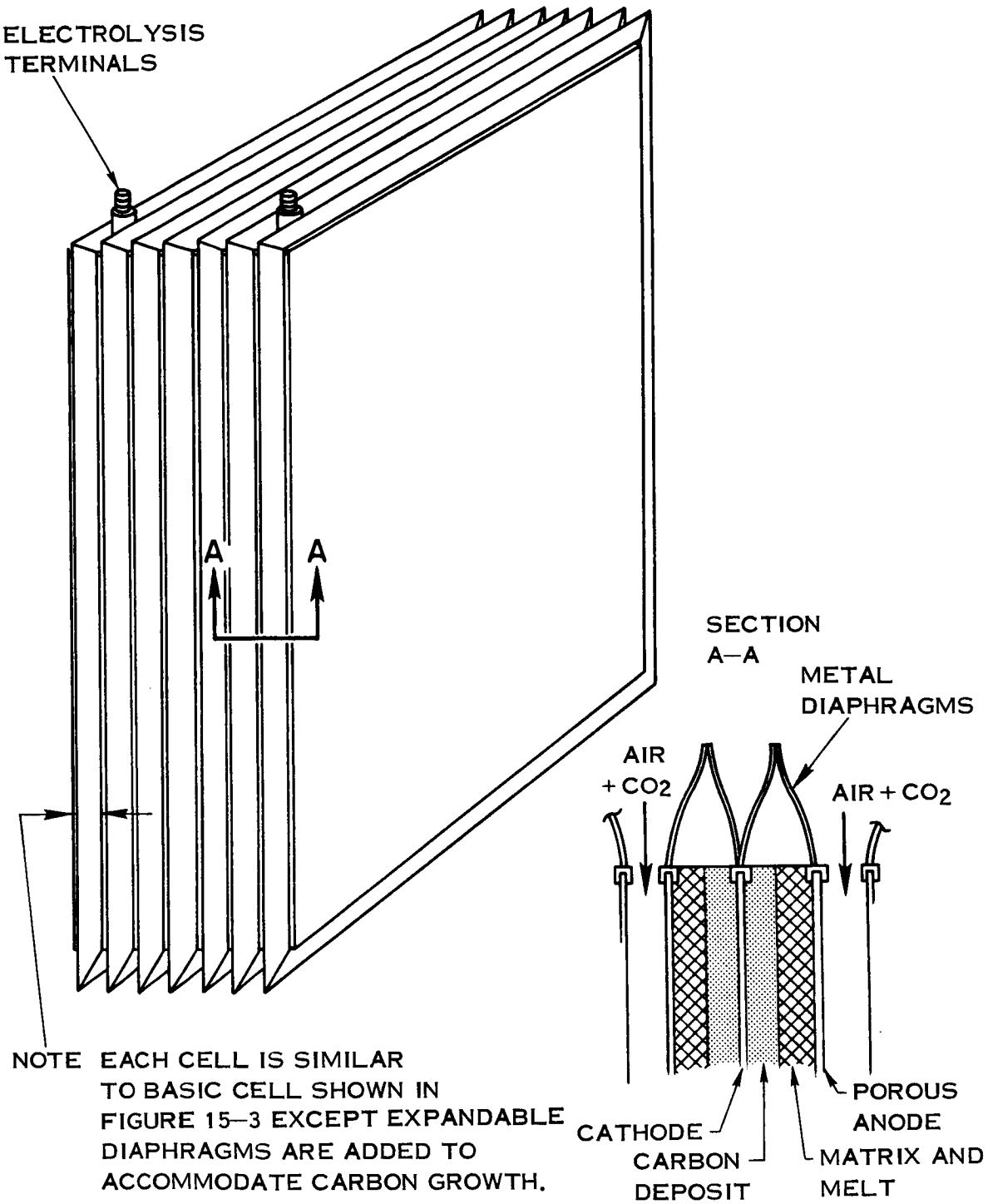

FIGURE 15-6 EXPANDABLE CELL STACK

HAMILTON STANDARD
DIVISION OF UNITED AIRCRAFT

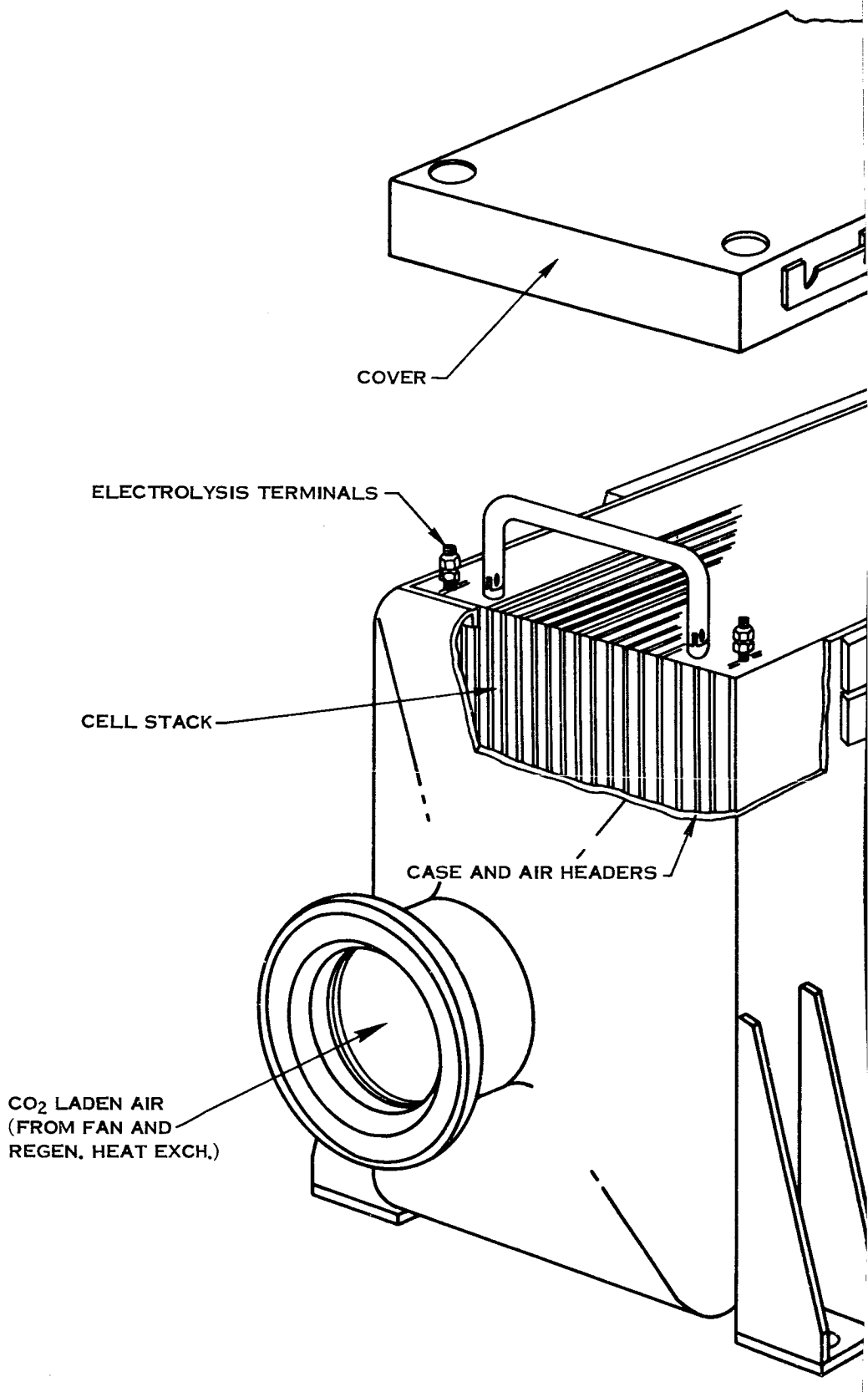

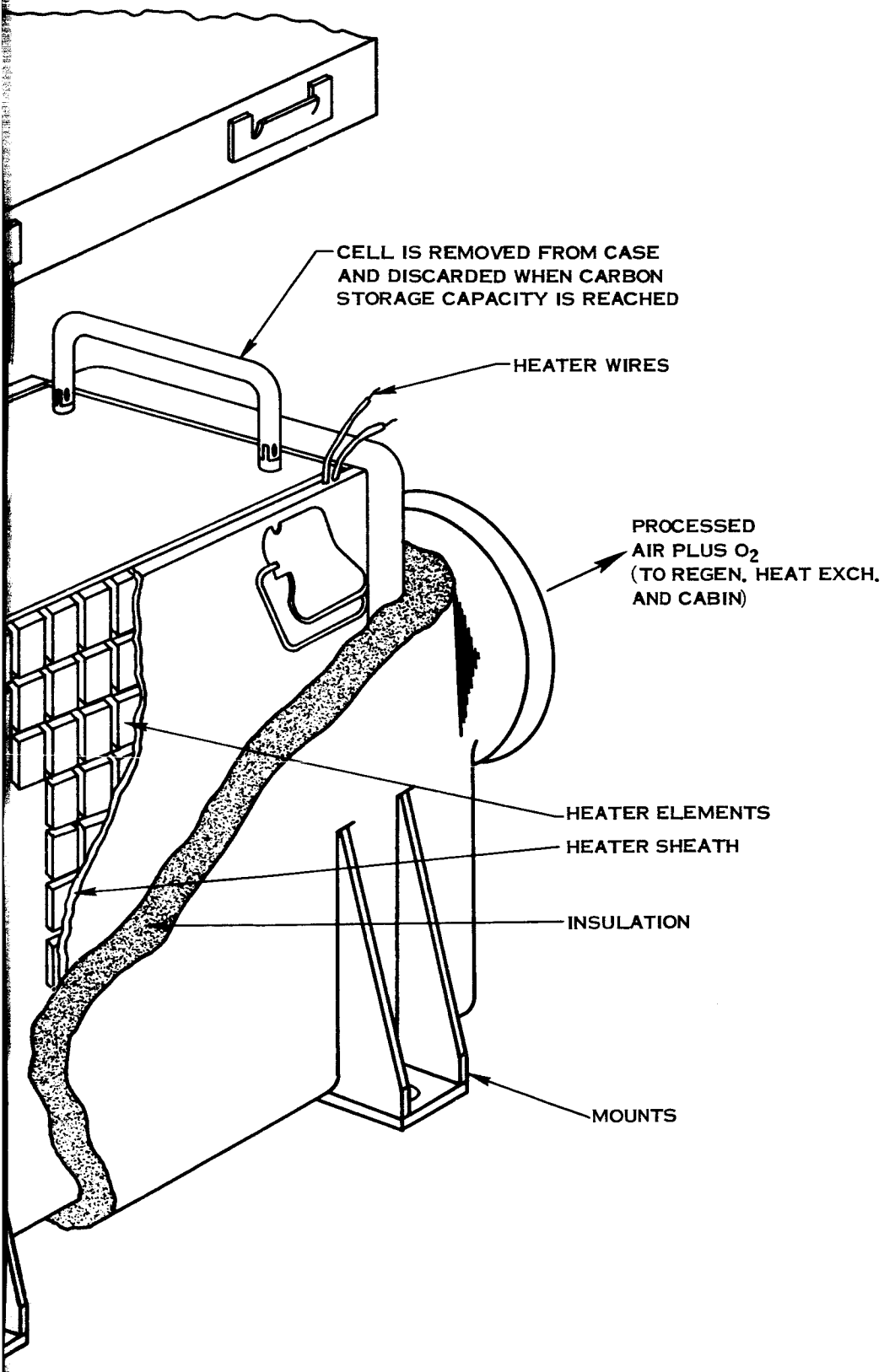

FIGURE 15-7 CELL STACK INSTALLATION

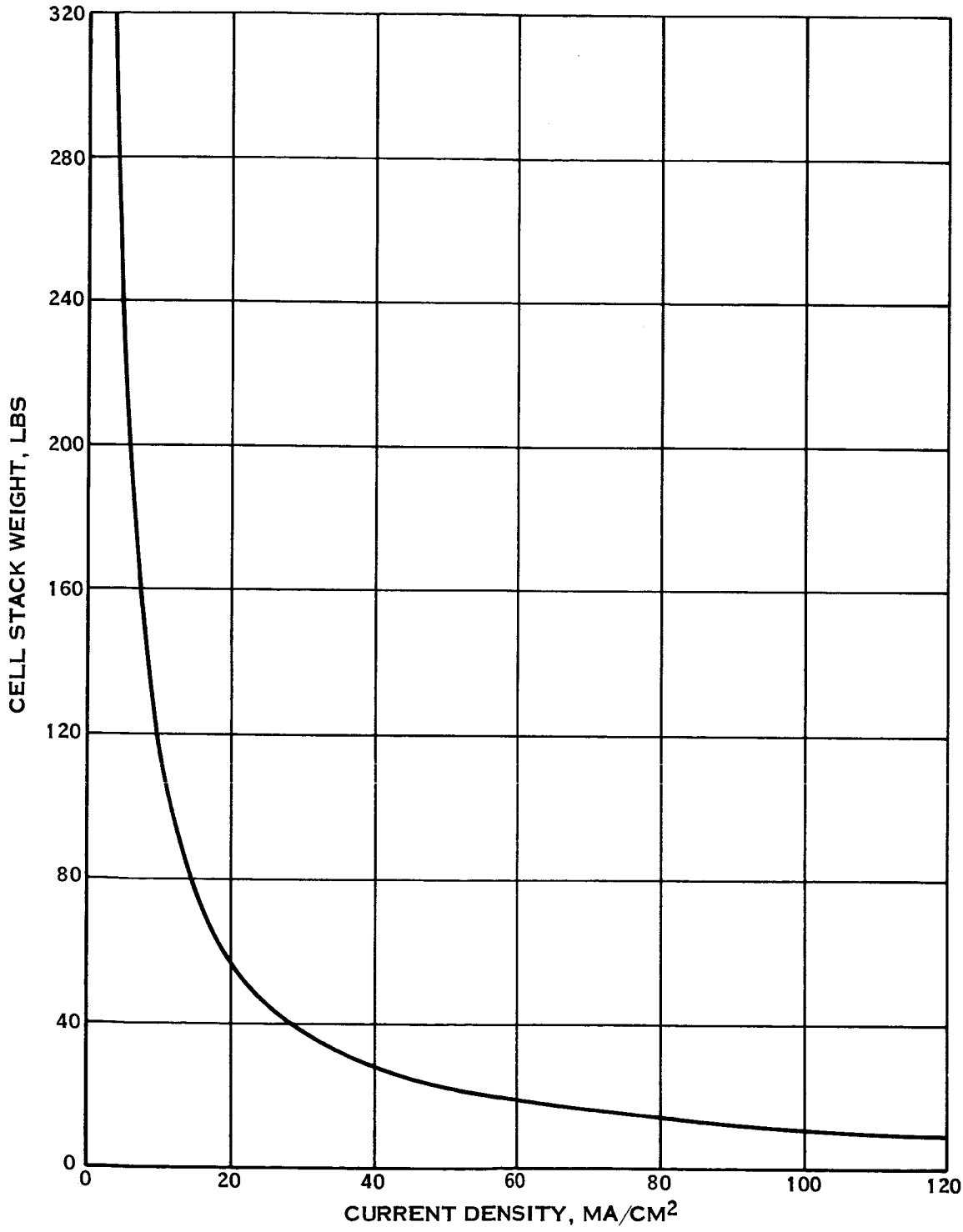

FIGURE 15-8 EFFECT OF CURRENT DENSITY ON CELL WEIGHT

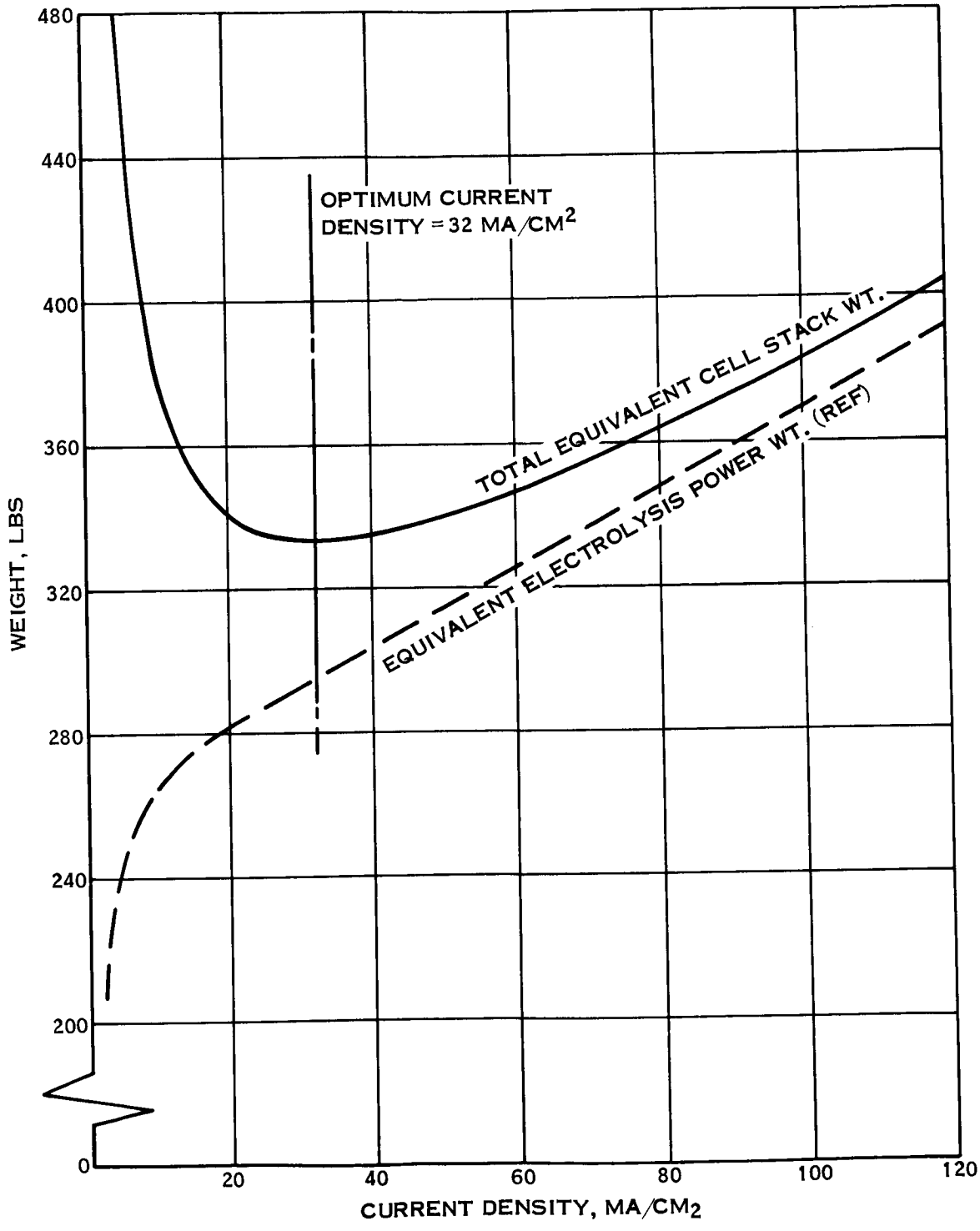

FIGURE 15-9 ELECTROLYSIS CELL CURRENT OPTIMIZATION

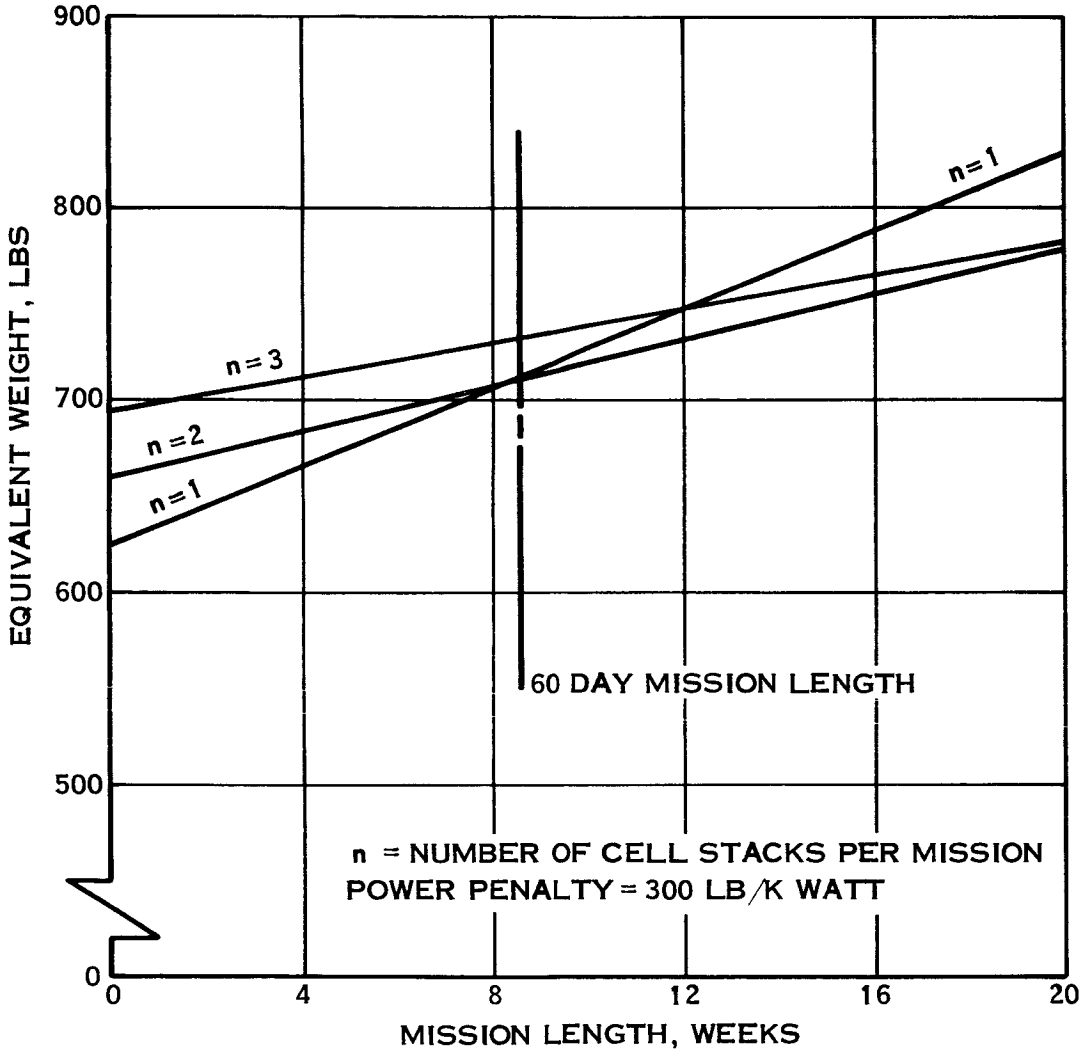

FIGURE 15-10 EFFECT OF MISSION TIME ON NUMBER OF CELLS FOR EXPANDABLE CELL STACK

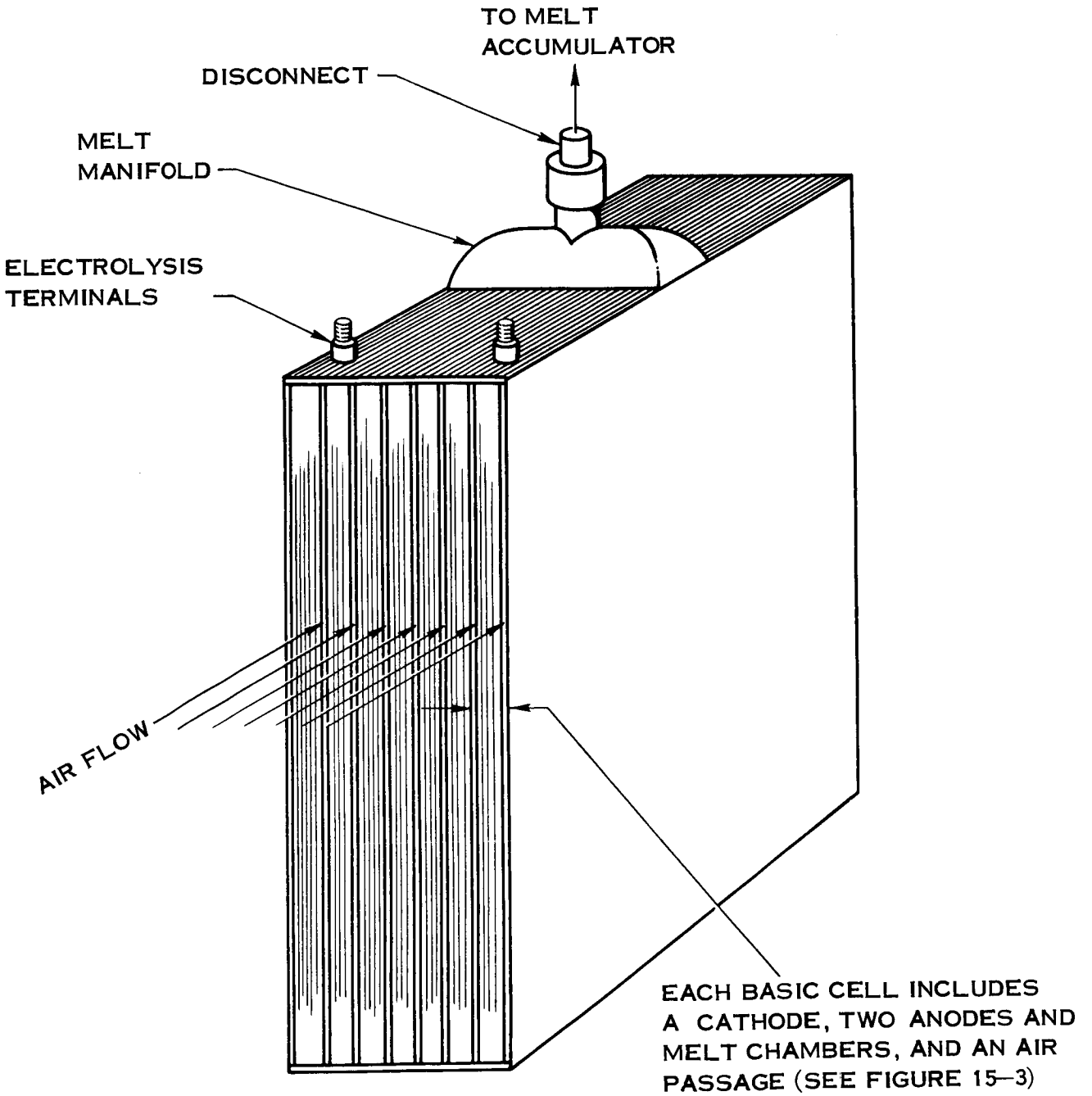

FIGURE 15-11 RIGID CELL STACK

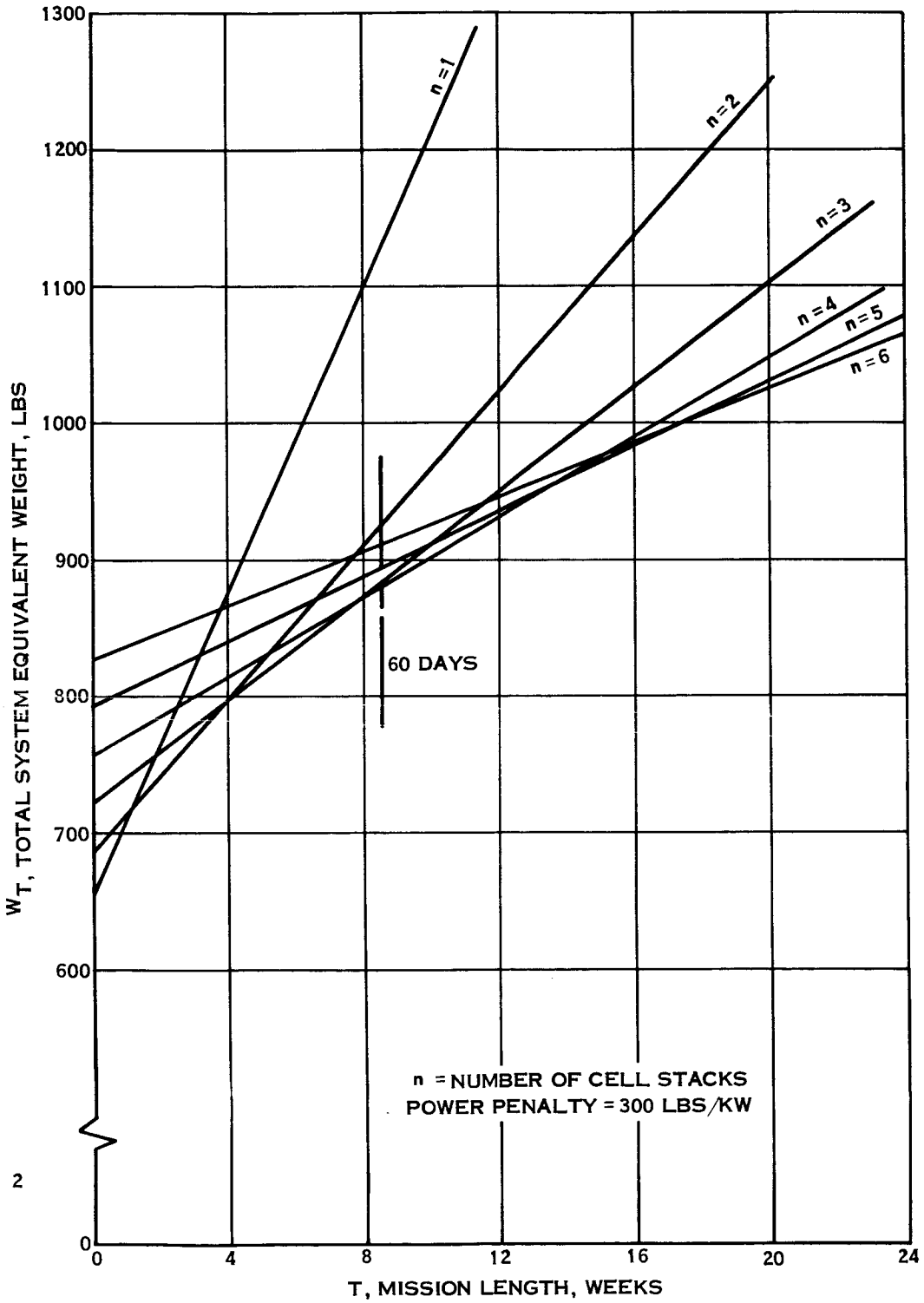

FIGURE 15-12 EFFECT OF MISSION TIME ON NUMBER OF CELLS RIGID CELL STACK

16.0 BIBLIOGRAPHY

1. Shearer, R. E., J. C. King, and J. W. Mausteller, "Electrochemical Recovery of Breathing Oxygen from Carbon Dioxide," Aerospace Medicine, 33, pp. 213-216, 1962.

2. Chandler, H. W. and W. Oser, Study of Electrolytic Reduction of Carbon Dioxide, Technical Documentary Report No. MRL-TDR-62-16, 1962.

3. Reddy, Thomas B., The Electrochemistry of Molten Salts, Electrochemical Technology, pp 325-351, 1963.

4. Emmet, P. H., Catalysis Volume IV, Reinhold Publishing Company, New York, pp 388-389, 398-404 and 416-417, 1961.

5. Burkhard, W. J., and J. D. Corbett, "The Solubility of Water in Molten Mixtures of LiCl and KCl," American Chemical Society Journal, 79, pp. 6361-6363, 1957.

6. Laitinen, H. A., W. S. Ferguson, and R. A. Osteryoung, "Preparation of Pure Fused Lithium Chloride-Potassium Chloride Eutectic Solvent, "Journal of Electrochemical Society, pp. 104, 516-520, 1957.

7. Janz, G. J., C. Solomons, and H. J. Gardner, "Physical Properties and Constitution of Molten Salts: Electrical Conductance, Transport and Cryoscopy," Chemical Reviews, pp. 461-508, 1958.

8. Janz, G. J., and M. Ingram, Department of Chemistry, Rensselaer Polytechnic Institute, Troy, New York; Private Communication.

9. Maricle, D. L., and D. N. Hume, "A New Method for Preparing Hydroxide-Free Alkali Chloride Melts," Journal of the Electrochemical Society, pp. 354-356, 1960.

10. Gardner, H. J., C. T. Brown, and G. J. Janz, "The Preparation of Dry Alkali Chlorides for Solutes and Solvents in Conductance Studies," Journal of Physical Chemistry, 60, pp. 1458, 1956.

11. Janz, G. J., and A. Conte, "Corrosion of Gold-Palladium, Nickel and Type 347 Stainless Steel in Molten Alkali Carbonates," Corrosion, 20, pp. 237-238, 1964.

16.0 (Continued)

12. Janz, G. J., A. Conte, and E. Nuenschwander, "Corrosion of Platinum, Gold, Silver, and Refractories in Molten Carbonates," Corrosion, 19, pp. 292 and 294, 1963.

13. Janz, G. J., and A. Conte, "Potentiostatic Polarization Studies in Fused Carbonates: Part II Stainless Steel," Electrochemica Acta, 9, pp. 1279, 1964.

14. Solomons, C., and G. J. Janz, "An Electronic Recording Differential Potentiometer," Analytical Chemistry, 31, pp. 623, 1959.

15. Lorenz, M. R., and G. J. Janz, "A Dynamic Method for Measuring Dissociation Pressures," Journal of Chemical Education, 40, pp. 611, 1963.

16. Ostroushko, Y. I., Lithium, Its Chemistry and Technology, AEC Report AEC-TY-4940, 1962.

17. Littlewood, R. V., "Electrochemical Studies of the Behavior of Metals in Fused Chloride," Electrochemica Acta, 4, pp. 55-69, 1961.

18. De Zubay, E., High Temperature Fuel Cells, SAE Preprint, 159E, 1963.

19. Vinograd, S. P., "Nutritional Trends in Future Manned Space Flights," Proceedings of the NASA-University of South Florida Conference on Nutrition in Space and Related Waste Problems, NASA SP-70, pp. 17-21, 1964.

20. Hamilton Standard, Space and Life Systems Division, "Mars Landing and Reconnaissance Mission Environmental Control and Life Support System Study," Volume 2, SLS 414-2, 1964.

21. Hamilton Standard, Space and Life Systems Division, "Manned Orbiting Space Station Environmental Control and Life Support System Study," Volume 3, SLS 410-3, 1964.

22. Young, G. J., "Fuel Cells," Reinhold Publishing Corporation, New York, pp. 78-93, 1960.